THE GEOLOGICAL EVOLUTION OF THE EASTERN RICHTERSVELD

by

Ulrich Ritter

Thesis submitted for the degree of Doctor of Philosophy in the Faculty of Science, University of Cape Town

Department of Geology,

December, 1978

ABSTRACT

The lithology of the early Proterozoic (~1950-1750 my) Richtersveld is characterised by predominantly calc-alkaline volcanics, (De Hoop Subgroup) overlain by and intercalated with quartzitic metasediments into which the mainly granodioritic rocks of the Vioolsdrif Intrusive Suite (VIS) were emplaced. Metavolcanics and sediments of the De Hoop Subgroup have been subdivided into formations, and their paleogeographic environments have been deduced from lithological criteria. In the northeastern Richtersveld systematic reconstruction permitted the recognition of four distinct depositional domains:

a) a high altitude volcanic terrain in the northeast, characterised by a great thickness of an entirely volcanic succession.
b) a synvolcanic graben structure in the southeast, infilled by melanocratic volcanics and immature sediments.
c) a low-lying volcanic terrain in the southwest, possibly representing a coastal plain, lithologically characterised by volcanic debris and redeposited volcanics of domain (a).
d) marine quartzites in the south, indicating a marine ingression from the southwest towards the end of the volcanic cycle.

In the southeastern Richtersveld more strongly metamorphosed acid to intermediate volcanics overlie metasediments of the Namaqua Metamorphic Complex (NMC).

Within the Vioolsdrif Intrusive Suite four intrusive phases can be distinguished. The oldest phase, a fine-grained granodiorite, is only tentatively assigned to the Vioolsdrif Intrusive Suite and probably constitutes a subvolcanic member of intermediate metavolcanics of the Kookrivier Formation. It was followed by syntectonic even-grained granodiorite and by posttectonic granite and leucogranite. Textural analysis of the undeformed granite phase provided information as to its intrusion and crystallisation history and the sequence of crystallisation. Since the latter allows the estimate of the water content of the initial magma, and as water content of the magma determines - according to some models - geological position and extent of porphyry ore deposits, predictions could be made as to the probable site and extent of possible porphyry ore deposits, which are in agreement with preliminary results obtained during fieldwork.

The metamorphic and tectonic development probably started soon after or even during deposition of the supracrustal rocks. Low grade metamorphism of low-pressure type (andalusite-sillimanite facies series *sensu* Miyashiro, 1973) in the central northeastern Richtersveld (associated with tight to isoclinal F_1-folds of different magnitudes) and migmatisation in the south and northeast (mainly postdating F_1) suggest an essentially zoned metamorphic complex with increasing grade of metamorphism towards the margins of the Richtersveld.

During decreasing metamorphic temperature a left-lateral wrench-fault system developed, causing northeast-trending early (F_2) open folds

and later north-south shear zones (Devilscastle Event) which in the south formed initially at ~5kb and 500 to 550°C but continued while pressure and temperature were further decreasing, thus supporting the assumption of crustal uplift during this time. In the northeast, shearing took place under very low metamorphic or near-surface conditions, suggesting a rather high crustal level for this area.

Contemporaneously with and possibly initiated by, crustal uplift, the northeast-southwest trending line of alkaline to peralkaline intrusives of the Richtersveld Igneous Complex (RIC) was emplaced in the southeastern Richtersveld. While its early members in the northeast (~900 my) are deformed by Devilscastle-type shearing, its youngest members in the southwest (~700 my) are undeformed.

The mafic north-south trending dykes of the Gannakouriep Suite are partly intrusive into the lower parts of the Stinkfontein Formation. Structurally, their emplacement must be related to east-west extension preceding the Pan-African deformation.

Comparison of the Richtersveld with the surrounding Namaqua Metamorphic Complex leads to the conclusion that the transition between them is continuous and that both have gone through essentially the same tectonothermal history. Differences in style and degree of apparent deformation as well as of metamorphic grade can be accounted for by different crustal levels. Rock assemblage, geochemistry and metamorphic facies series suggest that the Richtersveld originated as part of an Andean-type continental margin.

TABLE OF CONTENTS

ABBREVIATIONS

ab	albite
and	andalusite
ap	apatite
bi	biotite
carb	carbonate
cc	calcite
chl	chlorite
chtd	chloritoid
ep	epidote
gar	garnet
gros	grossular
hbl	hornblende
kao	kaolinite
kf	K-feldspar, potassic feldspar
ky	kyanite
mu	muscovite
ol	oligoclase
plg	plagioclase
pr	prehnite
qtz	quartz
rt	rutile
ser	sericite
sill	sillimanite
sph	sphene
zi	zircon
zo	zoisite

VIS	Vioolsdrif Intrusive Suite
RIC	Richtersveld Igneous Complex
HMC	Helskloof Migmatitic Complex
PGU	Pink-gneiss Unit
BMC	Blockwerf Migmatitic Complex
NMC	Namaqua Metamorphic Complex

$\bar{x}$	arithmetic mean
s	standard deviation
n	number of samples per population

DEFINITIONS

Richtersveld Province : this term refers in a general way to the area along the Orange River in which volcanics of the Orange River Group and of the VIS are exposed. It does not include definitions in terms of a tectonic province etc., since this is subject to this investigation. The usefulness of the term Richtersveld Province will be discussed in a later chapter.

Eastern Richtersveld : area east of the line Sendelingsdrif-Eksteenfontein

Northeastern Richtersveld : area investigated north of the northernmost occurrence of the RIC.

Southeastern Richtersveld : area investigated south of the northernmost occurrence of the RIC

Namaqua Metamorphic Complex : this term is used irrespective of previous definitions to denote predominantly high grade metamorphic rocks to the south, east and north of the Richtersveld Province. It may be used synonymously with Kröner and Blignault's (1977) *Namaqua Province*.

The textural nomenclature suggested by Moore (1970), is used to describe all those textures that show low degrees of preferred orientation.

Terms referring to metamorphic grade and the Al-silicate boundaries are used after Winkler (1974) unless stated otherwise.

The term *metamorphic facies series* refers to pressure characteristics and is either used *sensu* Miyashiro (1973) or Sassi and Scolari (1974).

The term *sericite* is used in a textural sense only and denotes white mica smaller than approximately 0,02 mm.

An alphabetical list of frequently used geographical names and their coordinates is included in the Appendix.

Chapter 1

1. INTRODUCTION

1.1. GENERAL

The area on which this investigation is based forms the eastern part of a region known as the Richtersveld (Fig. 1.1.). It is roughly divided in half by the inaccessible mountain chain of the Rosyntjieberge. The Richtersveld north of this chain is accessible only from the west through Helskloof Pass, while the southeastern Richtersveld can more easily be reached from the surrounding areas.

The area investigated comprises approximately 3500 km^2 desert mountainland the relief of which ranges from 1400 m (Vandersterrberg) to 100 m (Orange River) and is, apart from the region around Eksteenfontein, not permanently inhabited.

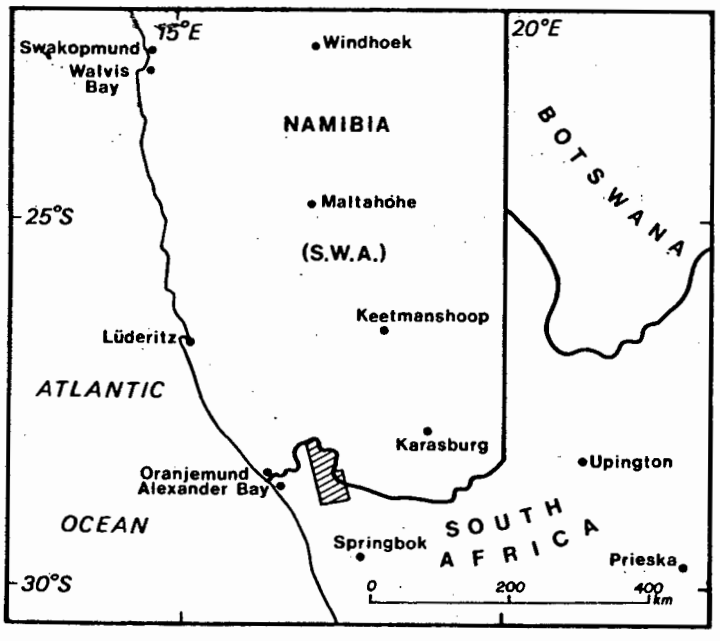

Fig. 1.1.

Regional setting of the area investigated

1.2. PREVIOUS WORK

Apart from reports by various prospectors traversing the Richtersveld in search of ore deposits since the early 19th Century, little geological research has been carried out in the Richtersveld. Rogers (1915) was the first to describe aspects of the geology between Vioolsdrif and Sendelingsdrif. The first comprehensive report on the geology of the Richtersveld, carried out by de Villiers and Söhnge between 1943 and 1945 was published in 1959 and provided the basic framework for further, more detailed studies like the present one. Taking into account different "philosophies" particularly on the origin of granitic rocks during the time of De Villiers and Söhnge's investigation (e.g. the concept of metasomatic granitisation), increased knowledge of the adjacent Namaqua Metamorphic Complex during the last few years and progress in modern igneous petrology, it is only natural that the conclusions now reached differ from theirs.

The geology between Sendelingsdrif and Witputs north of the Richtersveld proper was investigated by McMillan (1968). From this work it appears that the metavolcanics of the Richtersveld extend some tens of kilometres to the north where they are altered by increasing grade of metamorphism. Blignault (1977) investigated the area around Haib and at the Lower Fish River and Reid (1977) dealt with geochemical and isotopic aspects of the intrusives and volcanics of the Haib area. In the southeastern Richtersveld a detailed study of parts of the Richtersveld Igneous Complex and igneous rocks of the basement was carried out by Middlemost (1963). Köstlin (1971), Alsopp *et al.*, (1978) and Welke *et al.*, (1978) undertook radiometric dating of rocks of the Richtersveld Igneous Complex as well as of parts of the basement and overlying rocks. The area south of the Richtersveld was mapped by Joubert (1971) and the overlying Gariep Group was re-investigated by Kröner (1974).

1.3. OBJECTIVES OF THIS INVESTIGATION

The Richtersveld Province as defined by Kröner and Blignault (1977) differs lithologically, geochronologically in apparent degree of deformation and in apparent grade of metamorphism from the gneisses of the Namaqua Metamorphic Complex by which it is surrounded in the south, east and north. In the west it is unconformably overlain by the Late Precambrian Gariep Group, which led various authors to suggest an influence of Pan-African tectonothermal events on the Richtersveld basement (e.g. Kröner, 1974, Blignault, 1974b; Kröner and Blignault, 1977). Apart from the geology of the Richtersveld proper the present investigation therefore had to elucidate these relationships and in particular to answer the following questions:

a) what are the stratigraphic relationships between Richtersveld and

Namaqua Metamorphic Complex, i.e. what is the basement of the Richtersveld volcanics?

b) what are the metamorphic relationships : is the Richtersveld a homogeneously low grade metamorphic domain or does it display variable grades of metamorphism? Is the metamorphic facies series similar to or different from that of the Namaqua Metamorphic Complex?

c) has the Richtersveld been affected by the same structural events that affected the Namaqua Metamorphic Complex, i.e. is it the low strain subdomain suggested by Blignault (1977) or does it show the same degree of deformation?

d) to what extent did Gariep metamorphism and deformation influence the basement?

e) what deductions can be made as to the depositional and metamorphic ages of the Gariep rocks?

1.4. METHODS OF STUDY

The area was mapped between June 1975 and September 1977 by using air photographs (1:36000) and for parts of the area colour photographs on a scale of 1:10000. The data thus collected were later transferred on topographical sheets (1:50000) from which the final map 1:100 000 was prepared. The rather difficult topographic conditions of the eastern Richtersveld entailed a relatively variable density of observation points, which could be easily overcome, however, by the excellent outcrop conditions.

Two relatively new methods were used during the present project:

1) investigations of granitic textures based on the concept of grain transition probabilities

2) investigation of relative pressures during metamorphism in low grade pelitic rocks based on the determination of b_o-spacings of white micas

Both methods are, owing to their relative novelty, explained in the Appendix.

1.5. ACKNOWLEDGEMENTS

This project was initiated and initially supervised by A. Kröner. After his departure the supervision was taken over by P. Joubert. The project was funded by the Geological Survey of S.A. and during the first year also sponsored by a joint grant from DAAD (German Academic Exchange Service)

and the Department of National Education.

I am furthermore indebted to Messrs. South African Selection Trust, Messina Transvaal Exploration and Phelps Dodge who provided additional aerial photographs for selected areas as well as camp facilities, and to R. and H. Benecke for their hospitality at their camp at the Orange River. Chris Hartnady, A.C. Moore, A.R. Newton and D.J. Waters read parts and P. Joubert the complete manuscript and offered valuable advice. Thanks are finally due to Judy Elliott who typed the final manuscript and Pam Eloff for her outstanding work in drawing maps and figures.

Chapter 2

LITHOLOGY AND STRATIGRAPHY OF THE SUPRACRUSTAL ROCKS OF THE NORTHEASTERN RICHTERSVELD

2.1. METAVOLCANICS

2.1.1. Introduction

The metavolcanics of the northeastern Richtersveld are part of a belt of mainly calc-alkaline extrusive rocks extending from the Richtersveld to the Haib - Vioolsdrif area where they have been mapped by Blignault (1977) and petrographically and geochemically investigated by Reid (1977). Reid (1978a) suggested a mantle derived magma source for them and determined radiometric ages around 1950 my for their extrusion.

The present investigation was conducted with the aim of:

a) subdividing the supracrustal rocks of the Richtersveld into formations

b) establishing stratigraphic relationships with the Haib area, and

c) defining the depositional environment of the supracrustal rocks involved.

More than 90 percent of the supracrustal rocks of the eastern Richtersveld consist of acid and intermediate metavolcanics but only those of the central northeastern Richtersveld have retained some of their original volcanic textures, while those of the southeastern and northernmost Richtersveld are completely reconstituted and are consequently dealt with in the chapter on metamorphism.

The volcanics of the central northeastern Richtersveld are exposed in two regions

a) between the Nabasberge and the Pokkiespramberge in the northeast, and

b) underlying the Rosyntjieberg quartzites between Aussenkehr and Kodaspiek in the southwest.

These regions are nowhere in contact with each other and therefore age relationships are difficult to establish. Unequivocal facing criteria, however, suggest that both regions form the limbs of a regional anticline, in the following referred to as the Richtersveld anticline, into the core of which syn- and posttectonic rocks of the VIS were emplaced during and subsequent to its formation.

Table 2.1. Major element chemistry of some metavolcanics of the northeastern Richtersveld

	1	2	3	4	5	6	7	8	9	10	11	12
	159	161/3	182/3	59/1	A4	165	145/1	138/13	163	23	24	123
SiO_2	62,52	62,32	75,33	68,33	66,39	63,97	71,01	61,68	61,87	67,16	63,49	67,71
TiO_2	0,59	0,68	0,18	0,37	0,43	0,55	0,33	0,63	0,58	0,44	0,61	0,44
Al_2O_3	16,43	16,85	13,05	16,80	16,66	16,37	15,03	15,35	16,38	16,51	16,62	16,72
FeO*	5,78	6,21	0,98	2,00	2,48	5,21	1,40	5,90	5,00	2,71	4,86	2,47
MnO	0,20	0,18	0,08	0,06	0,06	0,15	0,05	0,14	0,11	0,14	0,12	0,09
MgO	3,44	3,12	0,37	0,29	0,79	2,29	0,42	2,17	2,06	0,93	1,80	0,85
CaO	2,11	3,71	0,43	2,13	3,20	2,55	1,25	5,39	3,62	3,37	4,38	2,82
Na_2O	1,58	0,65	3,03	3,62	2,62	3,98	3,87	2,40	3,17	3,05	2,45	3,70
K_2O	5,06	2,90	5,66	5,68	5,44	3,56	5,39	3,61	3,41	4,51	3,73	4,02
P_2O_5	0,16	0,13	0,03	0,07	0,13	0,15	0,07	0,16	0,16	0,12	0,18	0,12
LOI	2,36	3,26	1,08	0,97	1,99	1,42	1,49	2,86	4,18	1,41	2,13	1,30
Total	100,23	100,05	100,21	100,33	100,19	100,19	100,30	100,30	100,52	100,35	100,38	100,23
DI	66	56	94	84	77	71	90	60	66	75	64	75

1) Melanocratic lava, lower Abikwarivier Formation; Xenolith within Vioolsdrif Intrusive Suite granodiorite
2) Melanocratic lava, lower Abikwarivier Formation; 1 km southwest Tatasberg
3) Leucocratic welded tuff, Abikwarivier Formation, Pokkiespramberge
4) Mesocratic volcanic, Abikwarivier Formation, 1 km north of Springbokkloof
5) Mesocratic tuff, upper Abikwarivier Formation, 2 km northwest of Tatasberg
6) Melanocratic, aphanitic volcanic, Klipneus Formation, 1,5 km east of Kwaggarug
7) Leucocratic rhyolite with flow banding, Klipneus Formation, 1 km east of Kwaggarug
8) Melanocratic lava, Kuamsrivier Formation, Kuamsrivier profile
9) Mesocratic tuff or volcanic greywacke, Paradysrivier Formation, underlying Rosyntjieberg quartzite, Paradyskloof
10) Quartz-feldspar porphyry, Kookrivier Formation, foot of Rooiberg
11) Quartz-feldspar porphyry, Kookrivier Formation, Kookrivier
12) Quartz-feldspar porphyry, Kookrivier Formation, Kookrivier

Analyst : D. Reid, Geochemistry Department, University of Cape Town

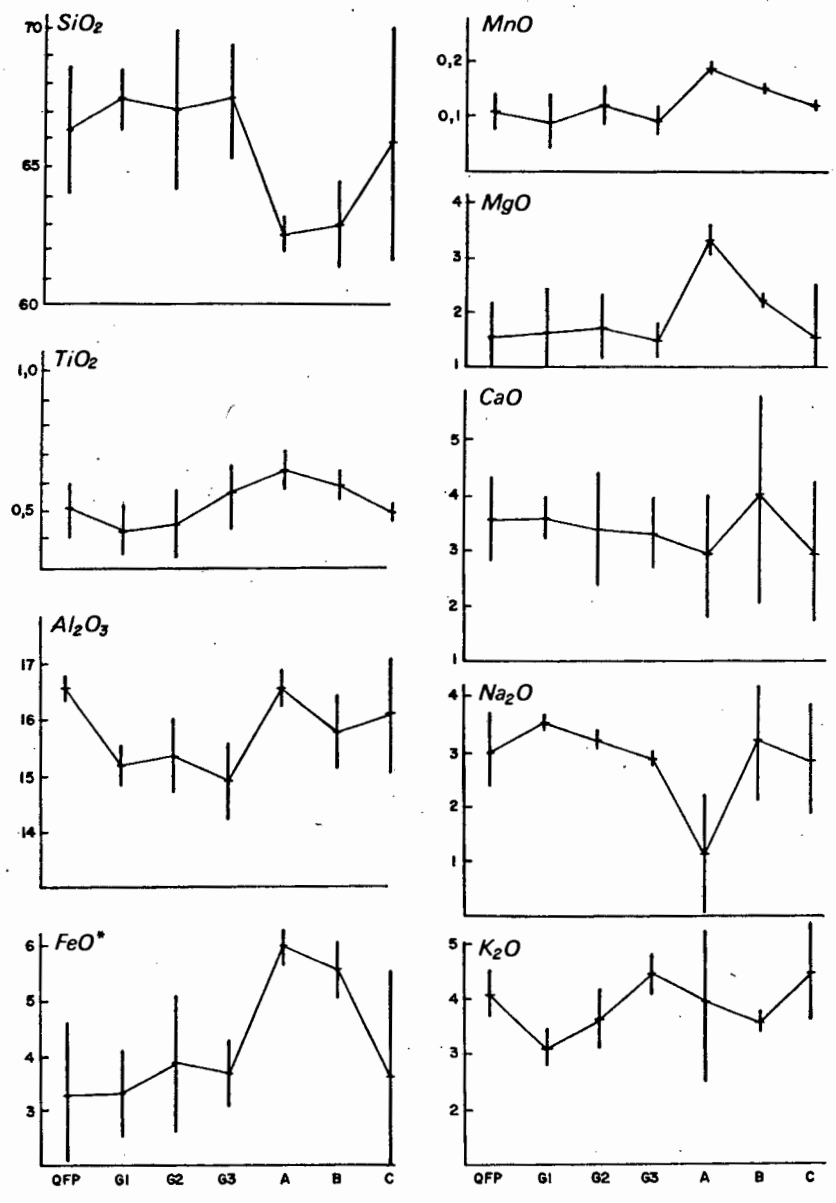

Fig. 2.1 Diagram comparing major element analyses of different groups of volcanic and intrusive rocks of the northeastern Richtersveld. There appears to be a relatively good agreement between the quartz-feldspar porphyry of the Kookrivier Formation and G_1 of the Vioolsdrif Intrusive Suite (apart from K_2O and Al_2O_3) providing further support for field evidence that the latter is a subvolcanic equivalent of the quartz-feldspar porphyry.

QFP : quartz-feldspar porphyry, Kookrivier Formation, n=3
G_1 : fine-grained granodiorite n=2
G_2 : even-grained granodiorite n=3
G_3 : granite n=4

A : melanocratic volcanics, lower Abiekwarivier Formation, n=2
B : melanocratic volcanics, Kuamsrivier and Klipneus Formation n=2
C : leuco- and meso-cratic volcanics, Abiekwarivier Formation, n=3

vertical line : standard deviation

2.1.2. Composition

The extremely weak compositional differences among the volcanics can only be established by chemical analysis. In Table 2.1 a selection of samples that are likely to comprise the compositional extremes is listed. It is apparent from these data that compositional mapping, either in the field or by means of thin section, is virtually impossible.

2.1.3. Textural classification

Because of the difficulty in recognising compositional differences, particular emphasis had to be laid on distinguishing features based on textural differences and an artificial classification scheme had been devised that is nevertheless thought to reflect some original features of lavas, tuffs and welded tuffs. It is complemented by the descriptive prefixes leuco, meso and melanocratic.

a) *Welded tuffs*

If pumice fragments, glass shards and rock fragments contained in a highly mobile matrix of ash particles and volcanic gases undergo compaction, welding and flattening will result, giving rise to the characteristic "fiamme" structures (eutaxitic structures) of welded tuffs. This process is essentially a tectonic one of pure shear (Roberts and Siddans, 1971) and consequently features similar to true tectonism will arise (Higgins, 1971).

That textures such as those shown in Figs. 2.2, 2.3 and 2.4 are the result of processes during deposition of a highly mobile gas-ash-suspension and not due to tectonic activities, can be deduced from the different state of material properties during these processes:

Features such as pressure shadows are mainly due to differences in ductility between groundmass and phenocrysts (Spry, 1969, p.240). In pelitic rocks the mica-rich parts are more ductile (less competent) than the porphyroblasts or phenocrysts (e.g. quartz, feldspar). The same relationship exists in ashflows before solidification, where the groundmass consists of a highly mobile suspension of rock particles, while the suspended phenocrysts and rock fragments are already solid. This relationship, however, does not exist in volcanic rocks during metamorphism. Since both groundmass and phenocrysts consist basically of the same crystalline material, there is no difference in ductility between them and thus textures such as shown in Fig. 2.2 and 2.4 can form only during the volcanic stage.

Mylonites or blastomylonites, which these textures may also typify, are likely to have strongly deformed phenocrysts (porphyroblasts), angular in incipient stages and increasingly more rounded in later stages, wrapped in a mortar-textured matrix. Euhedral phenocrysts piercing through the foliation cannot be imagined in mylonites (Higgins, 1971).

b) *Non-welded tuffs*

Rock fragments, glass shards and pumice fragments of variable size and composition are also the main constituents of non-welded tuffs. They will, during lithification, devitrification and metamorphism recrystallise in slightly different ways into sub-textures of different composition and grain size, giving rise to rather inhomogeneous textures in thin section or in hand specimen.

Inhomogeneous and isotropic textures are therefore classified as non-welded tuff, which may include ash-fall tuff and non-welded ashflow tuff.

c) *Lava and fine-grained non-welded tuff*

Lavas will consist of a fairly homogeneous groundmass with relatively well-preserved phenocrysts. If a rock of this kind has in addition a massive field appearance, it can be regarded as lava or fine-grained tuff with some justification.

d) *Additional criteria*

In addition to textural parameters, the following simple scheme has been applied:

leucocratic : light grey to nearly white
mesocratic : grey to dark grey
melanocratic : greenish grey to dark greenish grey on fresh surfaces.

2.1.4. Texture and mineralogy

a) *Introduction*

The textural classification devised for the metavolcanics is based on isotropy and homogeneity of texture. Naturally all transitions between the extremes are encountered and in many cases a clearcut classification is difficult. In the following therefore, mainly those textures are presented that are, so to say, end members of one of these extremes and show the characteristic features particularly well.

b) *Volcanics with strongly anisotropic textures* (Figs. 2.2, 2.3, 2.4)

Field appearance

Volcanics of this type can only be recognised in the field if flattened rock fragments or mineral aggregates are visible to the naked eye. In this case they also appear to be slightly foliated. Rare eutaxitic textures in the

cm range have also been recognised. Rocks of this type are mostly leucocratic and occur exclusively in the Abiekwarivier and Paradysrivier Formations.

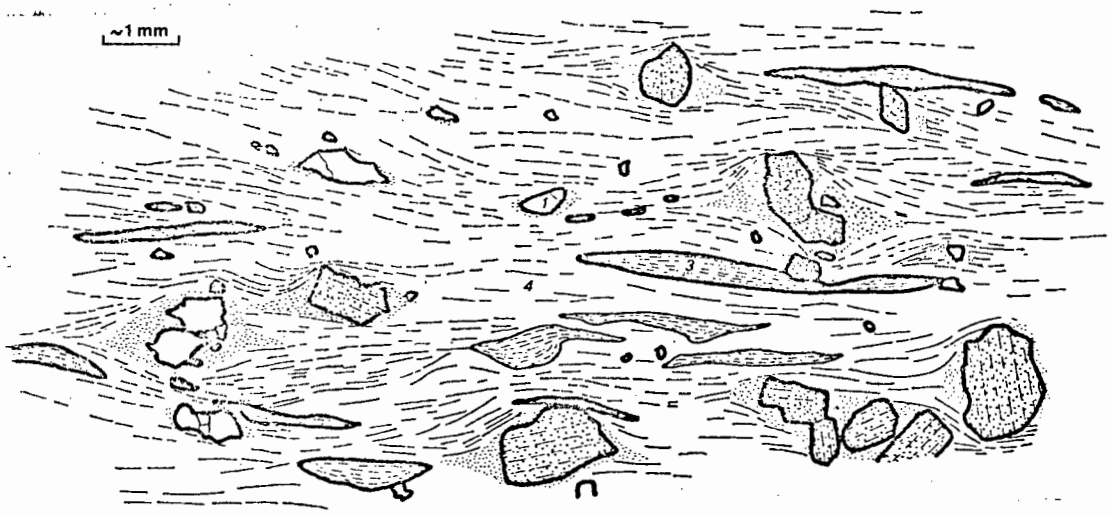

Fig. 2.2 Strongly anisotropic volcanic texture interpreted as welded tuff. (1) quartz (2) plagioclase, partly euhedral (3) flattened aggregates (outlines exagerated) (4) matrix with variable texture and mineral content.
Dashed lines represent "foliation" imparted on the rock during flattening. Note the pressure shadows around phenocrysts. (55/2)

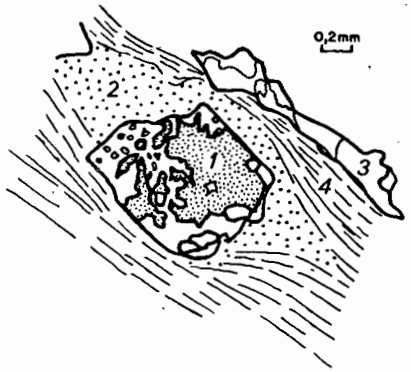

Fig. 2.3 Detailed view of the relationship between phenocrysts and "foliation".
(1) antiperthite (2) pressure shadow
(3) flattened quartz aggregates (4) sericite-quartz aggregates. (55/2)

Phenocrysts

Plagioclase is often euhedral and mostly weakly, but occasionally also strongly altered.* In some cases a strongly altered core and a non or weakly altered margin appear to reflect an original normal zonation.

Quartz is mostly anhedral, frequently with angular, irregular boundaries. Euhedral crystals, sometimes slightly rounded and embayed, occur occasionally.

K-feldspar is euhedral and exclusively present as microcline. Perthitic and antiperthitic patchy exsolutions are common.

Groundmass

The groundmass is highly anisotropic and made up of subtextures of variable composition, which is mainly reflected by variable proportions of sericite and quartz. The grain size is generally smaller than 0,01mm.

Sericite and sericitic subtextures impart a distinct foliation to the rock. This foliation does not, however, cut or otherwise affect the phenocrysts, but is either wrapped around or truncated by them.

Sericite has been observed to be less distinctly or not orientated at all in the vicinity of phenocrysts and this must be interpreted as shielding effect of the adjacent phenocrysts. According to Hobbs *et al.* (1976, p.281) pressure shadows "are generally believed to develop in parts of the rock where the mean stress is low due to a shielding effect of the host grain, which is a relatively rigid body within the deforming matrix." Spry (1969, p.240) defined a pressure shadow as an "approximately ellipsoidal region adjacent to a central rigid crystal; the texture within the shadow differs from that of the host rock and the foliation wraps around the crystal plus its shadow." He attributed the formation of pressure shadows to differential compaction of the matrix in sediments adjacent to rigid bodies, to flow in porphyritic igneous rocks and to various kinds of deformation in metamorphic rocks.

Ash-flow tuffs, consisting of a highly ductile groundmass and relatively rigid phenocrysts and rock fragments, therefore seem to be the ideal material for the formation of pressure shadows during compaction and by

---

* Definition of plagioclase alteration:
Secondary alteration products are common in plagioclase and consist of epidote and sericite in variable proportions. The degree of alteration of plagioclase is defined by the amount of feldspar that is still recognisable.
Weakly altered : only few grains of epidote or sericite are developed. An-content can be determined by optical means (1000x).
Moderately altered : dense alteration products. An-content can only sometimes be determined optically.
Strongly altered : crystal completely altered. No optical determination of An-content possible.

differential flow. In the present case, however, compaction seems to be the most likely mode of formation, as features such as the "piercing through" of the foliation by phenocrysts with their long axis can best be explained by mere compaction, while differential flow would have led to orientation of the phenocrysts parallel to the foliation.

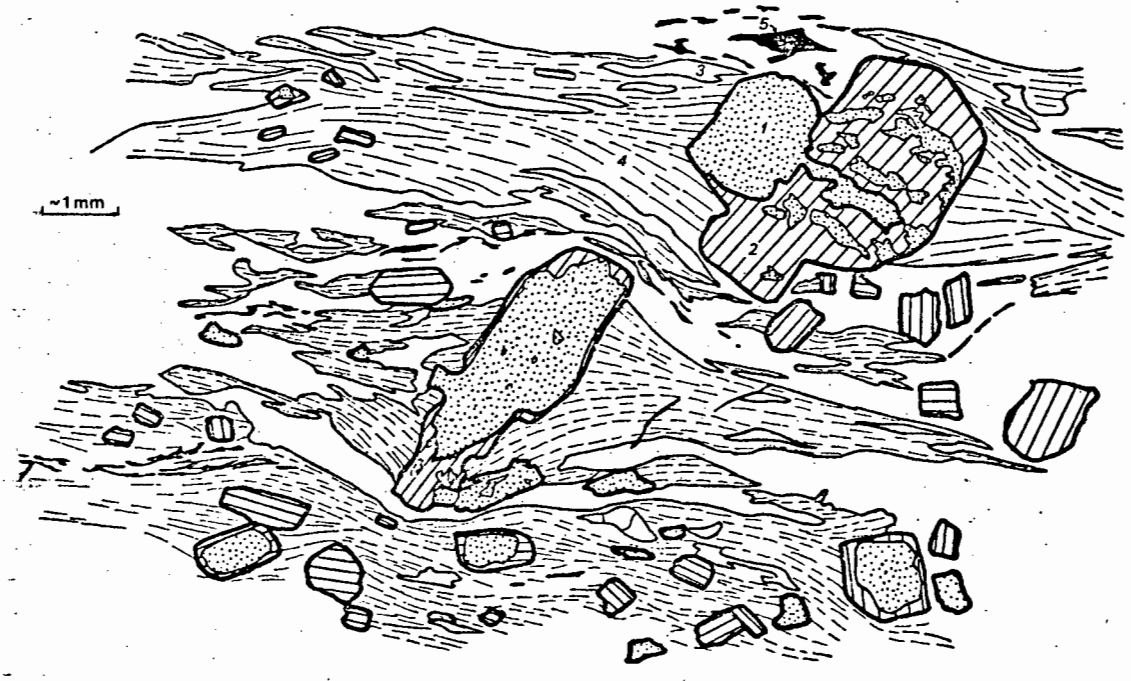

Fig. 2.4 Particularly well-developed eutaxitic texture. (1) altered plagioclase (2) fresh plagioclase (3) flattened quartz-rich subtexture (4) flattened mica-rich subtexture (5) opaque minerals. Note the divergent attitude of the "foliation" in the vicinity of phenocrysts caused by the shielding effect of phenocrysts during flattening. In contrast to tectonic foliation the foliation caused by welding does not wrap around the phenocrysts but is cut by them. (85/2).

c) *Volcanics with intermediate textural properties*

Field appearance

Rocks of this type are mesocratic to leucocratic and display a moderate to weak schistosity. In a fresh handspecimen quartz, greenish feldspar (plagioclase) and pink K-feldspar can be recognised in an aphanitic groundmass, while weathered surfaces allow only the recognition of plagioclase phenocrysts. Occasional narrow veins of epidote occur parallel to the foliation.

Volcanics of this type occur mainly in the Abiekwarivier Formation and are interpreted as moderately welded or ash-fall tuffs.

Phenocrysts

Plagioclase is weakly to moderately altered and sub- to euhedral. In one sample (55/5) phenocrysts of plagioclase enclose an earlier generation of plagioclase phenocrysts.

K-feldspar is invariably microcline and euhedral to anhedral. Patchy perthitic and antiperthitic exsolutions are common and in one sample examined (2/1) K-feldspar is clouded by tiny opaque minerals, possibly iron exsolutions.

Quartz is generally subhedral to euhedral, although euhedral outlines are frequently slightly rounded. Equigranular polygonal aggregates of quartz may either be parts of rock fragments or recrystallised anhedral phenocrysts.

Mafic phenocrysts : Phenocrysts of this kind occur in a few samples (2/1) and appear as aggregates with prismatic outlines, filled mainly by very fine-grained epidote and some albite. Their origin is unknown, but a formation after mafic minerals such as pyroxene or amphibole can be imagined.

Ore : Subhedral to euhedral ore (magnetite) is found in some samples and occurs within the groundmass and plagioclase phenocrysts. Its size ranges from 0,1-0,3 mm.

Groundmass

The groundmass is slightly to moderately heterogeneous, weakly to moderately anisotropic and consists of variable amounts of plagioclase, quartz, K-feldspar, epidote and sericite. The size of individual grains is approximately 0,01-0,02 mm, but some samples have a wider grain-size range between 0,02 and 0,1 mm.

d) *Volcanics with isotropic textures* (Figs. 2.5, 2.6, 2.7, 2.8)

(i) Mesocratic and leucocratic volcanics

Quartz-feldspar porphyry of the Kookrivier Formation (Fig. 2.5)

Field appearance

This rock is immediately recognisable in the field by its massive appearance. It makes up the whole of the Kookrivier Formation and must be interpreted as intermediate to acid lava. Weathered surfaces are white-grey and show phenocrysts of quartz and feldspar particularly well.

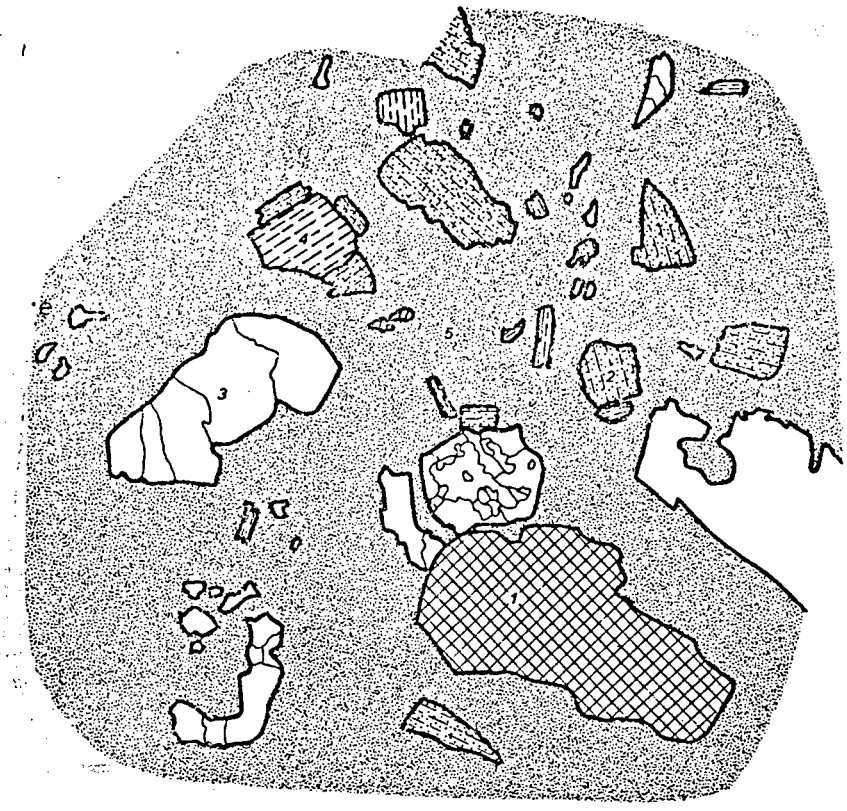

Fig. 2.5 Quartz-feldspar porphyry of the Kookrivier Formation. (1) microcline (2)plagioclase (3)quartz (4)pseudomorphs of biotite and chlorite after mafic mineral (5) groundmass. Note the strongly corroded quartz phenocrysts.

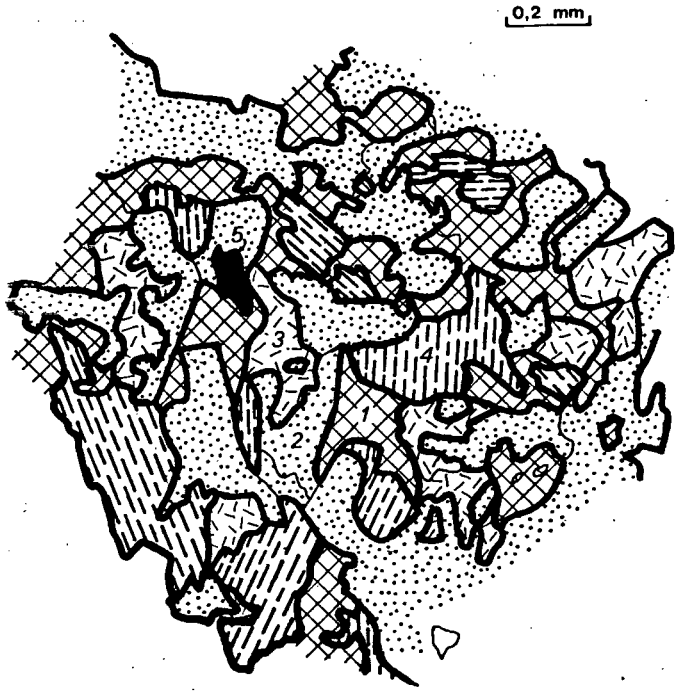

Fig. 2.6 Texture of melanocratic, non-porphyritic volcanic, Lower Abiekwarivier Formation. (1)alkalifeldspar and quartz (2) epidote (3) sericite aggregates (4)biotite (5)opaque mineral (55/6)

Phenocrysts

Plagioclase forms the most abundant phenocryst; it occurs as subhedral to anhedral crystals and is moderately to strongly altered.

Quartz is found in rounded subhedral to anhedral phenocrysts, which are often corroded and show embayments containing inclusions of the groundmass. Quartz phenocrysts are sometimes recrystallised into subgrains.

K-feldspar occurs as subhedral to anhedral microcline and is present only in subordinate amounts.

Mafic phenocrysts : Occasional aggregates with euhedral outlines of coarse epidote and green chlorite may be pseudomorphs after mafic phenocrysts.

Groundmass

The groundmass is rather homogeneous and consists of feldspar-quartz, epidote and sericite with a grain size of approximately 0,01-0,03 mm.

Other leucocratic volcanics (Figs. 2.7, 2.8)

Field appearance

Apart from the Kookrivier Formation leucocratic volcanics which can be interpreted as lavas occur mainly in the lower Abiekwarivier Formation where they are found as intercalations of only few metres thickness in a rapidly changing succession of various volcanics and metasediments.

They are leucocratic, massive and frequently display a slightly pink tinge.

Phenocrysts

Plagioclase is euhedral to subhedral and moderately altered. The cores are sometimes more strongly altered than the margins suggesting normal zonation.

K-feldspar is rare and occurs as subhedral microcline with perthitic exsolutions.

Quartz is mostly anhedral, but occasionally euhedral to subhedral phenocrysts may also be encountered.

Biotite occurs as subhedral flakes and is most likely of primary origin.

Groundmass

The groundmass is very homogeneous and consists of quartz, K-feldspar and slightly altered plagioclase with a grain size of up to 0,2 mm.

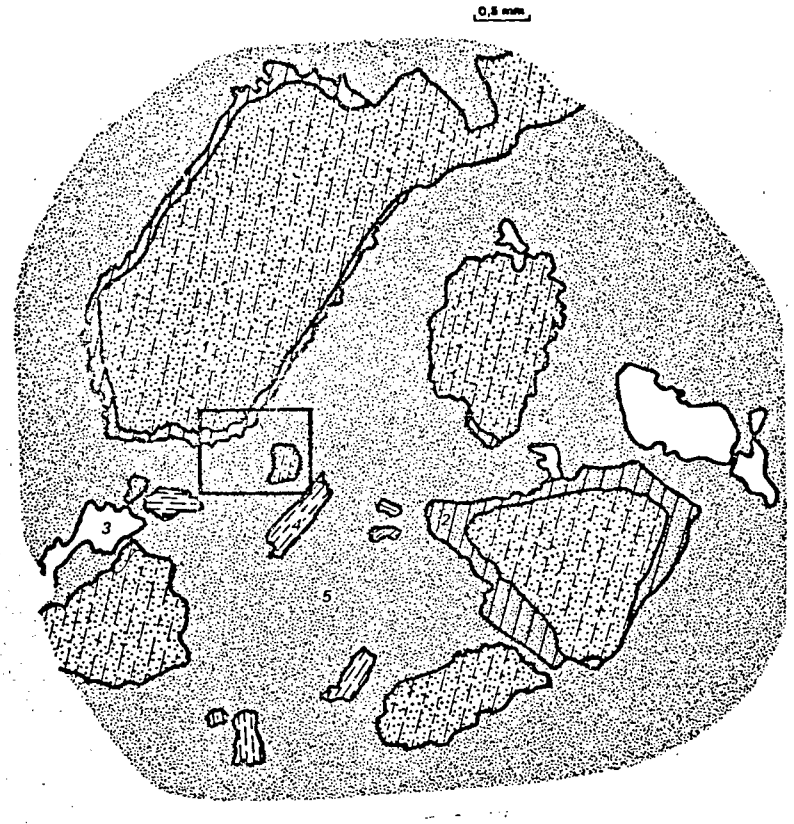

Fig. 2.7 Porphyritic leucocratic lava, Lower Abiekwarivier Formation. (1)moderately altered plagioclase (2)slightly altered plagioclase (3)quartz (4)biotite (5)groundmass. Except for moderate reconstitution of plagioclase by epidote and sericite the original volcanic texture is preserved. (31/2a).

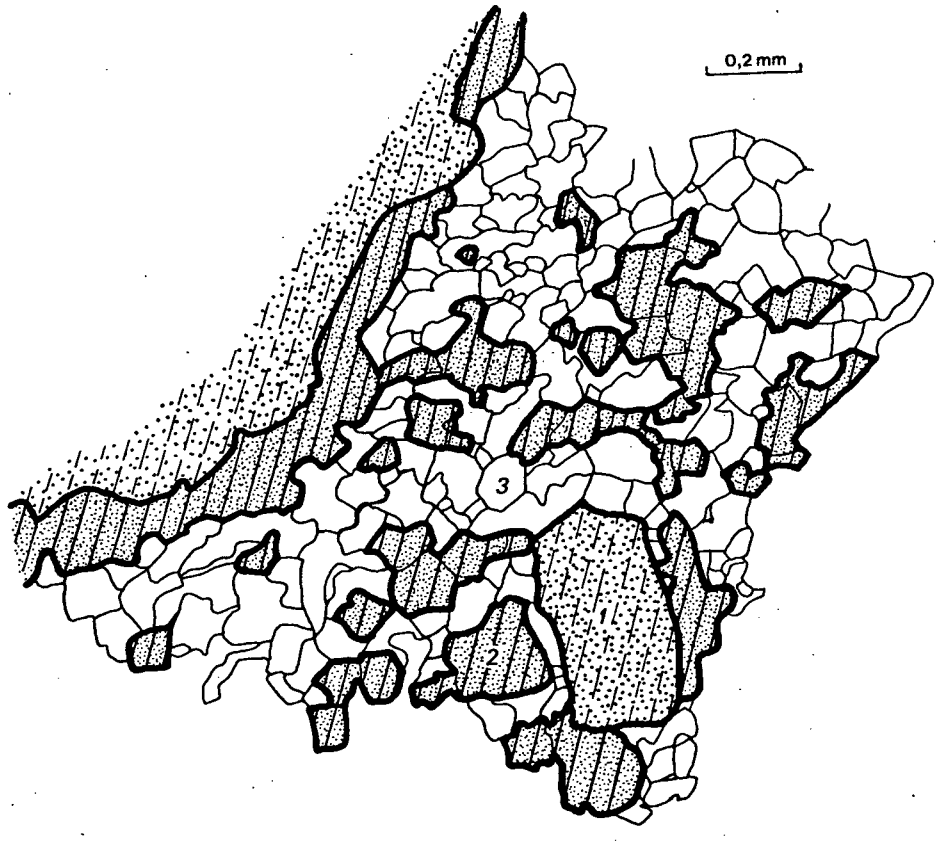

Fig. 2.8 Section of Fig. 2.7 showing textural relations within the groundmass. (1)moderately altered plagioclase (2)slightly altered plagioclase (3) quartz, K-feldspar. (31/2a)

(ii) Melanocratic volcanics

Compared with the leucocratic to mesocratic volcanics, melanocratic volcanics are texturally rather uniform and anisotropic features are completely absent. As a rule their primary minerals are strongly reconstituted by secondary epidote, biotite and chlorite and therefore no attempt has been made to illustrate their textural relationships.

Two types can be distinguished:

(1) Porphyritic lavas (mainly Kuamsrivier Formation)

Field appearance

In the field they are dark grey, often nearly black and massive. They are holocrystalline, but very fine grained and in the typical case, display euhedral plagioclase phenocrysts with a greenish tinge caused by alteration to epidote. Plagioclase phenocrysts sometimes also have irregular and indistinct boundaries and the rock then assumes a slightly flecky texture. In some specimens quartz is visible to the naked eye.

Phenocrysts

Plagioclase is mostly euhedral, moderately to strongly altered and is recrystallised into subgrains. This feature occurs particularly when approaching the higher metamorphic rocks of the Blockwerf Migmatitic Complex. Despite reconstitution and recrystallisation the original plagioclase phenocryst can still be recognised (Fig.6.16b).

Groundmass

The groundmass is granoblastic equigranular polygonal, homogeneous to slightly heterogeneous, anisotropic and consists of plagioclase, epidote, biotite and minor amounts of alkali feldspar and quartz. Biotite occurs interstitially and has a maximum length of 0,2-0,3 mm, while the average grain size of other minerals in the groundmass is approximately 0,1 mm.

(2) Vesicular lavas (mainly Klipneus Formation)

Field appearance

Vesicular lavas are massive and characterised by their brown to light-brown tinge on weathered surfaces and greenish grey to dark greenish-grey colour on freshly fractured surfaces. Vesicles are abundant and form holes and cavities on weathered surfaces.

Phenocrysts

Plagioclase is strongly altered and subhedral to euhedral. Mafic phenocrysts : epidote, chlorite, biotite, carbonate and feldspar occur in aggregates occasionally with hexagonal outlines, which suggests that they

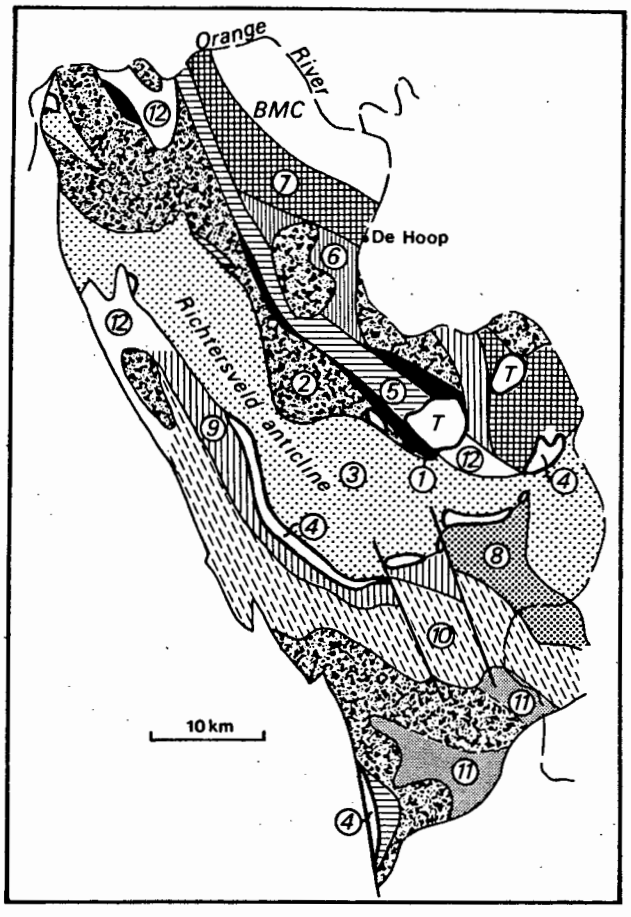

Fig. 2.9 Key map of the northeastern Richtersveld

Map units:
1) fine-grained granodiorite (G_1)
2) even-grained granodiorite (G_2)
3) granitic (G_3)
4) leucogranite (G_4)
5) Abiekwarivier F. (V_1)
6) Kookrivier F. (V_2)
7) Kuamsrivier F. (V_3)
8) Klipneus F. (V_4)
9) Paradysrivier F. (V_5)
10) Rosyntjieberg F. (R)
11) Windvlakte F. (northern part)
12) Volcanics, undifferentiated

may have formed after amphibole.

Groundmass

Individual primary minerals are not recognisable in the groundmass. Instead, complete reconstitution has taken place into tiny secondary minerals, mainly epidote (<0,01 mm).

2.1.5. Stratigraphic relationships

a) *Introduction*

De Villiers and Söhnge (1959) correlated the supracrustal rocks of the Richtersveld with the Marydale, Kaaien and Wilgenhoutdrift "Series" of the Kheis "System", but since this correlation has never been satisfactorily established, an independent nomenclature has subsequently been proposed (Kröner and Blignault, 1977; Blignault, 1974a) which subdivides the volcanics of the Richtersveld Province (*Orange River Group*) into the *Haib Subgroup* (Haib area) and the *De Hoop Subgroup* (Richtersveld and Lower Fish River) and the Haib Subgroup again into the *Nous* and *Tsams Formations* (Blignault, 1977).

For this reason an attempt has been made in the following to distinguish formations within the volcanics of the De Hoop Subgroup on the basis of criteria of lithology and depositional facies.

b) *Abiekwarivier Formation (map unit V_1)*

Leucocratic volcanics, particularly welded tuffs, dominate this formation, but subordinate amounts of melanocratic tuffs and lavas are intercalated. The lower Abiekwarivier Formation is characterised by a rapidly changing vertical succession of different volcanics and a lateral variation from volcanics and re-deposited volcanics to metasediments. Even some phyllitic intercalations are found in the area around the Peilkop, indicating reworking of the volcanic material or of preRichtersveld basement. The upper Abiekwarivier Formation is exclusively made up of leucocratic volcanics volcanics, mainly welded tuffs.

The Abiekwarivier Formation can be followed for more than 40 km from the Tatasberg to the northern bend of the Orange River and seems to continue for some tens of kilometres into South West Africa (Mc Millan, 1968).

Its lower boundary is not exposed. The upper boundary is made up by the Kuamsrivier Formation in the northwest and by the Kookrivier Formation farther to the southeast. The boundary between upper and lower Abiekwarivier Formation is taken as a thin band of non-porphyritic melanocratic volcanics, which can be followed for more than 20 km.

The maximum thickness of the lower Abiekwarivier Formation is 1,5 km and the upper Abiekwarivier Formation reaches 2-2,5 km in the southeast and 0,8-1 km in the northwest.

The formation is best exposed in the Tatasberg area and in the valley of the Abiekwarivier. Its development there is shown in Annex. 2.

c) *Kookrivier Formation (map unit V_2)*

This formation consists exclusively of quartz-feldspar porphyry and can be followed from northwest of the Kookrivier to the east of the Tatasberg.

It overlies the Abiekwarivier Formation throughout and underlies the Kuamsrivier Formation in the northwest and the southeast. The upper boundary to the east is undefined and not exposed.

Its maximum thickness can be inferred to be approximately 4000 m, but thins and disappears towards the northwest and southeast.

The type locality is the Kookrivier valley at the foot of the Richtersberg where this rock type is particularly well exposed.

d) *Kuamsrivier Formation (map unit V_3)*

The predominant rock type is a porphyritic melanocratic lava. Intercalated are layers of pink quartz porphyry and finely laminated biotite and biotite-muscovite gneisses,* which display cross-bedding and contain conglomerates with well-rounded pebbles. Phyllitic rocks are also found in subordinate amounts.

---

* The term "gneiss" is applied here with reluctance only because other terms such as "schist" are even more inappropriate due to lack of significant foliation.

Its geographic distribution extends from the Kuams River area in the northwest to the area southeast of the Tatasberg.

The Kuamsrivier Formation overlies the Kookrivier and Abiekwarivier Formations disconformably. This disconformity must be regarded as an intra-volcanic disconformity caused by the overlapping of different volcanic sequences. The upper boundary is not exposed. Amphibolites and gneisses of the Blockwerf Migmatitic Complex are, however, likely to represent parts of this formation. An approximate minimum thickness of 1500 m can be inferred from a profile across the Noms River Fold Belt (Fig.5.15).

Type locality and stratotype are found in the valley of the Kuams River. The stratotype is shown in Annex. 2 .

e) *Klipneus Formation (map unit V_4)*

The Klipneus Formation comprises the greatest variety of rock types of all the volcanic formations. It is composed of mesocratic and melanocratic tuffs, melanocratic aphanitic, vesicular lavas with small intercalations of leucocratic lavas and possible ash flow tuffs. Towards the east the amount of sedimentary rocks increases (conglomerates, green cherts). On the farm Aussenkehr dirty quartzites are intercalated in the reworked melanocratic volcanics.

Some of the conglomerates contain pebbles or mesocratic volcanics and one of the samples collected has a coarse porphyritic texture with a coarser groundmass than that of the volcanics, but finer than the Vioolsdrif granodiorite. Rocks of this type have only been found east and north-east of the Tatasberg and are, for reasons outlined later, regarded as subvolcanic transitions between volcanics and the Vioolsdrif intrusives. If this is the case, the area north of Klipneus must already have been subjected to erosion when the Klipneus conglomerates were being deposited. They therefore constitute an important link in the establishment of relative age relations.

The western boundary is arbitrarily drawn at Kwaggarug. In the east the formation is bounded by a post-Karoo fault and abuts against the Rosyntjieberg quartzites at the farm Aussenkehr.

The formation unconformably underlies the Rosyntjieberg Formation. Its lower boundary is not known. Judging from the rock types contained in conglomerates, the formation must be younger than the Abiekwarivier and Kookrivier Formations.

The thickness cannot be established with certainty, but probably exceeds 3000 m.

The formation is typically developed along a profile between Oudannisieprivier and the Rosyntjieberg quartzites. Due to rapid lateral lithological change, by which this formation is largely defined, no

stratotypes or type localities can be established.

Structural setting of the Klipneus Formation

As is evident from mapping (Annexure 1a) the rocks of the Klipneus Formation make up a marked unconformity with the overlying Rosyntjieberg Formation which can only be explained by the assumption of a trough having formed prior to the deposition of the Rosyntjieberg quartzites.

Although other modes of origin are imaginable (e.g. gradual downwarping of the basement) an explanation in terms of a graben-fault system has been preferred here (Annexure 3a) despite the fact that individual faults could not be proved at the present scale of mapping. However, graben structures and block faulting are common in volcanic terrains and it is only surprising that there are no more signs of synvolcanic block faulting in the Richtersveld. In addition, major graben systems are usually made up of numerous closely spaced faults rather than of a few big fractures and may account for the non-recognition of individual faults, together with the lack of lithological contrast and overprinting by subsequent metamorphism and deformation.

f) *Paradysrivier Formation (map unit V_5)*

In the north around the Paradys River the formation is made up of leucocratic lavas, welded and unwelded tuffs similar to the Abiekwarivier Formation. In addition, extensive layers of reworked material are found. About 1 km southeast of Die Koei on the road between Grasdrif and Numees, rocks are exposed that strongly resemble fanglomerates. The grain size and degree of sorting are extremely variable and the thickness of bedding is rather irregular and varies from the dm to the m scale. Some layers contain angular to slightly rounded fragments up to several dm in diameter, while others contain only fragments in the cm scale. Coarse layers show much more turbulent sedimentation than layers containing fine fragments. The rock fragments are invariably leucocratic volcanics. Towards the southeast leucocratic volcanics wedge out and instead the originally overlying mesocratic volcanics, mainly tuffs, make up the whole of the formation.

The formation extends from Kodaspiek in the northwest to the Kwaggarug in the southeast, where the boundary with the Klipneus Formation has been arbitrarily drawn.

2.2. METASEDIMENTS OF THE ROSYNTJIEBERG FORMATION

2.2.1. Lithology and texture of the main rock types

Texture and mineralogy of these rocks is only described here with respect to their general characteristics. Textural and mineralogical features relevant to metamorphism will be discussed and presented in Chapter 6.

a) *Quartzite* (Fig. 2.13)

Quartzite is white to light grey in hand specimen and outcrop. It is well bedded in the dm to m range or unbedded and massive without any sign of layering. Well-layered quartzites tend to display cross-bedding and ripplemarks.

In thin section quartz forms an equigranular polygonal texture with a grain size between 0,1 and 0,2 mm (Fig. 2.13)

Aggregates of very fine sericite of the same size occur interstitially while muscovite flakes up to 0,2 mm long are sometimes slightly bent. Chlorite, euhedral magnetite and interstitial anhedral fine ore dust are present in variable amounts. Tourmaline and zircon are accessory minerals while muscovite-chlorite porphyroblasts have been observed (0,3-0,4 mm) in some of these rocks.

b) *Iron quartzite* (Fig. 2.14)

Quartzites enriched in iron make up only a small part of the succession, but are conspicuous by their dark-grey to black colours. They occur in a continuous band 50 - 100 m in thickness near the base of the formation and can be followed for more than 40 km between the Orange River and Paradyskloof. Minor occurrences are also encountered in other parts of the formation. Owing to their dark colour, their iron content is easily overestimated in hand specimen, but microscopic investigations have shown that even nearly black samples may contain 30 to 40 percent ore only (Fig. 2.14). In one rock a considerable amount of zircon has been seen in magnetite-rich layers.

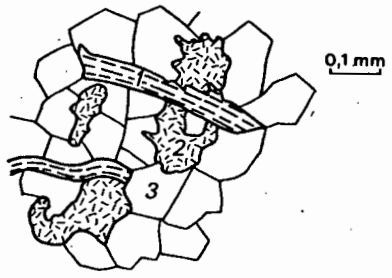

Fig. 2.13 Texture of fine-grained Rosyntjieberg quartzite (1) muscovite (2) sericite (3) quartz

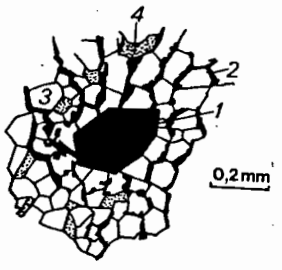

Fig. 2.14 Texture of magnetite quartzite (1) euhedral magnetite (2) interstitial anhedral ore (3) quartz (4) sericite (432/3)

c) *Chloritic quartzites and schists*

Rocks of these types are only distinguishable in the field from melanocratic volcanics if they are associated with distinct layering.

In thin section they reveal a granoblastic polygonal texture of quartz with interstitial flakes and aggregates of chlorite. The former may have preferred orientation and impart a weak foliation on the rock. The chlorite content is variable but frequently reaches or even exceeds the amount of quartz. Muscovite flakes and sericite aggregates are sometimes present in variable amounts. Porphyroblasts of biotite are seen in one thin section while magnetite and interstitial ore dust are invariably present in minor amounts.

d) *Pelitic rocks*

Pelitic rocks make up less than one percent of the Rosyntjieberg Formation. In field appearance they are intermediate between phyllitic and schistose. Muscovite dominates in thin section and imparts a distinct foliation to the rock. Minor amounts of quartz and chlorite are sometimes present as well, while chloritoid and kaolinite are common as accessory mineral in pelites of the northwestern Rosyntjieberg Formation.

2.2.2. Stratigraphic relationships

a) *Type locality and stratotype*

The Rosyntjieberg Formation comprises most of the former Kaaien Series of De Villiers and Söhnge (1959). The reference section for the southeastern part of the formation is the gorge of the Orange River, where the following succession can be established : (from below)

- R1 : well-bedded pure quartzites, minor sericite and chlorite schists and intercalated iron-bearing quartzite and schist
- R2 : well-bedded dark quartzites with intercalated reworked melanocratic and mesocratic volcanics
- R3 : coarse, massive, light grey to white quartzite
- R4 : melanocratic and mesocratic volcanics and reworked volcanics with intercalated thin quartzite bands
- R5 : melanocratic to mesocratic volcanics
- R6 : impure, massive, grey quartzite with well-layered intercalations.

b) *Stratigraphic boundaries*

The Rosyntjieberg Formation overlies all volcanic formations of the northeastern Richtersveld and is, in the Orange River area, overlain by melanocratic volcanics that have been included in the Windvlakte Formation (cf. Chapter 4).

c) *Areal variation and extent*

In contrast to R_1 which extends from the Orange River to the Paradyskloof with only minor interruptions, all other members of the formation can be followed with certainty only from the Orange River to the area around Mt Terror. To the west of Mt Terror the volcanic intercalations of the Orange River profile peter out and instead quartzites and pelitic rocks predominate, but with strongly reduced overall thickness. Even further to the west, in the Tswaies and Omsberge, an upper and a lower quartzite are separated by a thick volcanic succession. The Rosyntjieberg Formation is therefore not only subject to a vertical but also to a threefold lateral subdivision :

Table 2.2.

Orange River :	*Rosyntjieberge :*	*Tswaies-, Omsberge :*
R_6		
R_5		upper quartzite
R_4		mesocratic and
R_3		leucocratic volcanics
R_2	quartzites and	lower quartzite (R_1)
R_1	pelitic rocks	

d) *Thickness*

A total thickness of 3500 m in the Orange River area and 3300 m in the Rosyntjieberg-Tswaies area (Annex. 3) shows that this terrain must have experienced a rather uniform subsidence. A much lower thickness in the Rosyntjieberg area is, however, not in agreement with this view. Great amounts of intercalated volcanics and great total thickness of the formation in the southeast and the northwest, lack of volcanic intercalations and reduced total thickness in the central part, suggest that the southeastern and northwestern parts were closer to a possible coastline than the central part. In this case the reduced thickness of the central part would only reflect the lack of sufficient sedimentary material but not lack of subsidence.

e) *Current direction and coastline*

Ripplemarks throughout the formation indicate northnortheast-south-southwest current directions (Fig. 2.15). They are usually symmetrical or nearly symmetrical, so that water movements in both directions can be assumed. This is in agreement with an interpretation as coastal marine sediment. Judging by the direction and geographic distribution of flow marks, a southwest-northeast current direction appears to dominate in the Rosyntjieberg Formation. This direction appears to change more towards east-west in the southeastern Rosyntjieberg Formation and is thus in agreement with a coastline running in a northwesterly direction and changing more towards a north-south direction farther east.

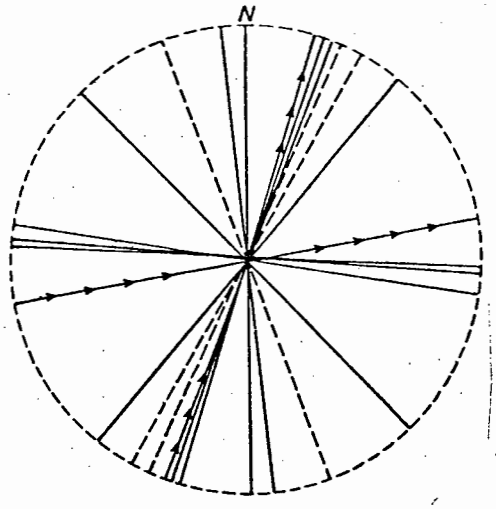

Fig. 2.15 Current directions from flow marks in Rosyntjieberg quartzites after rotation back into the horizontal position. Solid line : direction of current, arrows: sense of direction as deduced from ripple-marks; dashed line: direction of grooves.

f) *The Tswaies conglomerate*

Conglomerates are rare in the Rosyntjieberg Formation. One occurrence, however, in the Tswaies Mountains, which had been interpreted as a Stinkfontein inlier by De Villiers & Söhnge (1959), contains angular and very poorly rounded fragments of Rosyntjieberg quartzite of rather chaotic appearance. Rock fragments are contained in a matrix of quartz and sericite displaying the same foliation as the underlying volcanics. It is therefore distinguishable from the Stinkfontein conglomerates which are always composed of well-rounded boulders. The conspicuous band of iron-bearing rocks always associated with the lower quartzite is missing at the site of the conglomerates and instead iron quartzites occur as rock fragments within the conglomerate.

Rocks of similar appearance occur within the underlying volcanics nearby (Die Koei) and have been interpreted there as fanglomerates.

If the same interpretation also applies here, it has to be concluded that the sea where the Rosyntjieberg quartzites were being deposited withdrew temporarily and exposed the already solidified quartzites to erosion. This erosion is then likely to have been caused by mud-flows or temporary rivers, since singular events such as volcanic mud-flows or ash-flows, which may display similar features, tend to be constructive rather than destructive and are unlikely to erode a quartzitic succession of over 100 m thickness.

Table 2.3 Comparison of Precambrian iron formations with the Rosyntjieberg iron deposits. Algoman and Superior-type iron formations after Hutchinson (1978)

	Archean	Proterozoic	
Type	Algoman	Superior	Rosyntjieberg F.
age (by)	>2,5	~2,0	~2,0
character of sedimentation	alternating thin-bedded bands of chert and iron minerals, quiescent conditions, chemical	chemical alternating bands of chert and iron minerals, quiescent depositional conditions	clastic, shallow littoral conditions
rock association	dominant volcanics, differentiated, subaqueous volcanoclastic sediments	dominant epiclastic sediments, minor amounts of tholeiitic basalts, subaqueous	dominant andesitic to rhyolitic volcanics, subaerial, mature quartzite, volcanic greywacke
depositional environment	deep basin "eugeosynclinal"	shallow shelf "miogeosynclinal"	intravolcanic basin, shallow littoral
texture	fine grained	fine grained oolitic	medium to coarse grained, euhedral
extent			
- lateral	10's miles	100's miles	10's kilometres
- vertical	100's feet	1000's feet	10's metres
continuity	limited	great	limited
oxides	magnet. >hem.	hem.> magnet.	magnet.> hem.

g) *Origin of the Rosyntjieberg iron deposits*

Iron formations are chemically precipitated sedimentary rocks typically thinly-bedded and containing 15 percent or more ore (James, 1954). In Table 2.3 their characteristic features (taken from Hutchinson, 1978) are compared with those of the Rosyntjieberg Formation and it is evident from this table that particularly their clastic sedimentary origin does not allow them to be classified as iron formation as defined by James (1954). Although the present crystal shape of magnetite must largely be regarded as being due to later (metamorphic) crystal growth, close association of magnetite with sedimentary structures and mixtures of relatively coarse, clean quartzite with magnetite suggest clastic sedimentation, and the absence of cherty quartzites and the presence

of ripplemarks and cross-bedding suggest a littoral, shallow depositional environment not favourable for chemical sedimentation.

The Rosyntjieberg iron formation therefore does not fit into the scheme of Precambrian iron formations and must be regarded as being generated by the particular geological conditions prevailing in the Richtersveld during early Proterozoic times. The source of the iron minerals can either (and most probably) be seen in the melanocratic volcanics of the Orange River Group or alternatively in an independent source outside the Richtersveld.

2.3 CONCLUSION

In reviewing this chapter particularly the difference of the depositional environment at both limbs of the Richtersveld anticline must be noted: while the northeastern limb appears to be a centre of igneous activity throughout its development, the southwestern limb can be seen as an area of continued subsidence and as a recipient of sediments derived from the volcanic terrain farther in the northeast. If this interpretation is correct the stratigraphic relationships of the formations of the northeastern Richtersveld are as shown in Table 2.4.

Table 2.4 Approximate time correlation of formations of the northeastern Richtersveld

Rosyntjieberg F.		Kuamsrivier F.
	Klipneus F.	Kookrivier F.
Paradysrivier F.		Abiekwarivier F.

While the time correlation within each of the limbs is relatively safe, the correlation between the northeastern and southwestern limbs poses more problems. Particularly important in this regard is the presence of pebbles in conglomerates of the Klipneus Formation which strongly resemble subvolcanic equivalents of the Kookrivier Formation and have only been found in the area around the Tatasberg (G_1, see next Chapter). For this reason this area must already have undergone erosion when the Klipneus Formation was deposited.

In summary : the depositional evolution of the northeastern Richtersveld has been dominated by a shield volcano in the northeast which underwent a development from acid ash flow tuffs to intermediate lavas and which was surrounded in the south and west by basinal structures in which detrital volcanic sediments together with occasional lava flows accumulated, followed by a regionally restricted marine ingression towards the end of the volcanic cycle.

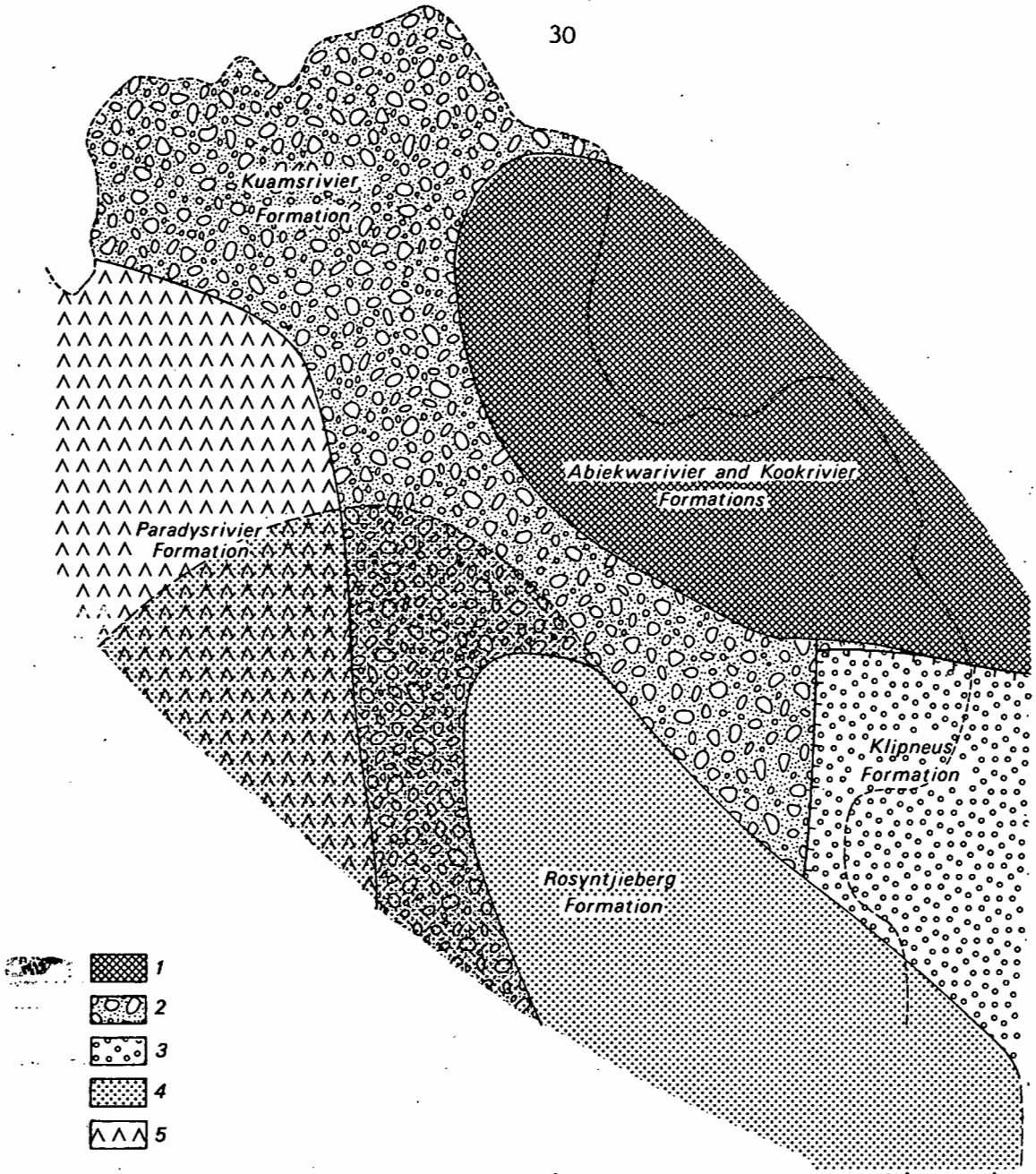

Fig. 2.16. Interpretative reconstruction of the paleogeographic environment during deposition of the lower Rosyntjieberg Formation in the confines of the present-day outcrops. The original distance between the northeastern and southwestern limbs of the Richtersveld anticline has probably been between 70 and 100 km. Legend:

1) High-rise inactive volcanic terrain
2) Volcanic lowlands and coastal plains with erosion products of 1) and 5) and individual ashflows.
3) Klipneus Graben structure with melanocratic volcanics and metasediments derived from 1.
4) Lower Rosyntjieberg Formation
5) Possible active volcanic terrain, mainly leucocratic ashflow tuffs and lavas. Volcanic activity leads to temporary regression of the Rosyntjieberg Sea. The maximum northern extension of the Rosyntjieberg Formation is indicated by dashed lines.

Table 2.5. Stratigraphy of supracrustal rocks of the northeastern Richtersveld

Formation	*Lithology*	*a)underlying b)overlying*	*type locality stratotype*	*thickness*	*paleogeographic interpretation*
Abiekwarivier Formation (v_1) lower :	melanocratic to leucocratic volcanics, pelitic rocks, volcanics partly redeposited	a) Kookrivier F. Kuamsrivier F. b) unknown	valley of the Abiekwarivier (Annex. 2)	0-1,5 km	basal part of shield volcano
upper :	leucocratic to mesocratic tuffs and ash flow tuffs			0,8-2,5 km	basal part of shield volcano
Kookrivier Formation (v_2)	quartz-feldspar-porphyry	a) Kuamsrivier F. b) Abiekwarivier	valley of the Kook River at foot of Richtersberg	4 km	central part of shield volcano
Kuamsrivier Formation (v_3)	melanocratic lava, pink qtz-porphyry, finely laminated leucocratic metasediments	a) unknown b) Abiekwarivier F. (NW) Kookrivier F. (SE)	Kuams River	minim. 1,5 km	transitional part between slope and foot of shield volcano
Klipneus Formation (v_4)	tuffs, lavas, conglomerates, cherts, quartzites, leucocratic to melanocratic	a) Rosyntjieberg F. b) Kookrivier F. (inferred)	no type locality	variable, locally exceeding 3 km	synvolcanic graben system, predating Rosyntjieberg Formation
Paradysrivier Formation (v_5)	NW: leucocratic volcanics, welded and unwelded, fanglomerates. SE: mainly mesocratic tuffs	a) Rosyntjieberg F. b) unknown	Paradys River	unknown, but exceeding 2 km	low lying volcanic terrain, possibly initial graben formation.
Rosyntjieberg Formation (R)	pure quartzites, chloritic quartzites and schists, ferruginous quartzites and schists, metavolcanics, very few pelitic intercalations	a) Windvlakte F. b) Klipneus and Paradysrivier Formations	SE: Orange River valley NW: area around Rosyntjiewater.	3-3,5 km	marine ingression into intravolcanic basin of limited extent

Chapter 3

THE VIOOLSDRIF INTRUSIVE SUITE (VIS) IN THE NORTHEASTERN RICHTERSVELD

3.1. INTRODUCTION

3.1.1. General

The plutonic rocks of the northeastern Richtersveld form part of a Proterozoic (1950-1750 my) intrusive complex of batholithic proportions situated mainly in the lower Orange River area between Haib-Vioolsdrif and the Richtersveld. They comprise diorites, granodiorites, tonalites, granites and leucogranites of calc-alkaline provenance. Their early phases are regarded as being comagmatic with the volcanic rocks of the Orange River Group (Reid, 1977) into which they are intrusive.

In this chapter only those rocks of the Vioolsdrif Intrusive Suite are dealt with that occur in the northeastern Richtersveld, since they are least altered by subsequent tectono-thermal events and thus provide the best material to investigate their primary igneous texture.

3.1.2. Previous investigations

The earliest investigations were carried out by Rogers (1915), Gevers *et al.* (1937), Mathias (1940) and Coetzee (1941). In the Richtersveld proper, rocks of the VIS were first described by De Villiers and Söhnge (1959) who applied the term "grey gneissic granite" to them and assumed a partly magmatic and partly metasomatic origin. Middlemost (1963) used the term "adamellite gneiss" for some of the basement rocks in the southeastern Richtersveld. More recently, Ward (1977) and Blignault (1977) mapped and described rocks of the Vioolsdrif Intrusive Suite in the Haib - Vioolsdrif area. Reid (1977) investigated geochemical aspects of the VIS in the Haib-Vioolsdrif area with special emphasis on source and mode of magma formation. He concluded from major and trace element modelling that the tonalitic and granodioritic phases could have been produced by fractional crystallisation

of a dioritic parent magma and the adamellitic and leucogranitic phases by a stepwise fractionation of a tonalitic parent. He also carried out radiometric age determinations by various methods and found that the intermediate and mafic members yield an age around 1900 my and the acid members 1730 my (Reid, 1978b).

3.1.3. Objectives of this investigation

Petrography and field relationships of the VIS have already been investigated extensively in previous publications (e.g. Blignault, 1977; Ward, 1977) and its geochemistry has been thoroughly dealt with by Reid (1977).

The approach to this investigation was therefore guided by the following ideas:

a) Most of the publications dealing with granites and related rocks either neglect or totally omit textural relationships. Quantitative textural data on granites are virtually unknown. However, methods based on statistical approaches have been developed in recent years, which allow for the quantitative determination of textural properties. One of these methods (grain transition probabilities) has been adapted to suit the requirements here (see Appendix). It will be particularly useful in the comparison of different magmatic rocks of the Richtersveld, which otherwise could only be distinguished with difficulty, due to lack of significant compositional differences.

b) Calc-alkaline intrusive rocks are frequently the site of porphyry ore deposits. According to now widely accepted views, the water content of the magma is at least partly responsible for the formation of such deposits, together with geological factors such as depth of intrusion and type of wallrock. It was therefore important to determine the intrusive history of the Vioolsdrif Intrusive Suite as accurately as possible, with particular emphasis on the crystallisation sequence of the main mineral phases, as this sequence permits the estimation of the original water content. The aim of the investigation was therefore:

a) unravelling of the intrusion and cooling history subsequent to the formation of the magma

b) determination of the original water content of the magma

c) extent of metasomatism

This had to be achieved by the following means:

a) thorough investigation of qualitative textural relationships

b) application of the concept of grain transition probabilities

c) evaluation of the results thus obtained in the light of experimental data

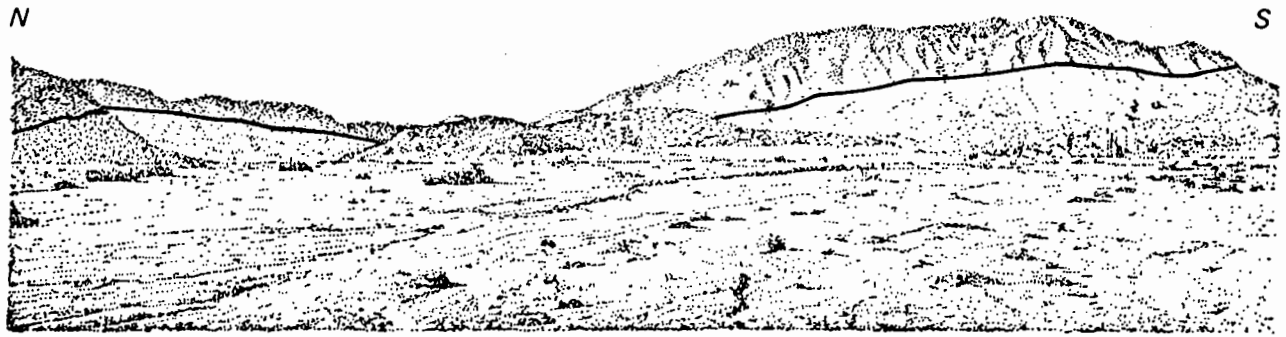

Fig. 3.1 Contact granodiorite - quartz-feldspar porphyry near Maerpoort. Gently dipping contacts of this type are rare.

3.2. FIELD RELATIONSHIPS

3.2.1. General

In the Richtersveld north of the Rosyntjieberge, the Vioolsdrif Intrusive Suite occurs in several major intrusive bodies; the largest, in the core of the Richtersveld anticline, has a length of nearly 50 km and a width of 20 km.

South of the Rosyntjieberge, the area between BakRiver and Kahams is underlain by several smaller intrusions.

Intrusives of the Vioolsdrif Intrusive Suite south of the Klipbokkop are increasingly tectonically overprinted and recrystallised and therefore are not dealt with here. Numerous small outcrops of pink granite in the northeast between De Hoop and Oenas and in the Pink-gneiss Unit in the south, are not included in the Vioolsdrif Intrusive Suite proper.

On the grounds of field relationships, texture and composition, four intrusive members have been distinguished in the northeastern Richtersveld which may, however, consist again of a variety of different intrusions.

3.2.2. Fine-grained granodiorite (map unit G1)

Fine-grained granodiorite occurs in a narrow sheet along the northeastern boundary of the main intrusion, bordering the Abikwarivier Formation. A weak, but persistent foliation is developed. In hand specimen it is frequently so fine-grained that it is easily confused with mesocratic volcanics.

Textural and field relationships suggest that it might constitute a transitional subvolcanic link between Vioolsdrif granodiorite and Orange River volcanics, a relationship that has already been indicated by geochemical data for early members of the Vioolsdrif Intrusive Suite (Reid, 1977). The uppermost, subvolcanic part of this intrusion can only be recognised in thin section and not in the field, as it is macroscopically virtually identical with metavolcanics and only distinguished by its groundmass grain size.

3.2.3. Even-grained granodiorite (map unit G2)

Even-grained granodiorite occurs to the west of the fine-grained granodiorite in the main intrusion and comprises by far the majority of the Vioolsdrif Intrusive Suite. It is finer grained than the granite member (G3) and coarser than the fine-grained granodiorite. A weak foliation is occasionally displayed in the field, but in thin section is present only as sporadic

recrystallisation of biotite and quartz.

A Rb-Sr whole rock age of 1900 ± 30 my has been determined for intermediate members of the Vioolsdrif Intrusive Suite in the Haib area (Reid, 1978 b).

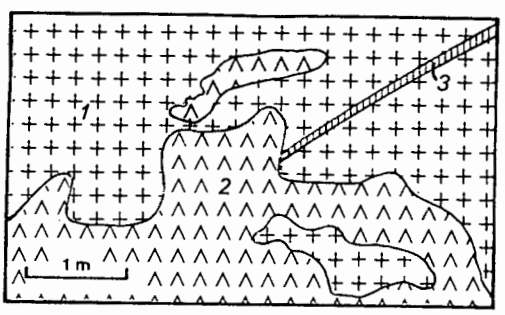

Fig. 3.2 Discordant, but sharp contact on outcrop scale between granite (1) and intermediate lava (2). (3) epidote vein. SE of Tatasberg.

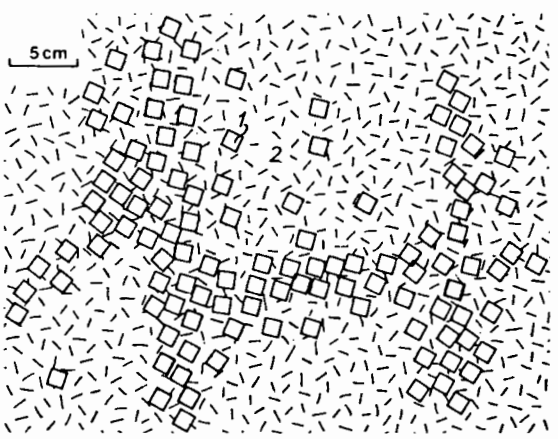

Fig. 3.3 Schematic sketch of metasomatic growth of feldspar porphyroblasts (1) along pre-existing joints within fine-grained granodiorite (2), approaching contact with granodiorite (G_2).

3.2.4. Granite (map unit G3)

Granite is coarser grained than granodiorite (G_2) and frequently porphyritic (kf), but it must be noted that plagioclase of the same size also occurs at places.

Although rocks of this type have been named adamellite by previous

writers (Blignault, 1974b, 1977; Reid, 1974, 1977; Ward, 1977) the term granite is preferred here, as the present writer does not see any reason why an intrusive rock, the modal composition of which occupies the granite field in the IUGS classification of igneous rocks, should not be called granite. In addition, the term adamellite seems to be rather ill defined. It was first used for an orthoclase-bearing tonalite at Monte Adamello, Italy, and is at present in use for a quartz-monzonite of United States usage (Glossary of Geology). Streckeisen (1973) in an attempt to standardise igneous rock terms advocated its abolition. The granite member of the Vioolsdrif Intrusive Suite is restricted to the core of the main intrusion and to minor outcrops around Kahams in the south, where it is clearly intrusive into the even-grained granodiorite.

3.2.5. Leucogranite (map unit G4)

Leucogranite is devoid of mafic constituents and forms easily recognisable intrusions as dykes, plugs and minor plutons. It may but need not be more K-feldspar-rich than granites and is usually easily recognised by its white to pink colour, finer grain size and angular weathering as opposed to "woolsack weathering" of granodiorite and granite. Although its contact with granite is usually sharp, transitional contacts with granite may occur. A Rb-Sr whole rock age of 1731 ± 20 my has been determined for granitic rocks of the Haib area (Reid, 1978b).

3.2.6. Summary

In summary, it appears that the fine-grained granodiorite is the oldest member of the Vioolsdrif Intrusive Suite in the northeastern Richtersveld. Textural and field relationships suggest furthermore that it constitutes a subvolcanic link between the other members of the Vioolsdrif Intrusive Suite and the metavolcanics. It is followed by even-grained granodiorite. Both granodiorites display foliations in the field and recrystallisation and reconstitution in thin section, but even-grained granodiorite displays these features less strongly than the fine-grained granodiorite.

In contrast to this, granite and leucogranite are devoid of deformational features and thus make up a distinct posttectonic intrusive phase. This agrees well with radiometric data derived from the Vioolsdrif Intrusive Suite in the Haib area, which indicates an intrusion of the intermediate members around 1900 my and that of the more acid members around 1730 my (Reid, 1978b).

3.2.7. Intrusive contacts

The rocks of the Vioolsdrif Intrusive Suite are intruded concordantly to subconcordantly on a regional scale. Contacts are usually steep and frequently, if only slightly, sheared. Undisturbed contacts are mostly sharp in the cm to dm range.

Only on a local scale can discordant contact relationships be observed. The best example is the contact of the Maerpoort intrusion at the western slope of the Rooiberg (Fig. 3.1) where the eastern contact dips gently to the east, while the northern and western contacts are steep to vertical. Gently dipping contacts can also be observed in the steep incision the Abiekwarivier forms in volcanics of the Abiekwarivier Formation.

On an even smaller scale (m), granitoids at places cut the structural grain of the country rock and display patterns such as shown in Fig. 3.2. Fragmentation of wallrock at contacts is, however, rare and the example depicted is the only convincing one encountered in the Richtersveld. Samples of the wall rock taken immediately from the contact show no signs of melting or recrystallisation, even in thin section. Contact migmatites at the western boundary of the Die Koei intrusion should be noted here, although they are most probably due to contact shearing during cooling and solidification of the intrusive rock.

Metasomatic alteration of the wall rock has been encountered only once: northwest of the Kook River near the contact between fine-grained granodiorite (G1) and even-grained granodiorite (G2), feldspar porphyroblasts are developed in increasing amounts within the fine-grained granodiorite along joints and other ways of facilitated migration, becoming more numerous and more densely spaced on approaching the even-grained granodiorite (Fig. 3.3). This, in addition, suggests that the fine-grained granodiorite must already have cooled when it was intruded by the even-grained granodiorite.

3.3 COMPOSITION

Modal compositions of the intrusive rocks of the Vioolsdrif Intrusive Suite have been estimated by point-counting 800 - 1200 counts per thin section per sample. Epidote and sericite occurring as alteration products of plagioclase have been counted as plagioclase. Epidote occurring outside plagioclase has been included in mafic minerals. The values plotted in Fig. 3.4. therefore provide only a rough estimate of the composition of the individual sample, more accurate for granodiorites and leucogranites because of finer grain size than for granites. The greater spread of granite values is largely due to this effect. Figs. 3.4 a-d reveal the following compositional features:

a) quartz-content is independent of the rock bulk composition
b) alkali feldspar and colour index display a distinct negative

Table 3.1. Major element analyses of rocks of the Vioolsdrif Intrusive Suite, northeastern Richtersveld

	1	2	3	4	5	6	7	8	9	10	11
	A11	68/3	169	A2	134/2	62	117/3	132	175	90	146
SiO_2	68,20	66,76	70,70	66,11	64,22	65,86	70,46	66,91	66,28	78,65	76,97
TiO_2	0,34	0,47	0,31	0,48	0,54	0,66	0,43	0,57	0,58	0,10	0,10
Al_2O_3	15,51	14,36	14,86	15,07	16,15	15,51	13,93	14,93	15,32	11,75	12,44
FeO	2,81	4,13	2,40	4,29	4,98	4,17	2,87	3,98	3,99	0,37	0,58
MnO	0,05	0,12	0,09	0,14	0,13	0,09	0,08	0,12	0,07	0,04	0,05
MgO	1,15	2,18	0,99	2,01	2,15	1,78	1,07	1,50	1,61	0,19	0,16
CaO	3,35	3,81	2,22	4,02	3,88	3,66	2,42	3,41	3,64	0,16	0,29
Na_2O	3,56	3,46	3,32	3,07	3,23	2,80	2,84	2,94	2,89	2,86	3,69
K_2O	3,21	2,98	4,16	3,29	3,29	4,10	4,57	4,67	4,34	5,71	5,22
P_2O_5	0,16	0,14	0,10	0,16	0,17	0,23	0,12	0,18	0,18	0,04	0,05
LOI	1,98	1,56	1,33	1,76	1,59	1,44	1,42	1,23	1,43	0,50	0,74
Σ	100,32	100,57	100,48	100,39	100,28	100,24	100,14	100,44	100,32	100,34	100,28
DI	75	70	81	68	66	70	80	74	72	98	97

1) Fine-grained granodiorite (G1), 3 km northwest Tatasberg
2) Fine-grained granodiorite (G1), 0,5 km north of Tatasberg
3) Even-grained granodiorite (G2), Maerpoort
4) Even-grained granodiorite (G2), 3 km northwest of Tatasberg
5) Even-grained granodiorite (G2), upper Kuams River
6) Granite (G3), Springbokkloof
7) Granite (G3), 3 km southwest of Tatasberg
8) Granite (G3), upper Abikwa River
9) Granite (G3), upper Abikwa River
10) Leucogranite (G4), Tswaies
11) Leucogranite (G4), Grasdrif

Analyst : D. Reid (1978) Geochemistry Department, University of Cape Town.

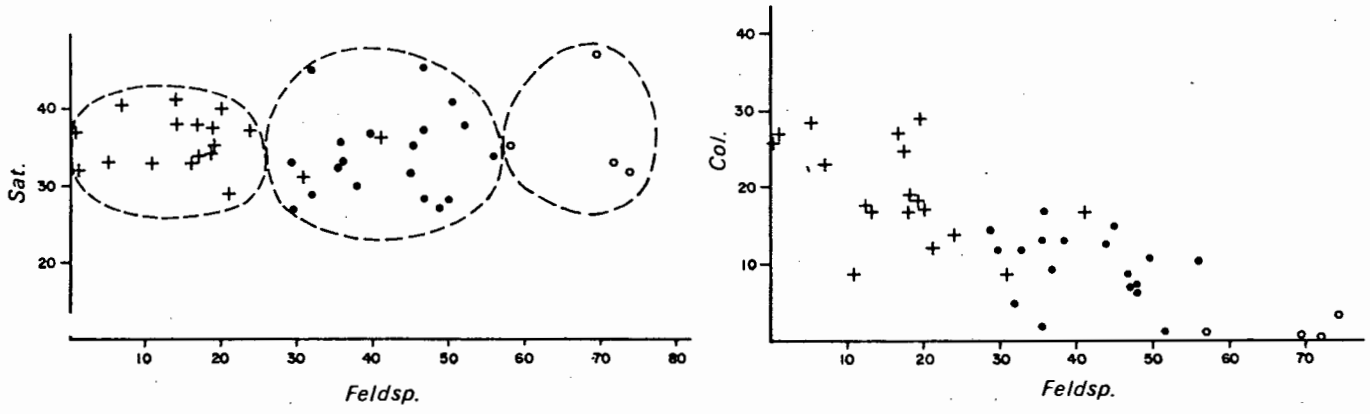

(a) (b)

Fig. 3.4 (a), (b) Legend: Crosses : G_1 and G_2, dots : G_3, circle G_4. The different members of the Vioolsdrif Intrusive Suite occupy distinctly different fields. The negative correlation between feldspathic Index and Colour Index is noteworthy (3.4.b). The Saturation Index remains constant throughout the compositional range of the intrusives and is thus consistent with chemical analyses.

Saturation Index (Sat.) $= \frac{qtz}{qtz + plg} \times 100$

Colour Index (Col.) $= 100 - qtz - kf - plg$

Feldspathic Index (Feldsp.) $= \frac{kf}{kf + plg} \times 100$

(after Jung and Brousse, 1959)

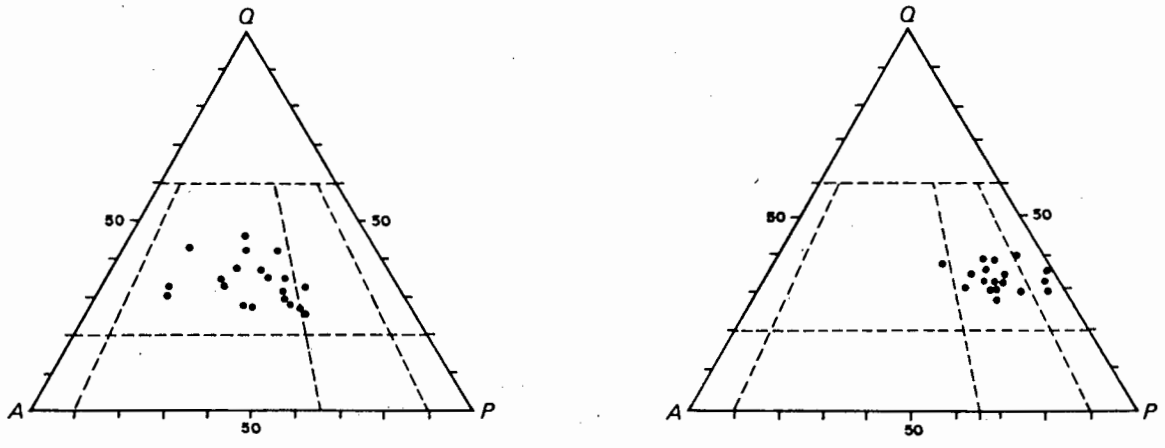

(c) (d)

Fig. 3.4 (c), (d) The compositional range of fine-grained granodiorite and even-grained granodiorite (G_1, G_2, Fig. 3.4(c)) and granite/leucogranite (G_3, G_4) is slightly overlapping.

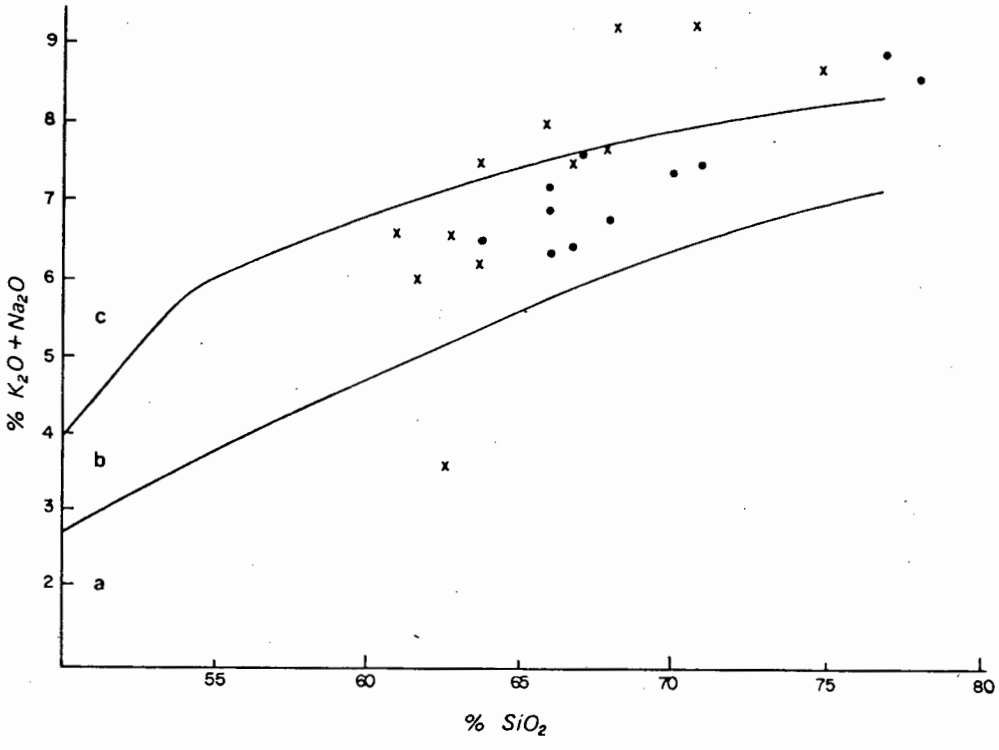

Fig. 3.5 Variation diagram of K_2O and Na_2O versus SiO_2 of volcanics and intrusives of the northeastern Richtersveld.
crosses : volcanics
dots : intrusives
(a) tholeiitic (b) calc-alkaline (c) alkaline (after Kuno, 1968)

Fig. 3.6 These figures suggest that the positive correlation of alkalis with SiO_2 is mainly due to the strong positive correlation of K_2O and SiO_2, while Na_2O appears to be independent of SiO_2. This is in agreement with modal analyses (Fig. 3.4c, d) which show that granodiorite and granite are mainly distinguished by their different K-feldspar content.

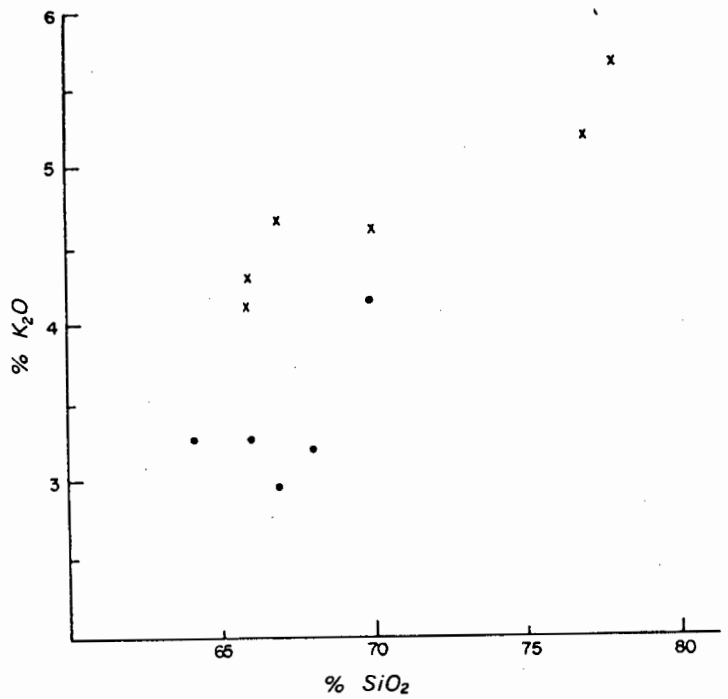

Fig. 3.6a

Variation diagram K_2O versus SiO_2.

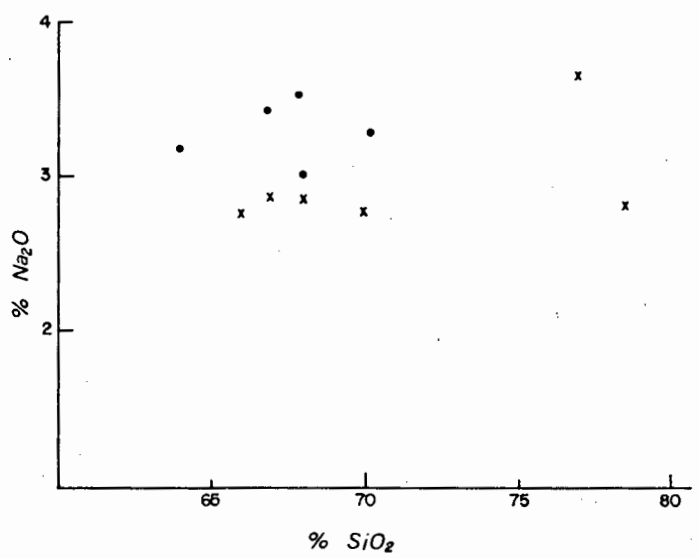

Fig. 3.6b

Variation diagram Na_2O versus SiO_2. Crosses : G_3 and G_4; dots : granodiorite G_1 and G_2.

correlation

c) leucogranites show a tendency towards higher alkali-feldspar content, but do not occupy the alkali-feldspar field of the AQP-diagram.

The compositional variation is therefore mainly expressed by different K-feldspar/plagioclase ratios and by different contents of mafic minerals.

This is also evident from major element analyses, where the granite phase (G3) is characterised more by an increase in K_2O than by an increase in SiO_2. (Table 3.1, Figs. 3.5, 3.6).

3.4. TEXTURE AND MINERALOGY

3.4.1. Introduction

Mode of occurrence of the main mineral constituents and their mutual textural relationships are described and discussed below.

Since textural features between granodiorites and granite are not significantly different, the textural descriptions apply to all rock types unless the contrary is mentioned. Because the granitic members of the Vioolsdrif Intrusive Suite are not affected by post intrusive tectono-thermal events, most examples described relate to the granitic phase, as it is the aim of this chapter to present magmatic features and not metamorphic ones.

3.4.2. Plagioclase

Plagioclase occurs as euhedral to subhedral, short prismatic crystals with a predominant grain size of 0,5 - 1 mm in the fine-grained granodiorite, 1 - 2 mm in even-grained granodiorite and 2 - 3 mm in granite and leucogranite. Phenocrysts of 5 mm and more also occur in some cases.

Plagioclase in hand specimen usually displays a greenish tinge due to the development of epidote.

The An-content in granites ranges between albite and oligoclase with occasional andesine. Significant differences in An-content between granite and leucogranite have not been found, although Reid (1977) reports lower An-contents in leucogranite of the Haib area.

Plagioclase of the fine-grained granodiorite and even-grained granodiorite is usually so strongly altered that its An-content cannot be determined optically.

Crystal boundaries are sharp or are slightly interlobate when in contact with K-feldspar, but amoeboid and strongly interlobate grain

boundaries also occur in some granites. No primary inclusions except zircon, hornblende and finely disseminated opaque oxide minerals (the latter two in fine-grained granodiorite only) have been observed. Unaltered or less altered rims of plagioclase are nearly always present at contacts of plagioclase with K-feldspar.

Alteration of plagioclase

Plagioclase crystals in rocks of the Vioolsdrif Intrusive Suite are altered to variable degrees into aggregates in which epidote and sericite predominate. While plagioclase of granite and leucogranite is only weakly altered, leaving the main features of the original mineral well recognisable, the plagioclase of the granodiorites tends to be completely filled with dense alteration products which virtually form pseudomorphs after plagioclase.

Epidote occurs in colourless to slightly pleochroic, subhedral crystals with diameters around 0,02 mm, sericite in flakes of 0,02 - 0,03 mm.

3.4.3. Potassium feldspar

K-feldspar grains occur in variable sizes from a fraction of a mm to several cm. Anhedral crystals predominate but euhedral crystals are present as well. In granite and granodiorite microcline with characteristic albite-pericline twinning is the only optically detectable polymorph. Two investigated specimens show maximum obliquity values of 0,95. Evaluation of the X-ray diffraction pattern after the method given by Parson and Boyd (1971) suggests that orthoclase might be present in minor amounts as well.

Texturally at least two types of K-feldspar can be distinguished:

K-feldspar I is characterised by a tendency to subhedral and euhedral forms. Symplectic intergrowth of quartz and biotite is not encountered here. Instead uncorroded and euhedral plagioclase phenocrysts are often enclosed. String perthite is the only perthite type.

K-feldspar II forms irregular grains and aggregates of variable size. Symplectic intergrowth of quartz and biotite is common. Perthite occurs as widely spaced string perthite and as irregular patches of perthite without sharp boundaries (e.g. Fig. 3.9).

3.4.4. Biotite

Biotite is the most common mafic mineral in the Vioolsdrif Intrusive Suite. It is generally olive green; only in fine-grained granodiorite can a tendency towards brown green be observed.

Two textural types of biotite can be recognised:

b_f : This type is made up of relatively big flakes of up to 1 mm in length. It is marginally corroded by K-feldspar and quartz containing exsolved, fine grains of a highly refractive material (? leucoxene). Sagenitic webs are frequent.

b_a : This type forms lepidoblastic aggregates with diameters between 0,5 and 3 mm, made up of flakes between 0,1 and 0,3 mm in length. Although biotite is the predominant constituent, epidote and quartz occur as well. Apatite occurs in minor amounts. Features indicative of assimilation, corrosion or exsolution within the individual flakes are absent except when in contact with *K-feldspar II*.

b_a also occurs within plagioclase where it occasionally fills subhedral forms, suggesting pseudomorphic growth after another mineral.

In even-grained granodiorite and fine-grained granodiorite aggregates of biotite frequently occur in an elongated foliation-like manner. Only in this case can a tectonometamorphic origin for these aggregates be regarded likely.

Another textural type of biotite occurs less frequently and is shown in Figs. 3.15, 3.16 and 3.18. It appears to have formed after a single biotite flake, since a continuous sagenitic web structure is frequently retained (Fig. 3.18). In cases of possibly more advanced reconstitution it is, however, not retained anymore. Furthermore, the tendency of biotite to crystallise at the margins of these "replacement" structures (Fig. 3.16, 3.18) is noteworthy.

In order to obtain an indication as to the significance of the textural modifications of biotite, *grain transition probabilities* have been determined for samples containing abundant b_f and b_a (for explanation see Appendix I). The system *quartz* - *plagioclase* - *K-feldspar* - b_f - b_a was investigated (i.e. b_a was treated as if it was a mineral phase, the various transitions within b_a were thus not recorded. Doubtful cases were treated as b_a).

The results of this investigation are displayed in *grain association diagrams* in Fig. 3.7.

Particularly striking is the complete mutual exclusion of b_a and b_f, i.e. the probability of b_a and b_f occurring in contact with each other is less than expected in random distribution. A further significant feature is the strong association of b_f with *quartz* and of b_a with *plagioclase*. While b_f may also be associated with *plagioclase*, the association of b_a with *quartz* is negative in both cases.

The spatial distribution of the two biotite-modifications is therefore distinctly non-random, which suggests a different mode of origin for each of them.

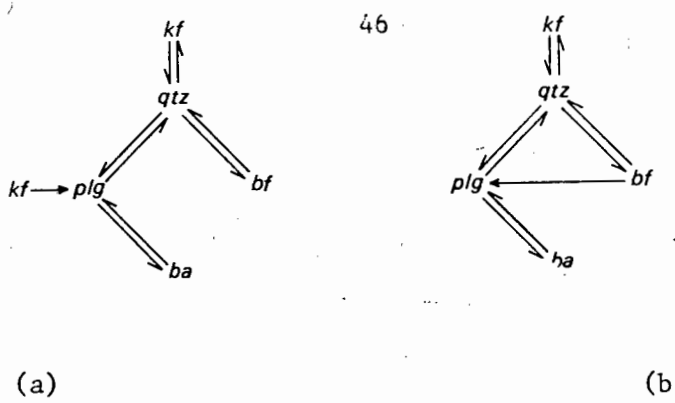

Fig. 3.7 Grain association diagrams for two rock types with particular emphasis on the association of biotite modifications. The arrows indicate positive associations. For further explanation see appendix.
(a) sample 420, granodioritic composition; (b) sample 425, granitic composition.

3.4.5. Quartz

Quartz occurs in interstitial aggregates of 0,5 - 4 mm in diameter, forming a granoblastic equigranular to inequigranular polygonal to interlobate subtexture. Undulatory extinction seems to be accompanied by increasing inequigranularity and development of interlobate grain boundaries while normal extinction of *quartz* is mostly found in equigranular textures with polygonal grain boundaries (see Fig. 3.22).

Occasionally a bimodal grain size distribution of quartz can be observed, although rarely as distinctly as in sample 427, where corroded subhedral quartz phenocrysts coexist with groundmass quartz (Fig. 3.23).

3.4.6. Hornblende

Fine-grained granodiorite is the only member of the Vioolsdrif Intrusive Suite that may contain hornblende. It is characteristically associated and surrounded by biotite of the type b_a, a feature which seems to be particularly well expressed in the vicinity of K-feldspar. Tiny inclusions of biotite are, however, also found in hornblende. Frequently hornblende is included in plagioclase. Typically it occurs as green hornblende in long, prismatic crystals which are poikilitically intergrown with quartz and biotite. If surrounded by quartz it is strongly corroded.

3.4.7. Accessory minerals

Epidote, apart from that grown in plagioclase, is the most abundant accessory mineral. It is often slightly more pleochroic than that of plagio-

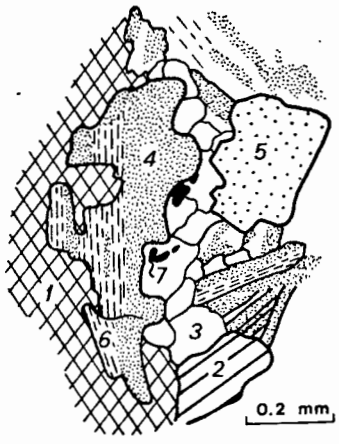

Fig. 3.8 Development of muscovite at the margins of biotite at contact with K-feldspar. It can be interpreted as transformation of biotite into muscovite at the contact with K-feldspar. (1)K-feldspar (2) plagioclase (3)quartz (4)biotite (5)epidote (6)muscovite (7)opaque. (424-11/55)

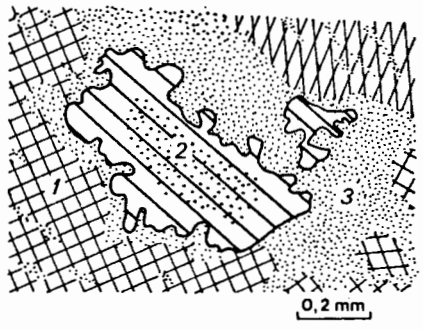

Fig. 3.9 Resorption of plagioclase by K-feldspar. Perthitic K-feldspar is more strongly albite-bearing in the vicinity of the resolved plagioclase. (1)K-feldspar (2)plagioclase (3)albite phase of perthite (248/3a)

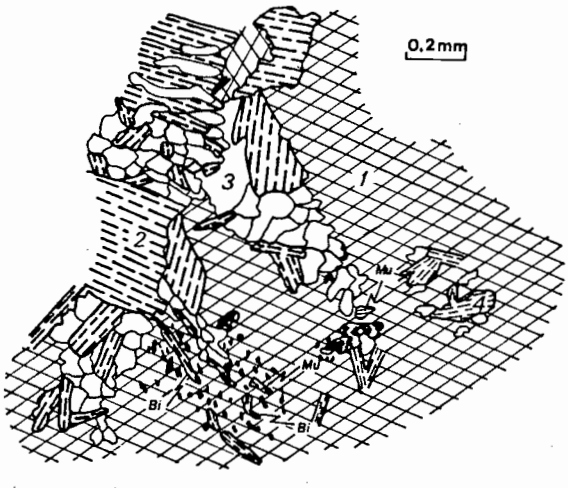

Fig. 3.10 K-feldspar porphyroblast, marginally resolving biotite aggregates (1) K-feldspar (2)biotite (3)quartz (4)muscovite (424 -12/48)

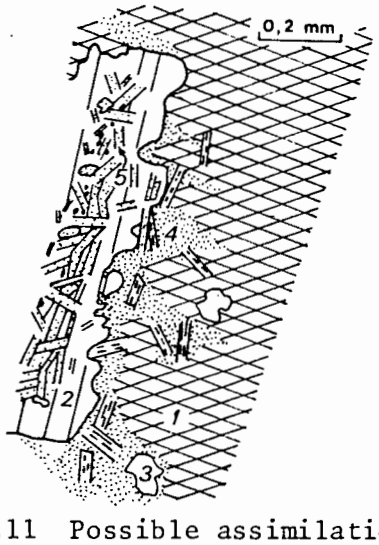

Fig. 3.11 Possible assimilation of plagioclase by K-feldspar after the formation of the plagioclase alterations. (1) microcline with small amounts of hairperthite (2)unaltered plagioclase (3)patchy albite in microcline (5)alteration products of plagioclase: epidote-sericite. Sericite of the same size occurs in the vicinity of plagioclase within K-feldspar, mostly closely associated with patchy albite (4) (248/3b).

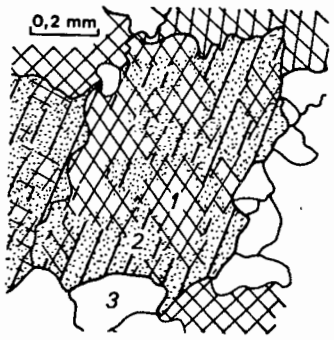

Fig. 3.12 Advanced stage of *in situ* plagioclase assimilation by K-feldspar. Primary plagioclase features like twinning are progressively obliterated. (1) newly formed K-feldspar (2) plagioclase (3) quartz (430-6/50)

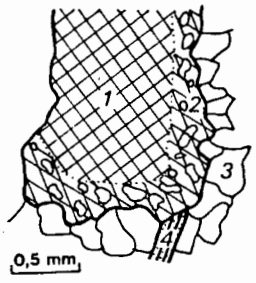

Fig. 3.13 Euhedral K-feldspar core surrounded by optically continuous poikilitic K-feldspar with anhedral outlines. The boundary between inner and outer K-feldspar becomes visible only at certain positions of the microscope stage. (1) inner K-feldspar (2) poikilitic rim (3) quartz from groundmass (4) plagioclase from groundmass (427-6/53)

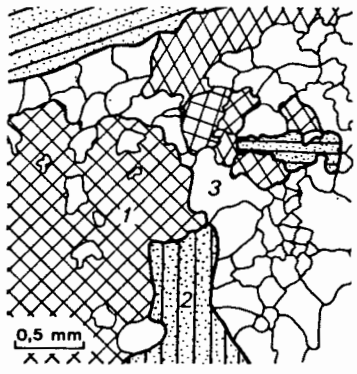

Fig. 3.14 K-feldspar porphyroblast growing into groundmass.
At its margin remnants of un-assimilated groundmass-quartz.
(1) K-feldspar (2) plagioclase (3) quartz (433b - 16/59)

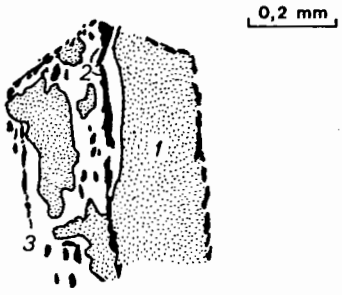

Fig. 3.15

(1) biotite with sagenitic webs
(2) ? leucoxene
(3) finegrained quartz
(427-6/53)

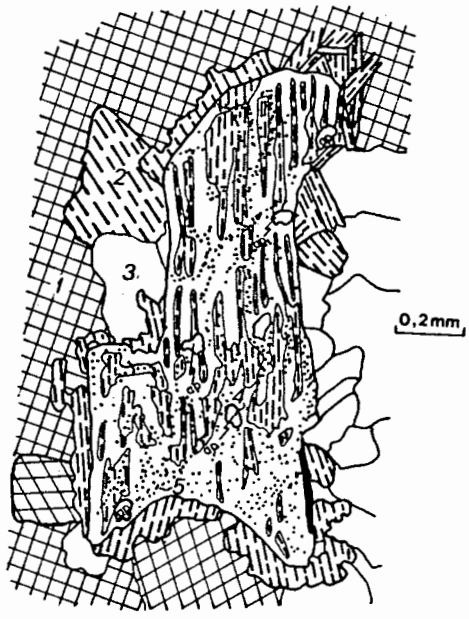

Fig. 3.16

Pseudomorphic quartz-biotite aggregates (1) microcline (2) biotite (3) quartz (4) apatite (5) ? leucoxene with very finegrained unidentified leucocratic minerals.

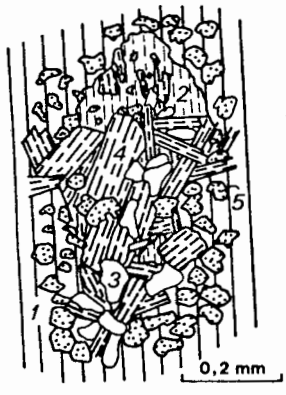

Fig. 3.17

b_a growing inside plagioclase crystal. (1) plagioclase (2)albite (3) quartz (4) biotite (5) epidote

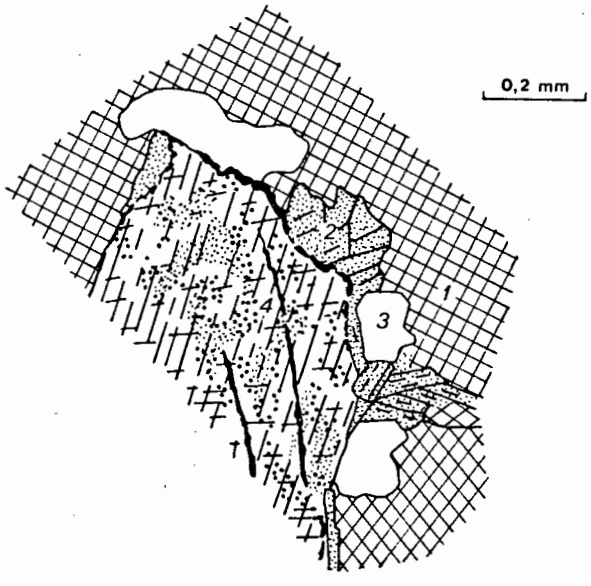

Fig. 3.18

Pseudomorphic finegrained quartz-biotite aggregate. (1) microcline (2) biotite (3) quartz (4) ? leucoxene (408-4/47)

clase fillings and occurs within b_a as irregular aggregates. Bigger grains (0,1 - 0,2 mm) tend to be marginally recrystallised. Occasionally it occurs interstitially in quartz.

Leucoxene is common as an exsolution product of biotite, within which, or at the margin of which, it occurs in small strings and lumps. Ilmenite or titanomagnetite are at places surrounded by leucoxene.

Sphene occurs as euhedral wedges or *is anhedral* and occasionally encloses plagioclase. It is commonly associated with quartz or biotite. Preferred occurrence within plagioclase as reported by Reid (1977) has not been observed.

Muscovite is the predominant mica in the leucogranites, but it also occurs in minor amounts in granodiorite and granite (apart from sericitic alteration products). Occasional flakes of muscovite occur within b_a, but it is most commonly developed interstitially in quartz.

3.5. TEXTURAL PROPERTIES

3.5.1. Grain association types

In order to obtain additional information as to the textural properties of the Vioolsdrif intrusives, grain transition probabilities have been established for selected samples involving the mineral phases *quartz - plagioclase - K-feldspar - M*. *M* includes mainly biotite and epidote, but also apatite and sphene.

The results are displayed in Table 3.2 and show the following characteristic features:

a) the *M - quartz* association is always positive, except in one leucogranite where the small number of transitions involving *M* renders them unrepresentative.

b) the associations *K-feldspar - quartz, plagioclase - quartz, K-feldspar-plagioclase* are in many samples positive.

c) the associations *K-feldspar - M, plagioclase - M* are negative in most samples. Since most grain associations are not consistently developed, a further inspection of the grain association diagrams suggests that there might be two different association types:

Association type 1) with positive *quartz - K-feldspar* association and negative *K-feldspar - plagioclase* association, and

Association type 2) with weakly positive *quartz - K-feldspar* association and strongly positive *K-feldspar - plagioclase* association.

Table 3.2 Comparison of grain association types with selected textural features

Sample No	Grain ass. diagram	Symplectic qtz in kf	Patchy perthite	Distorted plg crystals	Grain size distribution	plg boundary
408		X		(X)	bi	int
422			X	(X)	eq	str
423			X	(X)	(bi)	str/int
424		X	X		eq	str
425			X		eq	str
427		X			bi	int
428					(eq)	str
429		X	X		bi	int
430		X			bi	int
431		X	X		eq	str
433		X		X	bi	int
146			X	X	eq	str/int
90					eq	str/int
428/2					(bi)	str

Legend: qtz, plg, M, kf

bi = bimodal
eq = equigranular
int = interlobate
str = straight
(bi) = occasional, weak

3.5.2. Textural modifications

Further textural properties can be obtained from the description of individual mineral phases on the preceding pages. The following features might be useful for the definition of textural modifications:

a) The outline of plagioclase (straight-interlobate-amoeboid)

b) Grain size distribution of the main mineral phases (equigranular-bimodal-porphyritic)

c) The occurrence of symplectic quartz in K-feldspar

d) The distortion of plagioclase twin lamellae

e) The type of perthite in K-feldspar

These features have been compared in a contingency table (Table 3.3), which shows the following association of textural properties:

Textural modification A:

Straight plagioclase boundaries are associated with

a) equigranular grain size distribution

b) patchy perthite in K-feldspar

Textural modification B:

Interlobate plagioclase boundaries are associated with

a) bimodal grain size distribution

b) symplectic quartz in K-feldspar

c) distorted plagioclase

Table 3.3.

	A	B	C	D	E	F	G
plagioclase boundary straight	0	1	5	4	2	1	13
plagioclase boundary interlobate	5	1	2	3	5	4	19

A: grain-size distribution bimodal; B: grain-size distribution weakly bimodal; C: grain-size distribution equigranular; D: patchy perthite in *K-feldspar*; E: symplectic *quartz* in *K-feldspar*; F: distorted *plagioclase* phenocryst; G: number of observations.

3.5.3. Correlation of textural modification types and grain association types

In order to establish whether grain association types and textural modifications derived from observation can be correlated with each other Table 3.4 has been devised. It contains the synoptic difference matrices (cf. Appendix I) from those samples that show the most distinct affinities to either of the two textural modifications.

It is evident from Table 3.4 and Fig. 3.19 that the observed textural modifications can at least to some extent be correlated with grain association types.

Table 3.4 Difference matrix Texture A

	qtz	*plg*	*kf*	*M*
qtz	-	-0,042	-0,001	0,043
plg	0,001	-	0,085	-0,086
kf	0,044	0,036	-	-0,081
M	0,139	-0,071	-0,068	-

Texture B

qtz	-	-0,033	0,039	-0,006
plg	0,068	-	-0,028	-0,04
kf	0,135	-0,047	-	-0,088
M	0,163	-0,064	-0,099	-

Synoptic difference matrices derived from samples most typical for texture A and B respectively.

Texture A from samples : 422, 424, 425, 431
Texture B from samples : 408, 427, 429, 430, 433

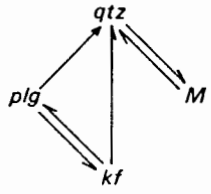

Fig. 3.19a

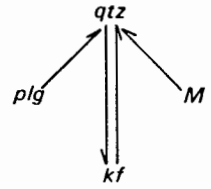

Fig. 3.19b

It is therefore possible to conclude that the population of samples investigated here is made up of two textural types:

Textural type A:

is even-grained, contains plagioclase with straight boundaries, its K-feldspar contains apart from string perthite also patchy perthite. Its grain association diagram is characterised by a positive *plagioclase - K-feldspar* association. Its texture is best represented by Fig. 3.21.

Textural type B:

is uneven-grained to porphyritic, contains plagioclase with interlobate to amoeboid boundaries. Some plagioclase grains, usually those of the larger grain fraction, show distorted twin lamellae. K-feldspar contains symplectic quartz. Its grain association diagram is characterised by a negative *plagioclase - K-feldspar* and a positive *K-feldspar - quartz* association. Its texture is particularly typically developed in Fig. 3.23.

3.5.4. Parameter related to mutual inclusion of mineral phases

Further indications as to the relative position of mineral phases within a texture can be obtained by recording the mutual inclusion of mineral phases. This has been done in Table 3.5 and the mutual relationships are depicted in Fig. 3.20 in a way similar to that of the association diagrams, but with the difference that the arrows here indicate inclusion and not association.

The analysis shows that:

K-feldspar encloses *quartz*, *plagioclase*, b_f, b_a

quartz encloses *plagioclase*, b_f, b_a

b_f encloses *quartz*

plagioclase encloses b_a

b_a encloses no other minerals (except *epidote* and some *quartz*, but they are included in the definition of b_a).

3.6. DISCUSSION

3.6.1. The significance of water in the crystallisation of a granitic melt

The stability of phase assemblages in the system T-XH_2O has been

Table 3.5 Synoptic diagram showing mutually enclosing relationships of mineral phases in granodioritic rocks.

enclosing mineral

	plg	*bf*	*ba*	*qtz*	*kf*	*sph*	*ep*	*ap*	*zi*	*ore*
plg				x	xx	x				
bf				x	(x)					
ba	xx			x	x					
qtz		x			x	x				
kf				x	x					
sph	x									
ep		xx	x	x		x				
ap	x	xx	x		x	x				
zi	x	x	x		x	x				
ore	x	x	x							

xx common occurrence
x occasional occurrence
(x) rare occurrence

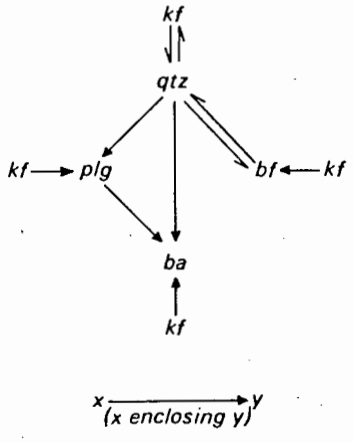

Fig. 3.20 Graphical representation of textural relationships as derived from Table 3.5. See text for discussion.

experimentally determined by a number of authors (e.g. Piwinskii, 1968; Gibbon and Wyllie, 1969; Lambert *et al.*, 1969; Piwinskii and Wyllie, 1970; Mc Dowell and Wyllie, 1971; Robertson and Wyllie, 1971; Maaløe and Wyllie, 1975; Whitney, 1975a) and since it is of particular importance for the following discussion, this problem is presented here first.

Recent investigations stress the importance of water undersaturation in the crystallisation of melts. Maaløe and Wyllie (1975), investigated natural samples of the Bohus granite (Norway/Sweden) and determined its phase relationships experimentally at 2 kb and various degrees of water saturation. By comparison with the natural crystallisation sequence deduced from textural

evidence, they suggested a water content of less than 1,2 percent for the original magma and concluded that granite formation under water saturated conditions might generally be rare.

The most comprehensive experimental study on the stability of phase assemblages in granitic systems has been undertaken by Whitney (1975a), who investigated four different synthetic compositions under various P/T conditions and with different wt percent H_2O in the original melt. He particularly pointed out the helpfulness of studies of this kind in the interpretation of the crystallisation and intrusion history of a granitic body and for these reasons simplified schematic T-XH_2O diagrams have been included here (Fig. 3.24). Although the liquidus temperatures and the temperatures of first occurrence of mineral phases differ between different investigations and with the bulk composition of the system, the crystallisation sequence *plagioclase - K-feldspar - quartz* emerges as a constant feature at lower pressures and independent of water content. Since the stability curve for biotite is less strongly dependent on XH_2O than that for anhydrous minerals, the textural relationships of biotite are most important, when as in the present case, deductions as to the original water content of a magma are attempted.

3.6.2. Two biotite generations : possible explanations

Biotite has been shown to occur in two textural modifications, which are associated with different mineral species. This of course, raises the question as to a difference in the mode of origin of each of these modifications.

One possible explanation is the crystallisation of b_a and b_f at different stages during crystallisation of the magma. Particularly the inclusion of b_a in plagioclase suggests contemporaneous crystallisation of plagioclase and b_a, while the positive association of b_f and quartz suggests a contemporaneous crystallisation for both of them during a later stage.

Formation of both types of biotite at two different stages during crystallisation, however, appears to be incompatible with crystallisation sequences suggested by T-XH_2O diagrams, unless a variation of water content or pressure of the magma are assumed during crystallisation. This could include repeated crystallisation and refusion of the magmatic rock during intrusion into higher levels and has been suggested as a mode of formation for many intrusive rocks by Cann (1970) and Martin and Bonin (1976). In this case, b_a would be the relic of an earlier crystallisation under different conditions of water saturation, pressure and temperature, and b_f would represent the latest crystallisation of biotite.

Another explanation that should be considered is the incongruent melting of hornblende during crystallisation of a magma. Biotite-hornblende reactions have been reported only from melting experiments (e.g. Gibbon and Wyllie, 1969). Büsch *et al.*, (1974) described the textural development during the formation of hornblende from biotite during melting of a granodioritic

rock. Knabe (1970) investigated experimentally the influence of biotite composition on the temperature of the biotite-hornblende*-reaction and found that the reactions involving Fe-rich biotite take place at lower temperature than those involving very Mg-rich biotite.

Since there is no reason to assume that this reaction is not reversible, hornblende formed at early stages of crystallisation may eventually become unstable with progressive crystallisation of non-K-bearing phases and concomitant increase in H_2O and K_2O in the rest melt.

The reaction

biotite + quartz = hornblende + melt (K_2O, Al_2O_3, H_2O) (simplified after Knabe, 1970)

may thus be finally forced into the left direction.

In this regard it is noteworthy that formation of hornblende from biotite has actually been observed in the Helskloof Migmatitic Complex where granodioritic members of the Vioolsdrif Intrusive Suite undergo migmatisation (p.171, Fig.6.11).

This shows that this reaction is possible in principle in biotites of the Vioolsdrif Intrusive Suite at temperatures slightly above solidus.

The possibility of transformation of hornblende into biotite during crystallisation of a magma cannot therefore be ruled out and is adopted as a working hypothesis in the following chapters.

3.6.3. Metasomatism

Signs of large-scale metasomatism in the Vioolsdrif Intrusive Suite are rare. On a smaller scale various textural features have been observed that could be interpreted as being of metasomatic origin:

a) "digestion" of plagioclase by K-feldspar (Figs. 3.9, 3.11, 3.21)
b) assimilation of biotite aggregates by K-feldspar (Fig. 3.10)
c) muscovitisation of biotite in contact with K-feldspar (Fig. 3.8)
d) rims of unaltered plagioclase at the contact with K-feldspar.

However, most of these features may as well have formed at temperatures above solidus. Only in the case of partial assimilation of plagioclase by K-feldspar (Fig.3.11) is a subsolidus reaction likely, since in this case the saussuritic alteration products of plagioclase appear to be affected as well, provided

---

* This reaction is known in the literature as biotite-hornblende-reaction (Büsch *et al.*,1974) and therefore this term is maintained here. The modification of amphibole formed during this reaction depends largely on the composition of the reacting biotite (Knabe, 1970). It is simplified here and in the following as hornblende.

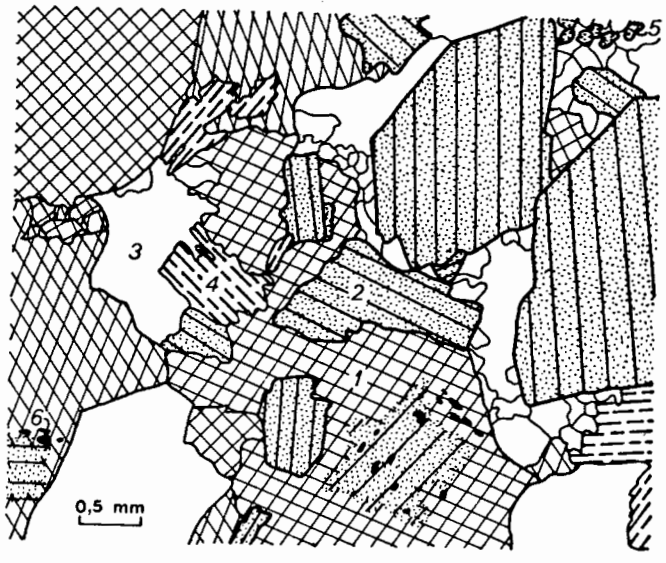

Fig. 3.21 Granitic texture of type A with anhedral K-feldspar (1), subhedral to euhedral plagioclase (2), and interstitial quartz (3). (4) biotite, (5) epidote. Some epidote grains also occur interstitially with quartz. Plagioclase is enclosed in K-feldspar as euhedral prisms with sharp boundary or as partly assimilated grains (below, centre left). Epidote as an alteration product of plagioclase is partly surrounded by K-feldspar, suggesting subsolidus metasomatic assimilation (6). (420-15/43)

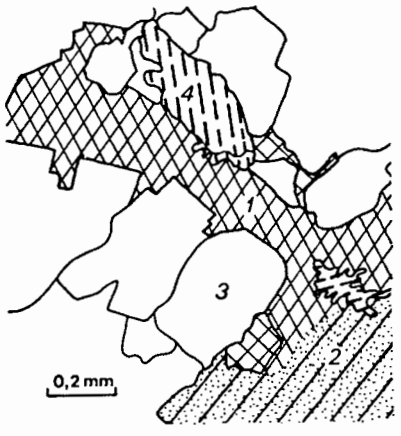

Fig. 3.22 Granitic texture. (1) K-feldspar (2) plagioclase (3) quartz (4) biotite. Biotite is corroded by K-feldspar. (425-7/66)

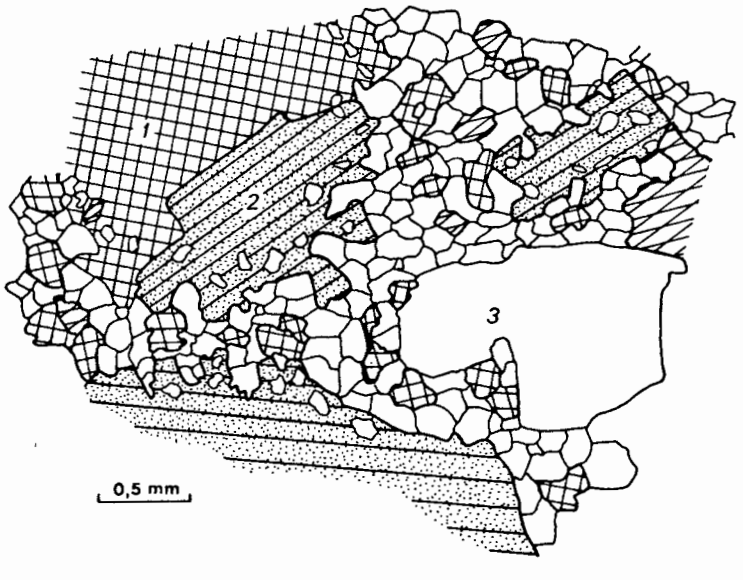

Fig. 3.23 Granitic texture with strongly developed bimodal grainsize distribution with quartz, K-feldspar, plagioclase as phenocryst phases and the same minerals as groundmass phases. Euhedral faces of plagioclase at contact with K-feldspar and anhedral faces at contact with groundmass indicate partial resorption of the phenocryst phases after their formation. (1) microcline (2) plagioclase (3) quartz. (427b - 15/56).

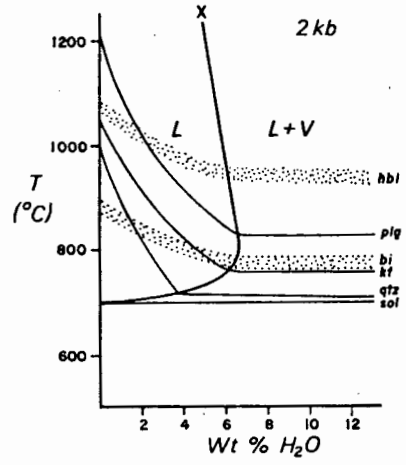

(a)

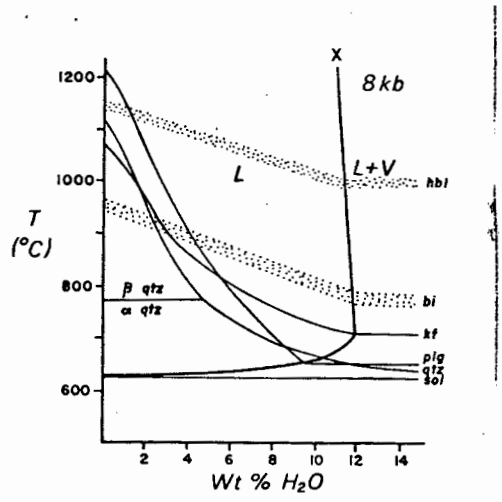

(b)

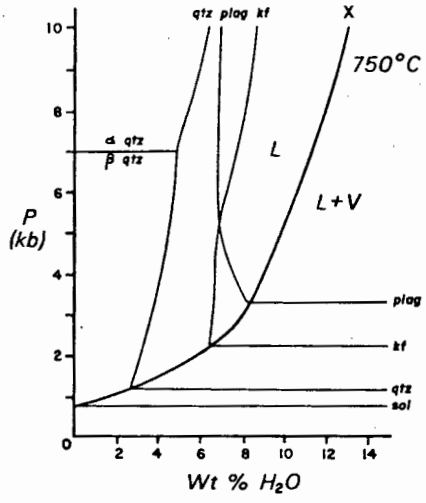

(c)

Fig. 3.24 T-XH_2O, P-XH_2O simplified after Whitney (1975a) illustrating melting relationships in a synthetic rock of granitic composition. Biotite is inferred after Piwinskii (1968), Gibbon & Wyllie (1969), Robertson & Wyllie (1971), Maaløe & Wyllie (1975). Hornblende is inferred after Piwinskii (1968), Gibbon & Wyllie (1969), Robertson & Wyllie (1971).
The boundaries are upper stability limits during melting.

X : water saturation boundary
L : liquid
V : vapour

that saussuritisation itself has taken place at subsolidus temperatures.

3.6.4. The problem of the lack of contact phenomena

In view of the large volumes of intrusive rocks in the northeastern Richtersveld the lack of contact phenomena is somehow surprising and has to be explained. It is possibly a problem of non-recognition and accounted for by several factors:

a) In volcanics of granodioritic to granitic composition no mineralogical changes will occur from the beginning of low grade metamorphism (*sensu* Winkler, 1974) to the breakdown of muscovite + quartz during higher grade metamorphism. If, as in this case, low grade regional metamorphism has occurred subsequent or prior to contact metamorphism, the latter is likely to be obliterated.

b) Relatively fine-grained metamorphic rocks have always been known from contact metamorphism (so-called hornfelses). There is therefore no need to assume a coarsening of the texture in excess of that of regional metamorphism.

c) Melting of the country rocks at intrusive contacts has been reported by De Villiers and Söhnge (1959) and Ward (1977) and was said by them to be responsible for basification of the intrusive rocks at contacts with mafic volcanics. Theoretically melting could have occurred at sharp angular contacts: using the equation given by Jaeger (1961) for the relationship between contact temperature and contact shape

$$T_c = T_i \frac{\alpha}{2\pi}$$

T_i = intrusive temperature
T_c = contact temperature
α = interior angle measured between planar contacts

the contact at a 90° outside corner will reach only 25 percent of the intrusive temperature and a 90° inside corner will reach 75 percent of the intrusive temperature. It also follows that rock fragments which are totally enclosed in intrusive magma will soon assume the intrusive temperature ($\alpha = 360°$). This means that only an intrusive magma of more than approximately 700°C (at 2 kb) would have been able to melt wall-rock fragments of the kind shown in Fig. 3.2.

The wall-rock temperature, however, decreases exponentially with the distance from the contact, which is shown in Fig. 3.25 for different intrusive temperatures and 200°C wall-rock temperature. Accordingly, the contact temperatures will decrease relatively rapidly away from the contacts.

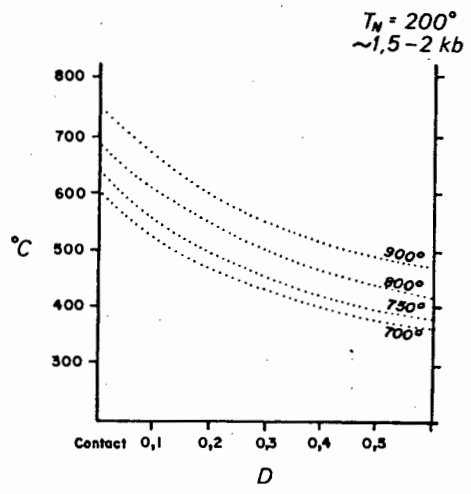

Fig. 3.25 Calculated wall-rock temperatures for sheet-like intrusive ($\alpha = 180^{o}$) in the vicinity of contact for various intrusive temperatures. (after Winkler, 1974; Jaeger, 1957) T_n = temperature of wall-rock prior to intrusion. D = thickness of intrusion. 0,1 - 0,5 = distance from contact as fraction of D.

Furthermore it must be taken into account that the main intrusion in the central northeastern Richtersveld is composed of several bodies of varying age. So, for example, in the east, the relatively thin sheet of G_1 can hardly be expected to have caused extensive contact heating. When the larger volumes of G_2 were intruded, G_1 must have been solidified already and therefore G_2 could not exert its contact influence directly on the volcanics. The same mechanism may have acted during the later G_3 and G_4 intrusions. The absence of notable contact phenomena can therefore be well explained if one takes into account the composition of the wall-rock, the duration and extent of contact influences and the temperatures that are likely to have been reached. Furthermore, the mineralogy insensitive to change in metamorphic grade, the effects of subsequent or previous regional metamorphism and the scarcity of water in the intruding melt, do not facilitate the recognition of contact phenomena.

3.6.5. The sequence of crystallisation as deduced from textural analysis

The crystallisation sequence outlined below assumes that b_a has crystallised as hornblende during early stages of crystallisation. For application to different hypotheses *"hornblende"* must of course be read as b_a and the reaction *hornblende* $\rightarrow b_a$ at lower temperatures is no longer necessary. The sequence of crystallisation of the main mineral constituents is supported by the following textural features:

hornblende (b_a) : enclosed in *plagioclase*, *K-feldspar*, *quartz* and enclosing no other minerals. Strong positive statistical association with *plagioclase* .

plagioclase : enclosed by *K-feldspar* and *quartz*, but enclosing b_a. Display of euhedral faces against *K-feldspar* and *quartz*. Positive statistical association with b_a .

quartz : enclosed only in *K-feldspar*, but enclosing b_f, b_a and *plagioclase*. Occasional euhedral faces against *K-feldspar*. Positive statistical association with *plagioclase* and b_f.

b_f : enclosing *quartz* and enclosed by *quartz* and *K-feldspar*. Positive association with *quartz*, negative or low association with *plagioclase* and b_a.

K-feldspar : enclosing all other minerals and occasionally enclosed by *quartz*. Euhedral faces against *quartz*. Positive association with *quartz*.

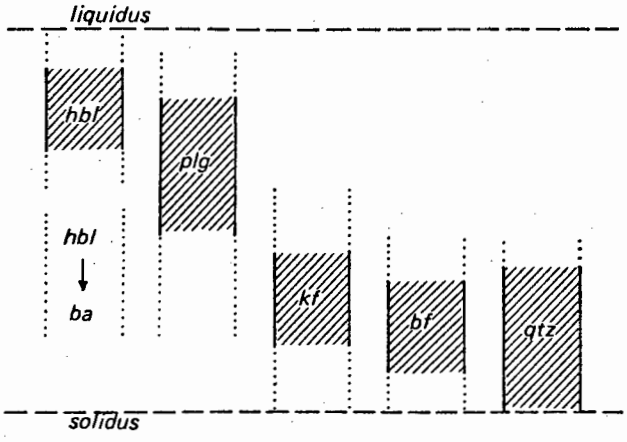

Fig. 3.26

The crystallisation sequence as shown in Fig. 3.26 therefore appears to be best in agreement with textural data.

3.6.6. The water content of the original magma

Comparison of the crystallisation sequence determined in Fig. 3.26 with possible crystallisation sequences (Fig. 3.24) indicates that the sequence found cannot be matched with any possible sequence in the water saturated region of the diagram. It can, however, be matched at 2 wt percent water (Fig. 3.24a).

Since the composition of the rock in diagram Fig. 3.24 is not completely consistent with the composition of the rocks investigated here, the value of 2 percent is naturally only approximate. Nevertheless, a water content of more than 3 percent is unlikely from comparison with other investigations (Robertson and Wyllie, 1971; Maaløe and Wyllie, 1975) which all show the intersection of the stability curves of biotite and quartz at 2 percent it and less. Water saturation can be ruled out completely, since in this case all biotite should show signs of crystallisation contemporaneous with plagioclase.

The rocks investigated have therefore crystallised from a melt which was undersaturated in water, possibly as low as 2 percent. Low water content is in agreement with lack of pegmatites related to the Vioolsdrif Intrusive Suite and rarely developed metasomatic features on the macroscopic and microscopic scale.

3.6.7. The significance of the two textural types

The presence of two textural types, however, if only weakly developed, indicates that conditions were not as simple as could appear from the preceding chapter. Whitney (1975a) pointed out that any change in pressure, temperature and wt percent water will lead to instability in already crystallised phases, causing either their disappearance or corrosion and partial assimilation. The phase boundaries in T- and P-XH_2O diagrams need not be crossed for this purpose. It is likely that events of this type will be recorded in the texture of the rock and that the features under discussion represent such an event.

In sample 427 texture B is most characteristically developed (Fig. 3.23) and it is therefore best suited to show in principle the mechanisms involved.

Separate estimates of the composition of its groundmass and phenocryst phase (*phase I*= ~50%) indicate that approximately 15 percent of the quartz 90 percent of plagioclase and 40 percent of K-feldspar had already crystallised when the texture-forming event occurred. Textural considerations suggest furthermore that only minor amounts of *phase I* have been assimilated (Fig.3.23) during this event. Judging from the composition of *phase I* it is unlikely to have formed below 800°C at 2 kb and 2 percent water. Taking into account these restrictions the following texture-forming mechanisms must be considered:

i) adiabatic intrusion:

Incipient crystallisation at low crustal level (Fig. 3.24b). At about 850°C relatively rapid intrusion into higher crustal levels occurs (Fig. 3.24a). It is evident from Fig. 3.24 that now particularly quartz becomes unstable as its stability boundary is likely to be crossed or approached. The result will be resorption of *phase I* material.

ii) change of water content of the melt:

Crystallisation at moderate pressure. Around 800°C influx of water occurs which causes a shift of the system to the right and thus results in assimilation of *phase I* material. It is evident from Fig. 3.24 that already small amounts of water may cause considerable instability in the system.

iii) rise in temperature:

This mechanism requires either exothermic reactions during cooling or sudden changes in heat conductivity of the wall-rock. Both are unlikely. A final solution to the question which of these mechanisms applies here is

difficult to find. The writer favours mechanism i) or ii). Mechanism ii) would result in a model similar to that proposed by Cann (1970) and Martin and Bonin (1976). The enrichment of potassium in the granitic phase favours this explanation. On the other hand this mechanism works only if the rock concerned is nearly completely crystallised, since diffusion of water is very slow in granitic liquids (Shaw, 1974), but the presence of a 50 : 50 crystal-liquid mush is one of the restrictions imposed on the discussion.

Mechanism i) is again favoured by occasionally distorted plagioclase twins, which may indicate a mechanical strain exerted on *phase I* crystals during rapid intrusion. In this case also b_a would have to be assumed to have formed from hornblende, which is supported by the previous theoretical consideration and by the occurrence of hornblende in a textural position similar to that of b_a in fine-grained granodiorite (G_1) (cf. p. 46), where it might have been preserved due to different mechanisms of intrusion. In case ii), however, repeated crystallisation and refusion makes a primary formation of b_a as biotite likely.

3.6.8. Economic applications

Various authors emphasised the importance of aqueous solutions to the formation of porphyry ore deposits. Holland (1972) pointed out the three main factors for the formation of this type of deposits:

1) Water, contained in a magma, released as hydrothermal solution during crystallisation

2) These hydrothermal solutions contain the metals that give rise to the ore deposits

3) Decrease of P/T and the reaction of the solutions with the wall-rocks leads to precipitation of the ore.

He found by means of experimental investigations that metals such as manganese, zinc and lead are the more soluble the higher the chloride content of the solution and that therefore the extraction of these metals from granitic magmas depended on :

a) the initial chloride content
b) the initial water content of the magma
c) the time relationship between the separation of a vapour phase and the crystallisation of the melt

Sillitoe (1973) in dealing with the main geological properties of porphyry copper deposits, emphasised their close relationship with calc-alkaline volcanic and plutonic activity and their general location at the boundary between volcanic and plutonic environments in many South American deposits. Whitney (1975b) in a study of exceptional clarity devised a synthetic model of vapour generation during cooling within an intrusive stock at the example

of a quartz-monzonitic magma, based on experimental investigations. He showed that the P/T range in which a free vapour phase coexists with melt, decreases with decreasing wt percent water of the original melt and that it is in a general way dependent on the composition of the magma. Using a simplified model of temperature distribution within a cooling intrusive stock, he arrived at a zonation pattern similar to that found by Sillitoe (1973) by geological means.

Looking at Fig. 5 of Whitney (1975b), it is obvious that in such a stock-like intrusion the size of the field in which liquid+vapour are stable:

a) decreases with decreasing water content of the original magma,
b) decreases with time, i.e. in the course of cooling.

However, it is exactly this field, where as implied by Holland (1972), the conditions are particularly favourable for the extraction of metals from the melt by chloride solutions. It follows that lack of sufficient initial water can prevent the formation of a porphyry ore deposit.

It is furthermore shown by Whitney's (1975b) results that the boundary of the field in which L and V coexist shifts towards lower pressures with decreasing wt percent H_2O of the original melt. This means in geological terms : the lower the water content of the magma, the higher the level to which mineralisation is restricted.

If therefore the assumption is correct that the water content of a granitic magma plays a major role in the formation of porphyry ore deposits, it follows that only those parts of the Vioolsdrif Intrusive Suite which are regarded as particularly high-level intrusions for geological reasons, can be expected to show significant ore mineralisation.

It has been indicated in a previous chapter that parts of the fine-grained granodiorite might belong to a subvolcanic environment and therefore meet the geological conditions for enrichment of metal phases. The fact that such enrichments have indeed been found in the area envisaged (and only there) and in notable amounts only in those parts that must be regarded as the highest subvolcanic level, speaks well in favour of the theory outlined here.

3.7. CONCLUSION

Four mappable members of the Vioolsdrif Intrusive Suite have been distinguished in the northeastern Richtersveld. The two older members - granodioritic - are syn- to late tectonic with respect to F_1 and, by analogy with the Haib area, approximately 1900 my old. The two younger granitic members are posttectonic and approximately 1750 my old.

The earliest member of the Vioolsdrif Intrusive Suite (G_1), is for geological reasons likely to constitute a subvolcanic link with the Orange River volcanics, thus corroborating a view earlier arrived at on geochemical grounds

Table 3.6 Rocks of the Vioolsdrif Intrusive Suite, summary

map unit / rock type	Structural and metamorphic environment, mode of origin	time age (my)	relationships evidence
G_1, fine-grained granodiorite	Subvolcanic with respect to volcanics of the Orange River Group	1957 ± 54	inferred from radiometric data of the Orange River Group in the Haib area Reid (1978)
G_2, even-grained granodiorite	syntectonic (F_1), intrusive into De Hoop Subgroup and Rosyntjieberg Formation	1900 ± 30	inferred from radiometric age determinations in the Haib area (Reid, 1978)
G_3, granite	intrusive into G_2, post-tectonic (F_1).	1731 ± 20	inferred from radiometric age determinations in the Haib area (Reid, 1978)
G_4, leucogranite	intrusive into G_3	as G_3	

(Reid, 1977). As to the composition, the granitic (G_3) phase is distinguished from the granodioritic members by its higher alkali content, while the SiO_2 content is virtually in the same range. This is supported by modal analysis which shows constant quartz but variable K-feldspar contents (Fig. 3.4).

Textural properties were investigated both qualitatively and quantitatively (grain transition probabilities) and revealed :

a) the presence of a texture-forming mechanism other than single-step crystallisation that imparted an imprint on the original magmatic texture (Texture A) in order to transform it into Texture B

b) the presence of two generations of biotite, statistically associated with plagioclase (b_a) and with quartz (b_f) respectively

c) the presence of a distinct crystallisation sequence which is indicative of low water content of the original magma.

a) and b) can be explained in terms of an intrusive history comprising multiple cycles of crystallisation and refusion by repeated influx of water and mobile elements prior to the final stage of intrusion. The fact that G_3 shows enrichment of alkalis with respect to the granodiorite is in support of this model and suggests alkalinisation of an originally granodioritic magma. The presence of two biotite generations can be explained by the transformation of primary hornblende into biotite at later stages of crystallisation (biotite-hornblende- reaction of Knabe, 1970; Büsch *et al.*, 1974).

The low water content of the original magma deduced from the crystallisation sequence has certain economic implications as it confines the site of possible porphyry ore mineralisation to the upper part of subvolcanic environments provided the water content of the intrusive magma plays a major role.

This and the fact that in the Richtersveld (uneconomic) enrichment of sulphides has as yet only been found in those parts that have been inferred from mapping to constitute a subvolcanic environment, support the findings presented here and also the assumption that porphyry ore deposits are dominantly controlled by the water content of the original magma.

Chapter 4

LITHOLOGY AND STRATIGRAPHY OF MARGINAL PARTS OF THE RICHTERSVELD

4.1. THE SOUTHEASTERN RICHTERSVELD

4.1.1. Rocks of supracrustal origin

Two stratigraphic entities of rocks of supracrustal origin can be recognised in the southeastern Richtersveld.

The metavolcanics have been assigned the rank of a formation in order to achieve a complete subdivision of the Orange River Group into formations.

The Namaqua rocks underlying the metavolcanics have been informally termed Pink-gneiss Unit in order not to anticipate a future stratigraphic correlation within the Namaqua Metamorphic Complex.

1. *Pink-gneiss Unit (map unit Gn)*

a) Field appearance and extent

Rocks informally referred to as Pink-gneiss Unit, mapped by De Villiers and Söhnge (1959) as "muscovitised granite" of Namaqualand and by Joubert (1971) south of the Richtersveld as "aplogranitic gneiss", were found to consist of a variety of rock types in the present area. Due to their importance as to the relative ages of "Richtersveld rocks" and "Namaqualand rocks", the area has been mapped in more detail. By applying a technique of grouping together rock associations rather than predominant rock types, with special emphasis on significant rock types occurring in minor amounts (Leitschichten Kartierung *sensu* Pilger, 1952), shown to be very effective in the detailed mapping of seemingly monotonous metamorphic terranes (Pilger *et al.*, 1975; Kleinschmidt *et al.*, 1975; Kleinschmidt and Ritter, 1976), it has been possible to distinguish the following succession : from below

Gnα a) *Pink-gneiss Zone* : Pink gneiss with minor amounts of muscovite schist

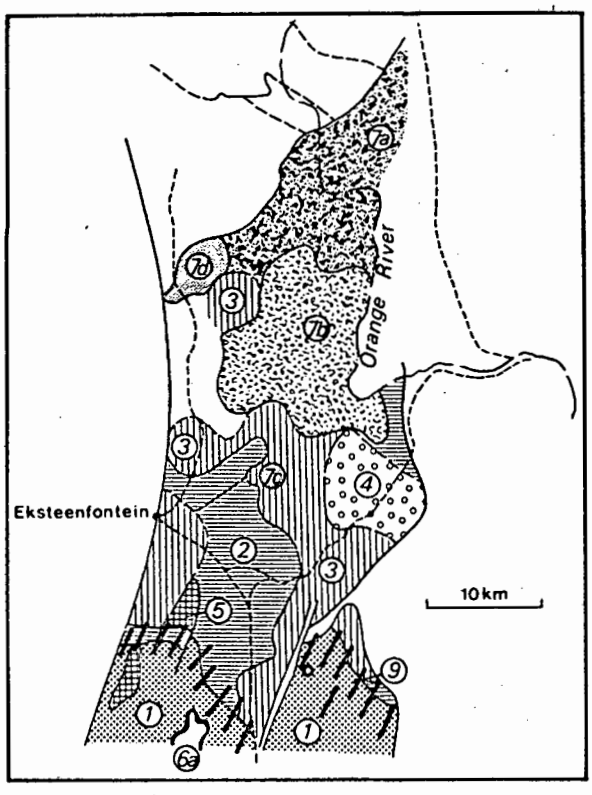

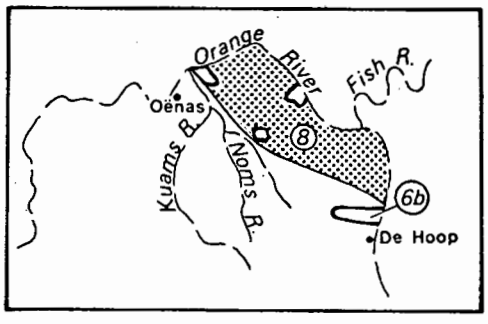

Southeastern Richtersveld

Noms River - Blockwerf area

Fig. 4.0 Key map of marginal parts of the Richtersveld

Map units:
1) PGU
2) Windvlakte F. (southern part)
3) Vioolsdrif granodiorite (G_2)
4) HMC
5) Megacrystic granite
6a) Kromnek granite
6b) Oenas granite
7a) RIC, Sambok River Intr.
7b) RIC, Xaminxaip - Blackface Mountain Intr.
7c) RIC, Rooiberg Intr.
7d) Klipbokkop Intr.
8) BMC
9) Pegmatites

Gnβ b) *Quartzite Zone :* muscovite-biotite schist, quartzites embedded in pink gneiss and muscovite schist

Gnγ c) *Transitional Zone :* metavolcanics of the Richtersveld type, often strongly deformed, muscovite and muscovite-biotite schists, amphibolite

V_R d) *Richtersveld metavolcanics*

According to this sequence, the rocks of the Pink-gneiss Unit structurally underlie the metavolcanics of the Richtersveld.

Although there is no direct evidence that this succession is the original sedimentary one, there is also no evidence for large-scale regional overturning. On the contrary, gently north-dipping S_1 and SS_1 of the Pink-gneiss Unit could be linked with south-dipping SS_1 of the Rosyntjieberg Formation to form a regional syncline which again is situated along strike of a major syncline underlying much of the Haib volcanics (Blignault, 1977).

b) Composition and mineralogy

No modal analysis has been carried out on rocks of the Pink-gneiss Unit since the mineralogy and composition are relatively simple. The mineral assemblage of major rock types is displayed in Table 4.1.

Muscovite schists contain rather variable amounts of muscovite and sericite but quartz generally tends to predominate over muscovite. Muscovite gneisses typically contain equal amounts of plagioclase, K-feldspar, quartz and muscovite, and biotite gneiss is approximately granodioritic in composition.

Some of the sericite in schists and gneisses seems to be formed after sillimanite. This and textural relationships will be discussed with regard to metamorphism in Chapter 6.

2. *Windvlakte Formation (map unit V_R, Vm, Vw)*

a) General

In order to achieve a complete subdivision of the supracrustal rocks of the Richtersveld into formations, all metavolcanics of the Richtersveld south of the Rosyntjieberge have been included in the Windvlakte Formation. These volcanics are distinguished from the volcanics in the north by stronger recrystallisation, the stronger the farther to the south, with finally only palimpsestic remnants of the original volcanic texture mainly in the form of volcanic phenocrysts.

The exact stratigraphic position of the Windvlakte Formation is not known. It overlies the Rosyntjieberg Formation in the north but also the Pink-gneiss Unit in the south. However, since this formation is torn apart by subsequent intrusions and deformational events, its various parts may represent rather different stratigraphic positions.

Table 4.1 Mineral assemblages of major rock types of the Pink-gneiss Unit

	qtz	*plg*	*kf*	*bi*	*chl*	*hbl*	*ep*	*mu*	*ser*	*fibr*	Rock type
210/1	x				(x)			x	x		muscovite-schist
285/5	x				(x)			x	x		muscovite-schist
285/3	x				(x)			x	x		muscovite-schist
343/2	x			(x)	(x)			x	x		muscovite-schist
355	x	x	x	(x)			x	x	x		muscovite-gneiss
389	x	x	x					x	x		muscovite-gneiss
340	x	x	(x)	x	x		x		(x)	x	biotite-gneiss
389/1	x	x		x	(x)	x	x		x	x	amphibolite

x = common
(x)= occasional

b) Field appearance and regional distribution

Metavolcanics of the southeastern Richtersveld are green-grey to light-grey and at places display fine banding and lamination. The latter has been found in association with cross-bedding and can therefore be regarded as primary layering (SS_1). They are markedly unfoliated and in the typical case therefore show the woolsack-type weathering of isotropic granoblastic rocks. From Rooiberg towards the south and east, the leucocratic volcanics are increasingly migmatised. Although migmatisation is only encountered locally, all types of migmatite are already present but stromatic, dictyonitic and agmatitic structures predominate. Even though deformation of neosomatic structures is common, completely undeformed veins and patches of neosome occur as well and emphasize the basically posttectonic character of migmatisation.

c) Composition

The modal composition of metavolcanics shows a spread between granitic and granodioritic composition (Fig. 4.1) and is thus in agreement with major element chemical analyses (Table 4.2) which indicate predominantly granodioritic composition. One sample plotting in the alkali granite field is likely to be metasomatically enriched in K-feldspar at the margin of an intrusion of the Richtersveld Igneous Complex.

d) Texture and mineralogy

As can be expected in rocks of $\pm$ dacitic composition, the mineralogy is uniform and consists of quartz, plagioclase, biotite (green to green-brown), muscovite (mostly unperthitic), epidote, sericite and

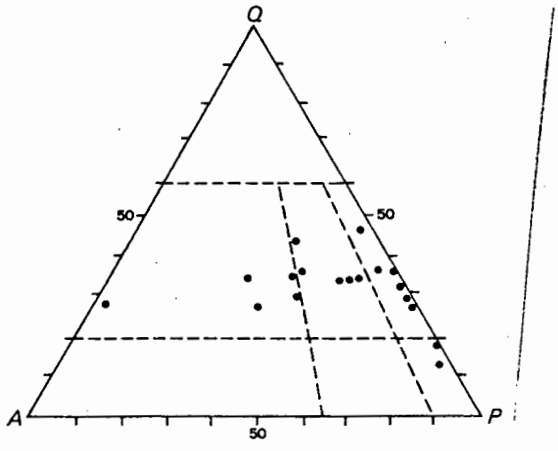

Fig. 4.1 Modal composition of metavolcanics of the southeastern Richtersveld.

occasional muscovite. These minerals make up a texture that can be described only unsatisfactorily as granoblastic inequigranular interlobate and is derived from the superposition of a metamorphic texture on the original volcanic texture.

Table 4.2. Major element analyses of metavolcanics of the Windvlakte Formation south of the Rooiberg. The oxides have been recalculated to 100% after analyses of the Geological Survey. They are included here only for the sake of completeness. Sample 221 : metasediment intercalated in volcanics.

	237/	238/1	267/	290/1	307/31	311/2	319/1	221/
SiO_2	61,98	56,87	62,47	62,5	68,76	61,58	69,25	80,49
TiO_2	1,05	0,77	1,08	0,77	0,33	0,67	0,36	0,67
Al_2O_3	16,75	17,50	16,79	17,14	14,74	17,16	14,36	11,50
Fe_2O_3	2,31	1,64	2,39	0,10	0,33	1,44	0,88	0,5
FeO	3,27	5,16	3,22	3,84	2,52	4,69	1,47	1,96
MnO	0,06	0,14	0,11	0,09	0,09	0,13	0,86	0,02
MgO	0,35	4,17	0,25	2,44	0,55	2,70	1,34	0,27
CaO	6,21	6,61	6,21	5,55	2,94	5,16	1,78	0,04
Na_2O	3,70	2,66	3,81	3,24	3,67	2,5	3,55	7,35
K_2O	1,66	1,82	1,66	2,50	3,28	2,96	4,27	0,32
P_2O_5	0,38	0,48	0,38	0,43	0,11	0,20	0,19	0,03
H_2O+	1,97	1,95	1,40	1,14	2,45	0,40	2,20	1,57
H_2O-	0,31	0,23	0,23	0,24	0,21	0,40	0,24	0,28
Ba	0,64	0,84	0,64	0,12	0,64	0,28	0,88	0,15
S	0,02	0,02	0,03	0,03	0,04	0,01	0,10	0,02

4.1.2. Intrusive rocks

In contrast to the central northeastern Richtersveld, a variety of intrusive rocks appear in the southeastern Richtersveld. They are presented here with decreasing age of emplacement.

1. *Rocks of the Vioolsdrif Intrusive Suite (map unit G2)*

a) Extent and field appearance

In contrast to the Vioolsdrif intrusives north of the Van Zyls River where metamorphic and tectonic features are discernible only with difficulty, the effects of such imprints are more evident in the meta-intrusives of the southeastern Richtersveld.

Most of the pre-Richtersveld Igneous Complex basement of the Richtersveld south of the Van Zyls River is made up of rocks of the Vioolsdrif Intrusive Suite which occur here as leucocratic to melanocratic relatively coarse-grained granodiorite (G2), while granite (G3) and leucogranite (G4) are missing. Distinctly melanocratic intrusives occur around the Van Zyls River and at Soetgat. The Struishoek intrusion appears to be variable between melanocratic and mesocratic, while parts of the intrusion east of Klipbok are leucocratic and mesocratic.

A north-south striking foliation (S_2) is particularly developed in granodiorites of the southernmost area and imparts a distinct gneissic appearance on the rock. It decreases in intensity towards the north and finally disappears.

Towards the southeast the Vioolsdrif granodiorites are increasingly migmatised and finally make up a migmatitic terrain that will be treated as Helskloof Migmatitic Complex.

b) Contact relationships

The size and outlines of individual intrusions are obliterated by deformation of the Devilscastle type (S_3) and therefore unaltered wall-rock-intrusive relationships are rarely observed. Minor intrusive bodies a few metres across are commonly found in volcanics of the Winvlakte Formation, and here the contacts are usually sharp.

It is especially in the area east of the Rooiberg that rather strong foliation and incipient migmatisation render the distinction between volcanics and intrusives difficult and it is possible that more supracrustal rocks are hidden in this region than have actually been mapped.

c) Composition

The modal composition is shown in Fig. 4.2 and in Figs. 4.6a-c the modal compositions of some granodioritic migmatitic paleosomes in relation to migmatitic neosomes are shown.

	Granodiorite, SE Richtersveld					Helskloof diatexites		
	194/1	208/12	287/1	295/	302/3	213/9	303/2	305/
SiO	63,36	67,09	65,32	63,48	70,69	63,44	70,04	70,93
TiO	0,91	0,45	0,61	0,72	0,33	0,77	0,48	0,37
Al_2O_3	17,09	14,31	14,15	16,23	11,85	16,60	16,18	13,65
Fe_2O_3	1,57	0,18	1,20	0,44	0,10	2,66	1,85	0,86
FeO	3,98	3,86	3,12	4,42	2;37	2,33	0,89	1,80
MnO	0,06	0,13	-	0,06	0,05	0,10	0,04	0,01
MgO	1,52	2,25	0,77	2,09	1,38	1,13	0,37	1,53
CaO	4,51	3,72	3,69	4,00	2,08	4,30	2,91	2,86
Na_2O	2,28	2,19	3,05	3,03	2,35	2,86	2,83	3,41
K_2O	3,04	3,50	2,97	3,42	3,93	3,52	3,32	2,38
P_2O_5	3,30	0,26	0,15	0,40	0,17	0,26	0,11	0,23
H_2O+	1,18	1,82	3,55	1,52	2,91	1,61	0,86	1,67
H_2O-	0,21	0,23	1,42	0,18	1,80	0,35	0,11	0,30
Ba	1,13	0,52	0,72	1,24	0,59	1,25	0,73	1,06
S	0,01	0,07	0,02	0,05	0,18	0,02	0,01	0,05

Table 4.3

Major element analyses of Vioolsdrif granodiorite and Helskloof diatexite of the southeastern Richtersveld. The oxides have been recalculated to 100% after analyses of the Geological Survey. They are included here only for the sake of completeness.

Localities:

194/1 : VIS granodiorite, Windvlakte
208/12: granodioritic paleosome (VIS) in Helskloof migmatites
287/1 : VIS granodiorite, Kliphoogte
295 : VIS granodiorite, Klipbok
302/3 : VIS granodiorite, Helskloof

213/9 : diatexite, Helskloof
303/2 : diatexite, Helskloof
305 : diatexite, Helskloof

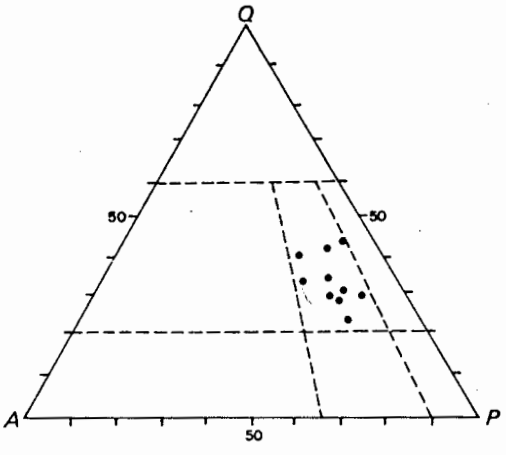

Fig. 4.2. Modal composition of Vioolsdrif granodiorites (G_2) of the southeastern Richtersveld.

d) Mineralogy and texture

The mineralogy is not different from that of granodioritic rocks of the northeastern Richtersveld (cf. p. 43). Although the texture is also similar to textures described from the northeastern Richtersveld, signs of metamorphic reconstitution can particularly be observed in the southernmost part of the Richtersveld (muscovitisation), while elsewhere the main alteration consists in alignment of biotite and biotite aggregates into the direction of foliation.

2. *Helskloof Migmatitic Complex (HMC) (map unit G_M, G_D)*

a) Introduction

While in the area west of the Rooiberg migmatites are only found in leucocratic metavolcanics, migmatites formed from granodioritic rocks of the Vioolsdrif Intrusive Suite are first encountered about 2 km east of the Rooiberg. The amount and structure of the neosomes vary widely even within the same outcrop, but generally the amount of neosome increases towards the east. Metatectic migmatites finally grade into a fine-grained, homogeneous, leucocratic rock, which is regarded as a product of advanced stage migmatisation (diatexite).

Although the western and northwestern boundaries of the Helskloof Migmatitic complex are gradational, its main areal extent appears to be controlled by faults of post-Stinkfontein age, which, through uplift of the eastern block, led to the exposure of deeper crustal levels in the east. In tectonic terms the Helskloof Migmatitic Complex is thus a post-Stinkfontein horst structure.

Migmatisation of the Vioolsdrif Intrusive Suite has also been observed by Bertrand (1976) from the area around Goodhouse, where it gives rise to the Goodhouse granite.

A Rb-Sr whole-rock age of 1750 ± 25 my from the Helskloof area (Corner, 1970, quoted in Köstlin, 1971), is thought to reflect the age of migmatisation and should not be related to the intrusion of the Vioolsdrif Intrusive Suite.

b) Definitions

In order to avoid confusion, only the terminology suggested by Mehnert (1968) for migmatitic rocks is used in the present chapter. The more comprehensive terms as applied in this chapter are defined as follows:

According to Mehnert (1968) a *migmatite* is defined as "a megascopically composite rock consisting of two or more petrographically different parts, one of which is the country rock generally in a more or less metamorphic stage, the other is of pegmatitic, aplitic, granitic or generally plutonitic appearance."

Metatexites (Mehnert, 1968) are formed by "partial, differential or selective anatexis of the low-melting components of the rock" and have thus a distinctly genetical connotation. In the present context, the term is used to describe those parts of the migmatitic terrain in which remnants of the parent rock (paleosome) are still visible, as opposed to diatexites where this is not the case.

The term *diatexite* has been defined by Mehnert *et al.*, (1973) as an anatectic rock " in which the initial melt has not moved from its origin and forms a pore liquid penetrating the rock like a network." Büsch *et al.*, (1974, p.347) and Mehnert (1968, p.253) in addition emphasise the melting of nearly the whole rock during formation of diatexites. In the present investigation the term diatexite is used to describe a massive, leucocratic to mesocratic rock - finer grained than the granodiorite of the Vioolsdrif Intrusive Suite and lacking its biotite aggregates, but coarser-grained than the Windvlakte metavolcanics - which develops gradationally out of schlierig and nebulitic metatexites and shows only subordinate signs of migration.

c) Field appearance

i) Metatexites (*map unit GM*)

A great variety of structural types of migmatites can be found in the present area. They vary considerably even within the same outcrop and it is therefore not possible to express any regional variation on the map. Only in a very general sense do nebulitic and schlierig structures increase towards the east.

In Plate 1 a rather good impression is given of the various types of migmatite encountered in close proximity : dictyonitic, phlebitic and stromatic structures occur virtually in the metre-range from each other. In Plate 2 a migmatite with partly unaltered paleosome (Vioolsdrif granodio-

rite) is shown together with stromatic neosomes. The nearly continuous development of neosome out of paleosome is noteworthy here (unfoliated paleosome - foliated paleosome - finegrained grey neosome in which aplitic leucosome and melanosome are intercalated).

Plate 3 shows a nebulitic migmatite. The whole rock must be regarded as consisting of neosome in an advanced stage of homogenisation but not yet homogenised enough to warrant the term diatexite as applied during this investigation. In Fig. 4.3 a migmatite is presented which had been termed "kryptomigmatite" during fieldwork, since its migmatitic nature is not immediately evident. It rather resembles a granodioritic paleosome with feldspar porphyroblasts. However, "porphyroblasts" of this type may attain sizes of 10 cm across in which case it is obvious even in the field that they are made up of quartz, plagioclase and K-feldspar and thus are of leucosomatic origin. This type of migmatite is most common during advanced stage migmatisation and may come close to what Mehnert (1968) termed "pseudo ophthalmitic structure" (= pseudo augen structure).

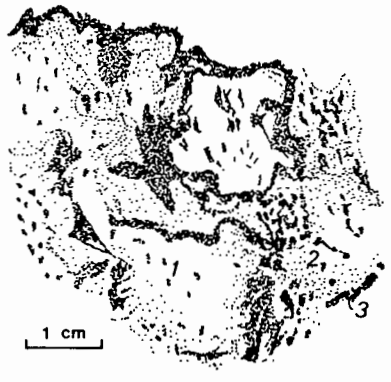

Fig. 4.3. Metatexite with *in situ* differentiation. Schematic view. ("Kryptomigmatite")

1) mainly quartz, plagioclase, k-feldspar = leucosome
2) biotite, epidote, plagioclase
3) biotite, epidote = melanosome

ii) Diatexites (*map unit* G_D)

The diatexites of the Helskloof are massive, leucocratic to mesocratic, finer grained than the granodiorite of the Vioolsdrif Intrusive Suite and lacking its biotite aggregates but coarser grained than the Windvlakte metavolcanics.

Although they develop gradationally out of schlierig to nebulitic metatexites, their main occurrence is bounded by a fault of post-Stinkfontein but probably pre-Nama age which separates them from metatexites in the west and unmigmatised metavolcanics in the east.

iii) Amphibolite (included in *map units* G_M *and* G_D)

In the area of advanced stage metatexis, relatively leuco-

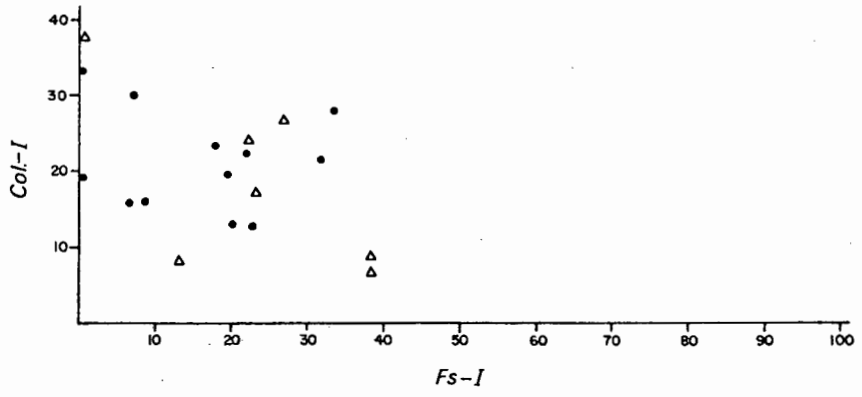

Fig. 4.4(a)
Compositional relationships within Helskloof migmatites

dots:VIS granodiorite, Southeastern Richtersveld;
triangle: granodioritic paleosome

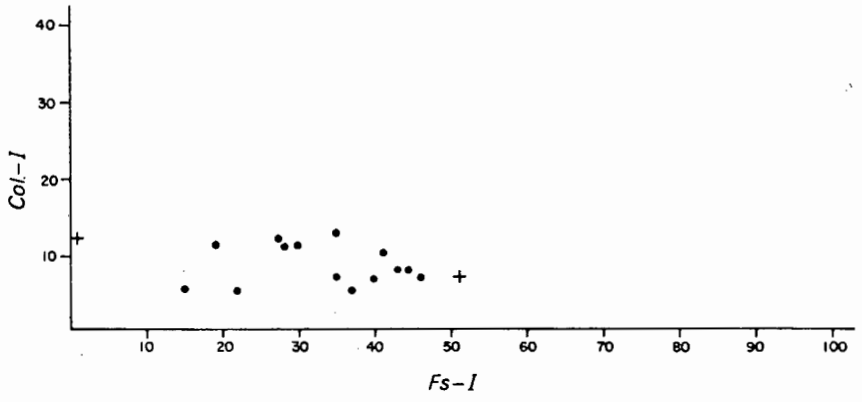

Fig. 4.4(b)
Compositional relationships within Helskloof migmatites

dots:diatexite
cross: leucosomatic diatexite

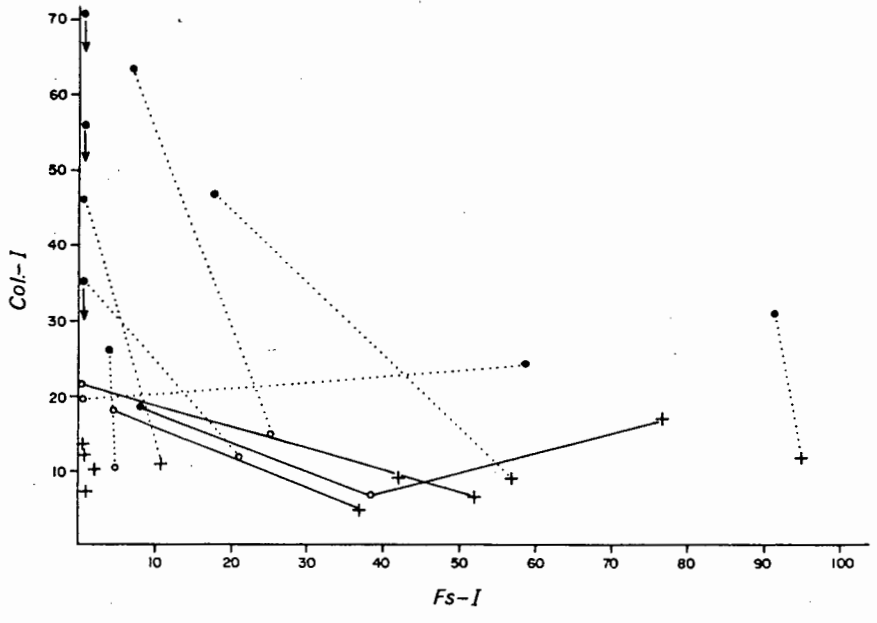

Fig. 4.5
Relationship between paleo-melanosome and leucosome;
Tielines stippled: compositional variation within hand-specimen;
solid:compositional variation within outcrop;

paleosome:circles
melanosome:dots
leucosome:crosses
arrow:melanosome associated with non-kf-bearing leucosome (crosses without tie-line)

Fig. 4.6 Compositional relationships within Helskloof migmatites
a) Modal composition of granodioritic paleosomes
b) Modal composition of diatexites
c) Modal composition of leucosomes

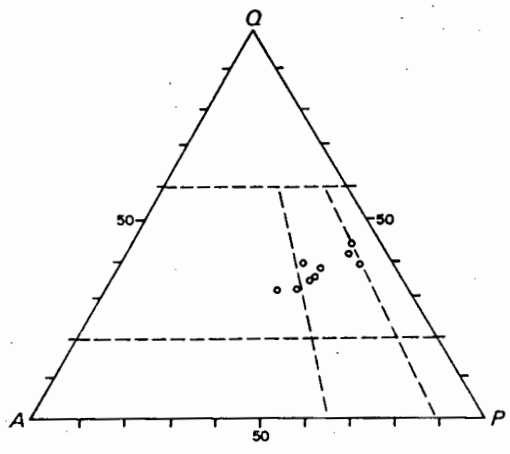

a

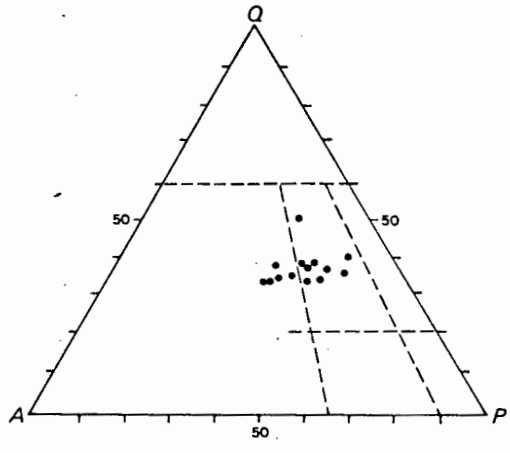

b

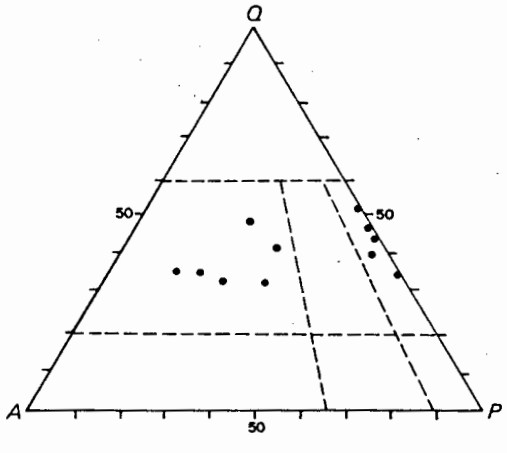

c

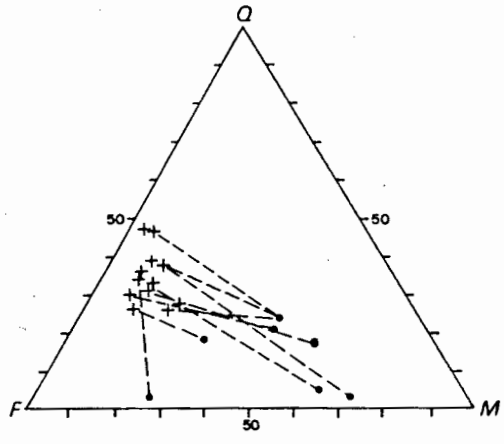

Fig. 4.7 Compositional relationship of spatially related paleosomes/melanosomes and leucosomes.

melanosome/paleosome : dots
leucosome : crosses

cratic amphibolites occur in isolated lenses of up to several hundred metres in length. They may or may not be layered and consist of equal amounts of hornblende and plagioclase with minor amounts of quartz, chlorite and epidote.

d) Composition

Modal compositions of migmatitic rocks are plotted in Fig. 4.4 to Fig. 4.7.

From these diagrams the following conclusions can be drawn:

1) Compared with granodioritic paleosomes, the diatexites are depleted in mafic minerals, but they tend to be enriched in K-feldspar (Fig. 4.4a, b; for meaning of Col. I. etc. see Fig. 3.4 p. 40).

2) In QPA-diagrams the modal composition of granodiorite and diatexite is similar. There is a weak tendency for the latter to be enriched in K-feldspar (Fig. 4.6a, b).

3) a) The K-feldspar content of leucosome is always higher than that in adjacent paleo-melanosome.
b) The K-feldspar contents of leucosome and paleo-melanosome are the more closely related the closer the spatial relationship.
c) The content of mafic minerals is always higher in paleo-melanosome than in leucosome (Fig. 4.5).

4) Leucosomes in metatexites are either granitic or tonalitic (trondhjemitic) (Fig. 4.6c).

5) There is a convergent compositional development of spatially related leucosomes and paleo-melanosomes resulting in a quartz/feldspar ratio close to 4:6 for the leucosome independent of the composition of the paleo-melanosome (Fig. 4.7).

The mineralogy of metatexites and diatexites is uniform and varies only in the relative amounts of plagioclase, K-feldspar, quartz, biotite, muscovite and epidote. In some samples incipient development of hornblende from biotite has been observed (biotite-hornblende reaction). This together with textural relationships will be discussed in Chapter 6.

3. *Megacrystic granite (map unit G_B)*

a) Field appearance and extent

Megacrystic granite occurs in north-south trending ridges south of Struishoek and east of Die Plate. It is characterised by densely spaced subhedral megacrysts of K-feldspar up to 5 cm across in a granodioritic groundmass.

The north-south foliation (S_2) that also affects the granodiorite of the Vioolsdrif Intrusive Suite of this area frequently imparts a distinct

gneissic foliation to this rock which wraps around the megacrysts. At its western margin the granite is strongly affected by S_3.

b) Contact relationships

Its contacts with adjacent Vioolsdrif granodiorite and Windvlakte volcanics are sharp and in some places it is intruded by pegmatites and aplitic veins.

c) Mineralogy, texture and composition

In thin section the same type and degree of metamorphic alteration is displayed in the groundmass as in the adjacent metavolcanics and granodiorites of the Vioolsdrif Intrusive Suite. Although its groundmass is granodioritic, the composition in hand specimen and on outcrop scale is granitic to alkali granitic where the amount of K-feldspar exceeds the amount of groundmass.

d) Age and origin

Metamorphic alteration of the groundmass texture and deformation by S_2 suggest an age of intrusion older than M_1 and S_2.

With regard to the formation of the megacrysts, De Villiers and Söhnge, (1959) suggested feldspathisation as a result of metasomatism emerging from the intrusives of the Richtersveld Igneous Complex. This interpretation is, however, unlikely, since the megacrysts are older than S_2, while the Richtersveld Igneous Complex is younger than this foliation. Introduction of K-feldspar-bearing material by aplitic veins, as suggested in this connection by De Villiers and Söhnge, is also unlikely since these veins cross granodiorite and metavolcanics without causing growth of megacrysts there.

Although no definite mode of origin could be determined during the present investigations, it seems nevertheless likely that this rock constitutes a member of the Vioolsdrif Intrusive Suite, or at least is not significantly younger than the latter, in which for unknown reasons the K-feldspar component crystallised as megacrysts.

4. *Kromnek Granite (map unit G5)*

a) Field appearance and extent

This relatively fine grained, pink granite is typically developed near Kromnek, but minor bodies of similar appearance and structural position occur throughout the formerly high grade metamorphic terrain of the south-eastern Richtersveld.

b) Mineralogy, texture and composition

In thin section quartz, microcline, plagioclase occur in approximately equal amounts together with minor amounts of muscovite and biotite

Contacts between ultramafic intrusions and country rock are sharp and no alteration of the wall rocks has been observed. Some ultramafics intruded into the Pink-gneiss Unit have in turn been intruded by pegmatite.

On the scale of the Richtersveld no particular order along particular lines of intrusion has been recognised, as suggested by De Villiers and Söhnge, (1959) and confirmed by Middlemost (1963) for the Rooiberg area (east-west line of intrusions). It is, however, correct that on a local scale, several minor intrusive bodies may be aligned in a nearly linear fashion. This has been observed in the Pink-gneiss Unit west of Bluff for a northwesterly direction (i.e. parallel to layering) and west of Rooiberg for a north-south direction.

b) Age

Serpentinites and hornblendites are intruded by pegmatites and fragments of serpentinite have been found in protomylonites of the Blackface Mountain Mylonite Belt. Their minimum age can therefore be inferred to be pre-pegmatitic.

All the ultramafic rocks observed are at least partly in contact with or fully included in supracrustal rocks. This may be a coincidence, but nevertheless suggests a post-Orange River Group and pre-Vioolsdrif age.

Mafic and ultramafic intrusives occur throughout the Namaqua Metamorphic Complex (Benedict, *et al.*, 1964; Joubert, 1971; Toogood, 1974; Clifford *et al.*, 1975; Moore, 1975) mostly in minor bodies. Little is known about their mutual relationship and age. Syn- and posttectonic intrusions into the Tantalite Valley Lineament (= Pofadder Lineament, Moore, 1975) and an assumed age of 1100 my (on account of isotopic data) for the Noritoid Suite at Nababeep (Clifford *et al.*, 1975), indicate that at least some of these intrusions are relatively late within the context of the crustal development of the Namaqua Metamorphic Complex.

6. *Pegmatites*

a) Field appearance and extent

The pegmatites of the southeastern Richtersveld are the western extension of an approximately 600 km long and 20-30 km wide east-west-trending belt known as Orange River Pegmatite Belt. In the present area pegmatites are confined to the high grade metamorphic zone and their northern limit coincides approximately with the boundary medium/high grade as inferred from metamorphic investigations. Pegmatites do not, however, occur in the high grade terrain of the Helskloof Migmatitic Complex. Their shapes and sizes range from irregular patches to cross-cutting veins and from the cm scale to bodies of hundreds of metres across. Their strike, statistically, is northwest, but locally they deviate from this direction.

b) Composition and mineralogy

The structure, mineralogy and chemistry of pegmatites of the Orange River Belt have been investigated by Hugo (1969) for the Kenhardt and Gordonia districts and partly by De Villiers and Söhnge (1959) for the Richtersveld.

Since there is no reason to assume distinctly different textures and compositions for the pegmatites in the present area, and since their investigation would not have contributed to the main objectives of this project, no textural and compositional investigations have here been carried out.

c) Age and origin

Radiometric age determinations yielded uniform ages around 1000 my throughout the Orange River Pegmatite Belt (e.g. Burger *et al.*, 1965) and it can safely be assumed that the present pegmatites are of approximately the same age.

Apart from De Villiers and Söhnge (1959), who suggested a relationship with the Richtersveld Igneous Complex and Hugo (1969), who appeared to relate the pegmatites in his area with an assumed magmatic body underlying the Namaqua Metamorphic Complex, no particular mode of origin has as yet been brought forward. The wide extent of the belt and its consistent east-west trend parallel to the metamorphic zonation, indicate magmatic and metamorphic processes within the Namaqua Metamorphic Complex as a common source of origin for the pegmatite-forming liquids. Its position, furthermore, close to the boundary medium/high grade in the vicinity of the Richtersveld suggests the migmatitic zone of high grade metamorphism as a possible source of pegmatitic fluids. The pegmatites would then occupy a position relative to the high grade zone which is equivalent to the mostly marginal occurrence of pegmatites around plutonic intrusions. This concept of pegmatite formation as pseudo-pegmatites (*sensu* Schneiderhöhn, 1961) will be presented in detail during the discussion of the Richtersveld in its regional context (p. 231).

7. *The Richtersveld Igneous Complex (RIC) (map units G7, G8, G9,GR)*

a) Previous work

The term Richtersveld Igneous Complex was apparently first used by De Villiers and Söhnge (1959) for what they described as a series of granitic and syenitic intrusions of batholithic dimensions in the southern Richtersveld between the Van Zyls River and Rooiberg II. The southern part between Rooiberg and Xaminxaip was later intensively studied by Middlemost (1963), who gave a comprehensive account of petrography, chemistry and intrusive relationships of the rocks concerned. He found that the Rooiberg II intrusion is in fact a ring-dyke complex consisting of granular syenite, porphyritic syenite, alaskitic granite and porphyritic microgranite and deduced from field relationships that the syenite was intruded by alaskitic granite

and both by porphyritic microgranite. For the Xaminxaip intrusion he found similar rock types except for porphyritic microgranite, but the reverse intrusive sequence from that of the Rooiberg, i.e. alaskitic granite → syenite. To the north of Xaminxaip, however, he observed that syenite again cuts alaskitic granite. He postulated a palingenetic origin for the alaskitic granite by selective fusion of "adamellitic gneiss" by concentration of heat "probably generated by radioactivity" and a more complicated origin for the syenites that involved a) granitisation of wall-rocks and their enrichment in Fe, Mn, Ti, Mg; b) assimilation of these wall-rocks; c) escape through fractures and faults of silica-rich rest-magma to account for the high Fe, Mg, Mn, Ti content and low Si content of these rocks.

Swarms of dark, fine-grained, northeast-striking dykes of syenitic composition, which he termed bostonite, were regarded by Middlemost as being comagmatic with the plutonic members of the Richtersveld Igneous Complex and emplaced while the latter were not yet fully cooled.

Since the geology of the Richtersveld Igneous Complex is thus relatively well-known, only those observations will be presented in this chapter that complement or revise previous findings.

b) Field relationship and extent

During the present investigations four intrusive complexes could be distinguished which are characterised by progressively younger relative ages from northeast towards southwest.

i) The Sjambok River Intrusion

The Sjambok River intrusion extends from north of Xaminxaip to the northeastern margin of the outcrop area at the farm Aussenkehr and to the upper part of the course of the Van Zyls River to the west. It consists entirely of alaskitic granite and is cut by dense swarms of dark, fine-grained bostonite dykes. Dykes and granites are frequently dissected by small north-south-trending shear zones of the Devilscastle type which become more numerous towards the west. In the Van Zyls River area, much of the granite and bostonite are altered to iron-rich schists and in places the original nature of the rock can only be recognised occasionally in less strongly deformed remnants.

ii) The Xaminxaip - Black Face Mountain Intrusion

The Sjambok River intrusion is bounded to the south by the Xaminxaip-Black Face Mountain intrusion. This boundary is particularly well visible on aerial photographs through the sudden lack of bostonite dykes in the south. Bostonite dykes are, however, present in great abundance in intervening country rocks and in country rocks further to the south. It therefore appears that the Sjambok River intrusion is older than the Xaminxaip intrusion, which is in agreement with Middlemost's (1963) observations that north of Xaminxaip syenite again intrudes alaskitic granite.

The western continuation of the Xaminxaip intrusion, the Black Face Mountain area, has been found to be underlain mainly by coarse, dark granular syenite, which in places is strongly sheared and profoundly fractured, giving rise to tectonic breccia and mylonite (cf. p.139)

iii) The Rooiberg Intrusion

The Rooiberg intrusion is not connected with other parts of the Richtersveld Igneous Complex and relative age relationships can therefore only be inferred. As it is intrusive into the Black Face Mountain Mylonite Belt which deforms the margin of the Black Face Mountain Intrusion, it must be younger than the latter.

Close attention must be paid to a grey, rather non-magmatic looking rock at the summit of the Rooiberg which has been referred to as xenolith and described as gritty impure quartzite and porphyritic lava of the Stinkfontein Formation by Allsopp *et al.*, (1978). Samples and thin sections of this "xenolith" provided by Prof. Allsopp were studied and it was found that its derivation from a sediment was rather unlikely and that it most probably represented metasomatically altered porphyritic microgranite of the Richtersveld Igneous Complex as described by Middlemost (1963). This granite contains euhedral but slightly corroded quartz phenocrysts which, as a special feature, enclose flakes of muscovite particularly at their margins. K-feldspar phenocrysts are also subhedral to euhedral prismatic and slightly corroded. The groundmass is inequigranular interlobate and contains quartz and microcline as main constituents with interstitial flakes of muscovite. The very same texture is displayed in the xenolith with the exception of k-feldspar, which is thoroughly sericitised and occurs in aggregates depicting the outlines of the former k-feldspar phenocrysts. The grain size of groundmass and phenocrysts in both rock types is roughly the same. Although in principle a formation of the "xenolith" after Stinkfontein lava cannot be ruled out, the textural similarities between microgranite and xenolith are such that its derivation from microgranite must be regarded as nearly certain.

iv) The Klipbokkop Intrusion

The Klipbokkop intrusion consists, apart from the main body that makes up the crest of the Klipbokkop, of several minor intrusions, some of them only a few hundred metres in diameter. Particularly in the case of the smaller intrusions it is obvious that the Devilscastle schists are cut by them.

Petrographically the Klipbokkop rocks are made up of porphyritic

syenite and porphyritic granite. The latter reveals a large degree of bimodality and is locally so fine-grained (e.g. northeast of Klipbokkop) that it is neither in the field nor under the microscope distinguishable from an acid volcanic rock. Relationships of this kind have also been described from porphyritic microgranite of the Rooiberg, at Xaminxaip (Middlemost, 1963) and from the Sjambok River intrusion (Martin, 1965). This and its close relationship with the Richtersveld Igneous Complex (as plugs and dykes) rule out an origin as volcanics of the Orange River Group.

Parts of the Klipbokkop intrusion closely approach the unconformity with the Stinkfontein Formation. It could, however, not be definitely established whether the intrusives are cut by the unconformity, owing mainly to the fact that Stinkfontein rocks underlying the Stinkfontein quartzites are not easily distinguishable from sericite schists of the basement. Taking into account the rather linear nature of the western boundary of this intrusion parallel to the mapped unconformity and the uncertainty in the estimate of the thickness of the Stinkfontein rocks underlying the quartzites, it is likely that the Klipbokkop intrusion is cut by the unconformity.

c) Contact relationships

Contacts between the Richtersveld Igneous Complex and the country rock are usually sharp but alkali metasomatism with growth of secondary K-feldspar in the wall rocks is particularly evident in the Van Zyls River area. The contacts, inferred by Middlemost (1963) to dip nearly vertically, are frequently rather gently dipping as can be seen for example almost one km west of the mapped contact of the Rooiberg intrusion where small patches of rocks of the Richtersveld Igneous Complex are cropping out along sharp incisions of dry river courses. South of Basterfontein in the dry river bed next to the main north-south track, undeformed but coarse and strongly weathered rocks of the Richtersveld Igneous Complex crop out along shallow contacts within the schists of the Devilscastle Schist Belt. In other cases again, such as the western and southern margin of Black Face Mountain, contact relationships are obliterated by strong mylonitisation due to Late Precambrian left-lateral shearing (Black Face Mountain Mylonite Belt, cf 5.3.3).

d) Texture

Since no textures have been found that have not already been described by Middlemost (1963) only the newly found Klipbokkop texture will be described here. In contrast to the porphyritic textures described by Middlemost (1963), the porphyritic varieties of Klipbokkop appear to be less mature. They display a rather irregular, granoblastic seriate groundmass texture consisting mainly of microcline and quartz with some biotite. The phenocrysts are anhedral throughout and particularly K-feldspar phenocrysts have a distinctly rounded shape. Occasionally, as in Fig. 4.9, a rounded

K-feldspar core is surrounded by a K-feldspar rim with slightly different extinction angle. Features of this kind could be interpreted as signs of partial refusion postdating a previous crystallisation and are particularly important with respect to the possible intrusive history of this rock, to be discussed below.

e) Composition

The modal composition of the Richtersveld Igneous Complex is rather simple and consists of alkali granite and syenite (Middlemost, 1963). Some whole-rock analyses have been published by De Villiers and Söhnge (1959) from which Wright's (1969) alkalinity ratio has been calculated and plotted in Fig. 4.8. According to this classification the granitic members of the Richtersveld Igneous Complex are weakly calc-alkaline to alkaline and the syenitic members alkaline to peralkaline.

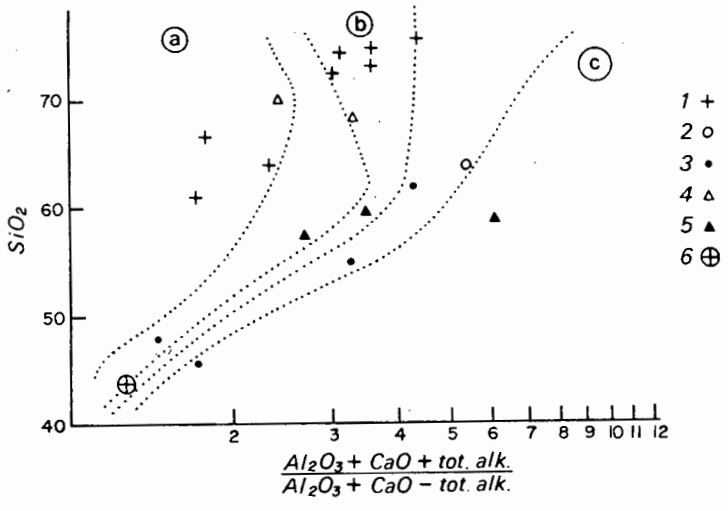

Fig. 4.8. SiO_2 versus alkalinity ratio after Wright (1969); a) calc-alkaline b) alkaline c) peralkaline.
Calculated after data from De Villiers & Söhnge (1-5) and D.L. Reid, 1978, pers. comm. (6).
Kuboos-Tatasberg : 1) granite 2) syenite 3) dykes
RIC : 4) granite 5) syenite
Gannakouriep Suite (mean) : 6)

f) Age

The relative intrusive sequence of the Richtersveld Igneous Complex determined during fieldwork is only partly in agreement with radiometric age determinations by Allsopp *et.al.*, (1978), who obtained U-Pb zircon ages of

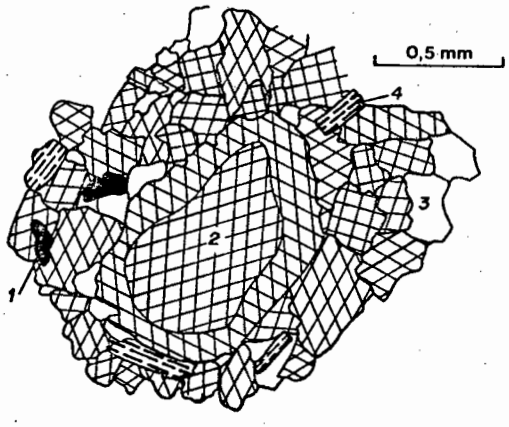

Fig. 4.9 Porphyritic microgranite from Klipbokkop. The texture shows signs of refusion and subsequent recrystallisation. The core of the microcline phenocryst (2) is anhedral and is surrounded by a rim of microcline with slightly different extinction angle.
1) opaque 2) microcline phenocryst
3) quartz 4) biotite in groundmass.

920 ± 10 my for the Richtersveld Igneous Complex and the older Bremen intrusives, but rather unreliable Rb-Sr whole-rock isochron ages for various localities in the Richtersveld Igneous Complex. According to them, alaskitic granite at Xaminxaip yielded an errorchron apparent age of 886 ± 90 my, alaskitic granite from Sjambokkloof and east of Klipbokkop a Rb-Sr age of 864 ± 12 my, porphyritic granite from the core zone of the Rooiberg a Rb-Sr whole-rock errorchron age of 809 ± 102 my and porphyritic granite at Klipbokkop a Rb-Sr whole-rock isochron age of 696 ± 16 my. Regarding the 920 my zircon age as the only reliable data, they are forced to invoke resetting events around 700 my and around 500 my connected with Gariep orogenic activity.

From the preceding chapters it appears, however, that the Rb-Sr ages agree much better with field evidence and reflect the relative intrusive succession outlined above.

g) Discussion

Alkaline intrusive rocks are known to occur preferably in stable continental areas (Sörensen, 1974) and it may therefore be useful to view their occurrence in the Richtersveld with respect to time of intrusion and structural environment. It is furthermore necessary to discuss questions arising from the obvious discrepancy of radiometric U-Pb and Rb-Sr whole-rock ages in order to evaluate their relevance with regard to the true intrusive age.

i) Theories on the origin of alkaline magmatic rocks

Butakova (1974) stressed the relationship of alkaline rocks of the Siberian platform to tectonic disturbances after periods of relative

tectonic quiescence. Consequently she pointed out that alkaline rocks are preferably developed at the limbs of arched uplifts and at deep faults and their intersections. She also stressed the coincidence in time of the development of alkaline rocks with maximum tectonic activity in adjacent orogenic zones.

Rhodes (1971) related alkaline intrusive complexes to the motion of continental plates. According to him, ring dyke complexes form when continents drift over hot spots, which "burn through" the continental plate.

A totally different but more sophisticated model has been proposed by Bailey (1964, 1974). He regarded local uplift as the particular force that initiated the formation of the magmatic cycle, which is, once in motion, self-perpetuating (see also Yoder, 1952). According to him local uplift of the crust, such as arching, causes a decrease in confining pressure in the underlying mantle with consequent release of volatiles and mobile elements which migrate into the crust. The effects are :
a) focusing of heat into the overlying crustal rocks, i.e. rising of the isotherms and
b) lowering of the solidus of the crustal rocks with increasing water content and addition of volatile elements. This in turn may cause partial or complete melting of crustal material if P-T conditions are appropriate.

The basic element of Bailey's model is thus the relief of pressure causing degassing in the underlying mantle and providing for the transfer of heat by means of volatiles and mobile elements into the lower crust and at the same time altering the chemistry of the crust.

The application of Rhodes' model to the Richtersveld Igneous Complex: Applying Rhodes' model to the Richtersveld Igneous Complex, a northeastward motion of approximately 100 km for the Richtersveld would ensue during a period of nearly 200 my. This is contradicted by the consistent 900 my zircon ages for all rocks of the Richtersveld Igneous Complex. It would also fit only partly with the proposed model of Late Precambrian geosynclinal development of the Gariep geosyncline (Kröner, 1974) which requires extension only for the time between 800 and 900 my. A crustal dilatation of 100 km furthermore seems somehow unsatisfactory for the creation of a proto South Atlantic.

In addition, mathematical modelling has shown that the change of surface heat flow is smaller the thicker the plate and the faster the plate motion, if a thermal disturbance at the base of the lithosphere is assumed (Gass *et.al.*, 1978), i.e. the thermal disturbance penetrates less into the overlying crust the faster the velocity of the plate. Already for this reason Rhode's mechanism must be regarded as unlikely.

The application of Bailey's model to the Richtersveld Igneous Complex: The intrusion of the Richtersveld Igneous Complex coincides with the following tectonothermal conditions in the southeastern Richtersveld:

(a) Low geothermal gradient, which comes close to that of stable continental areas
(b) Considerable crustal uplift
(c) Development of left-lateral shearing which could be related to a major wrench-fault system
(d) The magmatic axis of the Richtersveld Igneous Complex coincides with fold axes observed (F_2) and expected in a left-lateral wrench-fault system.

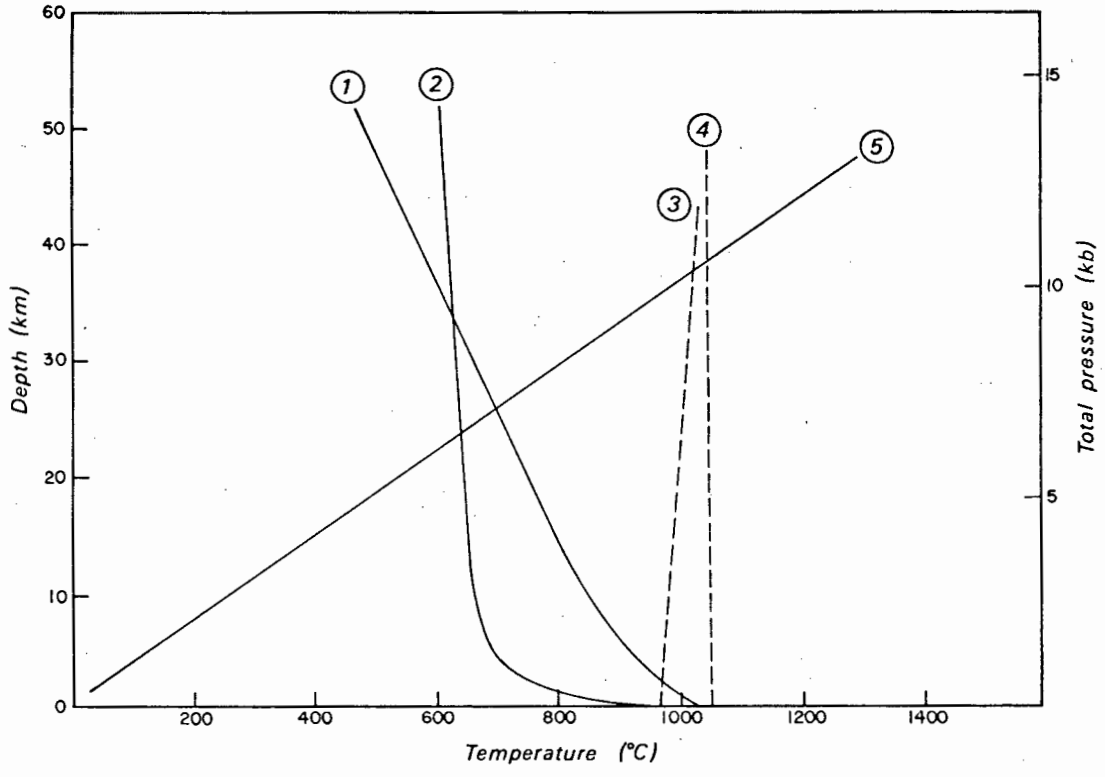

Fig. 4.10

Beginning of melting of
1) hydrous basalt;
2) hydrous granite;
3) anhydrous granite;
4) anhydrous basalt (after Bailey 1974 p.439);
5) geothermal gradient as inferred for the Devilscastle Event. Fully water saturated rocks of basaltic and granitic composition can be expected to melt already at a depth of 25 km.

These conditions meet the requirements proposed by Bailey: uplift to set the magmatic cycle in motion, and are also in agreement with the general observation that alkaline magmatic rocks tend to occur in relatively stable areas (a), but are nevertheless related to tectonic activity in the vicinity (c) (e.g. Butakova, 1974). The coincidence of F_2 and the magmatic axis of the Richtersveld Igneous Complex (d) may be accidental but may as well be an expression of the tectonic activity leading to magmatism.

ii) Speculations on the intrusive history of the Richtersveld Igneous Complex

In Figure 4.10 melting curves are shown for granitic and basaltic rocks (taken from Bailey 1974, p.439), together with a geothermal gradient as deduced from the early stages of Devilscastle metamorphism. At this geothermal gradient hydrous granitic and basaltic rocks melt already below a depth of 25 to 30 km, while anhydrous granite and basalt would only melt at a depth greater than 40 km. Assuming granulite facies conditions for the lower parts of the crust, influx of volatiles would lead to its immediate melting, and continued influx of volatiles and mobile elements to increasing syenitisation. Influx of water may also lead to refusion of already crystallised granites, a process on which Martin and Bonin (1976) focused attention. They suggested that hardly any magma will rise above the zone of partial melting without successive periods of freezing and refusion. Cann (1970) suggested that, due to the negative slope of the solidus, fully water saturated granite would rise only a short distance before crystallising again and that the distance a magma can rise depended basically on the ratio PH_2O/P_{tot}.

However, taking into account the relationships as depicted in $P\text{-}T\text{-}X_{H_2O}$ diagrams, the problem becomes more complicated and is best discussed in terms of Figure 3.24 (p. 59). Using this diagram as an example, a rock of granitic composition at 8 kb and 900°C with a water content of less than 1 percent can be expected to be solid, but influx of water to 4 percent would lead to its complete refusion and enable it to intrude to higher crustal levels. Cooling concomitantly, it would reach the solidus at e.g. 2 kb and 700°C or 1 kb and 750°C. It should furthermore be emphasised that most of the phase boundaries in Figure 3.24c have a positive slope in the water undersaturated region, which entails that K-feldspar, crystallising as liquidus phase (at 900°C, 8 kb, 4 percent water) will partly be resorbed, if adiabatic intrusion into higher crustal levels occurs. This may explain textures as shown in Figure 4.9.

The same mechanism can of course also be used to create granitic melt from rocks of non-granitic composition. It is evident from Whitney (1975a, Fig. 13) that a tonalitic rock (at 900°C, 8 kb, 4 percent water) would yield a granitic melt by fractional melting of all quartz and K-feldspar and some of the plagioclase. This melt then could be expected to behave according to the granitic system already described (Fig. 3.24) and much of the original granitic melt in the Richtersveld Igneous Complex can be envisaged to have formed in this way.

Additional complications may furthermore modify the conditions assumed:

a) partial refusion of already crystallised granite
b) incipient refusion, leaving only a weak or no textural imprint but disturbing the isotopic system
c) addition of alkaline material, leading to changes in composition of the system and lowering of the melting temperature.

The mechanisms leading to the intrusion of the Richtersveld Igneous Complex can therefore be envisaged as follows:

a) At a geothermal gradient like that of the late stage of metamorphism in the Richtersveld (Fig. 4.10), the lower crust is likely to have been in the state of granulite facies metamorphism.
b) Uplift due to tectonic activity results in the initiation of the magmatic process suggested by Bailey (1974): influx of water and mobile elements lower the solidus of the crustal rocks and cause their partial or total refusion. They may then migrate to higher levels until the specific conditions for their crystallisation are met.
c) Crustal uplift at the one hand and addition of volatiles to the crust on the other hand may result in two opposite trends of magmatic development:

   (i) uplift results in faster relief of pressure and rising granites will therefore attain their specific crystallisation conditions earlier and intrude over shorter distances

   (ii) continued uplift will maintain or even increase the influx of mobile elements and water and thus lower the solidus of existing rocks. This could lead, on the one hand, to the crystallisation of early granites already in rather low crustal levels and could, on the other hand, enhance the possibility of their later remobilisation and intrusion into higher levels. The intrusion into higher levels towards the end of the magmatic cycle will furthermore be facilitated by the fact that, due to continued uplift, the distance between the zone of remobilisation and the highest crustal level is continually decreasing.

iii) Intrusive history and the interpretation of radiometric ages

The evaluation of radiometric age data of the Richtersveld Igneous Complex (Allsopp *et al.*, 1978) should take into account the following:

a) The intrusive sequence as determined from field relationships is in agreement with whole-rock ages, but not with zircon ages.
b) The radiometrically and "geologically" oldest rocks show the smallest difference between whole rock and zircon ages.
c) The "geologically" and radiometrically youngest rocks show the greatest difference between whole-rock and zircon ages.

d) The texture of the youngest intrusives shows features that can be interpreted as signs of partial refusion. Textures of older rocks do not show these signs.
e) A prolonged intrusive history of repeated melting and crystallisation is possible.
f) There is no indication for metamorphic reconstitution of the country rock after the Devilscastle Event.

Melting conditions of zircon and temperatures at which resetting within zircon occurs are not exactly known and seem to be rather variable (Catanzaro, 1968). The fact that zircons frequently record much older ages in metamorphic terrains and are in intrusive rocks commonly found in early mineral phases points to a relatively high temperature of reconstitution. It is thus possible that zircon, once formed at relatively high temperature, remains stable throughout the prolonged intrusive history and records older ages than the whole rock. Martin and Bonin (1976) pointed out that even influx of volatiles at temperatures too low to cause refusion, will result in turbidity in feldspars, degradation in mafic minerals and disturbances in hydrogen, oxygen, strontium and lead isotopic systems.

The conclusions arrived at by Allsopp *et al.*, (1978) that many of the RIC Rb-Sr ages are reset is therefore certainly correct. However, the nature of this resetting event should not merely be seen in terms of a thermal modification connected with Gariep orogeny, but may also be related to a complicated intrusive history as outlined above.

iv) Summary

a) Geological evidence and theoretical considerations suggest that the emplacement of the Richtersveld Igneous Complex may have been initiated by tectonic activities related to F_2 and the Devilscastle Event.
b) Geological evidence, radiometric age pattern and theoretical considerations suggest that the Richtersveld Igneous Complex has a complicated intrusive history comprising repeated crystallisation and refusion.
c) The discrepancy of zircon and whole-rock ages can be explained by the intrusive history of the Richtersveld Igneous Complex and does not require a metamorphic resetting event.
d) If the Rb-Sr whole-rock ages are regarded as the true intrusive ages, the intrusive history of the Richtersveld Igneous Complex extended over a period of 200 my between ~900 and ~700 my, during which increasingly younger intrusives were emplaced into increasingly higher crustal levels from northeast to southwest.

4.2. THE BLOCKWERF MIGMATITIC COMPLEX (BMC) *(MAP UNIT M)*

The Blockwerf Migmatitic Complex is characteristed by a rapid transition from low grade in the west to migmatites in the east over a distance

of only a few kilometres. It is thus distinguishable from other metamorphic terrains of the Richtersveld where changes in metamorphic grade occur only over tens of kilometres.

In the west it is bounded by a zone of strong deformation parallel to the course of the Noms River. Its eastern boundary is not known, but since Blignault (1977) mapped unreconstituted granodiorite of the Vioolsdrif Intrusive Suite to the east of the Orange River it is likely that the Blockwerf Migmatitic Complex constitutes only a small horst-like structure in which lower crustal levels have been exposed during relatively late crustal uplift. Its structural position is therefore similar to that of the Helskloof Migmatitic Complex in the south.

4.2.1. Rocks of supracrustal origin

1. *Field appearance*

Supracrustal rocks of the Blockwerf Migmatitic Complex are distinguished from lower grade metavolcanics by coarser grain size, gneissic appearance and pervasive mineral foliation and lineation. Compositional boundaries can be traced in the field and on aerial photographs and are approximately parallel to the layering in the adjoining metavolcanics.

The following are the dominant rock types:

Augen gneiss is characterised by relatively dark groundmass consisting of biotite or chloritised biotite in which subhedral to anhedral K-feldspar porphyroblasts of up to 1 cm across have grown.

Amphibolite is readily recognised by its radial, garben-like clusters of black hornblende needles of up to several cm in length

Acid metavolcanic rocks appear like fine-grained mesocratic to leucocratic granites in the field, but can be identified as supracrustal rock by occasional preservation of the original layering, caused by small textural or compositional differences in the original rock sequence. Granoblastic texture and field appearance are similar to that of the metavolcanics of the Windvlakte Formation and also suggest volcanic origin for these rocks.

Migmatites display a variety of different structures and occur in increasing amount approaching the Orange River around Blockwerf.

2. *Origin*

The uniform mineral composition, consisting of *quartz, K-feldspar, plagioclase, hornblende, epidote, sericite, muscovite, biotite, chlorite* in variable amounts, suggests a derivation from volcanic rocks not only for the granoblastic metavolcanics. The frequent occurrence of amphibolite,

however, indicates that they have not been derived from the volcanic sequence west of Noms River (Kuamsrivier Formation) since their chemistry would not allow the formation of hornblende. Metamorphic rocks of the Blockwerf Migmatitic Complex can therefore not be stratigraphically correlated with the Kuamsrivier Formation and possibly represent volcanics underlying the latter.

3. *Age*

Radiometric age determinations have not been carried out on rocks of the Blockwerf Migmatitic Complex but metavolcanics collected immediately north of the present area at the Kuduboom River, opposite Oenas, yielded a Rb-Sr whole-rock age of 1000 ± 30 my (Welke *et al.*, 1978). It can therefore be assumed that this age also applies to the Blockwerf Migmatitic Complex and is indicative of the last metamorphic imprint.

4.2.2. Rocks of Intrusive Origin

1) *The Oenas Granite (map unit G5)*

a) Extent and field relationship

Pink, even-grained to porphyritic granite occurs as six major and minor intrusions. The largest intrusion is found north of De Hoop, but the small outcrops at and south of Oenas have been chosen as type locality since they are more readily accessible.

b) Intrusive relationships

Contacts are sharp and cut the regional foliation. Aplitic dykes emerging from this granite tend to be aligned in the foliation of the wall rock and for these reasons their crosscutting relationships are not always clearly recognisable. In the Oenas area contacts are occasionally disturbed by postintrusive shearing along the Noms River fault that caused the uplift of the Blockwerf Migmatitic Complex.

c) Texture and mineralogy

Quartz, plagioclase and K-feldspar occur in roughly equal amounts with minor amounts of biotite, chlorite and muscovite. Plagioclase is moderately altered into sericite and epidote, but in contrast to the surrounding country rock it is not recrystallised into subgrains. Biotite tends to be altered into chlorite and is associated with plagioclase. Muscovite, apart from sericite in altered plagioclase, occurs as anhedral flakes, mainly included in plagioclase. If undeformed, an equigranular polygonal to interlobate texture is displayed. All minerals are anhedral and only K-feldspar shows a weak tendency towards idiomorphism.

d) Age and origin

Cross-cutting relationships with the regional foliation and textural evidence suggest an age of intrusion younger than the texture forming metamorphic and tectonic events. Its age relative to metamorphism and tectonism is therefore similar to that of the Kromnek granite in the Pink-gneiss Unit. This granite is thus best interpreted as intrusive product of partial melting during metamorphism.

4.3 DYKES OF THE GANNAKOURIEP SUITE

4.3.1. Previous investigations

Dykes of the Gannakouriep Suite were first described by De Villiers and Söhnge (1959) as mafic to ultramafic dykes and Middlemost (1963), giving textural descriptions and chemical analyses, regarded them as comagmatic with the Richtersveld Igneous Complex and termed them hornblende diorite dykes.

4.3.2. Field relationships

Dykes of the Gannakouriep Suite occur in the whole Richterveld and surroundings as dark green, north to northeast-striking dykes of rather variable width between 2 m and 1,5 km (near Claimspeak in the northeastern Richtersveld) and in length from less than one km to nearly 100 km in the case of the main Gannakouriep dyke along the Gannakouriep River. They cut bostonite dykes as well as all members of the Richtersveld Igneous Complex and all deformational structures including structures of the Devilscastle event. The latter observation is important as these dykes frequently give the impression of being sheared, although they are simply deflected into the direction of foliation during later intrusion. Later reactivation of shear zones may have caused fracture and shearing in dykes, the effects of which are minor, however, with respect to the thorough mylonitisation encountered within the cores of shear zones.

Dykes of the Gannakouriep Suite are cut by the early Paleozoic Tatasberg Intrusion and have also been reported from the lower Stinkfontein formation (De Villiers & Söhnge, 1959; Kröner, 1974), but during the present investigations, only the main Gannakouriep dyke has been observed to intrude Stinkfontein conglomerate northwest of Rosyntjiefontein.

4.3.3. Composition

A detailed chemical investigation is at present in progress

(Reid, D.L., 1978, pers. comm.). First results are shown in Table 4.4. and display a rather unusual chemistry which does not justify the term hornblende-diorite dyke as proposed by Middlemost (1963). This term should be abandoned and instead the neutral term Gannakouriep Suite is used here.

4.3.4. Age

Since radiometric dating of the Gannakouriep Suite yielded rather inconsistent ages between 218 and 878 my (reported in Kröner and Blignault, 1977) its relationship to geological objects of known age such as the rocks of the Nama Group and the Richtersveld Igneous Complex may provide more accurate information : dykes of the Gannakouriep Suite intrude the microgranite of the Klipbokkop and are discordantly overlain by Nama. If it is assumed that Allsopp's *et al.*, (1978) inferred minimum age of 553 $\pm$ 13 my for the Nama Group is correct and that the Rb-Sr whole rock age for the Klipbokkop intrusion of 700 my represents the intrusive age of that body, it follows that the dykes of the Gannakouriep Suite cannot be younger than 550 my and not older than 700 my. If one takes furthermore into account that the upper Stinkfontein Formation apparently already overlies these dykes, an age far closer to 700 my than to 550 my is likely. On the other hand surprisingly few of these dykes have been observed to intrude across the unconformity with the Stinkfontein Formation and it can thus not be ruled out that many of them were emplaced prior to its formation. For these reasons it is likely that the dykes of the Gannakouriep Suite were emplaced over a considerable period of time prior to and following the deposition of the lower Stinkfontein Formation.

4.3.5. Structural setting

The consistent north-south strike of the Gannakouriep Suite in the Richtersveld as well as its mafic composition suggest an intrusion from a mantle source during a period of strong east-west extension. However, the emplacement of these dykes cannot be related to any of the known deformational events, since pegmatites are intruded into the north-west trending extensional features of F_2. F_1 can be ruled out on account of its age and the strain pattern during Gariep deformation suggests east-west trending extensional features. Crustal extension during the formation of the Gariep basin as suggested by Kröner (1974) is thus virtually the only remaining possibility. This agrees well with known structural environments of mafic dykes which may form parallel to lines of tensile stress as for example at the onset of the North Atlantic sea-floor spreading (May, 1971) and the emplacement of which may take place shortly before crustal

separation (Scrutton, 1973). Thus the intrusion of mafic dykes prior to and contemporaneous with the deposition of the Lower Stinkfontein Formation is possibly no coincidence and must be seen in the context of the structural development. In this regard the Messejana dolerite dyke system in Portugal/Spain (Schermerhorn *et al.*, 1978) is rather similar to the Gannakouriep Suite, since it was emplaced during a considerable period from the latest Triassic to Middle Jurassic, extends over several hundreds of kilometres and also intrudes a left-lateral shear system of regional dimensions (Messejana shear zone). Both are linked to the opening of the North Atlantic.

It therefore appears that the intrusion of the Gannakouriep Suite in fact represents a period of crustal extension during which either sea-floor spreading was initiated or a graben system developed in which the Gariep Group was deposited.

Table 4.4. Major element analyses from dykes of the Gannakouriep Suite

	1	2	3	
	156/1	D11	$\bar{X}$	S
SiO_2	47,86	45,57	45,91	1,18
TiO_2	3,60	2,83	3,37	0,68
Al_2O_3	18,42	15,62	16,03	1,40
FeO*	11,90	13,93	13,99	2,31
MnO	0,18	0,24	0,24	0,04
MgO	3,37	6,54	5,01	0,88
CaO	9,40	8,42	8,43	0,71
Na_2O	3,25	1,43	2,51	0,54
K_2O	1,00	1,67	1,65	0,58
P_2O_5	0,31	0,42	0,90	0,57
LOI	1,20	3,85	2,38	0,85
Σ	100,49	100,53		

1 - Main Gannakouriep dyke, near Claim Peak
2 - Small dyke, Springbokkloof
3 - Mean from 11 analyses from various localities outside the eastern Richtersveld

Analyst : D. L. Reid, (1978) Geochemistry Department, University of Cape Town.

Table 4.5 Intrusive rocks in marginal areas of the Richtersveld

map unit, rock type	*structural and metamorphic environment, mode of origin*	*time of emplacement age (my)*	*evidence*
G_D, *diatexite*	in situ melting of Vioolsdrif granodiorite, Helskloof, SE Richtersveld	1750 ± 25	Rb-Sr whole rock age (Corner, 1970 in Köstlin, 1971)
G_B, *megacrystic granite*	possibly related to VIS, unknown origin of megacrysts SE Richtersveld	~1800	affected by S_2, intruded by pegmatites, possible relationship with VIS
G_5, *Kromnek granite*	restricted to the vicinity of formerly high grade metamorphic terrain of the PGU	~1500–1000	not visibly affected by S_1 and S_2, intruded by pegmatites
G_5, *Oenas granite*	restricted to the vicinity of formerly high grade metamorphic terrain of the Blockwerf area	~1000	cutting S_1, 1000 my ages of surrounding metamorphic rocks Welke *et al.*, (1978)
ultramafic intrusives (hornblendite, serpentinite)	unknown	1900–1000	intruded into Orange River volcanics and VIS, intruded by pegmatites;
pegmatites	restricted to formerly high and medium grade metamorphic terrain. Related to closing stage of high grade metamorphism	~1000	inferred from various radiometric datings in Orange River Pegmatite Belt
RIC (alaskitic granite, melanocratic syenite) G_6–G_9, *GR*	incipient cratonisation; poss. initiated by tectonic activity in active orogenic belts to the N	~900–~700	interpretative from Rb-Sr and zircon ages; deformed by early Devils Castle Event, intrusion into Devilscastle shear zones
dykes of the Gannakouriep Suite	poss. during initial rifting prior to and during early Stinkfontein deposition	~700–650	circumstantial: only parts of the dykes intruded into Stinkfontein F. Intrusive into Devilscastle shear zones; min.age:~550 my (overlying Nama) (Allsopp *et al.*, 1978)

Chapter 5

STRUCTURE

5.1 INTRODUCTION

Detailed structural investigations of the Richtersveld Province have as yet only been carried out in the Haib and lower Fish River areas by Blignault (1977). Since he arrived at the conclusion that the Richtersveld Province is a low strain subdomain with respect to the early deformational events in the Namaqua Metamorphic Complex and that the later cross-cutting features (F_4, F_5 of Blignault, 1977) are not present in his part of the Richtersveld Province, it is one of the objectives of this investigation to establish whether this is also the case in the Richtersveld proper.

Degree and style of the early structural imprint vary considerably throughout the Richtersveld and for reasons of convenient description the area has been subdivided into four structural domains (Fig. 5.1.)

Later structural features (shear zones) of the Richtersveld have frequently been linked with Gariep deformation (e.g. Kröner, 1974), but it has been found during the present investigations that all available information speaks against this view and it is therefore necessary to incorporate these tectonic events within a comprehensive model of the structural development of the Richtersveld and surroundings.

5.2 EARLY STRUCTURAL IMPRINTS

5.2.1. The central northeastern Richtersveld

1. *General*

This area comprises most of the northeastern Richtersveld and is bounded in the north by the line joining De Hoop and the Pokkiespramberge and in the south by the line connecting Vandersterrberg with the Oudannissiep River and Klipneus. It is characterised by the absence of mesoscopic folding and by weak and non-penetrative structural elements (except in pelitic rocks) predating the intrusion of the G_3 (granite) member of the Vioolsdrif

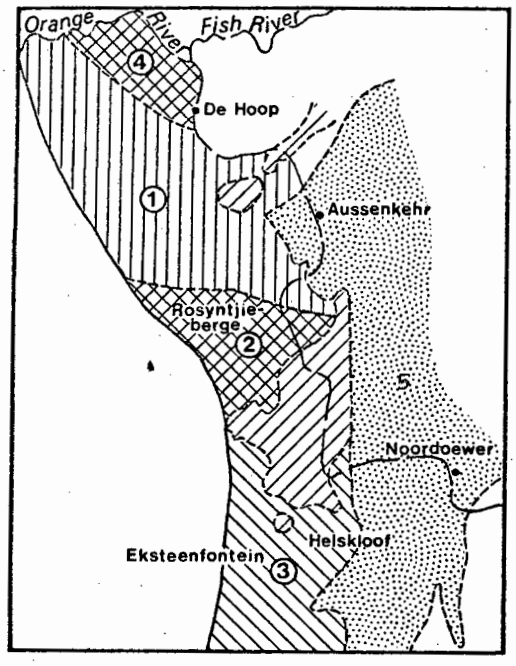

Fig. 5.1. Key map. Structural domains
1) Central northeastern Richtersveld
2) Southeastern Rosyntjieberg Formation
3) Southeastern Richtersveld
4) Nomsrivier-Blockwerf area
5) Areas younger than domains discussed here

Intrusive Suite.

2. *Fabric elements*

The elements used to define the structure of this area are listed in Table 5.1 and shown in Fig. 5.2.

In metavolcanics and early intrusives of the Vioolsdrif Intrusive Suite (G_1, G_2) secondary planar fabric elements are non-penetrative even on thin section scale and defined by narrow but irregular zones of recrystallisation. In metavolcanics they tend to be more strongly developed along bedding planes and then frequently obliterate the latter. Only in mica-rich pelitic rocks is the S_1 foliation always present and only here this foliation is occasionally deformed by a later crenulation cleavage S_2'. It does not, however, necessarily define a later deformational event since experiments in layered viscous materials suggest that loading normal to, or in the direction of the foliation produces conjugate sets of faults or kinks (Paterson and Weiss, 1966; Cobbold *et al.*, 1971; Means and Williams, 1972), while samples loaded at an oblique angle to the foliation yield only one set. The presence of S_2' might therefore only mean that the compressive strain causing F_1 and S_1 continued also after the formation of F_1 folds, acting oblique to S_1 and thus producing one set of crenulation cleavages. Although it cannot be ruled out that S_2' constitutes a distinct tectonic event this assumption is not essential and an explanation as suggested in Fig.5.20 is more likely.

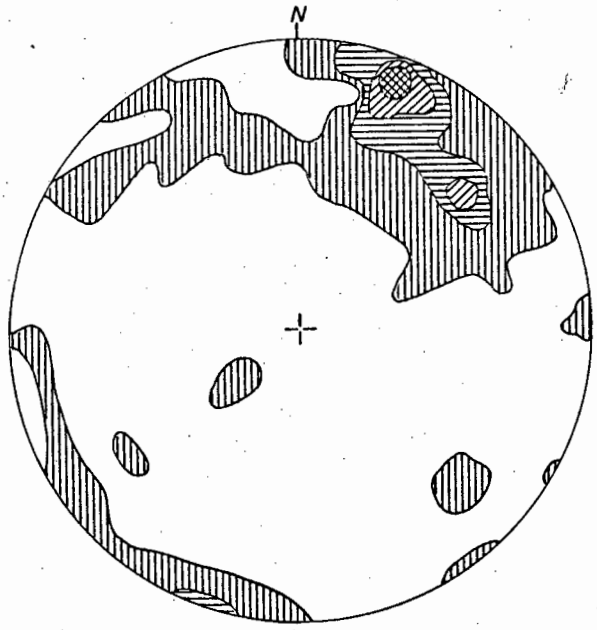

(a) n = 82
1-5-10-17%

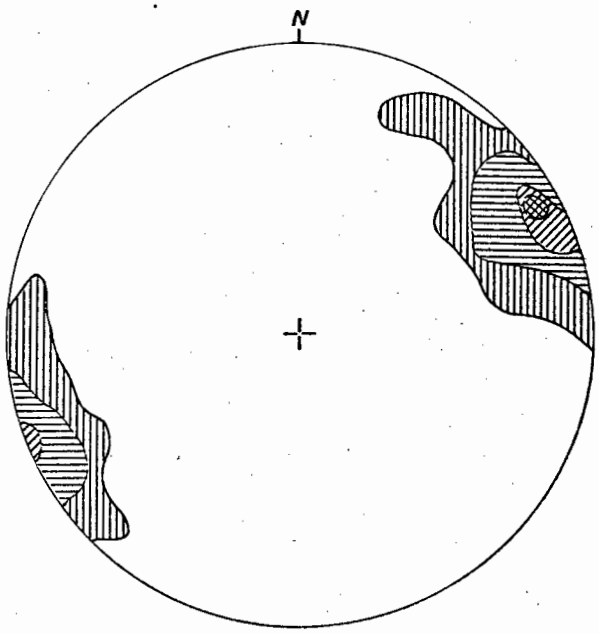

(b) n = 261
1-3-5-9%

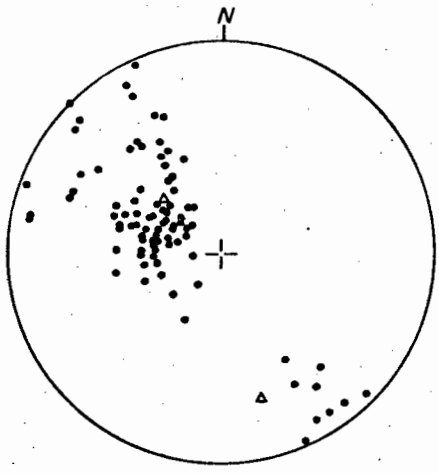

(c)

Fig. 5.2
Structural elements of the central northeastern Richtersveld.

a) Equal area projection of SS_1 in Kuamsrivier and Klipneus Formation.
b) Equal-area projection of SS_1 of the whole of the northeastern Richtersveld. The submaximum to the north is caused by aberrant directions mainly in Kuamsrivier and Klipneus Formation .
c) Scatter diagrams of linear elements (l_1) in the northeastern Richtersveld. Dots: l_1; Triangles: B_1

Table 5.1.

Structural elements of the central northeastern Richtersveld

bedding a) definition b) orientation	SS_1: a) change of material and grain size; often transitional in volcanics b) NW strike	
foliation a) definition b) orientation	S_1 : a) alignment of mica in pelitic rocks b) NW, vertical	S_2' : a) crenulation cleavage deforming S_1 b) NW, inclined to S_1
lineation a) definition b) orientation	l_1 : a) intersection of S_1 and S_2' b) horizontal, // B and variably inclined to B	
folding a) definition b) orientation c) wavelength d) shape	F_1 : a) folding of SS_1 b) NW, horizontal c) ~20 km d) probably tight to isoclinal	

3. *Major structural features*

a) Folds (F_1)

Most of the central Richtersveld is devoid of any indication of folding on a mesoscopic scale. It is only towards the southeast near Kwaggarug that folding on a metre scale can be observed in the valley of the Oudannissiep River (Fig. 5.6c). Isolated kinkfolds and ptygmatic folds at a sheared migmatitic contact of G2 granodiorite with leucocratic

volcanics west of Paradyskloof could also be correlated with F_1. West of the Tatasberg in a dry river valley (28°19'S; 17°12,5'E) moderate dips in opposite directions of volcanic layers could indicate the presence of an anticline. Dipping and younging towards the northeast in the Kuamsrivier and Abikwarivier Formations and towards the southwest in the Rosyntjieberg Formation suggests that nearly the whole of the northeastern Richtersveld is underlain by one single anticline (Richtersveld anticline), the significance of which with respect to the paleogeographic reconstruction of the northeastern Richtersveld has been discussed in Chapter 2.

5.2.2. The southeastern Rosyntjieberg Formation

1. *General*

This area is bounded in the north by the line connecting Vandersterrberg with the Oudannissiep River and Klipneus and in the south by the northernmost occurrence of the Richtersveld Igneous Complex. Structural observations are mainly restricted to outcrops within the Rosyntjieberg Formation along the gorge of the Orange River and to the area north of the Bak River.

2. *Fabric elements*

Structural elements occurring in this are are listed in Table 5.2. Apart from these elements the axial plane of F_2 and B_2 can be inferred from mapping. Similar to the central northeastern Richtersveld S_1 and 1_1 are weakly developed in intrusive and metavolcanic rocks.

3. *Major structural features*

a) F_1 folds

Although F_1 folds are predominantly tight to isoclinal, variations do occur even over short distances as shown in Figs. 5.4b & c. In Figure 5.3 folding and its variation on a medium scale are demonstrated at a profile along the Orange River Valley. Fold style and degree of deformation change from north to south from nearly concentric open folds which become tighter, become chevron type and finally similar folds. No folding occurs north of the profile. A weak asymmetrical shape (the southern limb of anticlines is slightly longer than the northern limb) may indicate a position of these folds at the southern limb of the Richtersveld anticline. The large cross-bedded structure (Fig. 5.3 right, below) is in agreement with other observations and indicates that the succession is not overturned. In Figure 5.4b quartzitic bands in a finely layered mica-schist matrix display parallel folds with an occasional tendency towards similar folds. The wavelength is dependent on the thickness of the quartzite layers and has a nearly constant

Table 5.2

Structural elements of the southeastern Rosyntjieberg Formation

bedding a) definition b) orientation	SS_1 : a) change of material and grain size b) NW and variable strike	
foliation a) definition b) orientation	S_1 : a) alignment of mica in pelitic rocks b) NW and variable strike where deformed, steeply SW dipping.	S'_2 : a) crenulation cleavage deforming S_1 b) NW and variable strike inclined to S_1.
lineation a) definition b) orientation	l_1 : a) intersection of S_1 and S'_2. b) // B, horizontal, moderately NW or SE plunging.	
folding a) definition b) orientation c) wavelength d) shape	F_1 : a) folding of SS_1 b) NW and variable c) 10-100m d) tight to isoclinal	F_2 : a) folding of F_1 fold structures b) steeply SW plunging c) km d) open

wavelength/thickness ratio of about 5,7 ($\bar{x}$=5,67, s=0,45) (see also Fig. 5.19). The similar fold in Figure 5.4c is from the same outcrop and is thought to have been caused mainly by relatively low viscosity and low ductility ratios of the rocks involved (immature quartzites with different degrees of impurity).

b) F_2 folds

F_2 folds occur as large, open structures on a kilometre scale. They are obvious from mapping along the Orange River north of Mike, and the large slopes of the R_3-stage of the Rosyntjieberg Formation between Gorgons Head and Devils Peak are also likely to be F_2 folds (Annex. 1a). The

crossgirdle patterns of the equal-area projections of S_1 and SS_1 can be attributed to deformation during F_2 (Fig. 5.6a, c).

c) The Mike Nappe

In the southeasternmost part of this structural domain horizontal, massive quartzite of the Rosyntjieberg Formation (R_3) covers the tops of certain mountains (Mike) and appears to be a nappe structure.

According to the thickness and lithological properties, the nappe is made up of 300-500 m thick quartzite of the R_3 stage of the Rosyntjieberg Formation. At its southwestern margin, exposed by the steep incision of the Orange River and other minor valleys it can be shown to overlie the Rosyntjieberg stages R_3 to R_6 which here have a northwesterly trend. R_3 is therefore partly overlying itself. In Plate 5 parts of the Mike Nappe structure are viewed from the northwest. Minor northwesterly striking and southwesterly dipping quartzite bands within the R_4 stage are cut off by banks of massive horizontal tectonic breccia. From this and from observations at other localities it is evident that the nappe quartzite is underlain by an approximately 100 m thick zone of extreme deformation, possibly consisting of authochthonous as well as allochthonous material. Examination of thin sections from the thrust zone indicates moderate recrystallisation and low grade metamorphic mineral assemblages (quartz, chlorite, sericite, epidote).

Any theory as to the mode of formation of the Mike Nappe must remain speculative as long as its origin is not known : to the southeast authochthonous quartzite peters out and is replaced by volcanics, and to the northeast and the north the succession of the Rosyntjieberg Formation is obviously undisturbed. An origin from the north or northeast (up dip) cannot be ruled out but can of course not be proved either.

It has been shown in 4.1.2. that the Richtersveld Igneous Complex and the tectonic processes leading to F_2 may be related to each other, and there is some evidence that the left-lateral wrench-fault system following and related to F_2 may have been of a convergent type (cf. p. 143) . Since major thrust structures have been reported from wrench-fault systems (Moody and Hill, 1956, Figs. 12 & 13), it is thus possible that the Mike nappe forms part of the shear system that developed during later stages of the tectonothermal history of the Richtersveld (Devilscastle Event). The contemporaneous intrusion of the alaskitic granite of the Richtersveld Igneous Complex may have played an additional role in the formation of this structure.

5.2.3. The southeastern Richtersveld

1. *General*

This domain comprises the area south of the northern margin of the Richtersveld Igneous Complex and is underlain by rocks of variable

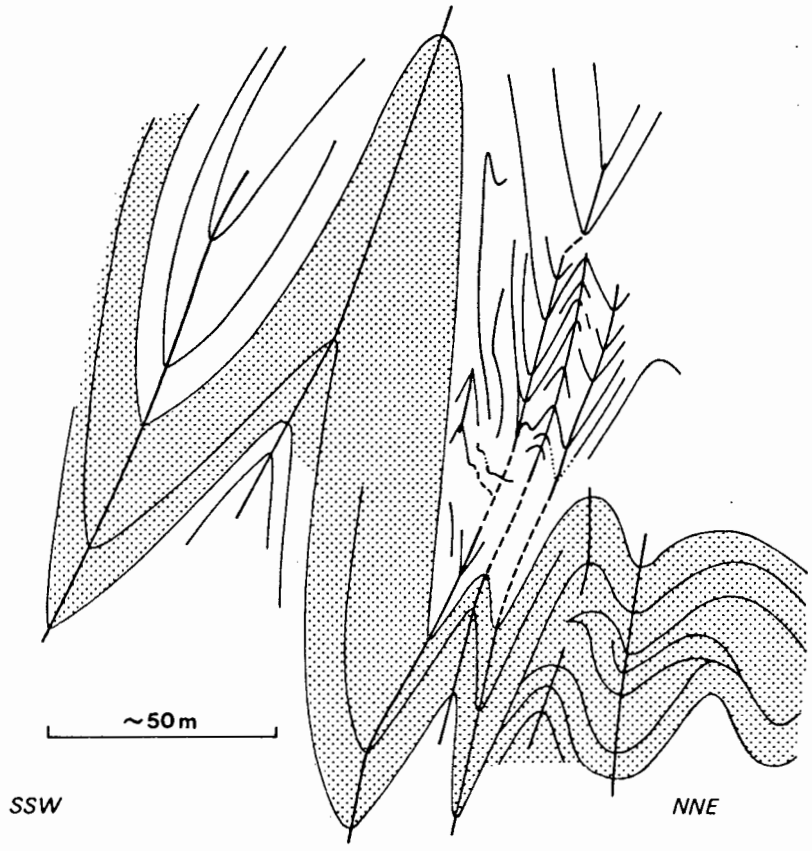

Fig. 5.3 Medium-scale folding along a profile in the valley of the Orange River west of Mike. Drawn after stereoscopic photographs. (B in Fig. 5.5 c)

lithology and metamorphic grade. Structural elements will therefore be discussed separately for the Pink-gneiss Unit, the Windvlakte Formation and the Helskloof Migmatitic Complex.

Two phases of folding can be recognised : early tight to isoclinal F_1 and large open F_2 folds. In addition, schists formed during the Devilscastle Event are most prominently developed in the west of this domain but will be treated in a separate chapter.

2. *Fabric elements*

Fabric elements occurring in the southeastern Richtersveld are tabulated in Table 5.3.

Sedimentary layering (SS_1) is found in the Pink-gneiss Unit and in the Windvlakte metavolcanics where it is defined by fine lamination on

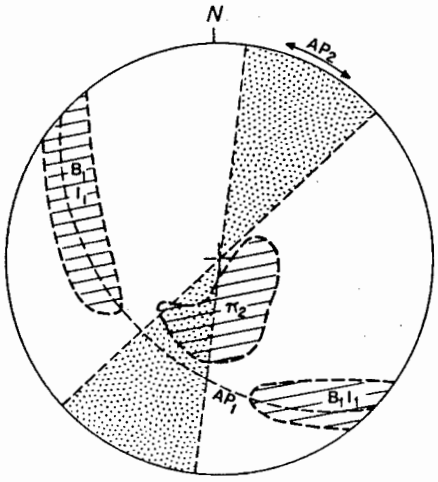

Fig. 5.4a Schematic presentation of the geometrical relationships between F_1 and F_2 structural elements. Fields of pole maxima and traces of axial planes are shown as derived from individual scatter diagrams.

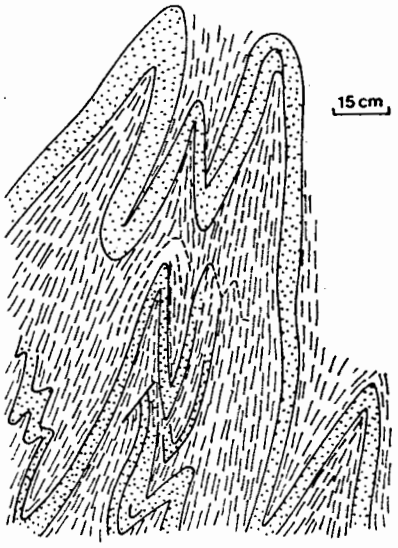

Fig. 5.4b Bands of pure quartzite in mica schist show parallel, partly concentric folds. Tendency to similar-type folds only at places. All folds shown here have a fairly constant wavelength-thickness ratio (w/t) of 5,7 ($\bar{x}$ = 5,67, s = 0,45) (See also Fig. 5.19)

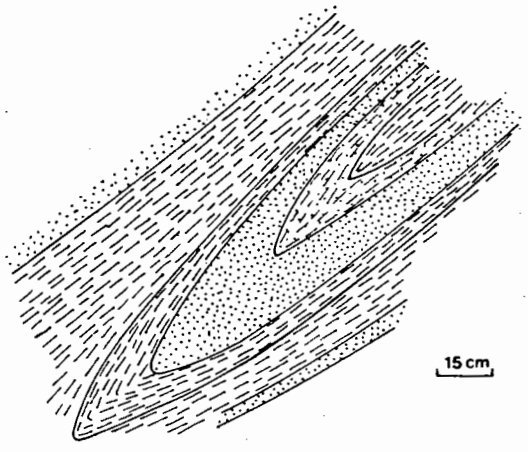

Fig. 5.4c Similar fold caused by higher ductility of impure quartzite and smaller differences of ductility.
Same locality as (b). The folds in (b) and (c) are from valley south of C (Fig. 5.5)

Fig. 5.5. Fabric elements in the Bak River area (A in Fig. 5.5c). The SS_1 poles in b) represent tight to isoclinal folds with nearly vertical axial planes. The foliation S_3 cuts F_1 perpendicularly and is also present in the adjacent Vioolsdrif granodiorite (G_2). Indications for the presence of S_1 in G_2 have not been encountered here.

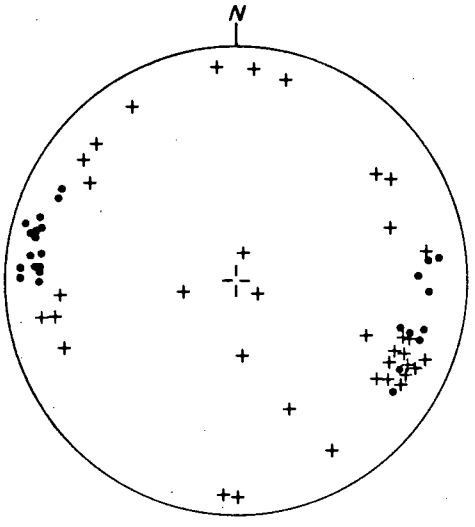

(a)
Fabric elements in Vioolsdrif granodiorite. dots: S_3, crosses: jointing

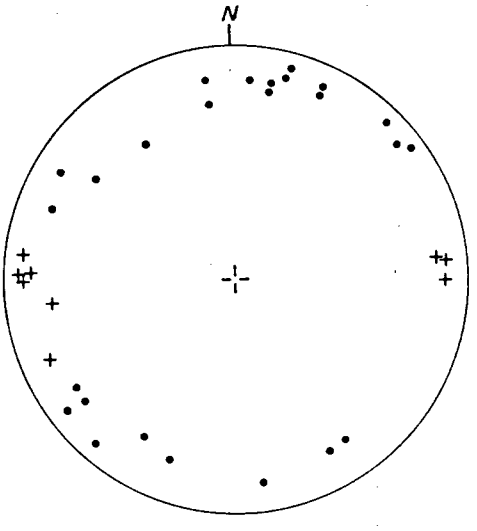

(b)
Fabric elements in Rosyntjieberg quartzites. dots: SS_1, crosses: S_3

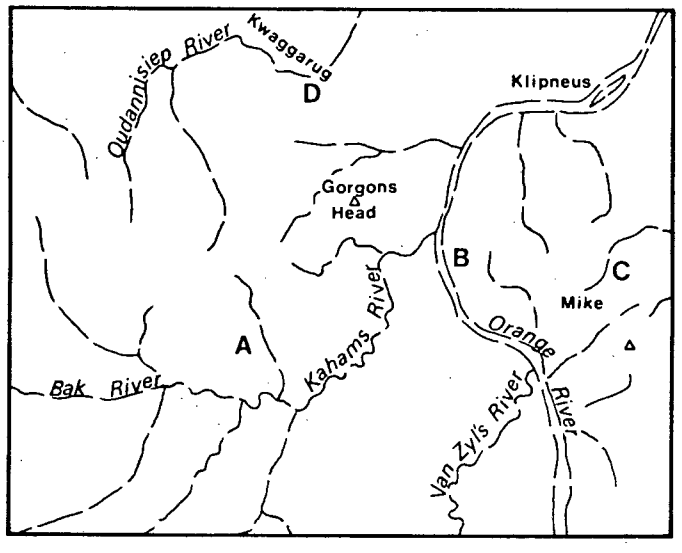

(c)
Key map with position of areas discussed:
A Bak River
B Orange River
C Mike (nappe structure)
D Kwaggarug

Fig. 5.6 Fabric elements of the southeastern Rosyntjieberg Formation

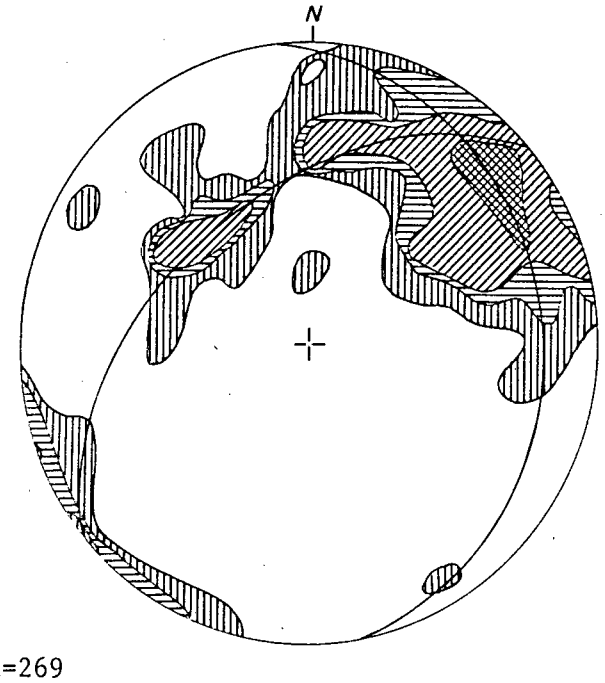

n=269
1-2-3-6%

Fig. 5.6a
Equal-area projection of all SS_1 elements. The girdle of SS_1 has been deformed by F_2, resulting in a cross-girdle distribution of the maxima.

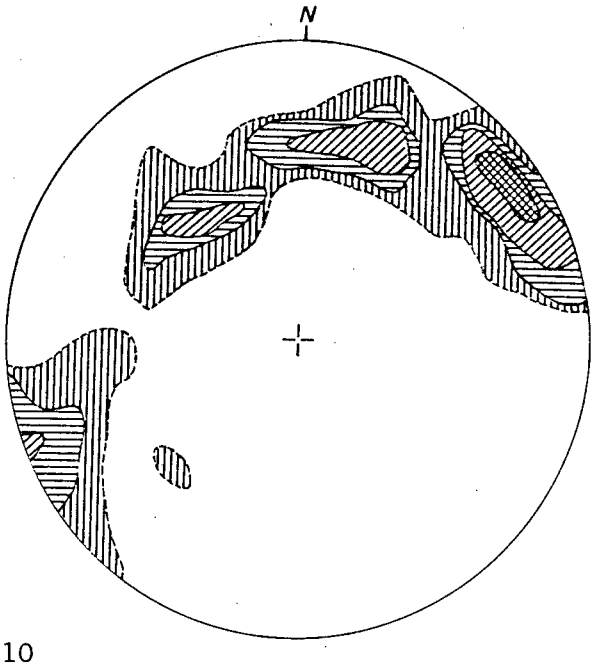

n=110
1-3, 5-6-15%

Fig. 5.6c
Equal-area projection of SS_1 elements in areas not affected by F_2. The maxima distribution can be described by a simple great circle.
(D in Fig. 5.5.)

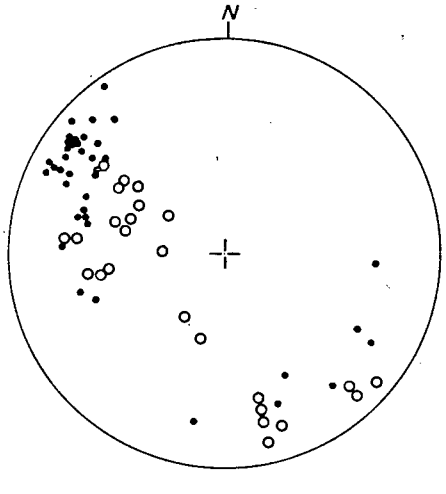

Fig. 5.6b
Synoptic scatter diagram of all linear elements.
dots B_1;
circles l_1

Table 5.3

Structural elements of the southeastern Richtersveld

primary elements	SS_1:	SS_2:	SS_3:
a) definition	a) sedimentary and volcanic layering.	a) neosomatic banding in migmatites; aplitic leucosome and mafic melanosome	a) aplitic veins cross-cutting SS_1 and SS_2, mm to cm thick.
b) orientation	b) variable	b) variable	b) variable, ptygmatically folded if striking NW
c) occurrence	c) Windvlakte volcanics, occasionally in PGU	c) Windvlakte volcanics and HMC	c) Windvlakte volcanics

foliation	S_1:	S_2:
a) definition	a) alignment of mica	a) alignment of mica
b) orientation	b) NW strike, gentle NE dip	b) N-S, steep
c) occurrence	c) mainly PGU, occasionally in Windvlakte volcanics	c) granodiorite of the VIS
lineation	L_1:	L_2:
a) definition	a) stretching of mineral aggregates	a) stretching of mineral aggregates in S_2.
b) orientation	b) down-dip N, $//B_1$	b) steeply N plunging
c) occurrence	c) mainly PGU, subordinate in Windvlakte volcanics	c) granodiorite of the VIS
folding	F_1:	F_2:
a) definition	a) folding of SS_1 in PGU and of SS_1 and SS_2 in migmatites and meta-volcanics	a) deformation of F_1 in PGU, mainly inferred. Ptygmatic folding of SS_3 in metavolcanics.
b) orientation	b) W to NW trend of axial plane, gently to moderately dipping to the NE	b) AP NE trending, dipping steep to vertical; B_2 steeply plunging to the NE
c) wavelength	c) dm to 10 m	c) km, mm to cm-range in ptygmatic folds
d) shape	d) tight to isoclinal	d) big folds open, small folds (SS_3) ptygmatic
e) occurrence	e) PGU and Windvlakte volcanics	e) big folds PGU and Windvlakte Formation (inferred), small folds (ptygmatic) in Windvlakte volcanics.

the mm-scale observed in connection with crossbedding-like structures. It can be inferred in most cases in the Pink-gneiss Unit by mapping and is on a regional scale subparallel to S_1 (Figs. 5.8a, 5.10b). Migmatitic layering (SS_2) may be folded but as a rule tends to be only weakly affected by deformation. If SS_1 is also present, the attitude of SS_2 tends to be controlled by sedimentary layering (Fig. 5.10a). Aplitic veins (SS_3) cut SS_1 and SS_2 and are only ptygmatically folded when trending approximately northwest (Fig. 5.10c). S_1 is most prominently developed in the Pink-gneiss Unit (Fig. 5.8a) and absent in the granodiorites of the Vioolsdrif Intrusive Suite. Coarse biotite gneiss of the Pink-gneiss Unit, strongly affected by S_1 may, however, be derived from Vioolsdrif granodiorite; the same applies for l_1 (Fig. 5.8b). S_2 is penetratively developed in the southeasternmost granodiorite (G_2) where it imparts a distinct gneissosity on the rock and disappears gradually to the north. It is less strongly developed in the Pink-gneiss Unit and present but not well recognisable in the meta-volcanics of the Windvlakte. The same mode of distribution applies for l_2 (Fig. 5.11).

3. *Major structural features*

F_1 folds are rare and can be identified with certainty only in the Pink-gneiss Unit. In Fig. 5.12 the structural elements of one of the best preserved F_1 folds are compared and measured and constructed fold axes can be shown to be approximately coaxial with l_1. It is therefore justified to interprete S_1 as axial-plane foliation and l_1 as axial lineation of F_1. It should be noted, however, that in contrast to F_1 folds elsewhere in the Richtersveld the fold axes here are down-dip, a fact which may create difficulties in the interpretation and correlation of F_1 folds. F_2 folds can only be inferred from mapping and are expressed in regional undulations of mapped stratigraphic units. Further indications for the presence of a F_2 fold phase can be obtained by structural analysis:

a) The scatter of l_1 can be reduced if each individual S_1 on which l_1 has been measured is rotated back into the reference great circle likely to represent the original position of S_1 prior to F_2 (Figs. 5.13b & c). This has been done for the area sketched in Fig. 5.13a using the great circle of the fold shown in Fig. 5.12 as reference. That way it can be demonstrated that S_1 and l_1 have been rotated together by the same amount and around the same northeast-trending axis.
b) In Figs. 5.10c, 5.7b it is shown that only those aplitic veins that strike in a northwesterly direction (stippled area) are ptygmatically folded. This suggests a direction of compressive strain for F_2 from the southeast, which is in agreement with directions inferred from F_2 elsewhere and also indicates that this deformation postdates the intrusion of the aplitic veins.
c) A northeast-trending axial direction is also evident from the dip isogon map in Fig. 5.14. This map, based on average dip values of

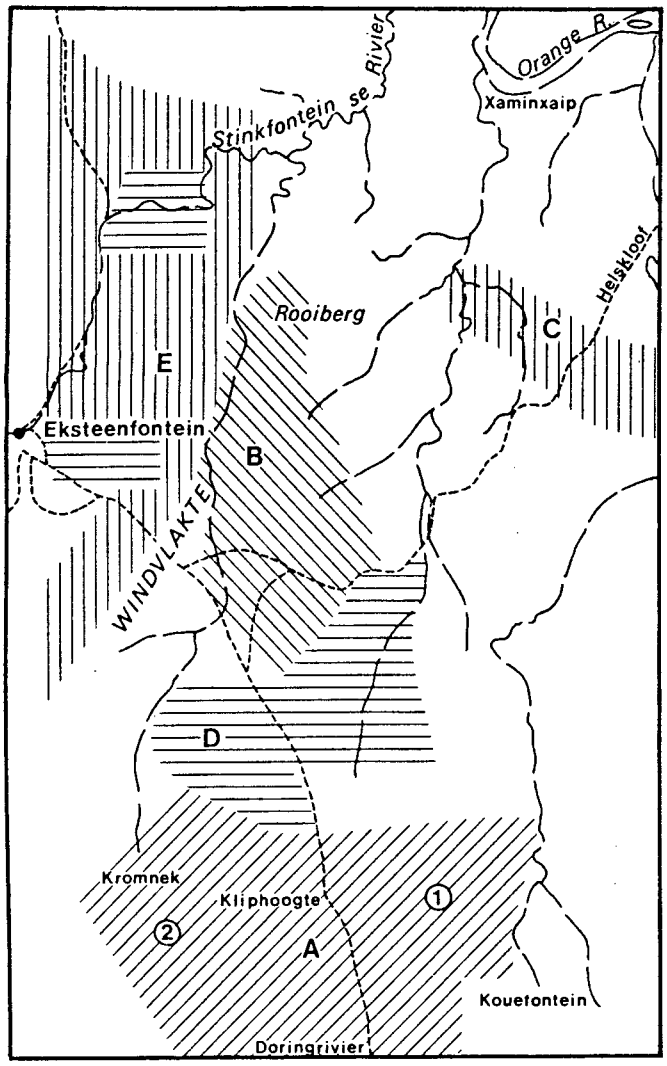

Structure of the southeastern Richtersveld

Fig. 5.7a
Key map:

A) Pink-gneiss Unit
B) Windvlakte metavolcanics
C) Helskloof Migmatitic Complex
D) Vioolsdrif granodiorite (G_2)
E) Devilscastle Schist Belt

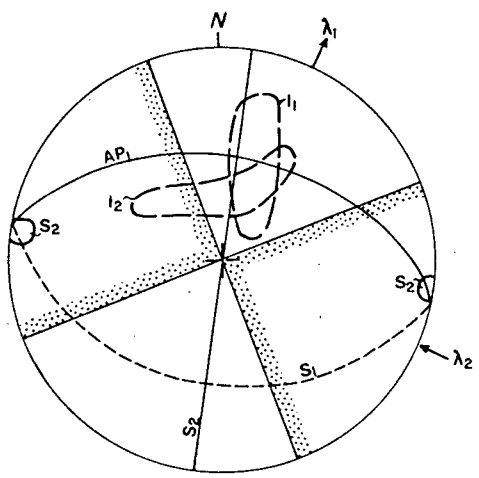

Fig. 5.7b
Schematic presentation of the geometrical relationships between F_1 and F_2 fabric elements. The fields of pole maxima and trace of axial planes are shown as derived from individual scatter diagrams.
Stippled field : direction in which ptygmatic folding of SS_3 (aplitic veins) occurs.

Fig. 5.8 Structural elements of the Pink-gneiss Unit (A, Fig. 5.7a)

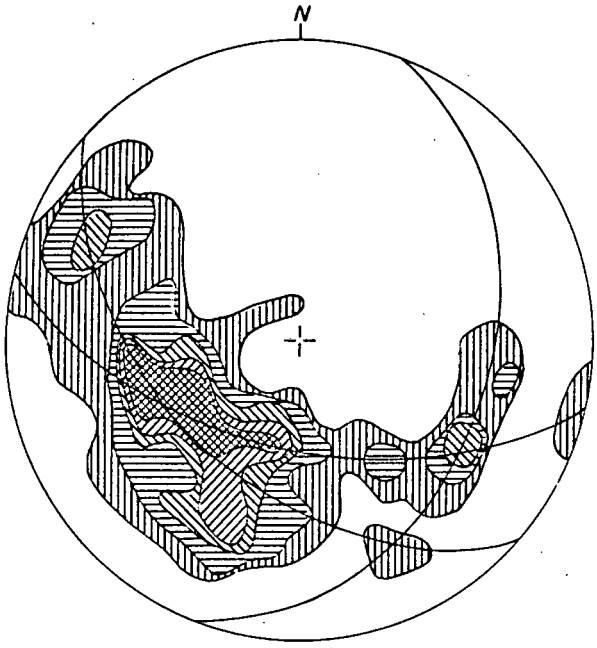

Fig. 5.8a
Equal-area projection of all S_1 poles

n = 180
1-2-3-4-5%

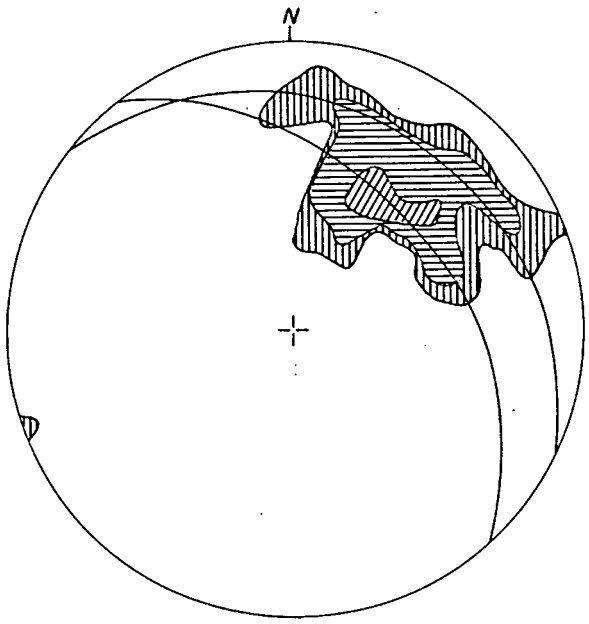

Fig. 5.8b
Equal-area projection of l_1

n = 62
2-5-12%

Fig. 5.9 Structural elements of the Helskloof Migmatitic Complex (C in Fig. 5.7a)

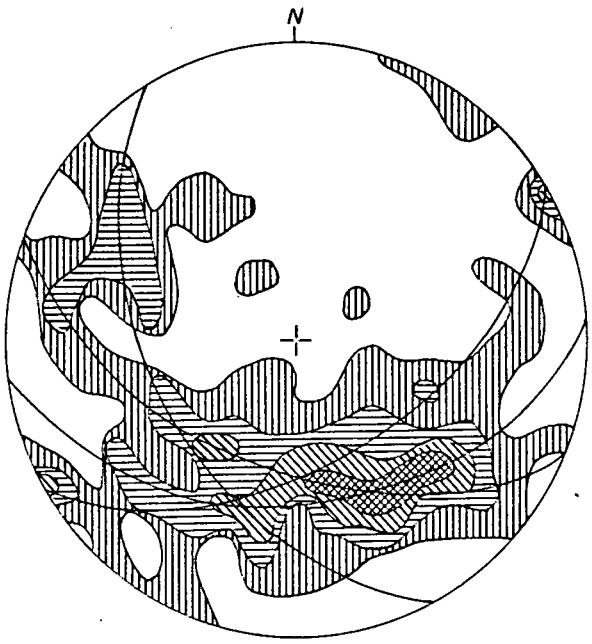

n = 179
1-2-3-4%

(a)

Equal-area projection of all SS_2 poles in the Helskloof Migmatitic Complex. The cross-girdle pattern may indicate a deformation of SS_2 around a northeast trending axis.

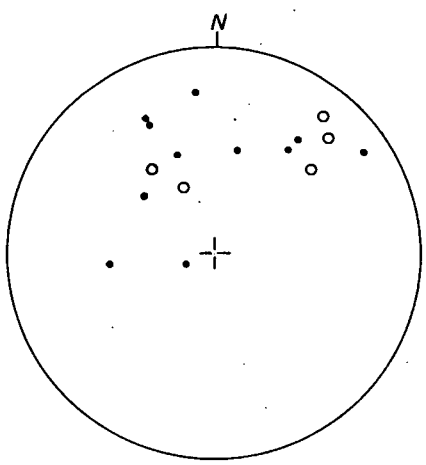

(b)

Scatter diagram of linear elements measured on SS_2
Circles: π; dots: lineations on SS_2

Fig. 5.10 Fabric elements (F_1 and F_2) in metavolcanics of the Windvlakte Formation (B in Fig. 5.7a)

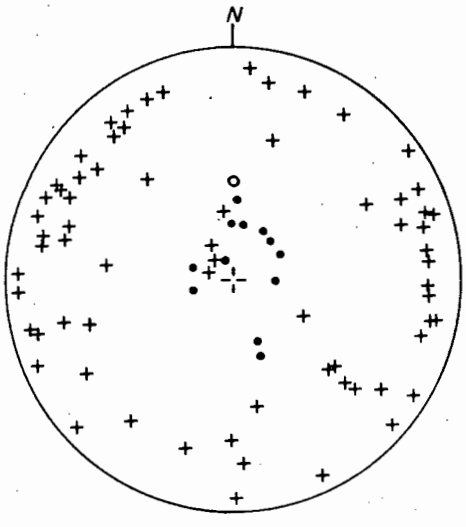

(a)
Scatter diagram of migmatitic neosome. The directional distribution appears to be influenced by primary layering

crosses: SS_2; dots: 1 on SS_2; circles: B_1

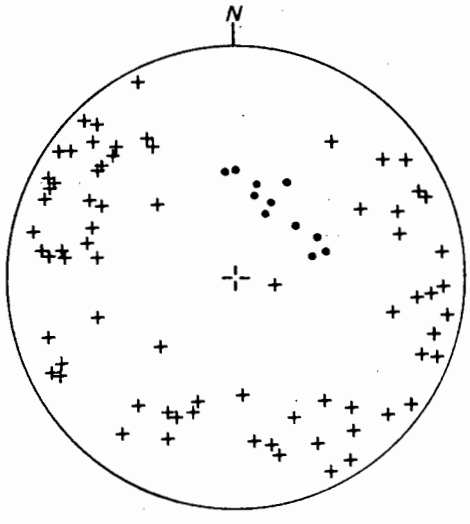

(b)
Scatter diagram of primary layering

crosses: SS_1; dots: 1 on SS_1

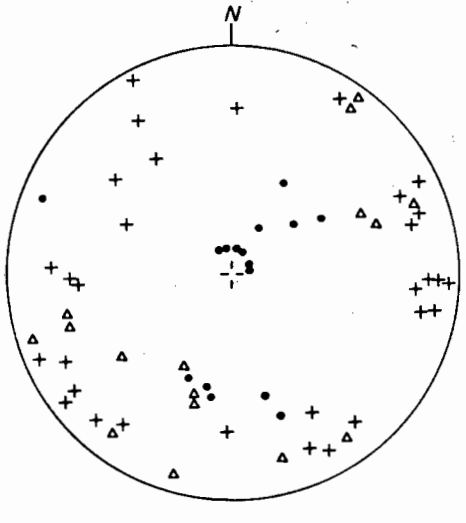

(c)
Scatter diagram of aplitic veins (SS_3). Only northwest-striking veins are ptygmatically folded.

triangles: SS_3 folded; crosses: SS_3 not folded; dots: 1 on SS_3

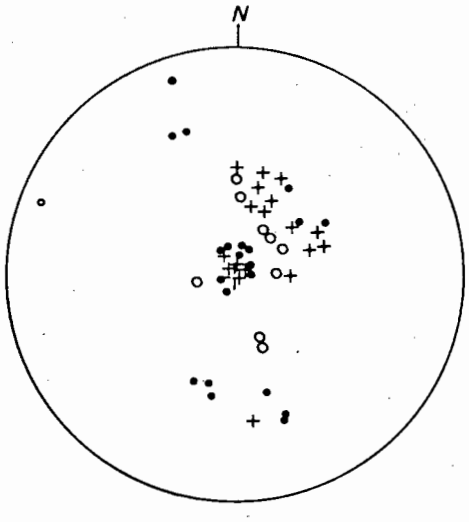

(d)
Synoptic scatter diagram of linear elements occurring in migmatitic metavolcanics

crosses: 1 on SS_1; circles: 1 on SS_2; dots: 1 on SS_3

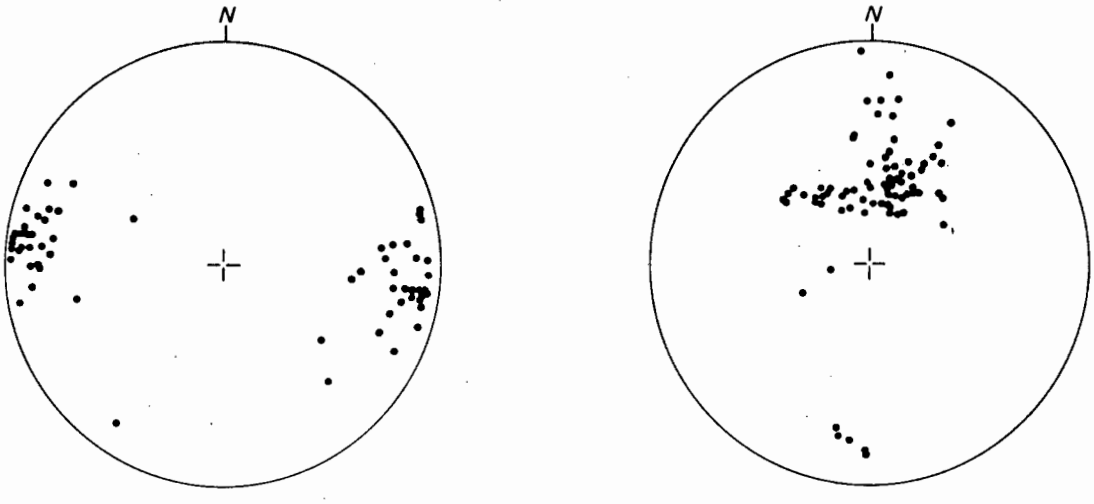

Fig. 5.11

Fabric elements in Vioolsdrif granodiorite (G_2) of the southeastern Richtersveld (D in Fig. 5.7a)

(a) foliation S_2

(b) lineation l_2

S_1, SS_1 and SS_2, has been constructed using a grid with squares of one cm^2 * in which all values within the same square were averaged again and noted in the centre of the square. From these values the isogons were constructed by standard geological methods. An isogon map of this kind displays variations of the amount of dip irrespective of its direction. Since a fold structure is characterised by a regular variation of the amount of dip with a minimum at the fold hinge, the distribution of isogons is likely to reveal axial trends. Because the influence of local variations (i.e. small-scale folds) has been eliminated by averaging the field readings several times, the data plotted on the map thus represent trends and not the local values of dip which might be rather variable.

By devising this map it had originally been intended to show the gradual decrease of dip angles in the direction of increasing metamorphism. Instead, a tectonic interference pattern emerged that appears to show the axial directions of F_1 and F_2 particularly well.

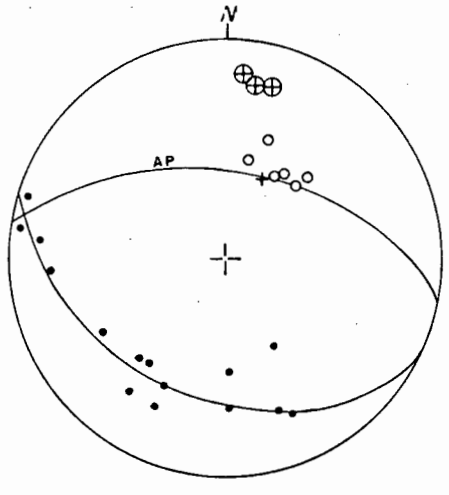

Fig. 5.12 Fabric elements of F_1 fold.
Dots : SS_1; circles: L_1; Crossed circles: B_1; cross : π_1.
F_1 fold near Kromnek (Domain A_2)

5.2.4. The Noms River-Blockwerf area

1. *General*

This domain is characterised by tight to isoclinal folding on the kilometer scale in the Noms River area and by penetrative tectonic elements in the Blockwerf Migmatitic Complex. It is bounded in the south-west by the line joining De Hoop and the Pokkiespramberge.

* On the original map 1 : 100 000

Fig. 5.13 Aberrant directions of F_1 fabric elements of the Pink-gneiss Unit (A_1 in Fig. 5.7a)

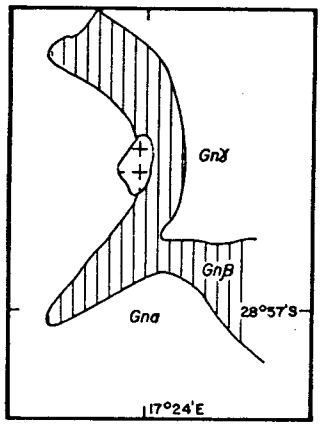

(a)
F_2 fold from which fabric elements are taken.

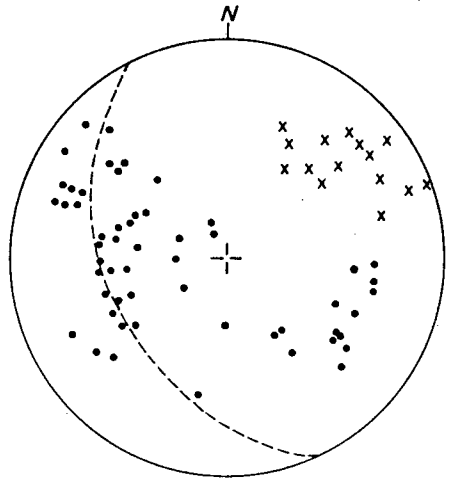

(b)
Scatter diagram of F_1 elements - dots: S_1; crosses: l_1.

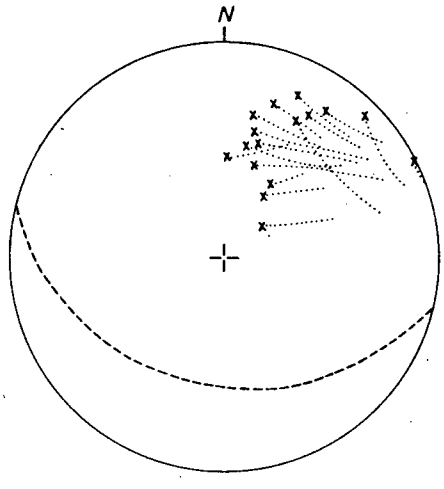

(c)
Movement of l_1 when their respective S-planes are rotated into the great circle indicated below. The scatter of l_1 is markedly reduced. See text for discussion.

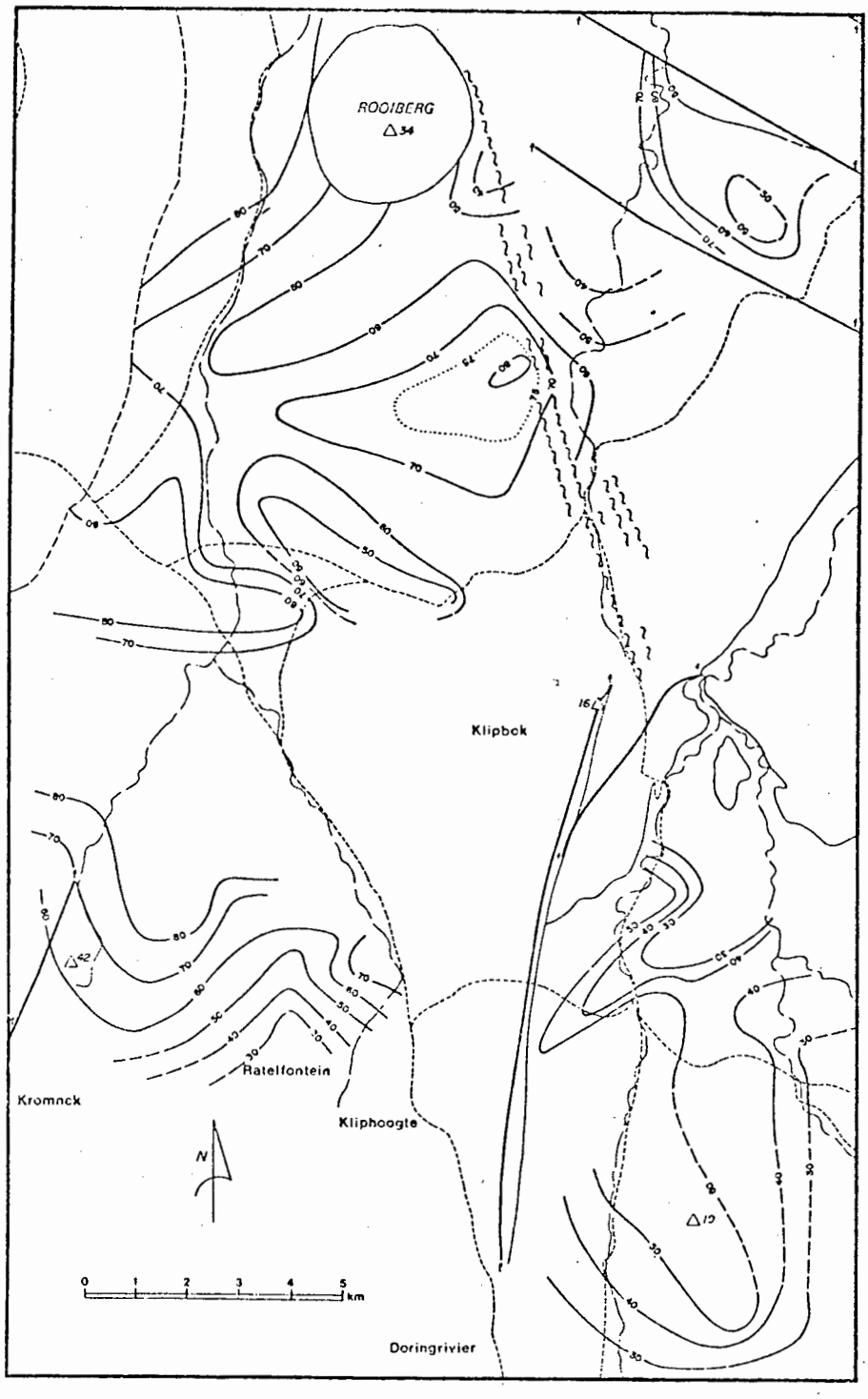

Fig. 5.14 Dip-isogon map of the southeasternmost part of the Richtersveld. Based on measurements of SS_1 and SS_2 in metavolcanics and S_1 in the Pink-gneiss Unit. The isogons are thought to reflect a tectonic interference pattern caused mainly by superposition of F_2 on F_1. Of all structures shown only the one southeast of Klipbok is obvious in the field. The isogon pattern within Helskloof migmatites is regarded as unreliable since dip variation within individual outcrops is too high and distribution of outcrops is too irregular. See text for further details.

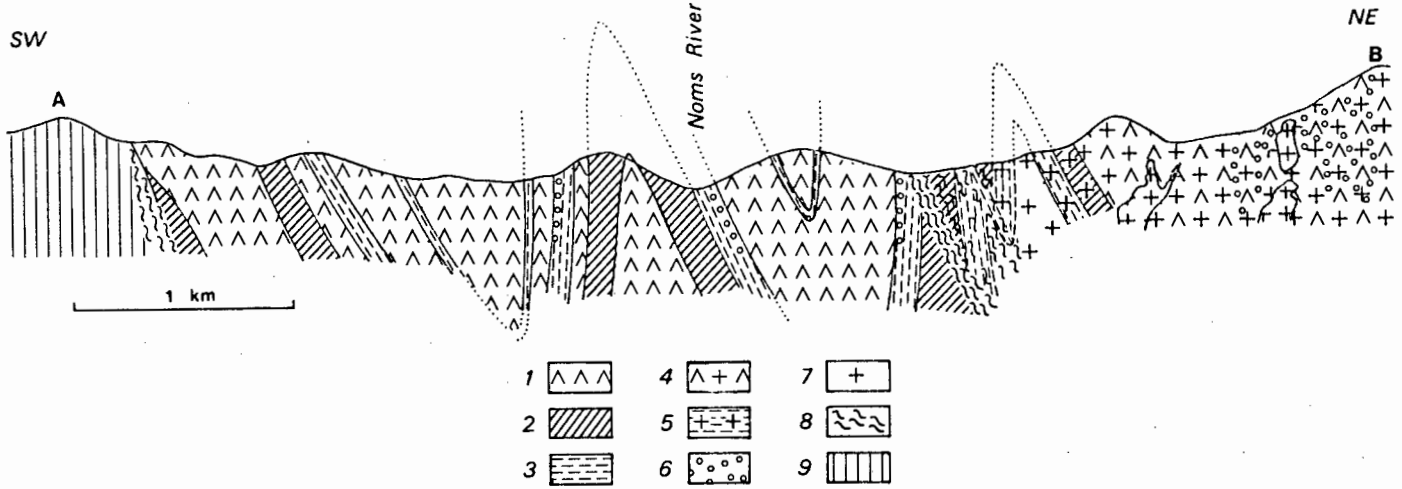

Fig. 5.15
Profile across the Noms River Fold Belt. 1)melanocratic volcanics 2)leucocratic volcanics 3)laminated metasediments 4)gneiss, amphibolite 5)leucocratic gneiss, muscovite schist 6)migmatite 7)Oenas granite (G_5) 8)Noms River fault zone 9)leucocratic volcanics of the Abikwarivier Formation

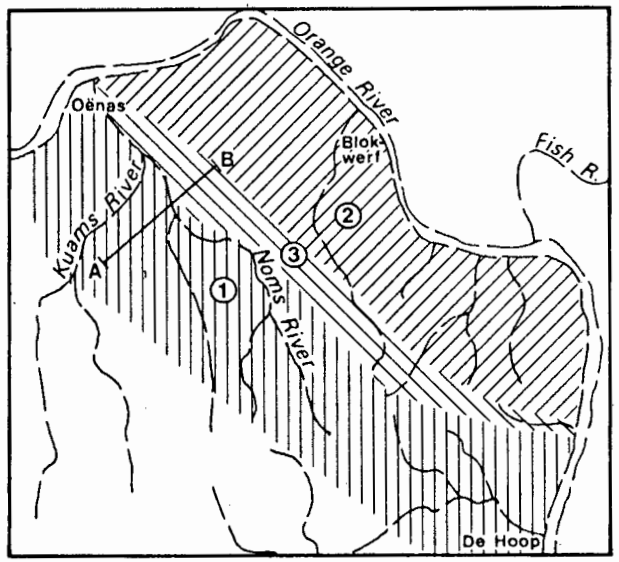

Fig. 5.16

Key map of the Noms River - Blockwerf area
A-B : Profile Fig. 5.15

1) Noms River Fold Belt
2) Blockwerf Migmatitic Complex (BMC)
3) Noms River fault zone

Fig. 5.17 Fabric elements of the Noms River - Blockwerf area

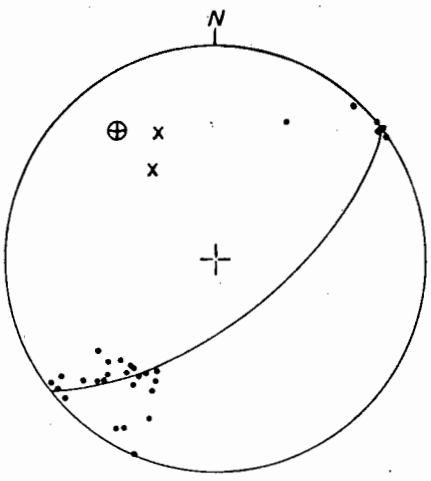

(a)
Noms River Fold Belt - dots: SS_1; crosses: l_1; crossed circle: π

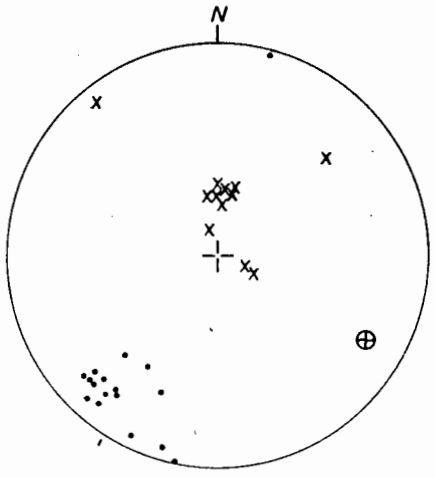

(b)
Noms River fault zone - dots: S ; crosses: l ; crossed circle: π of late kink fold .

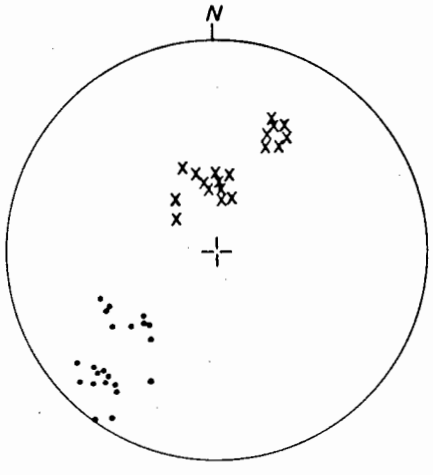

(c)
Blockwerf Migmatitic Complex
dots: S_1; crosses: l_1

2. *Fabric elements*

Fabric elements of this area are schematically tabulated in Table 5.4.

Table 5.4 Structural elements of the Noms River-Blockwerf area

	Noms River	Blockwert area
bedding	SS_1:	SS_1:
a) definition	a) change of material and grain size	a) change of material, inferred from mapping only
b) orientation	b) NW striking, variable dip	b) NW striking, moderately NE dipping
foliation	S_1 :	S_1 :
a) definition	a) alignment of mica in pelitic rocks, not or weakly developed in volcanics	a) alignment of mica
b) orientation	b) NW, steeply dipping	b) NW, NE dipping
	S_2' : (rare)	
	a) crosscutting S_1 in pelitic rocks	
	b) NW striking, inclined to S_1	
lineation	l_1 :	l_1 :
a) definition	a) unknown, rarely observed; possibly intersection of S_1 and S_2' in pelitic rocks	a) stretching of mineral aggregates
b) orientation	b) horizontal, //B	b) inclined to down-dip
folding	F_1 :	F_1 :
a) definition	a) deformation of SS_1	a) deformation of SS_1, inferred from mapping only.
b) orientation	b) NW, horizontal	b) NW trending axial plane
c) wavelength	c) 1,5 km	c) probably km-range
d) shape	d) tight	d) unknown

In the Noms River Fold Belt joints and cleavages parallel to the axial plane of F_1 have been interpreted as axial-plane foliation but since they become more pronounced towards the east they could as well be related to the Noms River fault zone. The linear elements of the two sub-domains display distinctly different directional attitudes. The lineation (l_1) of the Blockwerf Migmatitic Complex is down-dip or nearly down-dip, a feature also encountered in the high grade rocks of the Pink-gneiss Unit (Fig. 5.17a).

The planar fabric elements of the Noms River fault zone (Fig. 5.17b) strike and dip similar to SS_1 and S_1 and their formation seems to have been controlled by the latter. In many cases S_1 can actually be seen to be overprinted by the later foliation. The directional attitude of lineations of this zone is variable and although they are mostly plunging to the north-west, horizontal lineations are also encountered.

3. *Major structural features*

A profile through the Noms River Fold Belt is shown in Figure 5.15. Synclines and anticlines could easily be reconstructed since facing criteria (crossbedding) are abundant and the stratigraphic succession is uncomplicated. Folding within the Blockwerf Migmatitic Complex is not obvious but there are indications from mapping that suggest fold wavelengths similar to those of the Noms River area.

Noms River Fold Belt and Blockwerf Migmatitic Complex are separated by a narrow but persistent zone of intense deformation, partly of brittle fracture type, termed here *Noms River fault zone*, that appears to be part of a regional structural feature, since a zone of "intense foliation" mapped by Blignault (1977) in the Lower Fish River area is situated along strike of the Noms River fault zone. While most of its lineations suggest horizontal movement, horizontal axes of kink folds also indicate movement in a vertical direction. This view is supported by the rapid transition in metamorphic grade across this zone. It is suggested that the Noms River fault zone acted as a line of crustal weakness to the east of which crustal uplift occurred leading to the exposure of lower crustal levels in the Blockwerf area. Since it post-dates all other tectonic and metamorphic events it might be related to the Devilscastle Event, but a considerably younger age can also not be ruled out.

5.2.5. Summary

Fabric elements related to F_1 constitute the earliest structural imprint and affect G_2 (granodiorite, 1900 my) but not the younger intrusives. S_1 forms the axial-plane foliation to F_1, and l_1 on S_1 trends northwest in the central part and north to northeast down-dip in the marginal parts of the Richtersveld; in both cases it is parallel to B_1.

F_2 elements are present only in the southeastern part of the area. The large, open F_2 folds can only be inferred by mapping and deform F_1 around a northeast-trending axis.

Distribution and pervasiveness of structural elements are irregular and appear to be controlled by lithological properties at the time of deformation:

a) Fabric elements in metavolcanics in areas of low grade metamorphism are not penetrative
b) penetrative fabric elements are only developed in high grade metamorphic terrains and in metapelites of low grade metamorphic areas
c) folding (F_1) appears to be present everywhere but with rather variable wavelength : cm to m scale in the southeastern Rosyntjieberg Formation and Pink-gneiss Unit, km-scale in the Noms River Fold Belt and ~20 km in the Richtersveld anticline.

5.2.6. Discussion

Folds referred to as F_1 have been described from all parts of the Richtersveld. Their only common feature is a west to northwest-striking axial plane. The orientation of fold axes and linear elements differs between high and low grade metamorphic terrains and within low grade terrains folds of consistent orientation differ largely in magnitude. In addition, mesoscopic folds are only occasionally observed and thus raise the question as to the strain distribution within the Richtersveld. It is therefore necessary to discuss whether F_1 folds within the low grade terrain can be correlated despite their different magnitude, whether F_1 folds in high and low grade terrains can be correlated despite their different attitudes and whether the strain distribution within the Richtersveld can be regarded as homogeneous.

1. *Geometrical correlation of F_1*

While F_1 folds of the central northeastern Richtersveld (Richtersveld anticline), the Noms River Fold Belt and the southeastern Rosyntjieberg Formation are co-planar and co-axial, F_1 folds of the marginal area (Pink-gneiss Unit, Blockwerf Migmatitic Complex) are co-planar but not co-axial with respect to the central Richtersveld, raising the question as to their time of development. The following possibilities are imaginable:

a *Unconformity between horizontal and down-dip l_1 :*

Although this argument at first sight is strongly favoured by the sudden disappearance of structural elements when approaching the Windvlakte volcanics from the Pink-gneiss Unit, it is invalidated in the areas north of the Richtersveld: in the Blockwerf Migmatitic Complex rocks derived from Richtersveld volcanics show strongly down-dipping linear elements and Blignault (1977) described the same from the Haib and the Lower Fish River areas. In

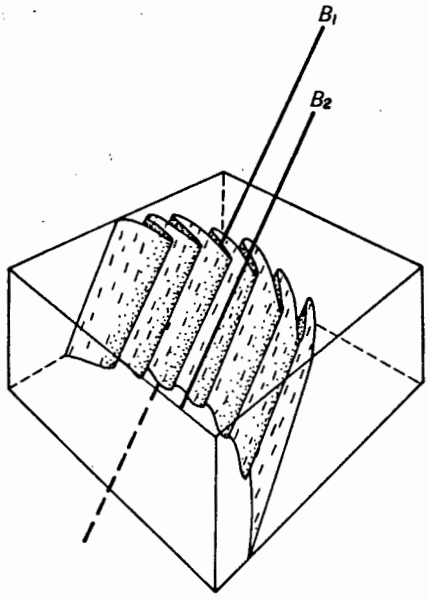

Fig. 5.18a
Relationship of F_1 and F_2 axial elements in different parts of the Richtersveld.

a) In the PGU F_1 and F_2 are coaxial but not coplanar (B_1// B_2; $AP_1 \perp AP_2$)

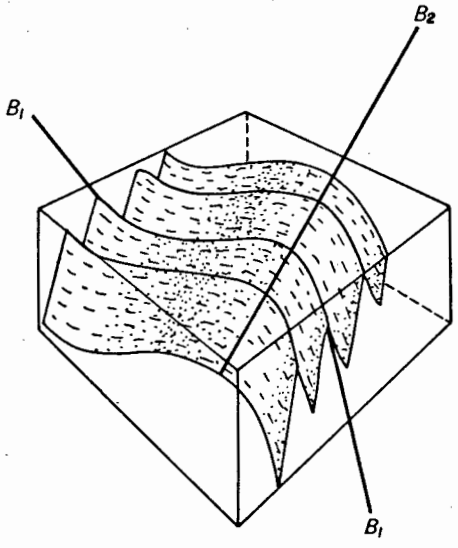

Fig. 5.18b
In the southeastern Rosyntjieberg Formation $B_1 \perp B_2$ and $AP_1 \perp AP_2$. In high grade metamorphic rocks B_1 appears to have formed // to the maximum extension direction while in lower grade rocks B_1 is normal to the maximum extension direction. (see text for discussion)

addition, even in the central Richtersveld occasional down-dip linear elements do occur (Fig. 5.2c). Since there are also no obvious signs for an unconformity between the Pink-gneiss Unit and the Richtersveld volcanics and even less signs for a major structural unconformity within the Richtersveld volcanics, an explanation involving a structural unconformity is rather unlikely.

b *Horizontal and down-dip structural elements have been superimposed on each other.*

This assumption is hard to substantiate since horizontal as well as inclined structural elements are imprinted on the Vioolsdrif granodiorite in the central Richtersveld while in other parts of the Richtersveld granodiorites of the Vioolsdrif Intrusive Suite are affected by neither of them. Similar observations have been made by Blignault (1977) in the adjacent areas and Joubert (1971) even dated his F_2 (which must for geometrical reasons be related to F_1 of the Pink-gneiss Unit) as prior to the intrusion of the Vioolsdrif Intrusive Suite. All this rules out a considerable difference in age between these two structural elements and it is therefore unlikely that they constitute distinct structural events.

c *Horizontal and down-dip structural elements have been formed during the same event.*

This would imply different axial directions formed under the action of the same strain pattern, which appears somehow unlikely and there is no known mechanism to provide for its explanation. It can, however, not be completely ruled out, as is indicated by the different nature of the axial lineations: while in the marginal parts l_1 is defined by stretching and may thus indicate a direction of maximum extension (see also Blignault, 1977, p.81), the axial lineation in areas with horizontal axial direction is defined by the intersection of the crenulation cleavage (S_2') with S_1, suggesting also here a vertical direction of maximum extension but normal to the fold axis. That way the same strain pattern would ensue for both domains, which does not, however, explain why the axial directions are different.

It is therefore not possible to arrive at a clear-cut solution for this problem, but the two alternative solutions: unconformity and superposition, are very unlikely and can be ruled out. Although the kinematic reasons in favour of a syngenetic relationship of "horizontal" and "down-dip" axial elements are rather weak and unconvincing, it is hard to imagine any other possibility than the contemporaneous development of these two structural elements. It is therefore adopted as a working hypothesis in the following.

2. *Layer thickness and wave length*

It is known from experimental investigations in layered viscous materials that the dominant wave length of a fold is dependent on the layer thickness and the viscosity ratios of the layers involved. This relationship

is expressed by the equation

$$W_d = 2\pi t \sqrt[3]{\frac{\eta_1}{6\eta_2}}$$

η_1/η_2 = viscosity contrast between different layers

t = thickness of layer

W_d = dominant wavelength

(Ramberg, 1963, 1964; Ramsay, 1967; Hobbs *et al.*, 1976)
Despite the fact that this equation can only strictly be applied to initial buckling (small amplitude folds), it can nevertheless be used to estimate the general proportions of folds generated in rocks with different layer thickness and viscosities, in which, however, the latter plays much less a role than the layer thickness, as can be inferred from Figure 5.19. In this diagram the w/t ratios of folds of various parts of the Richtersveld have been plotted and compared with calculated w/t ratios for different viscosity contrasts. It is evident that

a) the slope of the observed curve is regular, indicating no major variations in viscosity contrast

b) it is parallel to the calculated curves and thus in good agreement with the predictions.

It is therefore likely that the different magnitudes of F_1 folds are related to the layer thicknesses that dominated the respective areas (i.e. the layer thickness that finally produced the dominant wavelength (c.f. e.g. Hobbs *et al.*, 1976). Lack of mesoscopic folds in the central northeastern Richtersveld is therefore not due to lack of deformation but the expression of rather thick and homogeneous volcanic layers that dominated the process of folding and resulted in large scale regional folds. The same applies for the adjoining northern and southern fold belts which are distinctly dominated by layers of lesser thickness.

3. *The sequence of formation of F_1 folds of different magnitude and their relationship to the Vioolsdrif Intrusive Suite*

One of the questions not yet solved is the relationship of the Vioolsdrif Intrusive Suite and F_1 since granodiorite of the Vioolsdrif Intrusive Suite is partly weakly deformed by F_1 and partly unaffected, and even if deformed, does not show the degree of deformation displayed in supracrustal rocks. This problem can, however, be explained if the sequence of folding is investigated more closely.

Fig. 5.19. The dependence of layer thickness on wavelength in folds (F_1) of the eastern Richtersveld.
Dots : folds from Fig. 5.4b; Crosses : Fig. 5.3; Circle : Richtersveld anticline. Filled circle : Noms River Fold Belt; Solid line : observed w/t ratios. Dashed lines : calculated w/t ratios for different viscosity ratios : (a) = 1, (b) = 100. Dotted dashes : recalculated after Currie *et al.*, (1962).
t = layer thickness, W = wavelength

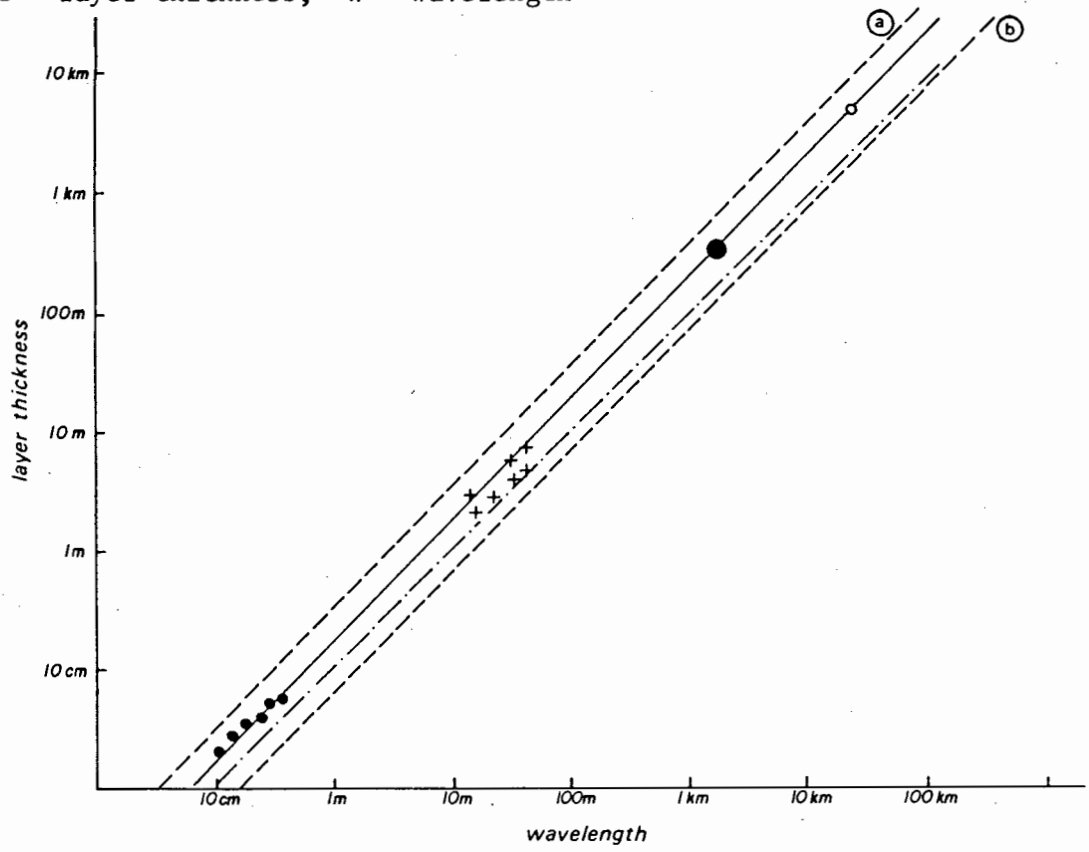

Ramberg (1964), investigating experimentally a competent/incompetent multilayer system occurring close to a thick layer of the same competency found that, subjected to compression, the thin layered multilayer buckled more readily and at an earlier stage than the thick layer of the same competency, which yielded essentially by layer parallel shortening and buckled only after continued shortening with a wavelength appropriate to its layer thickness. This experimental setting applied to the Richtersveld (thin-layered multi-layer = Rosyntjieberg quartzite, thick layer = Orange River volcanics) would result in a difference in age between the mesoscopic and the large-scale regional F_1 folds, the latter being younger than the smaller folds and could help to explain the ambiguous relationship of granodiorite and F_1. The sequence of events leading to the intrusion/deformation relationship is shown in Fig. 5.20 based on experimental results by Ramberg (1964) and observations in the Richtersveld. It may account for the variable degree of deformation of Vioolsdrif granodiorite even if all the granodiorite is assumed to have intruded contemporaneously and for the fact

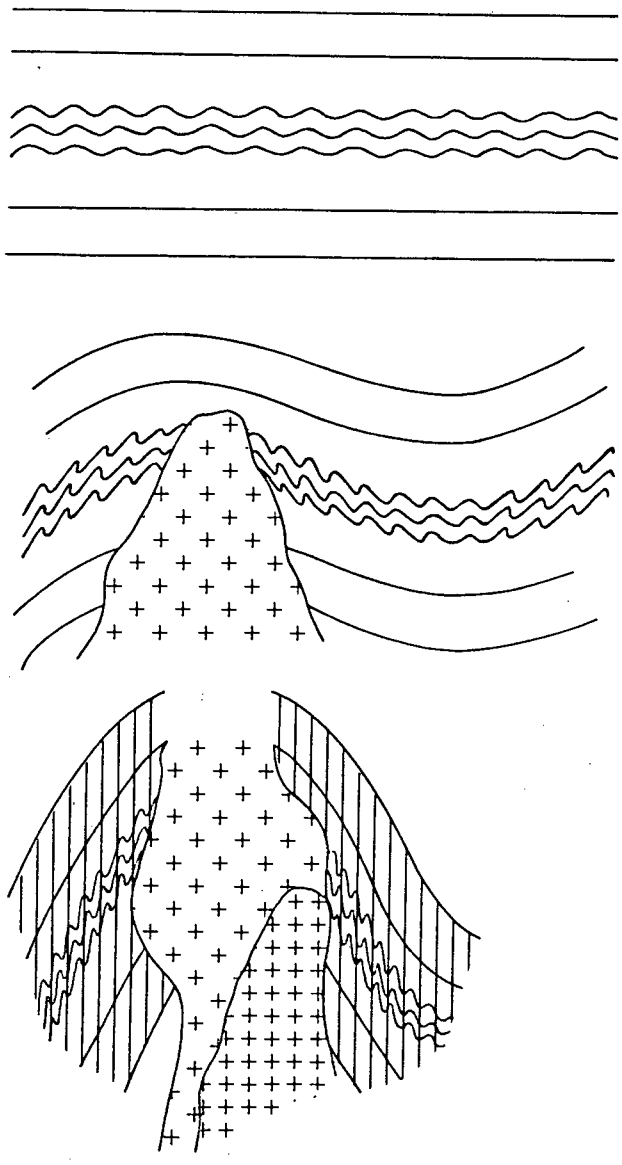

Fig. 5.20
Possible sequence of formation of F_1-folds of different magnitudes and their relationship to the Vioolsdrif Intrusive Suite. Based on experimental results (Ramberg, 1964) and field observations in the Richtersveld.

Early stage of deformation: thick layers yield by layer parallel shortening and the multilayered complex by buckling. (= early, mesoscopic F_1 folds).

Advanced stage of deformation: beginning of buckling of thick layers and distortion of early F_1 folds. Early Vioolsdrif intrusives.

Final stage of deformation: continuing deformation and formation of regional folds. Development of crenulation cleavage (S_2'), cf. 5.2.1.) and deformation of the early granodiorite. Undeformed granodiorite intruded after termination of deformation.

that supracrustal rocks tend to display much stronger deformation than syn-tectonic granodiorite.

5.3. DEFORMATION OF THE DEVILSCASTLE EVENT

5.3.1. General

The Richtersveld is transected by numerous north to northwest-striking zones of intense shearing referred to in the following as Devilscastle Event. In the southeastern Richtersveld shearing during this event has frequently resulted in complete transformation of the country rock into sericite schist and mylonite, comprising wide belts of coherent lithology referred to in the following as Devilscastle Schist Belt and Black Face Mountain Mylonite Belt. Apart from these two belts this event is documented by a variety of minor shear and mylonite zones. The left-lateral nature of shearing is most evident in the Rosyntjieberg Formation and west of Kromnek. The displacement of the Pink-gneiss Unit east of Kliphoogte (Fig. 5.27) can also be related to it, although it may have been reactivated in post-Nama times. The shear zone from east of Rooiberg to Klipbok is doubtful in origin since it displays left-lateral shearing but also deforms dykes of the Gannakouriep Suite. It is possible that this zone, originally formed during the Devilscastle Event, has been reactivated during pre-Nama but post-Stinkfontein (= post-Gannakouriep) times.

In the northeastern Richtersveld deformational zones of the Devilscastle Event traverse the Rosyntjieberg Formation in at least two fault zones near Devils Peak and Kwaggarug which, on entering the granitoids and volcanics, split up into several shear systems consisting of several individual shear zones. A maximum displacement of ~20 km can be inferred for the area between Rosyntjieberg and Kwaggarug

Definitions

Rock terms relating to cataclastic rocks are frequently not well defined. Their meaning as applied in the present context is therefore given below, mainly based on Higgins (1971).

Mylonite, according to Higgins (1971) is "a coherent microscopic pressure breccia with fluxion structure which may be megascopic or visible only in thin section and with porphyroclasts generally larger than 0,2 mm. The porphyroclasts make up about 10 - 50 percent of the rock. Mylonites generally show recrystallisation and even new mineral formation to a limited degree but the dominant texture is cataclastic." In contrast to this, *protomylonite* contains porphyroclasts making up more than 50 percent of the rock and features of the original rock may be preserved in larger fragments.

Microbreccia (Higgins, 1971) is "an intensively fractured but unground cohesive breccia in which grains and fragments are without form orientation. Fragments may range from megascopic to about 0,2 mm and are separated by finer grained material. Fragments larger than 0,2 mm make up more than 30 percent of the rock." In the present context only the term *tectonic breccia* is used, comprising rock fragments of all sizes.

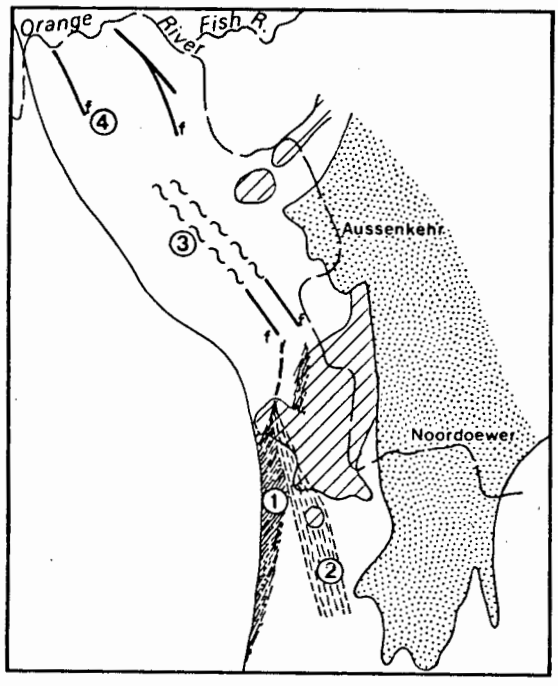

Fig. 5.21 Regional distribution of rocks of the Devilscastle Event.

1) Devilscastle Schist Belt
2) Black Face Mountains Mylonite Belt
3) Shear zones of the northeastern Richtersveld
4) Faults

5.3.2. The Devilscastle Schist Belt (*map unit S*)

1. *Field appearance and extent*

Rocks of the Devilscastle Schist Belt are found in a 1-3 km wide irregular belt with frequently intercalated weakly or undeformed remnants of the country rock extending from the southern margin of the map to the north of Basterfontein. Rocks of this belt are conspicuous in the field by their light pink colour. They form wide mountain ranges especially east of Eksteenfontein (Devilscastle) and around Vanzylsrus. The foliation (S_3) which is the predominant structural element frequently overprints older foliations of slightly different direction, but since this relationship is not systematically developed the whole of this set of foliations is regarded as S_3. Mineral

Table 5.5. Characteristic features of deformational zones of the Devilscastle Event

	Devilscastle Schist Belt	Black Face Mountain Mylonite Belt	Northeastern Richtersveld shear zones
foliation	S_3:	S_3:	S_3:
a)definition	a)alignment of sericite aggregates and quartz	a)compositional lamination	a)alignment of sericite and chlorite
b)orientation	b)N-S strike, E and W dip, steep	b)N-S, NW strike, dip steep, variable	b)NW, steep
	S_4:		
	a)crenulation cleavage deforming S_3		
	b)N-S, inclined to S_3		
lineation	l_3:	l_3:	l_3:
a)definition	a)stretching of mineral aggregates	a)rare, stretching of mineral aggregates	a)stretching of mineral aggregates
b)orientation	b)steep plunge to the north	b)N, steep	b)N, steep
	l_4:		
	a)intersection of S_3 and S_4		
	b)horizontal		
folding	not observed	not observed	not observed
macroscopic occurrence	belt of pink sericite schists	mylonite, protomylonite, tectonic breccia	brittle fracture-type shear zones
degree of recrystallisation after deformation	complete	variable, weak	very weak to weak
relative age	older than unconformity with Stinkfontein; younger than pegmatites and older members of the RIC	older than Rooiberg member of RIC; younger than Black Face Mountain member of the RIC	older than Gannakouriep dyke suite; younger than G_4

Fig. 5.22 Structural elements of the Devilscastle Event

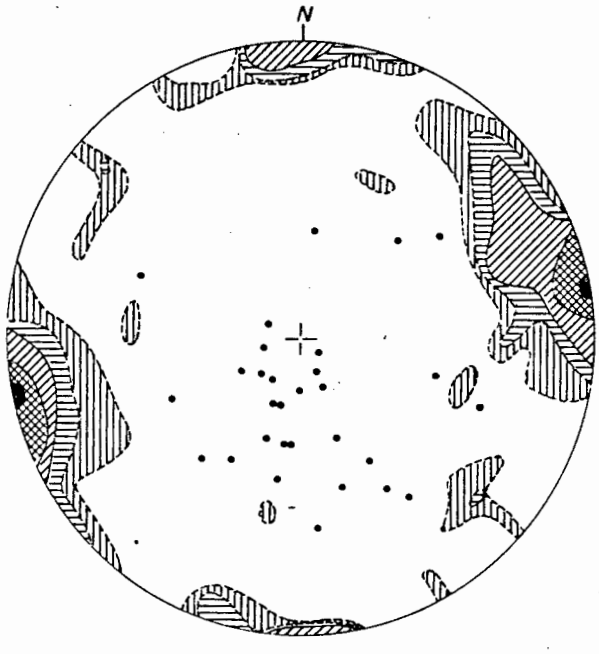

(a)

Northeastern Richtersveld:
Synoptic equal-area projection of shear planes in granites (G_3) that can be correlated with the Devilscastle Event. The frequency distribution of photo-lineaments in Fig. 5.25 is fairly well reflected. Dots: l_3

1-2-4-10-15%

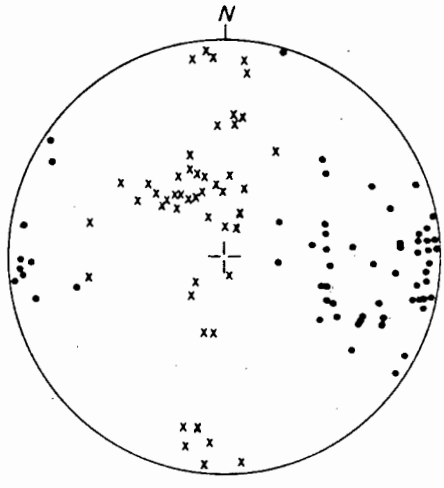

(b)

Southeastern Richtersveld:
Scatter diagram of S_3 (dots) and l_3, l_4 (crosses).
Devilscastle Schist Belt

grains are variable in size and as a rule not recognisable with the naked eye. Lenticular quartz "augen" of up to several mm across, wrapped by the foliation, are a significant feature and occur rather frequently.

Although the main belt is sharply bounded on its eastern margin transitions between the host rock and schistose rocks can be observed and it is obvious that even intermediate volcanics and granodioritic intrusives have been transformed into sericite schists when affected by deformation. Transitions are rather sudden but at places only partly deformed primary textures can be seen in thin section (Fig. 6.17b).

2. *Composition*

Compositional variations are unsystematic and can rarely be followed over long distances. Grey-green varieties interfinger with pink ones and at places, particularly in a ~10 km long and ~100 m wide zone east of Devilscastle, massive rocks are encountered in which quartz dominates over mica. The mineralogical composition is rather uniform and made up of quartz and sericite (~60%, ~40%). Occasionally kyanite and chloritoid occur as accessory minerals. The textural characteristics are complicated and display features of multiple deformation and recrystallisation during decreasing metamorphism, to be described in detail in Chapter 6.

3. *Age*

Despite the fact that the foliation (S_3) and the unconformity with the Stinkfontein Formation are basically parallel, it can be inferred from mapping that on a regional scale the Devilscastle Schist Belt forms an acute angle with the unconformity and is subsequently cut off by it in the south (see Fig. 5.27). Around Klipbokkop rocks of the Richtersveld Igneous Complex (~700 my) are intrusive into the Devilscastle Schist Belt while older members of the Richtersveld Igneous Complex (~900 my) are deformed by the Devilscastle Event. This delimits the period of tectonic activity to the time between 700 and 900 my.

5.3.3. The Black Face Mountain Mylonite Belt (*map unit* T_B)

1. *Field appearance and extent*

The Black Face Mountain Mylonite Belt is found to the east of the Devilscastle Schist Belt and is particularly well developed on the western slope of the Black Face Mountain, where the mylonites and tectonic breccias can easily be mistaken for volcanics and volcanic agglomerates.

Most of the rocks of this belt are in fact protomylonites and volcanic breccias, comprising the whole range of the size of porphyroclasts which are made up of material of the surrounding country rock as well as of mylonites. Their lithological properties are tabulated in Table 5.6.

Table 5.6 Rock fragments in tectonic breccias

Rock type	amount	shape	size	locality	groundmass
syenite of the Black Face Mountain	10-30%	angular to slightly rounded	mm - 10 m	S margin of the Black Face Mountain (28°45'S 17° 20,5°E	Protomylonite
bostonite	acc.	angular to slightly rounded	1 cm - 10 cm	as syenite	Protomylonite
serpentinite	acc.	rounded	one occurrence : 1 m	(28°45,7'S 17°22,3'E)	Protomylonite
mylonite	10-100%	angular to slightly rounded	cm - m range	west slope of Black Face Mountain and other localities	Mylonite and Protomylonite
mineral fragments	no estim. poss.	angular	cm	ass. with syenite and bostonite	Protomylonite

In discussing these cataclastic rocks the following should be stressed:

a) Syenite fragments attain in some cases sizes of nearly 10 m across and are then hard to recognise as fragments. Together with the often massive, dark, partly aphanitic groundmass in which they are embedded, they do not appear to be of tectonic origin at all and have been taken as mixtite or tillite during the early stages of the investigation. This interpretation, however, would entail serious difficulties in the assessment of the whole geological history of the Richtersveld and raise more questions than answers. A relationship with mixtites of the Gariep Group must also be ruled out since transitional boundaries between brecciated and non-brecciated basement rocks and the frequent occurrence of brecciated rocks in small patches render this possibility unlikely.

b) Tectonic breccias at the western slope of the Black Face Mountain may, due to their fine-grained nature, easily be mistaken for volcanics in the field, and also under the microscope a clear distinction is often difficult.

Features such as shown in Fig. 5.23a are, however, an indication of non-volcanic origin.

2 *Texture and mineralogy*

Judging by the field appearance as already described , it is only natural that also in thin section a vast variety of textures is displayed, ranging from weakly recrystallised mylonite to protomylonite in which much of the original texture is still recognisable. So, for example, the groundmass of sample 255 consists mainly of plagioclase, quartz and K-feldspar and minor rock fragments of variable size, displaying a weak compositional layering. In sedimentary terms this rock could as well be regarded as a weakly recrystallised arkose while in tectonic terms it meets the definition of a protomylonite (Higgins, 1971).

In more strongly deformed rocks a compositional lamination is developed and made up of either biotite-rich or quartz and feldspar-rich layers, biotite displaying no or only weak preferred orientation. Figure 5.23a could be regarded as mylonite and constitutes the other end-member on the scale of variable deformation. It is characterised by rounded to angular quartz grains embedded in a very fine-grained matrix in which only sericite can be recognised (<0,01 mm). Sericite is arranged in a fluxion texture but may also occur in random orientation. Particularly typical for this rock is the mostly marginal inclusion of sericite in quartz porphyroblasts and frequently a rounded, clear quartz core is marginally complemented by optically continuous but sericite-stippled quartz with angular outlines. Since this implies that quartz must have grown in an "authigenic-quartz-like" manner after the formation of the fine-grained matrix, an origin as mylonite or ultramylonite for these textures is most likely and can be explained rather easily by assuming this rock to be ground down except for the clear cores of quartz which then acted as nuclei for the growth of post deformational quartz around them, enclosing at the same time not so fast growing materials of the groundmass.

3. *Age*

The Black Face Mountain Mylonite Belt is intruded by the Rooiberg member of the Richtersveld Igneous Complex and by minor intrusive bodies south and east of Klipbokkop while fragments of the Black Face Mountain syenite are found in protomylonites and tectonic breccias. It thus post-dates the Black Face Mountain Syenite and pre-dates the Rooiberg member of the Richtersveld Igneous Complex. Its less well recrystallised nature could indicate an age younger than that of the Devilscastle Schist Belt.

Fig. 5.23 Microscopic and mesoscopic mylonite structures of the Blackface Mountain Mylonite Belt.

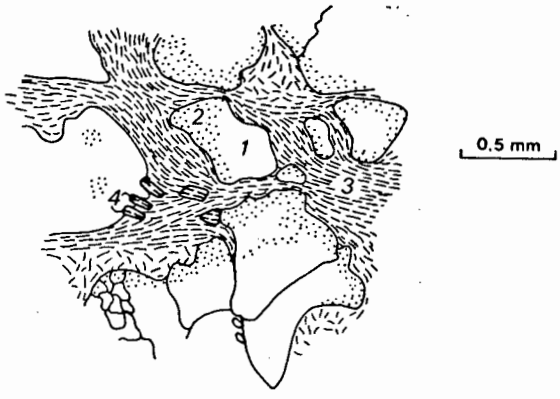

(a)

Microscopic mylonite texture
1) clear quartz, 2) stippled quartz (ser), 3) fluxion texture, 4) biotite.

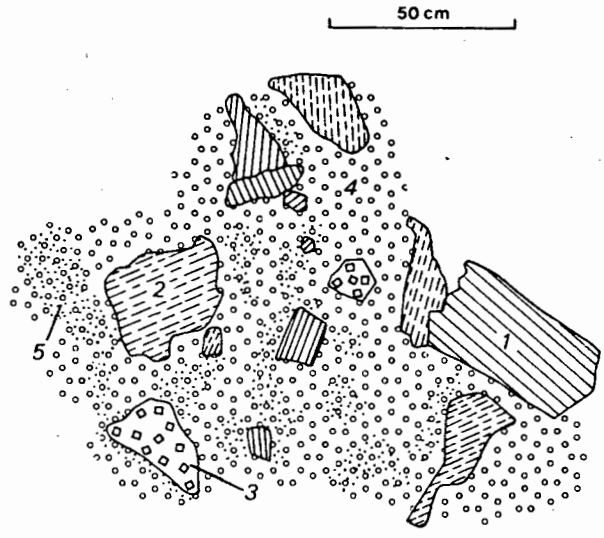

(b)

Sketch of "*mylonite in mylonite structure*" (Loc. 272). Light-grey mylonite(1), dark mylonite(2), coarse protomylonite(3) in a groundmass of variably coarse(4) and finer(5) protomylonite.

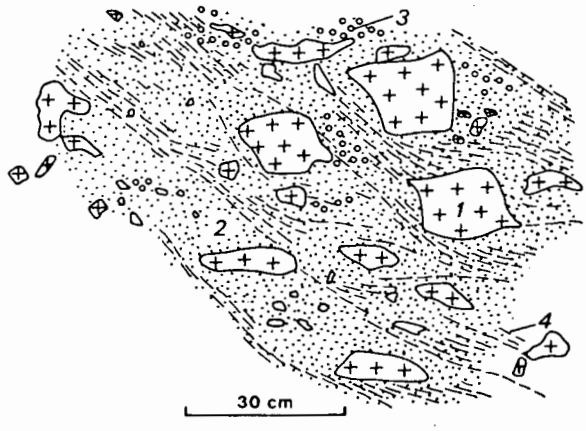

(c)

Fragments of Blackface Mountain Syenite (1) in dark fine-grained (2) to coarse-grained (3) groundmass. Weak foliation (4) appears to be later. Syenite fragments of up to 10 m in size are found at this locality. Riverbed Stinkfontein se Rivier, 2 km northeast of Rooiberg.

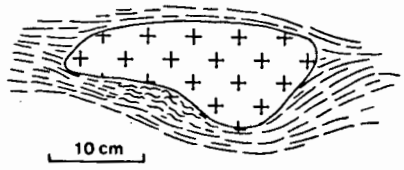

Fig. 5.24 Rounded syenite fragment in finely laminated dark aphanitic mylonite. Note crenulated lamination at the base. SE margin of Black Face Mountain.

5.3.4. Shear zones of the northeastern Richtersveld

1. *General*

In contrast to the southeastern Richtersveld, deformational zones in the northeastern Richtersveld are immediately recognisable as shear zones. Their cores are mylonitised, accompanied by strong quartz impregnation, facilitating their recognition in the field and on aerial photographs. Outside the immediate core the host rock is usually sufficiently preserved in order to recognise its original fabric. Thin sections of mylonite cores display incomplete recrystallised quartz textures (seriate, interlobate to amoeboid) with strings and strains of sericite and chlorite. Crosscutting and deformed foliations also occur and suggest a polycataclastic history.

2. *Photogeological analysis*

In order to obtain a more detailed picture of the deformation pattern during the Devilscastle Event, the Claims Peak area has been selected for a detailed inspection since it is underlain by G_3 granite which has not been affected by F_1 and is cut by the dyke suite of the Gannakouriep which intrudes the lower Stinkfontein Formation and is not affected by deformation of the Devilscastle Event. This ensures that all lineaments recorded represent the time after the intrusion of G_3 and prior to the emplacement of the Gannakouriep Suite. All lineaments have been mapped which were farther apart than 2 mm on a photomosaic (~1:40000) and their lengths were recorded. From these data the histogram in Figure 5.25a

was constructed and shows the frequency per azimuth of all recorded lineaments. It displays a distinct minimum between 20° and 50° and a distinct maximum between 140° and 160°, accompanied by submaxima between 80° and 90°, and 100° and 120°.

By comparing the added length per azimuth and the frequency per azimuth (= number of measurements) it can furthermore be shown that the directions between 140° and 170° tend to form relatively long lineaments while the directions between 80° and 140° tend to form their maximum through relatively more frequent but shorter lineaments. The directions 170° to 80° again show hardly any difference between added length and number of measurements per azimuth which is in parts already visible on the lineament map (Annex. 4). It also emerges from this map that dykes of the Gannakouriep Suite and quartz impregnated lineaments of the 150° direction are displaced along east-west trending faults while the main lineament direction (150°) is cut by the dykes and therefore older than the latter. East-west displacement of the dykes is therefore younger and (east-west features) should be regarded with caution when interpreting lineament map and histogram.

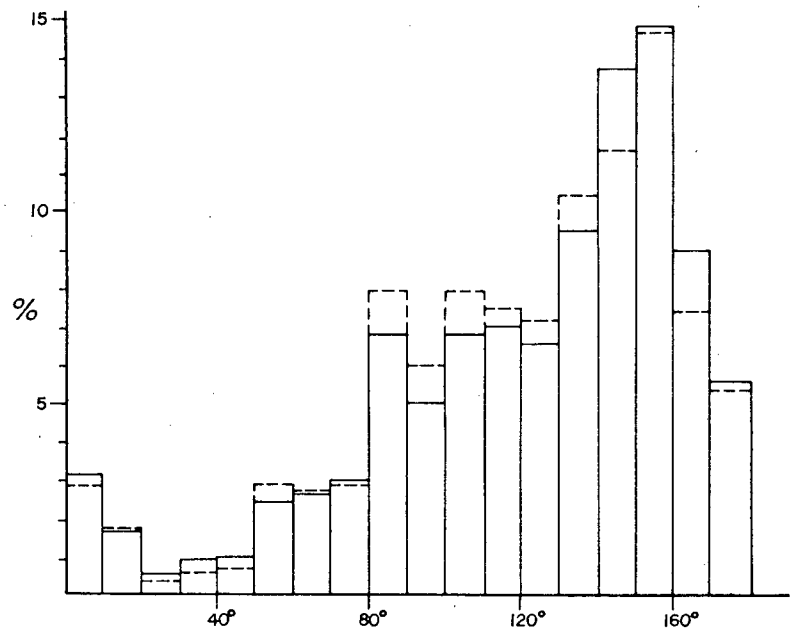

Fig. 5.25. Histogram of photolineaments of the Claims Peak area, northeastern Richtersveld; the lineaments are taken from Annexure 4 .
Bold lines : added length of lineaments per azimuth (in %)
Dashed lines : frequency (= number of measurements) per azimuth (in %)
Added length : 11559 length units ; Frequency : n = 1948
By comparing the added length and frequency, deductions as to the relative length of the lineaments can be made. The lineaments between 140° and 170° are relatively longer than those of other directions. This agrees with photolineaments as shown in Annexure 4 and is consistent with an interpretation as a left-lateral wrench fault system (p. 143-146).

5.3.5. Summary

The deformation of the Devilscastle Event is characterised by north to northwest-trending shear zones with left-lateral sense of displacement. Shear zones are of the brittle fracture type in the central northeastern Richtersveld, weakly recrystallised mylonite and protomylonite in the Black Face Mountain Mylonite Belt and sericite schists (interpreted as well-recrystallised mylonite) in the Devilscastle Schist Belt. While 900 my old members of the Richtersveld Igneous Complex are affected by Devilscastle deformation, the 700 my old members of the Richtersveld Igneous Complex are intruded into the Devilscastle Schist Belt and Blackface Mountain Mylonite Belt which agrees well with the assumption of a prolonged tectonic activity and evidence for multicataclastic deformation under increasingly higher crustal conditions.

5.3.6. Discussion

1 *Tectonic elements and their geometry in wrench-fault systems*

According to fold geometry the direction of the main compressive strain during F_1 must have been southwest-northeast while F_2 fold axes suggest a compressional strain from the southeast, which means that a re-orientation of the regional strain pattern by 90° must have taken place between F_1 and F_2. Since F_2 strikes in a direction expected for *en echelon* folds in a left-lateral wrench-fault system with north-south striking main wrench, the possibility of a cogenetic relationship of F_2 and the Devilscastle Event has to be investigated.

Moody and Hill (1956) first introduced the concept of wrench tectonics and concluded that for a given area at least four directions of wrench faulting and four directions of anticlinal folding and/or thrusting existed and that these directions have a symmetrical position with respect to the primary compressional stress. Their "primary tectonic elements" are adapted to left-lateral shearing and shown in Fig. 5.26a.

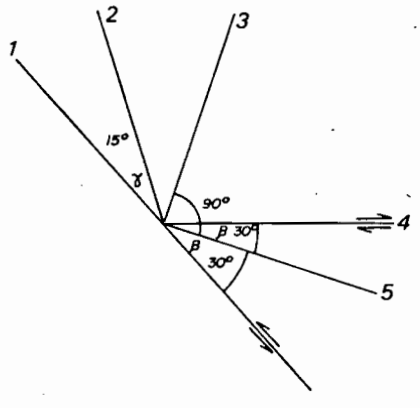

Fig. 5.26a

1) primary 1st order wrench
2) dragfolds, 2nd order
3) minimum compressive stress; primary fold direction
4) 1st order complementary wrench
5) maximum compressive stress

Similar results have been obtained experimentally by Wilcox *et al.*, (1973). Geometry and terminology of their tectonic elements are shown in Fig. 5.26b.

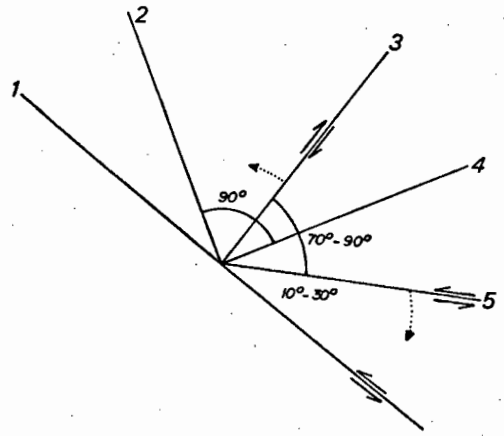

Fig. 5.26b

1) main wrench
2) minimum compression; *en echelon* folds
3) antithetic fault
4) maximum compression, normal faults
5) synthetic fault

They were able to show that *en echelon* structures form in the early stages of deformation, followed by synthetic and antithetic faults and the main wrench in the last stage. They also pointed out that convergent wrenching tends to enhance conjugate faults and folds and may even cause reverse faulting and thrusting while divergent wrenching on the other hand may enhance tensional structures like normal faults.

2 *Interpretation of the Devilscastle Event in terms of a left-lateral wrench-fault system*

The rather accurate data obtained by their experiments can also be used to predict a possible wrench fault pattern in the Richtersveld. The data compared in Table 5.7 show the expected and observed directions to be in rather good agreement and therefore suggest that the lineament pattern investigated has indeed been caused by a left-lateral wrench-fault system.

Wilcox and others' (1973) experiments showed furthermore that the conjugate faults tend to occur in swarms of short but densely spaced

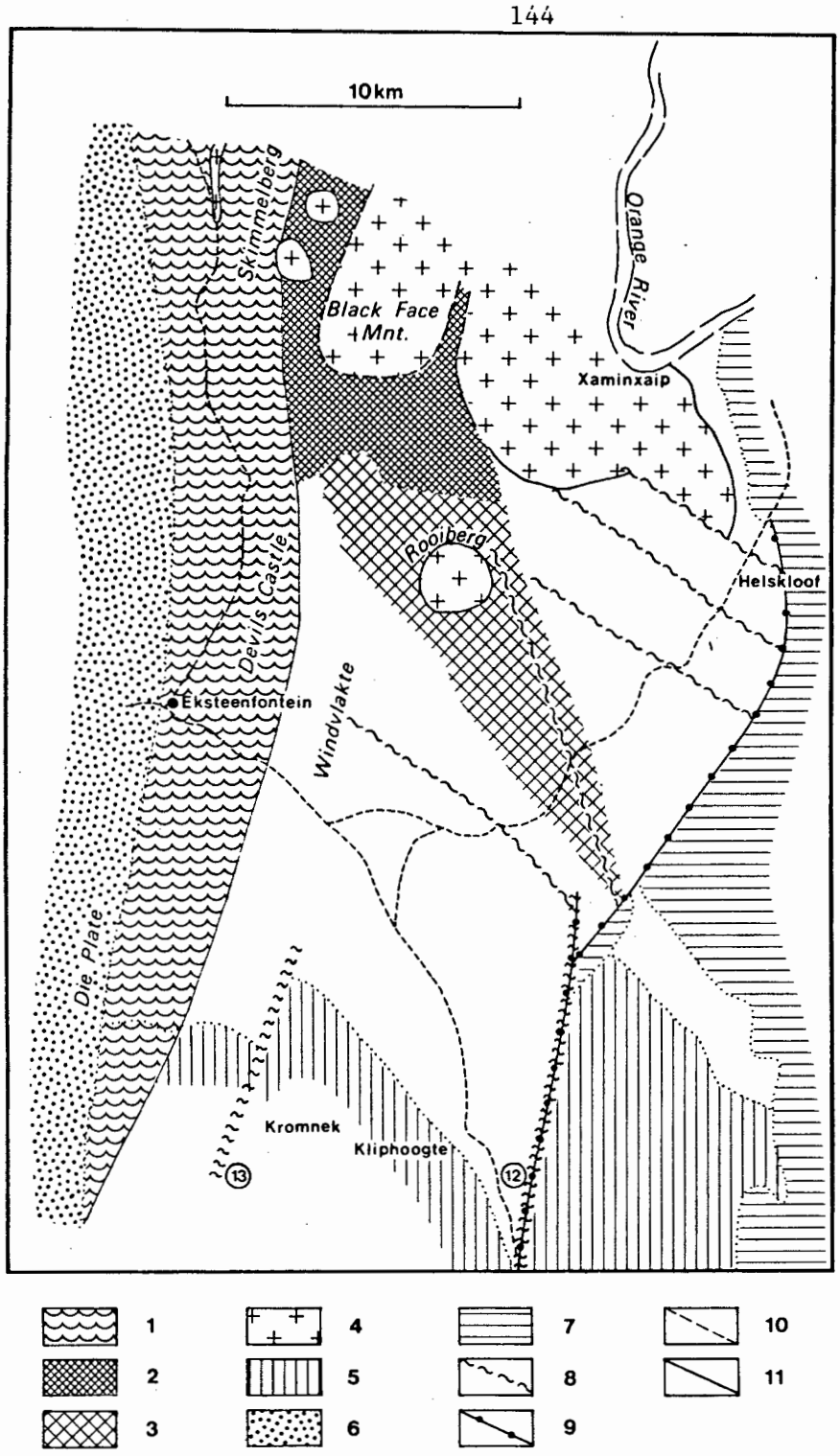

Fig. 5.27 Schematic map of Late Precambrian structural features of the southeastern Richtersveld.
Legend:
1) sericite schist (Devilscastle Schist Belt); 2) mylonites and proto-mylonites (Blackface Mountain Mylonite Belt); 3) occasional occurrence of mylonites; 4) Richtersveld Igneous Complex; 5) Pink-gneiss Unit; 6) Stinkfontein Formation; 7) Nama Group; 8) post-Stinkfontein and pre-Nama faults; 9) post-Nama faults; 10) tectonic contact; 11) intrusive contact; 12) Doring River fault; 13) Kromnek fault.

Element	expected directions	observed directions
main wrench	150°	155°
synthetic fault	120°-150°	120°-150°
normal faults	100°	105°
antithetic faults	80° and less	85°
fold axes (F_2)	~ 10°	NE and NNE

Table 5.7

Prediction of fault patterns for a left-lateral wrench fault system in the northeastern Richtersveld based on the main wrench striking 150° and experimentally determined fault patterns (Wilcox *et al.*, 1973). The expected maxima directions are compared with those observed in histogram Fig. 5.25.

shears while the main wrench is made up of few but longer elements. This also agrees with Figure 5.25, where the 150° direction reflects (if only weakly) few but long lineaments while particularly the maxima between 80° and 140° indicate shorter but more numerous lineaments.

The strike of pegmatites in the southeastern Richtersveld is 120° and thus not in agreement with the expected direction of tensional features. However, since the main wrench in the southeastern Richtersveld strikes north-south (instead of northwest in the north) a direction of 120° to 130° for tensional features is well in agreement with the wrench-fault model on a local scale. Compressional features are represented by S_4 and the Mike nappe structure and may be indicative of convergent wrenching.

3. *Some problems with respect to the Devilscastle shear zones*

Striking features of the shear zones of the southeastern Richtersveld are their rather irregular outline and strong deformation compared with the relatively modest amount of displacement. The irregularity of shape may be explained by taking into account the lithological variety within the southeastern Richtersveld: metavolcanics, possibly intercalated schists of the Pink-gneiss Unit, granodiorite of the Vioolsdrif Intrusive Suite, deformation at variable crustal levels and the intrusion of the Richtersveld Igneous Complex at various stages during deformation may have contributed to their rather irregular outline. It must also be taken into

account that the presently exposed shear zones might only be marginal parts of a major shear system that has subsequently been eroded along the unconformity. Similar explanations may be found for the relatively strong deformation relative to the modest amount of displacement.

Finally attention should be drawn to the fact that the schist belts of the Devilscastle Event trend northwest in the northeastern Richtersveld but north to north-northeast in the Richtersveld south of the RIC, while the later Black Face Mountain Mylonite Belt trends again northwest (see also Annexure 1b and Fig. 5.27). In Fig. 5.28 therefore an explanation has been brought forward which is based on the rotation of the southeastern Richtersveld caused by the intrusion of the early (and main mass of the) RIC and which may account for the phenomena observed.

4. *Geotectonic environment*

Wrench-fault systems are known to be active over rather long periods, and this appears to have been the case here, too. Most of the major wrench-fault systems occur in active orogenic terrains (e.g. San Andreas fault, Alpine fault, Anatolian fault) and are regarded as active plate margins with considerable lateral displacement. Intraplate wrench-fault systems are, however, also known, an example of which is the Messejana fault system in Spain/Portugal, which extends over several hundreds of kilometres and can probably be linked with the opening of the North Atlantic (Schermerhorn *et al.*, 1978). This shear system is particularly interesting in the present context since it is also posttectonically intruded by mafic dykes like the Devilscastle shear zones.

As for the Devilscastle shear zones, a non-orogenic intraplate origin appears likely since alkaline to peralkaline intrusives of the Richtersveld Igneous Complex as well as the geothermal gradient deduced from early Devilscastle metamorphism suggest a more or less cratonic environment. The Devilscastle Event should also be seen in relation to other major shear zones in the vicinity (Pofadder Lineament, Kannabeam shear zone, Kuckaus mylonite belt, etc) and to tectonic activity to the north of the Rehoboth Magmatic Arc (Watters, 1974).

5. *The Devilscastle Event and the age of the Stinkfontein Formation*

In the southeastern Richtersveld the Devilscastle Schist Belt and related shear zones have repeatedly been linked with Gariep and pre-Gariep deformation (Kröner, 1974; Blignault, 1974b; Kröner and Blignault, 1977) and Kröner (1974) envisaged a formation of the Gariep trough by down-faulting of the western parts along shear zones described here as Devilscastle Schist Belt. The present investigations, however, cast serious doubt on this interpretation since S_3 is cut by the unconformity and in addition formed under metamorphic conditions representative of a crustal depth of approximately 18 km (cf. section 6.5). Rocks formed by the Devilscastle Event must therefore have been eroded to their present level before the Stink-

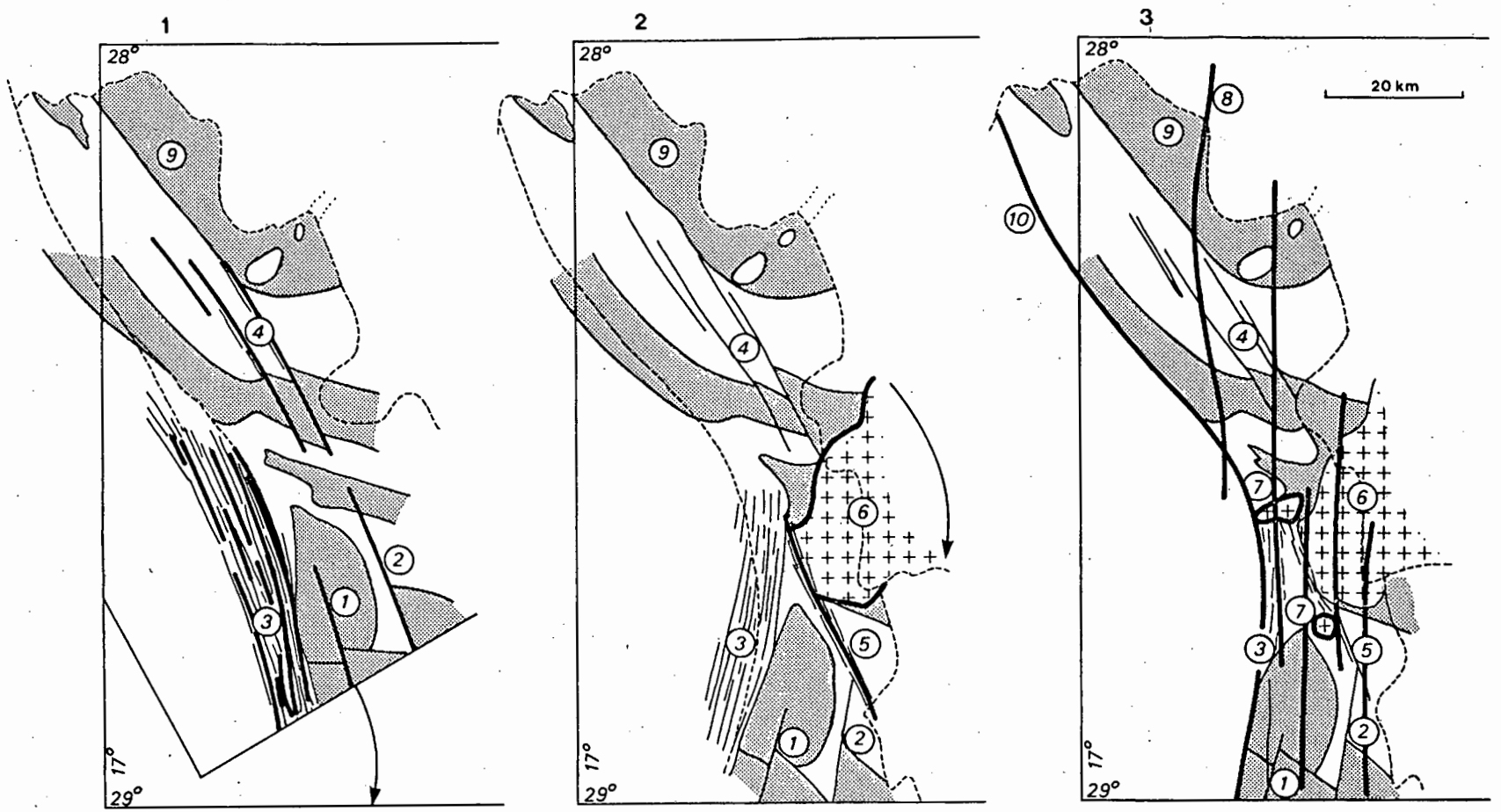

Fig. 5.28 Possible interrelationship of Devilscastle shearing and the emplacement of the RIC. This model implies that parts of the Devilscastle Schist Belt are older than 900 my.

Stage 1 : Richtersveld prior to the emplacement of the RIC. Devilscastle shear belts trend northwest in the northeastern Richtersveld as well as in the south.

Stage 2 : Intrusion of the early RIC causes clockwise rotation of parts of the southeastern Richtersveld. Translative movements are also likely but have not been particularly indicated in the model. Early Devilscastle shear zones now trend NNE. Continuing shearing in northwesterly direction accounts for the formation of the Black Face Mountain Mylonite Belt which deforms early RIC members. (cont.)

fontein Formation was deposited, i.e. uplift must have occurred instead of down-faulting, only subsequent to which a graben-forming mechanism as suggested by Kröner (1974) can be envisaged.

Fig. 5.28 (continued from opposite page)

Stage 3 : Intrusion of the youngest members of the RIC (Rooiberg, Klipbokkop). Emplacement of dykes of the Gannakouriep Suite. Deposition of the Lower Stinkfontein Formation.

Key : 1) Doring River fault 2) Kromnek fault 3) Devilscastle Schist Belt 4) Shear zones of the northeastern Richtersveld 5) Black Face Mountain Mylonite Belt and its possible extension towards S 6) early members of the RIC 7) younger members of the RIC 8) dykes of the Gannakouriep Suite 9) major units of supracrustal rocks 10) unconformity

Features formed during the respective stages are shown in heavy outlines.

Chapter 6

METAMORPHISM

6.1 INTRODUCTION

Detailed investigations of metamorphism within the Richtersveld Province have so far only been carried out in the Haib and Lower Fish River areas by Blignault (1977), who determined upper low grade metamorphic conditions (~4 kb, ~500°C) for the Lower Fish River area and Reid (1977) who concluded that metamorphism in the Haib area reached upper greenschist facies and constituted a "regional contact phenomenon".

For these reasons it was important during the present investigation to find out whether

a) the Richtersveld proper is also homogeneously low grade
or whether there is a spatial metamorphic zonation

b) the metamorphic facies series is the same in the Namaqua Metamorphic Complex and the Richtersveld Province

c) metamorphic grade and facies series vary with time

However, since the mainly granodioritic lithology of the Richtersveld does not allow for the formation of metamorphic index minerals in the temperature range concerned, particular emphasis had been laid on

a) microscopic investigation of non-volcanic rocks

b) texture and celadonite content of white micas in low grade pelitic rocks (investigation of b_o-values)

c) textural criteria in volcanic and intrusive rocks (recrystallisation, melting)

For reasons of convenient description the area has been subdivided into metamorphic domains largely consistent with those used in Chapter 5, except for the central Richtersveld which here also includes the structural domain of the southeastern Rosyntjieberg Formation and the Noms River Fold Belt with respect to biotite formation.

6.2. THE CENTRAL RICHTERSVELD

6.2.1. Texture and mineralogy

1. *Pelitic rocks*

Textural and mineralogical data that are important for the evaluation of metamorphic grade have been tabulated in Table 6.1. Kaolinite has been determined by careful optical comparison (after Tröger, Part I, 1971) with other clay minerals as well as minerals of the zeolite, nepheline and sodalite groups with respect to birefringence, pleochroism, refractive index, extinction angles and habit.

Quartz aggregates containing chlorite, chloritoid and kaolinite are mostly elongated and aligned in S_1. There is some doubt whether these aggregates can be regarded as pressure shadow or as primary compositional inhomogeneity of the sediment but since they frequently occur without host minerals in their cores (e.g. chloritoid, see Fig. 6.1) around which a pressure shadow could have formed and since they tend to be deformed by S_1,

Table 6.1 Textural and mineralogical properties of pelitic rocks

Rock types : mica schist, predominantly white mica (50-90%) *Main mineral phases :* muscovite, quartz *Accessory mineral phases :* chloritoid, kaolinite, magnetite *Fabric elements :* S_1, developed throughout predating G_3 S_2', occasional, crenulation cleavage		
	chloritoid	*kaolinite*
relation to S_1	aligned in S_1, deflects S_1, if oblique : corroded by S_1.	aligned in S_1, marginal alteration into unfoliated white mica
relation to S_2'	deformed by S_2' but also crosscutting S_2' (see Fig. 6.1. b)	rotated by S_2'
crystal habit	subhedral to euhedral	platy, columnar, sub-to anhedral, sometimes stained by opaque to dark red iron oxide, cloudy extinction.
$S_i - S_e$	$S_i \neq S_e$, rarely and weakly developed	$S_i \neq S_e$, weakly and rarely developed
paragenesis	quartz, muscovite	quartz, muscovite

Table 6.2 Mineral assemblages in metasediments of the Rosyntjieberg Formation

	bi	*mu*	*chl*	*qtz*	*ep*	*kf*	*plg*	*chld*	*kao*	*ore*
18/4		x	x	(x)				x		
M33/1		x		x					(x)	(x)
M33/2		x		x					(x)	(x)
M33/0		x	(x)	(x)				(x)	(x)	
151/1		x	x	x						(x)
151/2		x	(x)	x						(x)
364/5		x	x	x						
364/11	x	x	x	x		(x)				
339/0		x	x	x						(x)
364/12		x	x	x	x		x			gar,carb.
364/7		x	x	x				x		

( ) : occurring in minor amounts

they are likely to be of primary sedimentary origin. Possibly they originated as iron-rich concretions which are frequently formed in pelitic rocks during diagenesis, a probability which is supported by the relatively high chlorite and chloritoid content of these aggregates.

2. *Semi-pelitic rocks*

Textural and mineralogical data that are important for the evaluation of metamorphic grade have been compiled in Table 6.3. The rocks described here have all been collected within the southeastern Rosyntjieberg Formation and appear to be mainly derived from melanocratic volcanics and to comprise various degrees of maturity.

Of particular importance is one sample containing large crystals of garnet, since this is the only occurrence of garnet encountered in the Richtersveld. Its dark colour and mineral assemblage suggest it to be grossularite with considerable melanite content.

3. *Volcanic rocks*

Primary volcanic texture and mineralogy are rather well preserved and have been described in Chapter 2.

The growth of secondary minerals can either be ascribed to deuteric alterations during cooling of an extrusive sheet or to metamorphism following the formation of the volcanic texture. Since large-scale deuteric alterations in volcanics have never been reported from modern volcanic

Table 6.3. Texture and mineralogy in semipelitic rocks (mainly southeastern Rosyntjieberg Formation)

Rock type : chlorite schist and chlorite-rich impure quartzite *Main mineral phases* : quartz, muscovite, chlorite (epidote, feldspar) *Accessory mineral phases* : chloritoid, biotite, garnet, carbonate, zoisite *Fabric elements* : S_1, weak preferred orientation of platy minerals.			
	biotite	*chloritoid*	*garnet*
mode of occurrence	porphyroblasts, cutting foliation	porphyroblasts, sub- to euhedral, undeformed, poikilitic intergrowth with chlorite and quartz	undeformed, subhedral. *hand specimen* : dark grey to black, diameter several mm *thin section* : colourless, weakly pink, poikilitic with quartz, zoisite, carbonate
assemblage	K-feldspar	chlorite, muscovite, quartz	quartz, zoisite, carbonate, muscovite, chlorite, epidote, plagioclase

terrains and since secondary minerals in the Richtersveld volcanics are frequently associated with foliation-like features, the following deductions as to the metamorphic grade are based on the assumption that muscovite, biotite, chlorite and epidote are entirely of metamorphic origin.

6.2.2. Evaluation of textural and mineralogical data

1. *Temperature conditions*

a) Kaolinite

Apart from chloritoid which is known from a variety of metamorphic environments up to lower amphibolite facies (e.g. Zen, 1960; Halferdahl, 1961), particularly kaolinite deserves closer attention. Mineral assemblages containing kaolinite are known from diagenesis (Dunoyer de Segonzac *et al.*, 1968; Frey, 1970) up to assemblages with andalusite (Zen, 1961), and experimental breakdown reactions have been accomplished between 300° and 400°C (at 2 kb). They are schematically shown in Table 6.4. It thus appears that kaolinite may be stable even in assemblages with andalusite and that various

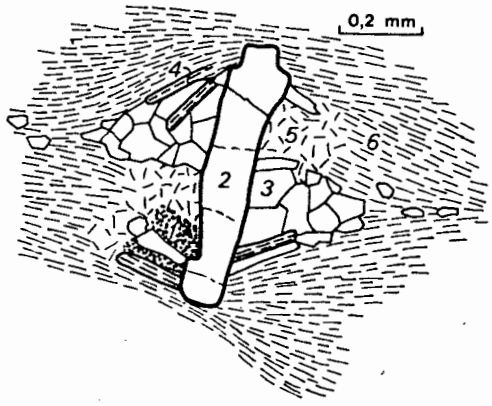

(a)

Fig. 6.1(a) Aggregate of chloritoid, quartz, chlorite, muscovite. The aggregate looks like a pressure shadow around chloritoid. However, quartz–muscovite–chlorite aggregates are also found without big crystals around which a pressure shadow could have formed.
1) chlorite; 2) chloritoid; 3) quartz; 4) muscovite; 5) sericite, unfoliated; 6) sericite, foliated.

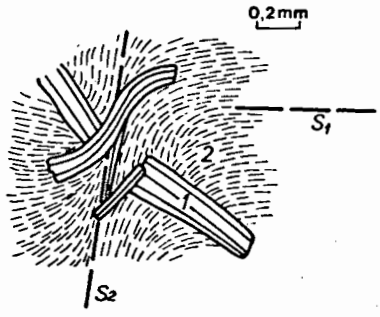

(b)

Fig. 6.1(b) Chloritoid deformed by S_2'. 1) chloritoid
2) sericite

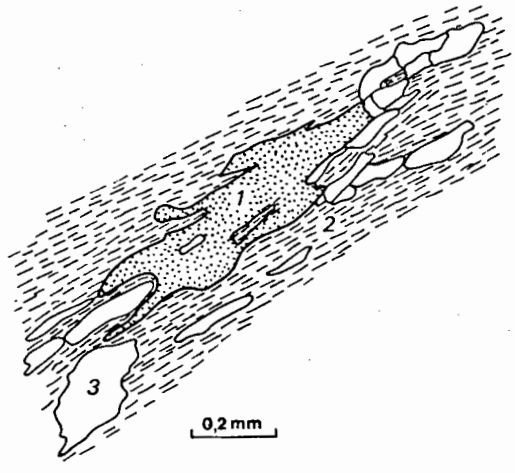

(c)

Fig. 6.1(c) Formation of kaolinite along planes of foliation.
1) kaolinite
2) sericite
3) quartz

Table 6.4 Some literature data on the stability of kaolinite

Author	*Break-down conditions*	*Evidence*	*Location*
Frey, 1970	diagenetic K.I. = 7,5	petrographic and field investigations on natural rocks	Alpine foreland
Dunoyer de Segonzac et al., 1968	diagenetic K.I. = 20	petrographic and field investigations on natural rocks	Upper Cretaceous, Bassin de Douala (Cameroun)
Zen, 1961	metamorphic, in paragenesis with andalusite	petrographic and field investigations	North Carolina, in volcanic sequence
Thompson 1970; review	between 300° and 400°C at 2 kb	review of experimental results from various authors	
Thompson, 1970, experiments	~350°C at 2 kb	experimental result	

K.I. = Kubler Index; K.I. = 4 : boundary diagenesis / very low grade.
K.I. = 2,5 - 3 : boundary very low grade / low grade (after Weber, 1972b).
Experimental formation of andalusite by the reaction pyrophyllite = andalusite + quartz + H_2O at 400°C (2kb). After Kerrick, 1968.

reactions under variable conditions may lead to its breakdown. Winkler (1974) therefore doubted that Thompson's and other investigators' experimental results are real equilibrium data but noted, nevertheless, that according to Thompson's data kaolinite may break down already during very low grade metamorphism if pressure was sufficiently low.

b) The formation of biotite

Mather (1970) investigating the biotite isograd in Dalradian rocks of Scotland found the initial formation of biotite to be dependent on rock composition and to take place by the reaction

1) microcline + chlorite + phengitic muscovite = biotite + less phengitic muscovite + quartz + H_2O

in greywackes of suitable bulk composition. His investigations furthermore showed the stability field of biotite-bearing assemblages to be enlarged

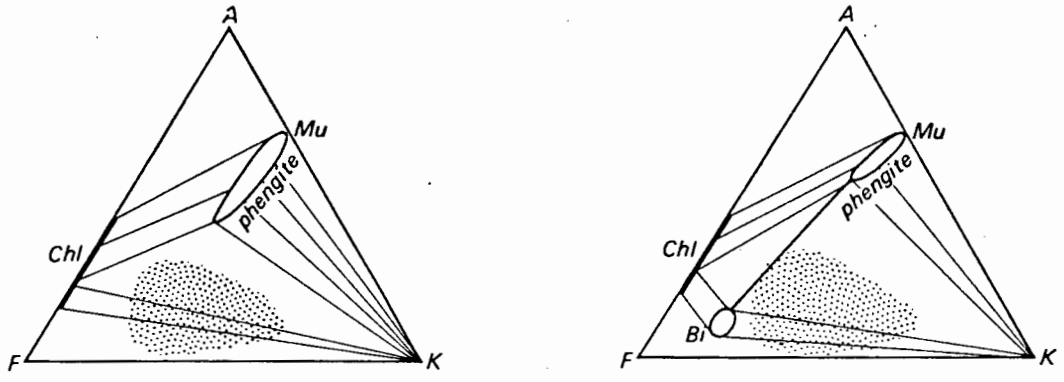

Fig. 6.2

a) AKF diagram of Mather's zone 1; K-feldspar and chlorite are always stable together if bulk composition permits.

b) AKF diagram of Mather's zone 2; K-feldspar and chlorite react to form biotite.

Stippled field : approximate composition of rocks investigated.

through the reduction of the amount of celadonite which can be tolerated in white mica, leading to the reaction

2) phengitic muscovite + chlorite = less phengitic muscovite + chlorite + biotite + H_2O

thus allowing for the formation of biotite in more and more aluminous rocks. He was therefore able to distinguish three metamorphic zones within the lower greenschist facies:

Zone 1 :chlorite and microcline are always stable in rocks of suitable bulk composition

Zone II :biotite is formed by reaction 1) with microcline in rocks of suitable bulk composition

Zone III :chlorite and phengitic muscovite react to form biotite in pelitic rocks, (reaction 2)

Since metavolcanics of the northeastern Richtersveld generally contain muscovite and K-feldspar, Mather's concept can be used to determine whether zone II has been reached (and whether it has been reached everywhere) by determining where and in what parageneses biotite and chlorite are present. This has been done by listing all relevant minerals per thin section as shown for a selection of the samples in Table 6.6 regardless of the amount in which they occurred, i.e. the mineral assemblage on the thin-section scale has been determined (from approximately 100 thin sections).

Table 6.5 Statistical evaluation of paragenetic mineral associations in the northeastern Richtersveld

a) mesocratic and leucocratic volcanics

	bi	*mu*	*chl*	*n=*
bi	-	95	58	40
mu	56	-	61	66
chl	50	95	-	40

$\frac{n(bi)}{n(chl)} = 1,0$ $n_{tot}=70$

b) melanocratic volcanics

	bi	*mu*	*chl*	*n=*
bi	-	92	58	12
mu	69	-	69	16
chl	50	79	-	14

$\frac{n(bi)}{n(chl)} = 0,86$ $n_{tot}=19$

c) "chlorite only" zone (all rock types)

	bi	*mu*	*chl*	*n=*
bi	-	100	100	3
mu	27	-	91	11
chl	18	91	-	11

$\frac{n(bi)}{n(chl)} = 0,27$ $n_{tot}=12$

d) "biotite only" zone (all rock types)

	bi	*mu*	*chl*	*n=*
bi	-	77	15	13
mu	91	-	9	11
chl	100	50	-	2

$\frac{n(bi)}{n(chl)} = 6,5$ $n_{tot}=14$

Explanation:

Table 6.5a - *bi*-row, *mu*-column : 95% of those thin-sections containing biotite contained also muscovite; n: 40 thin sections out of 70 ($=n_{tot}$) contain biotite independent of paragenesis. But (*mu*-row, *bi*-column) : 56% of those samples containing muscovite contained also biotite; 66 out of 70 thin-sections contain muscovite independent of paragenesis. Chlorite and biotite zones refer to Fig. 6.3.

Evaluation :

a) The composition within the compositional range of the volcanics of the northeastern Richtersveld has no influence on the frequency with which biotite and chlorite occur.

b) The geographical situation has considerable influence on the frequency of occurrence of biotite and chlorite.

c) The frequency of occurrence of muscovite is weakly related to composition and geographical situation.

The occurrence of biotite and chlorite may be influenced by

a) composition
b) homogeneity of the sample
c) degree of equilibrium within the sample
d) metamorphic grade

Only the latter is important here and it was therefore necessary to determine the influence of composition on the parageneses in Table 6.5a and b, which compare melanocratic with leucocratic to mesocratic volcanics. The only difference between both rock groups is a slightly less frequent occurrence of muscovite in melanocratic rocks while frequency of occurrence of biotite and chlorite are not significantly affected. Since the compositional influence thus appears to be negligible, the occurrence of biotite and chlorite is likely to be mainly dependent on the grade of metamorphism and justifies the mapping of biotite and chlorite as shown in Fig. 6.3. It is obvious from this map that biotite occurs more frequently in the northeast (De Hoop - Noms River) and in the southwest, while chlorite is more frequent towards the centre of the area. This zonal distribution can be checked by the contingency tables in Tables 6.5c and d which, in marked contrast to a) and b), display an obvious difference between samples of the "biotite zone" and "chlorite zone". This suggests that reaction 1 has in fact taken place. However, according to Figure 6.2 biotite and chlorite must not occur together in the compositional range of the samples investigated. The common association of biotite and chlorite can therefore only be accounted for by assuming

a) compositional inhomogeneities on thin-section scale

b) pre-metamorphic mineral phases to be present

c) disequilibrium on the thin-section scale

d) retrograde reactions

Since compositional influences have been shown to be negligible (Table 6.5a and b) and the existence of much premetamorphic biotite and chlorite is unlikely as indicated by the textures, disequilibrium must be particularly regarded as the main reason for the assemblage chlorite and biotite. It is therefore likely that zone II has been reached throughout in the northeastern Richtersveld, except for the central part where the few occurrences of biotite could as well be of deuteric origin or represent the lowermost part of zone II. The occurrence of actinolite in mafic rocks of Mather's zone II finally justifies the correlation of this zone with the lower part of low grade metamorphism.

c) Garnet

In semipelitic rocks the occurrence of grossular is of importance. Parageneses involving zoisite, quartz, grossular, calcite and anorthite are strongly depending on XCO_2 and have been investigated by various authors (Kerrick, 1970;

Table 6.6 Mineral assemblages in metavolcanics of the Northeastern Richtersveld

Sample	*bi*	*mu*	*chl*	*qtz*	*ep*	*kf*	*plg*	*ore*	
2/1		x	x	x	x	x	x		
23/1	x	x	x	x	x	x	x		
31/1	x	x	x	x	x		x		
31/2	x	x	x	x	x	x	x		Abikwarivier
32/2			x	x			x		
35/2		x		x	x)	x	x		
36/1		x	x	x	x)		x		
55/4		x)	x	x	x		x	x	Formation
55/5		x	x	x	x	x	x		
55/6	x	x	x	x	x	x)	x		
68/4		x	x	x	x	x	x	x	
73	x	x	x	x	x	x)	x		
17/1	x	x		x	x		x		
18/1	x	x		x			x		
19/2		x		x	x	x	x		
79	x	x		x	x	x	x		
80	x)	x	x)	x	x	x	x		Paradysrivier
81/1	x	x		x	x	x	x		
82/1	x	x		x	x	x	x		
83	x	x		x	x	x	x		Formation
85/1	x	x		x	x	x	x		
85/2		x	x)	x	x	x	x		
86/2	x	x		x	x	x	x		
87/2		x	x	x	x	x	x		
89/2	x		x	x	x				
74		x	x	x)					Nomsrivier
76		x		x	x	x	x		Formation
92/2		x		x	x)	x		x	
92/3	x	x		x	x	x	x		
93		x	x)	x	x	x			
94	x	x		x	x	x)	x		Klipneus
96/1	x	x	x	x	x	x	x		
96/4		x	x	x	x	x	x		
96/5	x	x	x	x	x)	x	x		Formation
96/8		x	x	x	x)	x	x		
97	x	x	x)	x	x		x		
152	x		x	x	x		x		
123	x	x		x	x	x	x		Kookrivier Formation

x) occurrence in minor amounts

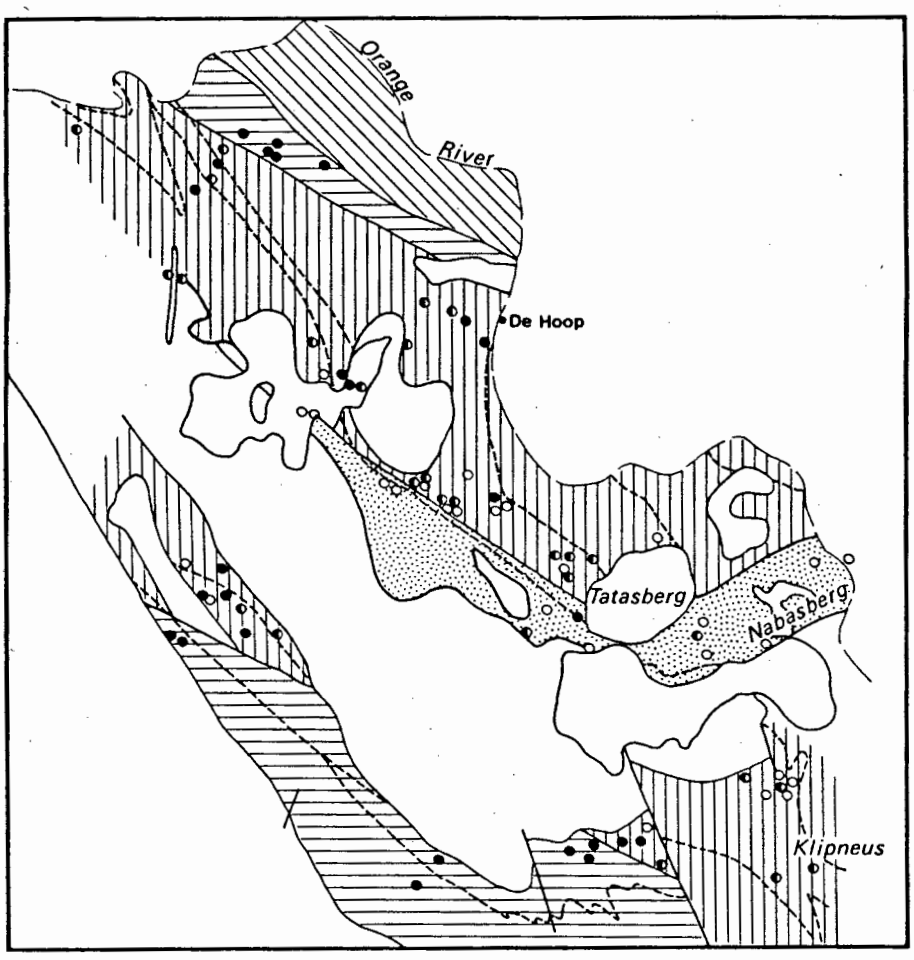

Fig. 6.3

Geographical distribution of biotite - chlorite parageneses in metavolcanics of the northeastern Richtersveld.

Legend:

- • - biotite only, no chlorite
- ◐ - biotite and chlorite
- ○ - chlorite only, no biotite

Inferred zonation:

- ▒ - "chlorite only" zone
- ▥ - "chlorite and biotite" zone
- ▤ - "biotite only" zone

- ▨ - Blockwerf Migmatitic Complex

Storre, 1970; Gordon and Greenwood, 1971; Storre and Nitsch, 1973, compiled in Winkler, 1974, Fig. 10.2). The assemblage zoisite, quartz, calcite, sericite (anorthite is most probably not newly formed and constitutes a remnant of the original volcanic rock) in the groundmass and the paragenesis grossular, quartz, zoisite in the garnet porphyroblast suggest a formation of the latter by one or more of the following reactions:

1) 2 zoisite + 5 calcite + 3 quartz = 3 grossular + 5 CO_2 + 1 H_2O

2) Prehnite = 2 zoisite + 2 grossular + 3 quartz + 4 H_2O

3) 1 prehnite + 1 calcite = 1 grossular + 1 H_2O + 1 CO_2

All these reactions suggest temperatures between 500° and 400°C at 2 kb and very low XCO_2 (Winkler, 1974, Fig. 10.2) but unless more samples with more elucidating textural relationships are found, nothing can be said about which of these reactions actually took place. The suggested temperature range is, however, in agreement with the occurrence of biotite in the presence of k-feldspar only and with the stability of chloritoid, merely allowing the conclusion that metamorphism was of low grade.

d) Summary

For the central Richtersveld maximum thermal conditions can be inferred from the upper stability limit of kaolinite + quartz at 420° if the highest experimentally determined breakdown temperature is used; but from the preceding discussion the breakdown temperature is likely to be lower and probably not exceeding lower low grade metamorphism. Minimum thermal conditions can be inferred from the occurrence of biotite in the presence of K-feldspar indicating that the boundary very low/low grade has been reached. The distribution of biotite-bearing assemblages suggests an increase in metamorphic grade towards northeast and southwest.

2. *Pressure conditions*

Baric conditions in low grade metamorphic rocks have been estimated by using a method developed by Sassi and co-workers and based on the measurement of the *d(060)* peak of white micas by means of X-ray diffractometry. Details of this method and the procedure employed are given in Appendix 3.

a) Relative baric conditions

The relative baric conditions have been determined separately for the central northeastern Richtersveld and the southeastern Rosyntjieberg Formation and suggest metamorphism intermediate between facies series 2 and

3 of Sassi and Scolari (1974) (Fig. 6.5), equivalent to the andalusite - sillimanite facies series of Miyashiro (1973).

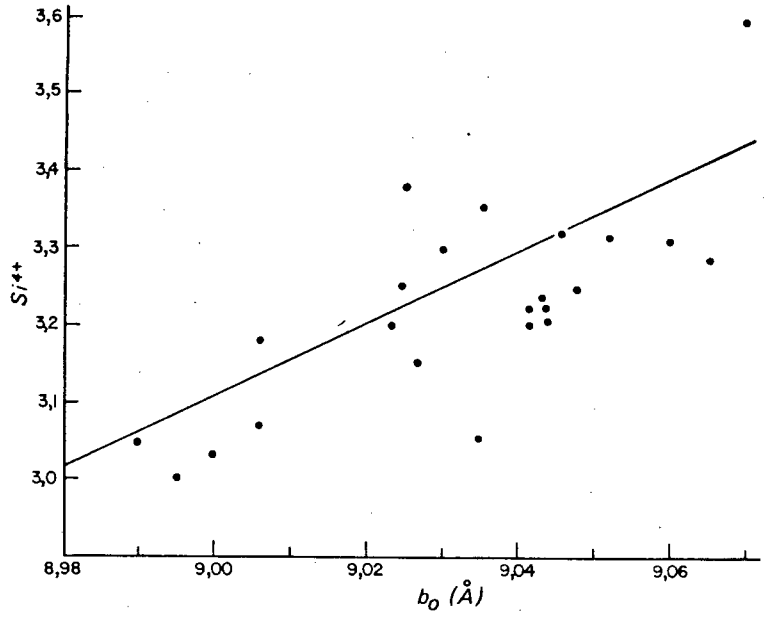

Fig. 6.4 Correlation of Si^{4+} and b_o after data from the literature (Ernst, 1963; Velde, 1967; Höck, 1974).

b) Absolute baric conditions

Absolute pressures can be inferred from this relative pressure scale either by comparison with experimental data or by comparison with areas where b_o values and independently estimated pressure conditions are known.

In the present case experimental data can only be used indirectly by applying Velde's (1967) equilibrium curves for different phengite contents (Fig. 6.6) to the data derived from Figure 6.4. This curve has been constructed from literature data (joint determinations of b_o and Si^{4+} in the same sample are rare) and displays a distinct positive correlation of Si^{4+} and b_o. It can thus be used to "translate" b_o into Si^{4+} values as necessary for the application of Velde's data. The b_o values in areas with pressure conditions reasonably well known from an independent source (for lower pressure ranges) are only available from the Bosost area/Pyrenees (facies series 1) where Zwart (1962) calculated a geothermal gradient of 150°/km from geological evidence. For the temperature range investigated here this geothermal gradient implies a pressure of approximately 1 kb. On the other hand, facies series 4 is characterised

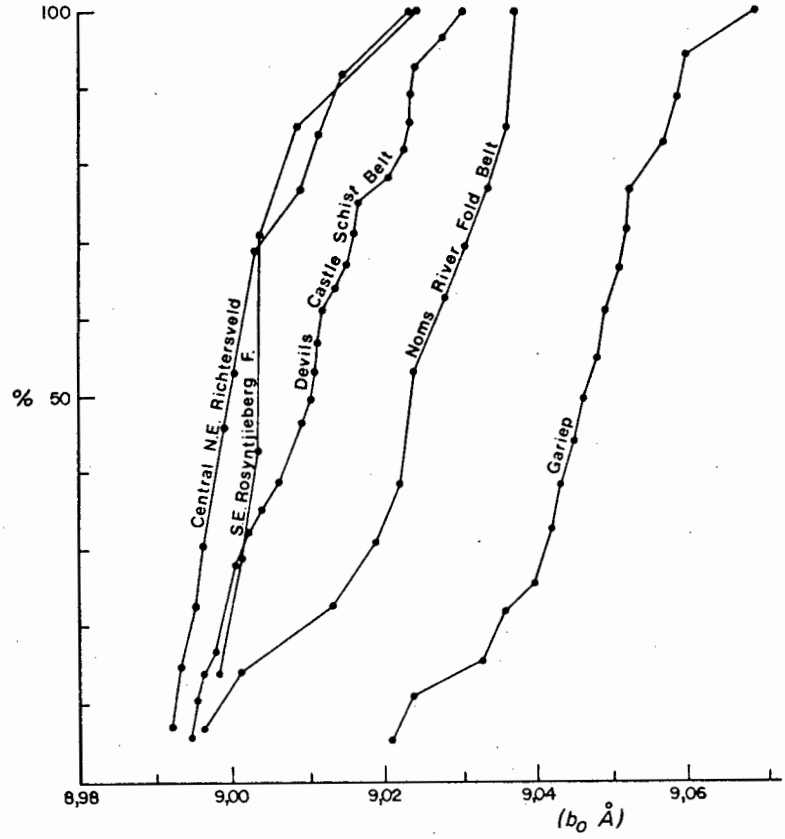

Fig. 6.5 Cumulative frequency curves of b_o-values

Central Northeastern Richtersveld : n = 13 $\bar{x}$ = 9,0031 s = 0,0092
SE Ros. Form. : n = 7 $\bar{x}$ = 9,0064 s = 0,0084
Noms River Fold Belt : n = 13 $\bar{x}$ = 9,0232 s = 0,0132
Devilscastle Schist Belt : n = 28 $\bar{x}$ = 9,0099 s = 0,0118 (all peaks)
Gariep : n = 18 $\bar{x}$ = 9,0464 s = 0,012

Table 6.7

Facies series	1	2	3	4	5	6
b_o (Å)	≅8,990	≅8,995	≅9,010	≅9,020 9,025	≅9,035	≅9,055

1) Low pressure metamorphism (and. + cord.) without chl zone (e.g. Bosost)
2) Low pressure metamorphism (and. + cord.) with chl zone (Hercynian metamorphism in Eastern Alps)
3) Low to intermediate pressure metamorphism (and) with the chl-bi-alm sequence in the greenschist facies (e.g. New Hampshire)
4) Typical barrovian metamorphism, (e.g. Dalradian metamorphism in Scotland)
5) Barrovian-type metamorphism, with simultaneous first appearance of bi and alm (e.g. Otago)
6) Glaucophanite greenschist facies (e.g. Sanbagawa)

From Sassi and Scolari (1974)

Fig. 6.6

Tentative absolute pressure scale for facies series 1 - 4 interpolated after data from the literature.

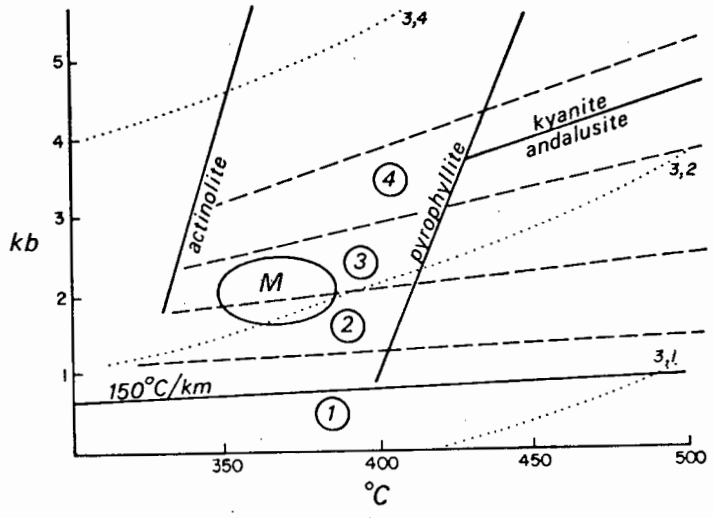

Explanation:

150°/km geothermal gradient : Bosost area (Zwart, 1962)
lower actinolite stability : (Winkler (1974)
upper pyrophyllite stability : (Kerrick, 1968)
phengite contents (stippled: Si^{4+}) after Velde, 1967
kyanite/andalusite stability : Winkler, 1974
1) - 4) : facies series after Sassi and Scolari (1974) as inferred from areas with known baric conditions.
M : approximate P-T conditions for metamorphism of the northeastern Richtersveld

by kyanite and would thus imply a pressure of ~3kb for the same temperature range. Assuming a linear dependence of b_o and pressure, the facies series 1-4 can tentatively be constructed as shown in Figure 6.6.

It is therefore evident from the above that the indirect use of Velde's (1967) equilibrium curves as attempted here leads to pressures that are too low and that a correlation of Sassi and Scolari's facies series with independently determined geological and experimental results is more promising. For this reason a pressure of ~2 kb for low grade metamorphism of the northeastern Richtersveld appears to be the most realistic estimate.

6.3. THE SOUTHEASTERN RICHTERSVELD

6.3.1. Texture and mineralogy

1) *Pelitic rocks of the Pink-gneiss Unit*

Textural and mineralogical data that are important for the evaluation of metamorphic grade are given in Table 6.8.

Biotite occurs in flakes up to several mm in length and is in most cases altered to chlorite. Its original red-brown colour is only present in cases of complete inclusion within quartz.

Muscovite occurs in several textural modifications:

Mu_1 consists of flakes up to several mm long as shown in Figure 6.8. Mu_2 is made up of aggregates of sericite (Fig. 6.8b) embedded in a well-crystallised "high-grade" texture while tectonically formed sericite is found in deformed and recrystallised quartz textures as depicted in Figure 6.8a and associated with deformed mu_1. Needle-shaped muscovite (Fig. 6.7) bears a strong resemblance to sillimanite as it occurs in sillimanite nodules elsewhere in the Namaqua Metamorphic Complex and the fine strings of sericite intergrown with equally fine "drops" of quartz both embedded in an original "high-grade" quartz texture strongly suggest a formation after sillimanite according to the reaction

$$\text{sillimanite} + \text{k-feldspar} + H_2O = \text{muscovite} + \text{quartz}$$

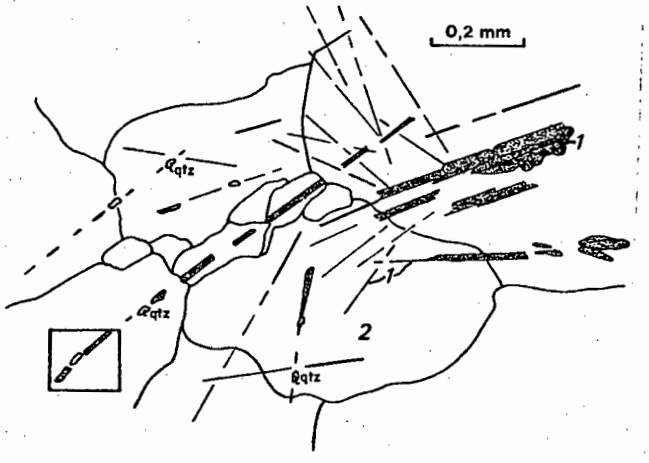

Fig 6.7(a) Needles of white mica assumed to have formed after sillimanite.
1) white mica
2) quartz

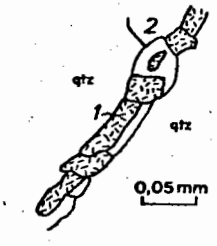

Fig. 6.7(b) Section of Fig. 6.7(a) showing very fine intergrowth of quartz and white mica. 1)white mica associated with fine quartz "drops". 2) quartz host grain.

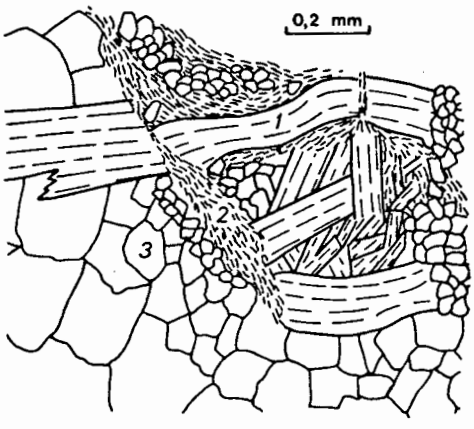

Fig. 6.8(a) Tectonically formed sericite associated with deformed mu_1 and recrystallised quartz. Deformation probably due to shearing of the Devilscastle Event.
1)mu 2) tectonically formed sericite
3) quartz

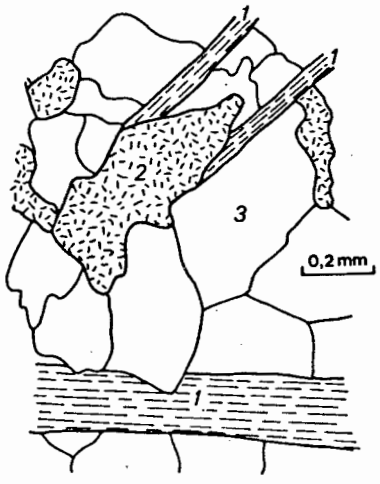

6.8(b) Aggregates of sericite in undeformed metamorphic texture suggest other than tectonic origin for the sericite.
1) mu_1 2)mu_2 3) quartz

See text for discussion

2) *Non-pelitic rocks of the Pink-gneiss Unit*

Textural and mineralogical data that are important for the evaluation of metamorphic grade are given in Table 6.8. A particular feature encountered in Pink gneiss is the normal zonation of plagioclase wherever it is in contact with K-feldspar (core An 7, rim An 0). Rambaldi (1973) suggested that features of that kind may have been produced by the equilibration of K-feldspar with an originally higher Na content (e.g. igneous) at metamorphic temperatures resulting in enrichment of Na in the rim of the plagioclase and in a decrease of Na in the K-feldspar itself.

In pink gneiss mu_1 occurs in big flakes which are only weakly orientated. When in contact with plagioclase it is surrounded by a rim of mu_2 which is never present when in contact with quartz. Mu_1 is therefore distinctly associated with quartz and mu_2 with plagioclase, which is also shown on a statistical basis by means of grain transition probabilities in Table 6.9 and Fig. 6.9.

Table 6.8

Textural and mineralogical properties of rocks of the Pink-gneiss Unit

	Pink gneiss	*biotite gneiss*	*amphibolite*	*schists*
texture	equigranular polygonal	inequigranular polygonal	lepidoblastic	equigranular polygonal
mineralogy	quartz, plagioclase (core An7, rim An0) microcline (non-perthitic), mu_1, mu_2. Composition : granitic	quartz, plagioclase, K-feldspar, biotite (green), epidote. Composition: granodioritic subtexture B in plagioclase	plagioclase (andes.) quartz, biotite (brown to green-brown) hornblende (blue-green) fibrolite in plagioclase = subtexture B.	qtz, mu_1, mu_2, tectonic sericite, "needle-shaped" muscovite, biotite
fabric elements	S_1, absent or very weakly developed	S_1, partly distinctly developed, alignment of biotite	S_1, preferred orientation of biotite and hornblende	S_1 by weak alignment of mica

Table 6.9

Difference matrix of grain transition probabilities in muscovite gneiss. Sample 389/4. Total tally 611 transitions. The concept of grain transition probabilities has been explained in Appendix 1 and Chapter 3 with respect to granites. The same concept can, of course, also be applied to the quantitative description of metamorphic parageneses.

	qtz	*plg*	*kf*	mu_2	mu_1
qtz		0,034	0,032	-0,093	0,027
plg	0,092	-	-0,014	0,008	-0,087
kf	0,125	-0,007	-	-0,032	-0,086
mu_2	-0,108	0,049	-0,028	-	0,087
mu_1	0,189	-0,166	-0,165	0,142	-

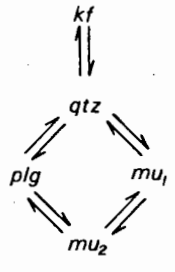

Fig. 6.9
Grain association diagram as derived from Table 6.9. Arrows denote associations higher than expected in random distribution.
For further explanation see Appendix 1.

3. *Metavolcanics of the Windvlakte Formation*

Textural and mineralogical data that are important for the evaluation of metamorphic grade are given in Table 6.10.

Yellow pleochroic cores of epidote in contact with biotite are frequently observed in prograde metamorphic terrains and probably denote reduction of ferric iron and its incorporation into biotite with rising temperature (Miyashiro, 1973).

Table 6.10

Texture and mineralogy of metavolcanics of the Windvlakte Formation

Texture	inequigranular interlobate metamorphic texture superimposed on volcanic texture. Remnants of volcanic phenocrysts are partly preserved as palimpsestic mineral aggregates
foliation	Not present on scale of thin section and hand specimen
plagioclase	recrystallised into aggregates of muscovite, quartz epidote, albite, making up distinct subtextures in the confines of the original plagioclase crystal (subtexture A) (cf. 6.3.1. - 4)
K-feldspar	content variable; structural state always microcline, minor perthitic exsolutions
biotite	flakes up to 1 mm in length, random orientation, green-brown, in few cases brown
muscovite	mainly as sericitic alteration of plagioclase. Occasional bigger flakes growing from sericite within plagioclase, occur more frequently when approaching Helskloof migmatites
epidote	anhedral to euhedral, 0,1 - 0,5 mm; yellow pleochroic core when in contact with biotite

4. *Plagioclase subtextures*

Plagioclase crystals in volcanic and intrusive rocks of the Richtersveld have repeatedly been shown to be particularly strongly saussuritised and to contain alteration products consisting of sericite, epidote, quartz and less An-rich plagioclase. These alteration products grow with increasing grade of metamorphism, form distinct granoblastic subtextures during medium grade metamorphism within the confines of the original plagioclase crystal*, disappear with further increasing metamorphic grade and finally give rise to homogeneously extinguishing plagioclase with fibrolite and epidote grains.

It is therefore possible to distinguish between two types of subtextures *within* the former plagioclase crystals:

* Recrystallisation textures in plagioclase similar to those described here but without fibrolite development had also been reported by Roddick *et al.*, (1976) from an Archean greenstone sequence in Western Australia.

Texture A (Fig. 6.10a) develops from the original products of saussuritisation and reaches its optimal stage during medium grade metamorphism.

Texture B (Fig. 6.10c) occurs mainly in association with migmatites and consists of homogeneously extinguishing plagioclase, epidote of the original size and fibrolite, which is in most cases altered into aggregates of fibrolitic sericite.

The transition between these two subtextures is not sudden and the first occurrence of *Texture B* appears to be related to the first occurrence of migmatites in granodioritic paleosome where both textures coexist even within the same grain.

Fig. 6.10
Development of quartz-albite-sericite-epidote and fibrolite-sericite-epidote subtextures within volcanic or intrusive phenocryst during metamorphism.
A stage preceding Texture A is shown in Figure 6.16b.

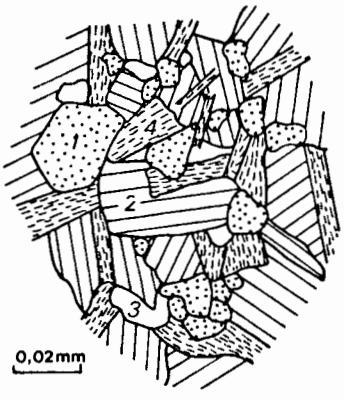

Fig. 6.10a Texture A : the original plagioclase phenocryst is completely recrystallised into albite of variable orientation and epidote, sericite and quartz
1) epidote; 2) albite; 3) quartz;
4) sericite

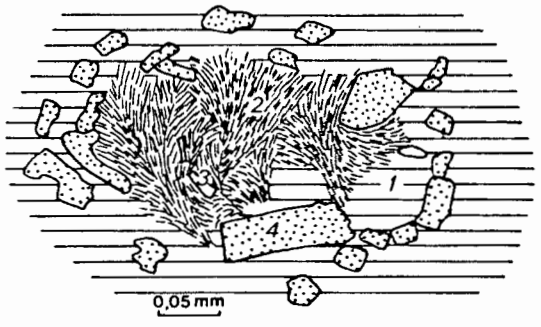

Fig. 6.10b Texture B : homogeneous plagioclase with epidote grains and occasional quartz. The fibrolitic texture consists of white mica and not of sillimanite.
1) epidote; 2) plagioclase;
3) quartz; 4) sericite

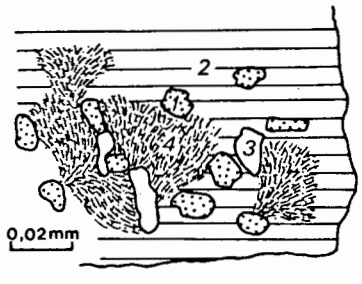

Fig. 6.10c Development of fibrolite in plagioclase.

1) homogeneously extinguishing plagioclase; 2) fibrolite;
3) quartz; 4) epidote

5) *Helskloof migmatites*

Textural and mineralogical data that are important for the evaluation of metamorphic grade are given in Table 6.11. Compositional relationships between paleosomes and neosomes have been discussed in Chapter 4.

Table 6.11
Texture and mineralogy of migmatitic rocks in the Helskloof area

Rock type	:	*paleosome* : granodiorite and tonalite of the VIS *leucosome* : trondhjemitic to granitic, depending on paleosome *diatexite* : granodioritic to granitic
Texture	:	inequigranular to equigranular interlobate to polygonal.
Fabric elements	:	S_1 in paleosomes, occasionally on outcrop scale
plagioclase	:	subtextures A and B. First occurrence of subtexture B is approximately identical with first occurrence of migmatisation in granodioritic rocks
K-feldspar	:	microcline, perthite as few and small flame-like exsolution lamellae, anhedral, as porphyroblasts and interstitially.
biotite	:	green to green-brown, in advanced stage neosomes as individual flakes rather than aggregates
epidote	:	euhedral to anhedral, within plagioclase up to 0,2 mm across, larger outside plagioclase, particularly when associated with biotite, development of yellow pleochroic core. Frequent marginal recrystallisation into tiny colourless grains with high refractive index.
muscovite	:	sericitic alteration products in plagioclase and occasional larger flakes. In advanced stage migmatites larger flakes occur interstitially with quartz and feldspar.
sillimanite	:	only found in one instance in advanced stage migmatite, enclosed in muscovite flake which is embedded in microcline.
amphibole	:	in granodioritic paleosomes of advanced stage migmatites, particularly growing at contact with biotite and quartz (see text and Fig. 6.11)

Of particular importance with respect to the anatectic nature of the migmatites is the growth of amphibole in granodioritic paleosomes as shown in Figure 6.11, since incongruent melting of biotite during anatexis is known from experimental

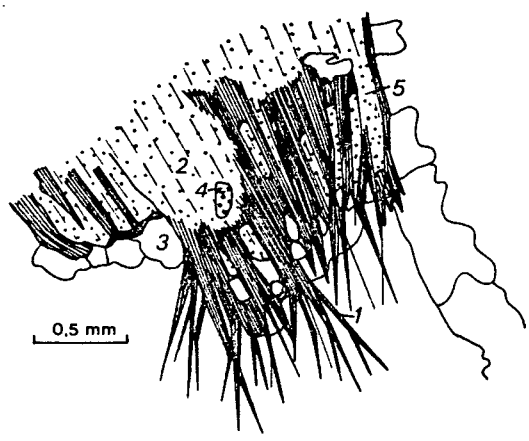

Fig. 6.11 Marginal alteration of biotite into hornblende at contact with quartz. Incipient growth of hornblende starts as fissile colourless needles (possibly actinolite) at the contact of biotite and quartz and proceeds from there towards the interior of the former biotite crystal.
1) needles of amphibole
2) biotite
3) quartz
4) epidote

See also Plate 7.

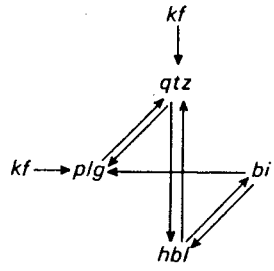

Fig. 6.12a Grain association diagram of the sample shown in Fig. 6.11. Total tally 797 transitions. For explanation of the concept of grain transition probabilities see Appendix 1.
(328/2)

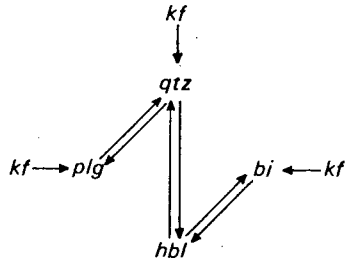

Fig. 6.12b Amphibolitic melanosome in which no biotite-hornblende reaction has been observed. The grain association pattern is, however, nearly identical to that of Fig. 6.12a and suggests a formation of hornblende by the same mechanism.
Total tally 300 transitions
301/1

work (Büsch, *et al.*, 1974, Knabe, 1970) and this occurrence may represent such a case. The preferred growth of hornblende in the presence of quartz is corroborated by the grain association diagrams in Figure 6.12 which show a particularly strong association between hornblende and biotite and hornblende and quartz. Grain association diagrams have also been constructed for some selected migmatites of advanced stage. They show at one glance (Fig. 6.13; Table 3.2) that, while the Vioolsdrif granodiorite is characterised by a persistent *M-qtz* and the absence of a *M-plg* association, migmatitic neosomes have variably developed positive *plg-M* associations but negative *M-qtz* associations.

Fig 6.13 Grain association diagrams of migmatitic neosomes of the Helskloof area.

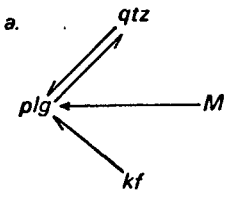

a) Nebulitic migmatite, total tally 757 transitions (213/10)

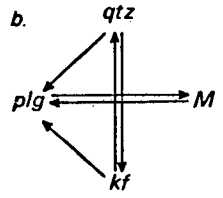

b) Diatexite at loc. type. total tally 543 transitions (303/2)

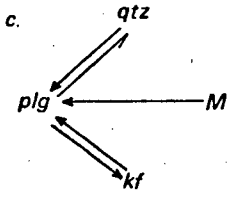

c) Diatexite, immature texture, total tally 275 transitions (213/2)

6.3.2. Evaluation of mineralogical and textural data

1. *General*

As is evident from the scarcity of index minerals, the elucidation of metamorphic grade will have to concentrate on two main problems :

a) indications for the presence of sillimanite
b) the problem of migmatisation

Evidence for the presence of sillimanite is suggested by:

a) the plagioclase subtextures in volcanic and intrusive rocks
b) needle-shaped mu-pseudomorphs in pelitic rocks
c) sericite aggregates and their parageneses within pink gneiss

The value of migmatites for the elucidation of metamorphic grade depends largely on whether they are of anatectic origin. The discussion of metamorphism in the southeastern Richtersveld is thus reduced to the problems of sillimanite pseudomorphs and anatexis.

2. *Indications for the presence of sillimanite*

a) The plagioclase subtextures

The occurrence of sericite, epidote, quartz and plagioclase within former plagioclase phenocrysts in medium grade metamorphism and the presence of fibrolite, homogeneously extinguishing plagioclase and epidote of the original size and shape in high grade metamorphism,suggest a reaction to have taken place that led to the formation of sillimanite and the reconstitution of plagioclase while leaving epidote unaffected. Two reactions able to produce transformations of that kind are known from the literature:

1) muscovite + quartz + albite comp. of plagioclase $\rightleftharpoons$ sillimanite + melt
2) muscovite + quartz + albite comp. of plagioclase $\rightleftharpoons$ sillimanite + albite-rich K-feldspar + H_2O

Reaction 1) has been experimentally investigated by Storre and Karotke (1971) (quoted in Winkler, 1974) and their equilibrium curve is virtually identical with the beginning of melting in granodiorite (Fig. 6.14), thus being in good agreement with field relationships in the southeastern Richtersveld. Reaction 2) was suggested by Evans and Guidotti (1966) who conceded that if this reaction took place in the field of water saturated granitic liquid, their reaction should have a liquid phase on the right-hand side instead of vapour. It would then be identical to reaction 1). If a reaction of that type has in fact taken place on the scale and the manner outlined above, it is of considerable importance with respect to the scale on which metamorphic reactions took place in the southeastern Richtersveld and would argue in favour of a very conservative metamorphism, ruling out metasomatic

migration of components over more than a fraction of a mm.

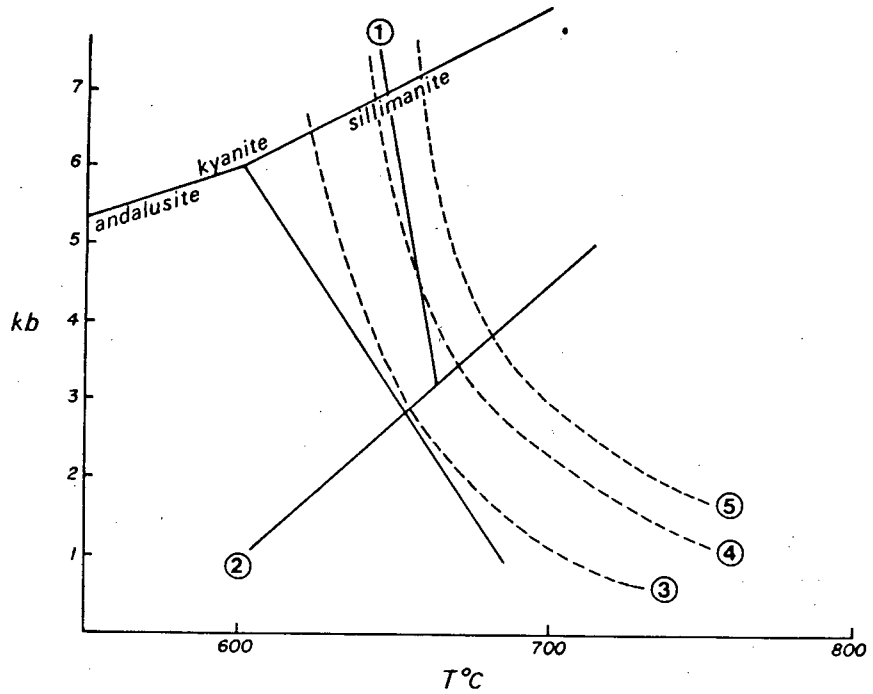

Fig. 6.14 Phase relationships in high grade metamorphism

1) Formation of *sillimanite* after the reaction albite + muscovite + quartz + $H_2O \rightleftarrows$ melt + sillimanite/kyanite (Storre & Karotke (1971) quoted in Winkler (1974) p. 83).

2) Formation of *sillimanite* after the reaction muscovite + quartz = K-feldspar + sillimanite + H_2O (Althaus *et al.*, 1970; Evans, 1965)

3) *Beginning of melting* in water-saturated granite (Sierra Nevada granite 104 of Piwinskii, 1968)

4) *Beginning of melting* in water-saturated granodiorite (after Piwinskii, 1968; Whitney, 1975)

5) Approximate temperature of "*quartz out*" during melting experiments in water-saturated granodiorite (after Piwinskii, 1968)

b) Muscovite pseudomorphs in pelitic rocks

Since sillimanite nodules in muscovite schists of the Pink-gneiss Unit have occasionally been observed in the field, textures as displayed in Fig. 6.7 suggest sillimanite to have formed at one stage during metamorphism, and the close relationship of muscovite needles and tiny quartz "drops" in Fig. 6.7b indicates that a retrograde reaction of the type

K-feldspar + sillimanite + water → muscovite + quartz

has taken place without destroying the original metamorphic texture.

c) Textural parameter in muscovite gneiss and the formation of sillimanite

The distinctly non-random distribution of the two muscovite modifications (Fig. 6.9, Table 6.9) suggests a formation by different processes, one of which could be the formation of mu_2 after sillimanite.

Sillimanite in high grade terrains may form by one of the two types of reaction:

1) albite + muscovite + quartz → melt + sillimanite (Storre and Karotke, 1971, quoted in Winkler 1974)
2) muscovite + quartz → K-feldspar + sillimanite + H_2O (Althaus *et al.*, 1970, Evans, 1965)

In textures as described for muscovite gneiss each of these reactions would lead to a different grain association provided there is no material exchange beyond the immediately reacting minerals.

If reaction 2 is assumed to have taken place, muscovite flakes should be expected to react to form sillimanite at least at the contact with quartz, resulting in a strong association of mu_2 and quartz, and the production of K-feldspar by the same reaction should have formed a strong association of K-feldspar and mu_2. Neither is evidently the case as can be seen from the difference matrix in Table 6.9 where the two mineral pairs are expressed by negative values.

If reaction 1) is assumed to have taken place, muscovite flakes in contact with plagioclase should be expected to react to form sillimanite if sufficient quartz is available and a similar reaction rim should be expected at contacts with quartz if sufficient plagioclase is available. The latter has, however, not been observed and it is therefore not possible to identify reaction 1) positively by textural criteria, but textural parameters do not rule it out either. Reaction 2), however, can be ruled out since none of the expected positive associations have been observed. On the contrary, they display rather negative values (Table 6.9).

d) Conclusion

While there is hardly any doubt that sillimanite did form during main metamorphism (fibrolite in plagioclase subtexture B, muscovite needles, Fig. 6.7) some uncertainty remains as to its mode of formation. From the two reactions that are likely to account for the formation of sillimanite, reaction 2) can be ruled out for textural reasons. Reaction 1) however, is weakly favoured by textural relationships in pink gneiss (Fig. 6.9, Table 6.9) and considerably favoured by the formation of fibrolite in plagioclase subtextures, where reaction 2) can also be ruled out. For these reasons the author tends to attribute the formation of sillimanite to reaction 1) rather than to reaction 2).

3. *The Origin of the Helskloof Migmatites*

a) General

The field appearance, structural position and compositional relationships of the migmatites have already been discussed and for details the reader is referred to 4.1.2. This paragraph therefore has only the purpose of evaluating the available evidence with respect to metamorphic grade.

De Villiers & Söhnge (1959) already noted the conspicuous association of Vioolsdrif intrusives and migmatitic rocks and related the latter to the intrusion of the Vioolsdrif Intrusive Suite. Middlemost (1963) divided the rocks of the Rooiberg-Helskloof area into Kheis supracrustal rocks, hybrid rocks and adamellitic gneiss. While it does not become clear from his descriptions and his map what exactly is meant by "hybrid rocks", the migmatites and Vioolsdrif granodiorite are obviously included with the adamellitic gneiss. According to him, Kheis supracrustal rocks have undergone an intense "granitisation process" with adamellitic gneiss in the core of the granitised area and unaltered supracrustal rocks farthest away. He attributed the granitisation to "permeating granitic solutions" and proposed an allochthonous origin for the leucosomatic banding of the migmatites (his banded gneiss).

b) Mode of origin

According to conventional views migmatites may be formed by

a) metamorphic differentiation
b) lit-par-lit intrusion
c) partial melting

- mechanisms which are, except for anatexis, rather ill defined. At Helskloof lit-par-lit intrusion is not favoured by the close compositional similarity of adjacent paleosomes and leucosomes and can hardly be imagined

to have taken place in the unlayered and only weakly foliated meta-intrusives of the Vioolsdrif Intrusive Suite. In addition, it fails to account for many of the gradual transitions between leucosome and paleosome on the outcrop scale.

Metamorphic differentiation is not supported by the indications for rather conservative metamorphism elsewhere in the southeastern Richtersveld (see the problems of plagioclase subtextures and the formation of sillimanite) and by the composition of the leucosome (~minimum melt).

Both of these mechanisms are improbable because of the gradual transition from metatexites to diatexites on the local scale and the formation of hornblende from biotite which is not possible during metamorphism.

The alternative theory of *in situ* melting of Vioolsdrif granodiorite is supported by the following observations:

a) There is no difference in field appearance between paleosomes of the Helskloof migmatites and Vioolsdrif granodiorite elsewhere in the Richtersveld.

b) the texture of the leucosome is magmatic

c) melanosomatic rims at the contact of paleosome and leucosome (Plate 2) indicate an anatectic origin (Mehnert, 1968)

d) compositional relationships of paleosome and leucosome:

   i) the modal composition of granodiorite and diatexite is similar with respect to leucocratic minerals (Fig. 4.6)

   ii) close relationship between K-feldspar content of paleosome and leucosome

e) biotite-hornblende reaction which is only known from melting experiments and not from metamorphism.

For these reasons anatexis of the Vioolsdrif granodiorite is regarded as the most likely mode of origin and in the following adopted as a working hypothesis.

c) The role of water during melting

That so little information is available as to the actual melting conditions in migmatitic terrains is largely due to the incomplete knowledge of textural and compositional relationships of the paleosomes which always leave some doubt as to their true nature. In the present case, however, texture and composition of the paleosome are safely known to be Vioolsdrif granodiorite and we are therefore in the position to evaluate changes in texture and composition of the rocks involved during migmatisation more accurately than in most other cases.

Schematic isobaric T-XH_2O diagrams as shown in Figure 6.15a for

a granodiorite similar in composition to the Helskloof paleosome, are useful for the interpretation of migmatites since they allow the demonstration of the general principle of the availability of water on the amount of melt and also allow a rough estimate of the composition of the melt during various stages of melting. So, for example, at 3 percent water and 725°C, all quartz and K-feldspar plus some plagioclase have already melted while at 2 percent water and the same temperature only small amounts of initial melt have formed. At water contents represented by the amount of hydrous minerals, no melting will occur up to nearly 900°C. At metamorphic conditions between 650°C and 750°C and P > 4kb, which can reasonably be assumed here, melting will be mainly controlled by the amount of water circulating through the rock. Since this will happen along planes of increased permeability such as joints, schistosity and cleavage, initial melting is likely to take place in areas of facilitated water circulation and to proceed from there towards the interior of the rock. The common observation in migmatitic terrains of strongly migmatised rocks coexisting with virtually unaltered paleosome can thus best be explained by variable availability of water, which in turn is controlled by structural features obtained during or prior to migmatisation.

d) Assessment of the degree of melting

The formation of melt as expected from experimental data.

Owing to the detailed work of Mehnert *et al.*, (1973) and Büsch *et al.*, (1974), textural and compositional developments during melting are relatively well known and can be used in addition to T-XH_2O diagrams to predict the formation of a melt in granodioritic rocks (see also Fig. 6.15 a and b).

Judging from Fig. 6.15a, a rather small increase in temperature is already sufficient to melt all K-feldspar and quartz in a granodioritic system and textural observations during initial melting suggest (Mehnert *et al.*, 1973, Büsch *et al.*, 1974) that K-feldspar and K-feldspar component of plagioclase melt wherever they are in contact with quartz. Recrystallised products of melting, forming narrow rims around quartz, consist of fine intergrowth of quartz and K-feldspar. It is evident that this melt if segregated at such a stage would form a K-feldspar-rich leucosome even if the parent rock was granodioritic.

In the advanced stages of melting more plagioclase-component will be included in the melt, giving rise to an increasingly more granodioritic composition of the leucosome, a trend which may be counterbalanced if the composition of biotite allows its incongruent melting with the formation of hornblende, resulting in an additional release of K-component into the melt (Büsch *et al.*, 1974). It can be estimated from Figure 6.15 that at temperatures of approximately 50°C above solidus (more than 50% of the rock already consist of melt) the remaining crystal phase is mainly made up of plagioclase and biotite/hornblende.

Table 6.12 Experimental melting temperatures of granites and granodiorites

References	Rock type as described by author	solidus, water sat. at 2 kb in °C		"qtz and Kf out," water sat. at 2 kb in °C	
1)	bi-hbl gneiss (natural)	700	675 (5 kb)		
	diatexite (granodioritic, natural)	690	660 (5 kb)		
2)	granodiorite (natural)	700		720	
	"	700		750	
	qtz monzonite (natural)	680		720	
	"	690		710	
	rhyolite (natural)	690		810	
	"	690		730	
	"	690		740	
3)	monzogranite (natural)	710		750	
4)	riebeckite granite (nat.)	650		700	
	riebeckite-aegirine granite (natural)	650		750	
5)	granodiorite Sierra Nevada				
	No. 102	710		740	
	No. 103	705		730	
	granite No.104	675		730	
6)	Needle Point Pluton, Wallowa Batholith				
	felsic body	670		710	
	main pluton	700		750	
7)	granodiorite (nat.)	700		725	
8)	all synthetic:		8 kb:		8 kb:
	granite	700	620	750	
	adamellite	705	620	760	700
	granodiorite	710	640	730	655
	tonalite	710	660	800	700

References: 1) Büsch *et al.* (1974), 2) Gibbon & Wyllie (1969), 3) Maaløe and Wyllie (1975), 4) McDowell and Wyllie (1971), 5) Piwinskii (1968), 6) Piwinskii & Wyllie (1970), 7) Robertson & Wyllie (1971), 8) Whitney (1975a).
"Qtz and Kf out" denotes the temperature at which all qtz and Kf are in a molten state during melting experiments or at which, during cooling from a melt, either of these minerals occurs first.

It is therefore possible to explain many of the observations encountered in terms of experimental results:

1) *Leucosomes in metatexites are either granitic or tonalitic.* (Fig. 4.6c). Granitic leucosomes in granodioritic paleosomes represent early stages of melting in which most of the K-feldspar and quartz but relatively little plagioclase had been incorporated in the melt. In the case of tonalitic leucosomes the parent rock was so devoid of K-feldspar that only the K-feldspar component of plagioclase could contribute to the formation of an early melt.

2) *The enrichment of mafic minerals* and plagioclase in melanosomes is evident from the sequence of melting and needs no further discussion.

3) *Incongruent melting of biotite* has been achieved experimentally by Knabe (1970) and Büsch *et al.*, (1974) and takes place during the formation of a melt in granodioritic rocks by the reaction

biotite + quartz = hornblende + melt (K_2O, Al_2O_3, H_2O)

However, the temperature of the reaction (Knabe, 1970) is strongly dependent on the composition of the biotite.

4) *Similar composition of granodioritic paleosome and diatexites.* In an advanced stage of melting increasing amounts of the plagioclase component will be included in the melt and if mobile and crystalline components of the diatexite are not or only weakly segregated a composition similar to that of the parent rock will result (with respect to the leucocratic components).

5) *Textural properties* (grain associations). If Vioolsdrif granodiorite melts (it has been shown in Section 3.4 to contain two generations of biotite associated either with plagioclase or quartz) those biotite crystals which are wholly or partly enclosed in plagioclase will be protected from melting up to much higher temperatures than those that are enclosed in quartz or K-feldspar. Thus the association biotite-plagioclase will selectively be preserved or even enhanced during melting (Fig. 6.15b). This effect will even be more pronounced if melting and recrystallisation take place under water-saturated conditions. Since in the paleosomatic granodiorite the strong association of bi_2 and quartz had been ascribed to crystallisation under water-*undersaturated* conditions, recrystallisation under water-*saturated* conditions after anatexis will promote crystallisation of biotite at an early stage together with plagioclase and thus favour once more this association. Grain associations as displayed in grain sequence diagrams therefore appear to be more than only descriptive and may reflect considerable parts of the geological history of a rock.

4. *Metamorphic grade*

In order to assess metamorphic grade from migmatisation,

Table 6.13 Comparison between some expected and observed features of migmatites of the Helskloof area, at different stages of melting.

	expected features	observed features
initial melting	Melt very kf-rich, except in parent rocks without kf-component	granitic composition of leucosome in granodioritic paleosome
incongruent melting of biotite	Formation of hornblende at the contact of bi with melt. Release of additional kf-component	formation of hornblende at the contact of biotite with quartz diatexites slightly more kf-rich than granodioritic parent rock
advanced stage melting	melt becomes increasingly more granodioritic, selective melting of biotite associated with quartz	granodioritic leucosomes in granodioritic paleosomes, strong plg-bi association in diatexites and advanced stage leucosomes

composition and solidus temperature of the paleosome as well as the degree of melting have to be known. While in the present case the composition of the paleosome is roughly known, its solidus temperature can only be inferred from melting experiments with similar rocks. For this reason Table 6.12 has been prepared which lists most of the presently available data on melting temperatures of granodiorites. While the solidus temperature of granodioritic rocks is fairly consistent, the "quartz and K-feldspar out" temperature depends much more on the composition of the rock, but can be estimated for granodiorites to lie approximately 20 to 40°C above the solidus temperature. It is thus possible to estimate the degree of melting if textural relationships are known, as in this case, where it is likely that at least the diatexites have undergone advanced stage melting with approximately 50-60 percent of the rock in a molten state. This degree of melting, represented in Figure 6.14 as curve 5, naturally is only a rough estimate, its exact position depending on the amount of kf and qtz, but it can nevertheless be used to show that metamorphic temperatures must have exceeded 650°C at pressures below ~8 kb.

Pressure conditions can only be estimated with a large degree of uncertainty. Assuming (Fig. 6.14) that

a) sillimanite is stable
b) sillimanite has formed by a reaction of type 1) and not 2) (Fig. 6.14)
c) the degree of melting in granodiorite is identical with curve 5

a pressure of 5,5 $\pm$ 1,5 kb is likely for the formation of the Helskloof migmatites.

6.4. THE NOMS RIVER - BLOCKWERF AREA

6.4.1. General

This domain is characterised by a rapid lateral transition from

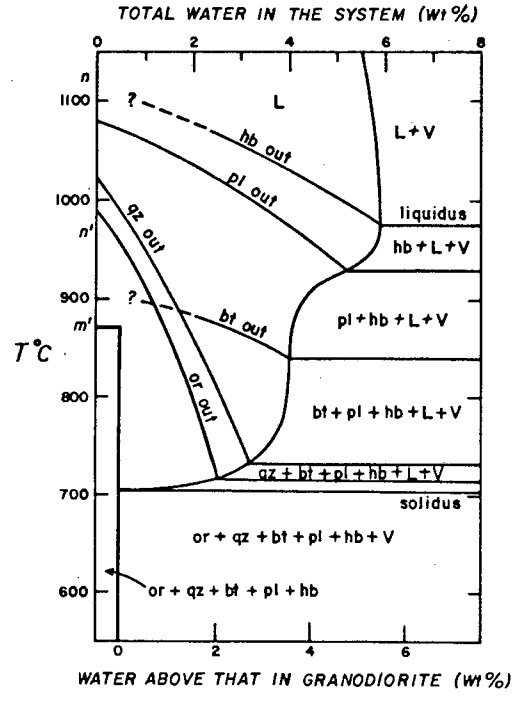

Fig. 6.15a T-XH_2O diagram for granodiorite after Robertson and Wyllie (1971)

low to high grade metamorphism and by intermediate pressure characteristics of b_o values in pelitic rocks. It is furthermore the only metamorphic domain in which indications for two tectonothermal imprints exist.

6.4.2. Texture and mineralogy

1. *The Noms River area*

Mineralogy and texture of metavolcanics are not markedly different from those of the central Richtersveld. Its biotite parageneses have already been treated in the paragraph on the central Richtersveld. It is evident from Table 6.14 that the occurrence of biotite is related to the maturity of the rock, i.e. to the K-feldspar component available, since all metavolcanics contain biotite while it occurs only occasionally in immature sediments and not at all in pelitic rocks.

Laminated leucocratic metasediments consist of a fine groundmass of sericite and quartz in variable proportions in which porphyroblasts of biotite, poikilitically intergrown by quartz, are embedded (Fig. 6.16a). Pelitic rocks are extremely rare and consist mainly of sericite with minor amounts of quartz and chlorite. In one sample two distinct crosscutting foliations have been observed.

2. *The Blockwerf area*

This area is made up of different rock types among which a variety

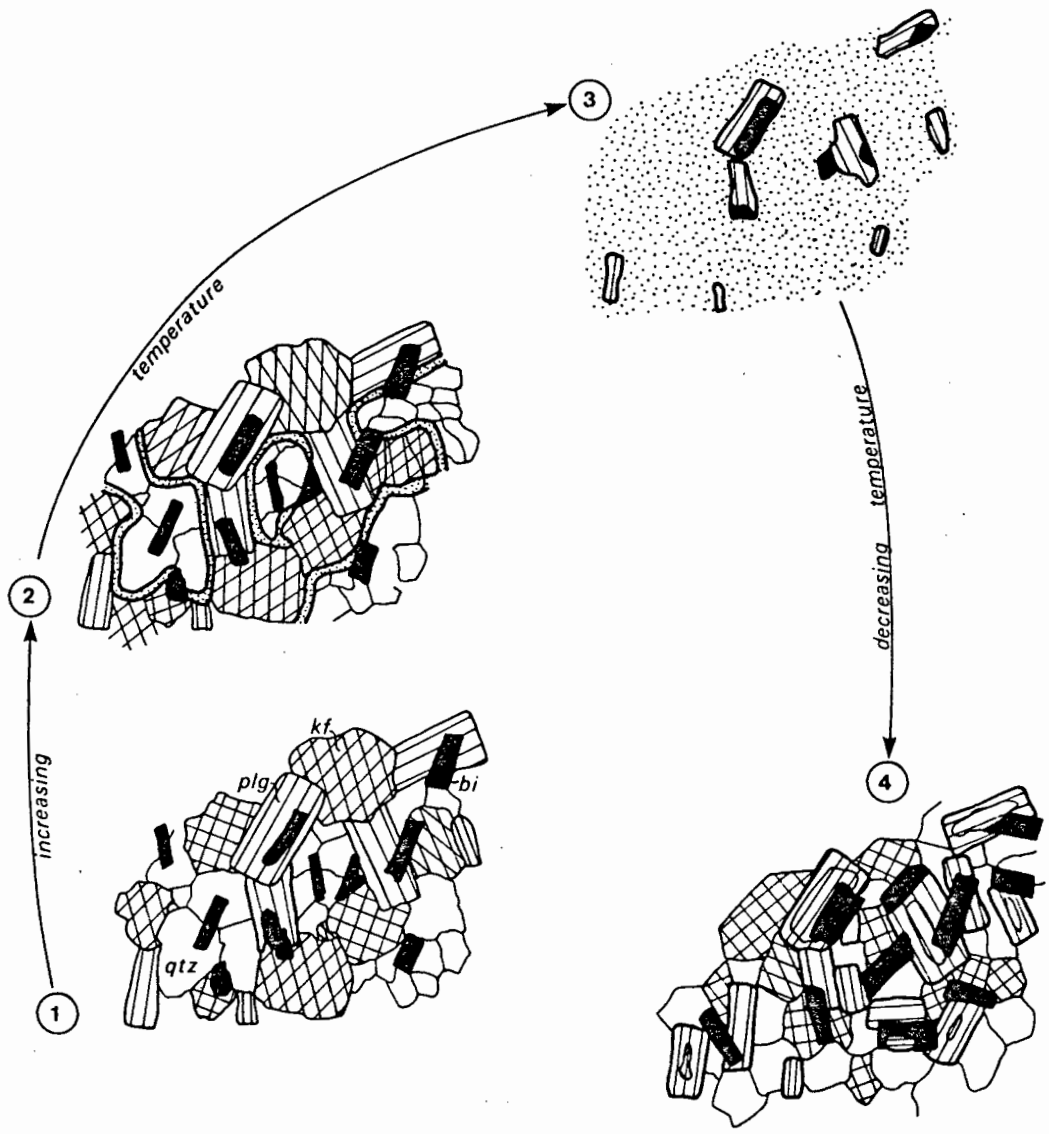

Fig. 6.15b Schematic diagram of the textural development during anatectic melting and recrystallisation of granodioritic rock. The relevant features are exaggerated for the sake of clarity.
Stage 1): Original texture formed under water-undersaturated conditions with *bi* associated with *qtz* and *plg* respectively
Stage 2): Initial melting. First melt forms at contact of *qtz* with *Kf* and *plg* (but not at contact *plg-Kf*) in narrow rims of *Kf*-granitic composition. This texture has been described from melting experiments by Büsch *et al.*, (1974) and has actually been observed during the present investigations in granodioritic samples collected at the contact with dykes of the Gannakouriep suite (see Plate 6).
Stage 3): Maximum melting. All *qtz* and *Kf* and some *plg* and *bi* has melted. *Bi* enclosed in *plg* is selectively preserved from melting.
Stage 4): Recrystallisation under water-saturated conditions. *Plg* and *bi* recrystallise together; pre-existing minerals may serve as nuclei for further crystallisation thus contributing to the preferred association of *bi* and *plg*; final crystallisation of *qtz* and *Kf*.

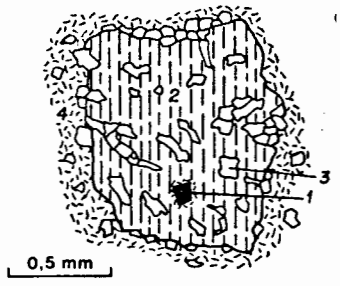

Fig. 6.16a
Porphyritic biotite in laminated metasediments. 1) ore with goethite rim; 2) biotite; 3) quartz; 4) sericite (411)

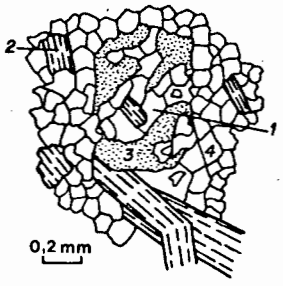

Fig. 6.16b
Partly recrystallised volcanic plg phenocryst. 1) recrystallised fspr of phenocrysts; 2) biotite; 3) fine-grained ep aggregates; 4) anhydrous groundmass minerals (416/1)

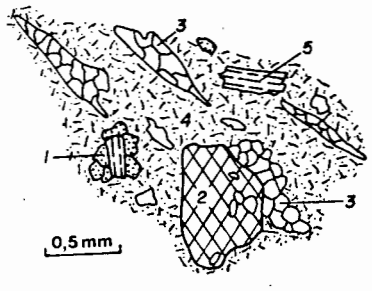

Fig. 6.16c
Augen gneiss (BMC)
The texture displays effects of considerable downgrading.
1) epidote; 2) Kf augen; 3) qtz aggregates; 4) groundmass, mainly sericitic; 5) biotite (409/2)

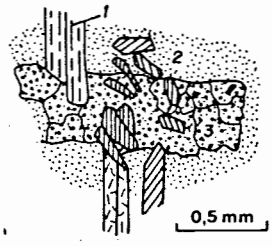

Fig. 6.16d
Amphibolite (BMC) Recrystallised plg phenocryst intergrown with amphibole, probably of metamorphic origin. 1) amphibole; 2) strongly saussuritised grm, individual grain boundaries not recognisable; 3) recrystallised plg phenocryst intergrown with amphibole and small grains of epidote (409/4)

Table 6.14 Mineral assemblages in rocks of the Noms River area

Sample Nr	bi	mu	chl	ep	plg	kf	qtz	ore	
126/1		x	x				x		
138/7		x	x				x		pelitic
138/17		x					x		
419/1		x	x				x		
138/9		x	x	x	x		x		
138/10	x	x	x	x	x		x	x	immature sediments
138/15		x	x	x			x	x	
138/23	x	x	x	x			x		
138/12	x		x	x	x		x		
138/19	x			x	x		x		metavolcanics
138/21	x	x		x	x		x		
138/22	x	x		x	x		x	x	
419/2	x	x		x	x		x		

of transitions exist. They are coarser grained than the rocks in the Noms River area and display a distinct gneissic appearance. Textural and mineralogical data are listed in Table 6.15 and field appearance and structural position have been described in Section 4.2.

6.4.3. Data related to the baric type of metamorphism

In Figure 6.5 it can be seen that the b_o-values of samples collected in the Noms River area are different from those of other parts of the Richtersveld in that their mean ($\bar{x}$ = 9,023 Å) is equivalent to facies series 4 of Sassi and Scolari (1974) and thus typical barrovian. It should be emphasised, however, that the cumulative frequency curve has its origin at the origin of all other curves, i.e. the lowermost values are in agreement with those found in other parts of the Richtersveld, although the mean reflects higher b_o-values.

6.4.4. Evaluation of textural and mineralogical data

1. *Thermal type of metamorphism*

Due to the uniform mineralogy and absence of indicator minerals little can be said about the actual metamorphic grade that has been reached in the Noms River area and the BMC.

Rock type	*muscovite schist*	*augen gneiss*	*amphibolite*	*granoblastic metavolcanics*
texture	equigranular polygonal (~0,5mm)	see Fig. 6.16c grain size: ~0,5mm		equigranular polygonal
fabric elements	weak alignment of mica	alignment of qtz aggregates and biotite		only weakly developed preferred orientation of mica
plagioclase		strongly altered, type A	strongly altered, type A	moderately altered, type A (Fig. 6.10a)
K-feldspar		augen, slightly perthitic (string perth.)		microcline, minor perth. exsolutions
quartz	equigranular polygonal subtextures (~0,5mm)	equigranular interlobate (0,5mm) in aggregates aligned in S		
biotite		brown to brown green in core of larger flakes, green at margins and in small flakes		green, flakes in mm range, weakly orientated.
muscovite	flakes in mm range, often kinked or bent, sericite aggregates	sericite in plg and partly in groundmass	ser. in plg	sericite in plg
chlorite	retrograde after biotite			
epidote		occasion. outside plg, sub- to euhedral	if outside plg marginally dissolved into very fine aggreg.	
amphibole			blue-green needles poikilitically intergrown by qtz & ep, radial arrangement in hand specimen	

Table 6.15 Texture and mineralogy of rocks of the Blockwerf area.

In the Noms River area, muscovite and chlorite are still stable with each other and therefore medium grade metamorphism cannot have been reached. In the BMC high grade conditions must have been attained at least in parts. However, since the mineralogy of the paleosomes of the migmatites is not known, no deductions as to the melting temperature can be made.

The belt of amphibole-bearing rocks within the BMC appears to strike towards southeast across the Orange River into South West Africa, where the amphiboles have been described as hornblende by Blignault (1977). The first occurrence of these hornblendes in the Richtersveld should, however, not be regarded as an isograd since

a) they occur first within and immediately beyond the Noms River fault zone
b) rocks to the west of this fault zone are not able to form hornblende for chemical reasons

The first occurrence of hornblende therefore should be regarded as a lithological boundary rather than a metamorphic one.

2. *The baric type of metamorphism*

The pressure conditions in the low grade part of the area are characterised by a mean b_o-value of 9,023Å with a relatively high standard deviation. In addition, the cumulative frequency distribution originates at low b_o-values (Fig. 6.5). This might indicate that either primary low-pressure characteristics have been overprinted by later intermediate-pressure characteristics, or primary intermediate-pressure characteristics by a weaker later low-P-event. Since b_o of the central Richtersveld indicates low pressure (in textures that can be related to F_1, and F_1 is likely to predate G_3) it can be regarded likely for the Noms River area that an earlier low pressure metamorphism has been overprinted by a later intermediate pressure metamorphism. This interpretation is in agreement with two foliations in at least one pelitic sample. A mean of b_o= 9,023Å is furthermore in agreement with the mean for the early Devilscastle Event and this again fits well with the ages of both events of ~1000 my in the Noms River and approximately 900 my in the Devilscastle area.

It therefore appears that intermediate-pressure type metamorphism has been caused by a later metamorphic imprint for which only radiometric and circumstantial but hardly any textural evidence is available.

3. *Conclusion*

The main metamorphism in the Noms River area is likely to have reached not more than upper low grade metamorphism of low pressure type. A later metamorphic imprint probably around 1000 my caused intermediate-pressure b_o-characteristics in white micas of pelitic rocks (barrovian-type

metamorphism). The degree of the main metamorphism in the Blockwerf Migmatitic Complex can only be inferred from textural data and the occurrence of migmatites. It is likely to have reached high-grade.

6.5 THE DEVILSCASTLE EVENT

6.5.1. General

Rocks formed by the Late Precambrian Devilscastle Event, lithology and structural relationships of which have been described and discussed in Chapter 5, are exposed in a broad north-south striking belt in the western part of the southeastern Richtersveld. In some of these rocks complete mineralogical and textural reconstitution has taken place subsequent to deformation reflecting the metamorphic conditions during recrystallisation and justifying their treatment not only as tectonic but also as metamorphic rocks.

6.5.2. Texture and mineralogy

1. *The Devilscastle Schist Belt*

Textural and mineralogical data that are important for the evaluation of metamorphic grade are given in Table 6.16. Field relationships and structural position have been discussed in Section 5.3.

The mineral composition of rocks of the Devilscastle Schist Belt is rather uniform, the main constituents being quartz (~60%) and muscovite (~40%). Sillimanite as reported by De Villiers and Söhnge from the Devilscastle area has not been encountered and is unlikely to occur in paragenesis with chloritoid. When embedded in isotropic textures, chloritoid and kyanite display random orientation as well but are aligned in S_3 when forming part of an anisotropic texture. Later deformation tends to cause either recrystallisation or undulatory extinction and marginal growth of white mica in kyanite.

Textural relationships are complicated. The smaller grain-sized texture frequently cuts in streaks and trains through coarser textures which may represent either an earlier stage of deformation and recrystallisation or parts of an original texture as shown in Figure 6.17b.

2. *The Black Face Mountain Mylonite Belt*

Mylonites, protomylonites and tectonic breccia of this belt have

Table 6.16 Textural and mineralogical properties of schists of the Devilscastle Schist Belt

Rock type	:	sericite schist, partly quartzitic, few chlorite schist intercalations
Texture	:	*textural type* : granoblastic equigranular polygonal (Fig. 6.17a) trains of orientated muscovite of variable size and amount *grain size distribution* : bimodal on thin section scale, developed as subtextures of different grain size but similar degree of recrystallisation
main mineral phases	:	quartz, muscovite, kyanite, chloritoid, (biotite)
muscovite	:	interstitially, random direction, poor in celadonite and paragonite
kyanite	:	tends to be restricted to rel. well-recrystallised textures; euhedral to anhedral; degree of orientation depending on anisotropy of texture; marginal alteration to sericite when deformed
chloritoid	:	tends to be restricted to relatively well-recrystallised textures; subhedral to euhedral, often associated with kyanite
garnet	:	anhedral, encountered only once in iron-rich biotite-sericite schist derived from alaskitic granite

been described in Section 5.3. Their contribution to the elucidation of metamorphic grade is fairly limited. In protomylonites in outcrops along the Stinkfontein River compositional lamination has been observed consisting in thin section of alternating layers of either quartz- sericite or biotite enrichment with phyllosilicates showing only weak preferred orientation, while other mylonites display no signs of recrystallisation.

6.5.3. Data relating to the baric type of metamorphism

The baric type of metamorphism has been estimated by means of

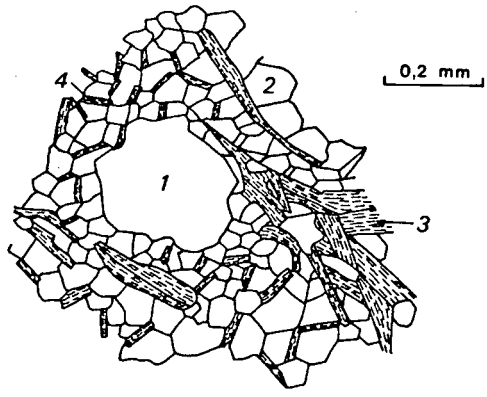

Fig. 6.17a Relatively isotropic texture with relic quartz. (1) The equigranular polygonal quartz texture (2) contains randomly orientated interstitial sericite (4). Larger muscovite flakes are aligned in S. (3).

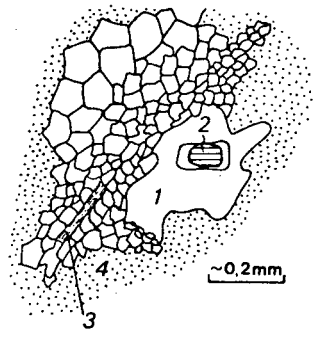

Fig. 6.17b Partly deformed granodiorite of the VIS. Trains of recrystallised quartz with aligned sericite (3) are cutting through the primary quartz aggregate, which still contains, in its undeformed parts, euhedral igneous plagioclase (2) crystals characteristic of Vioolsdrif granodiorite. Sericite (4).

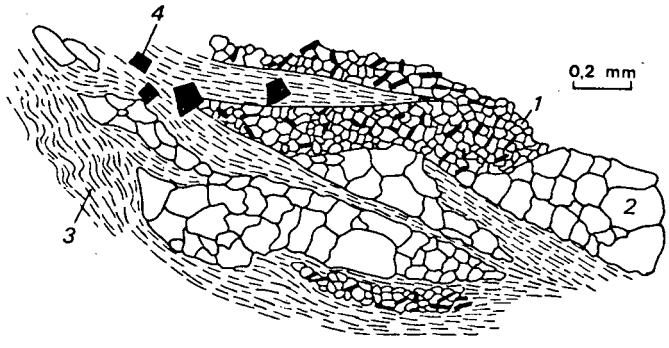

Fig. 6.17c Complex texture of Devilscastle schists. Well recrystallised but fine-grained granoblastic polygonal quartz texture (1) with interstitial sericite (black), aggregates of less well recrystallised bigger quartz (2) and trains of sericite (3). Euhedral ore (4).

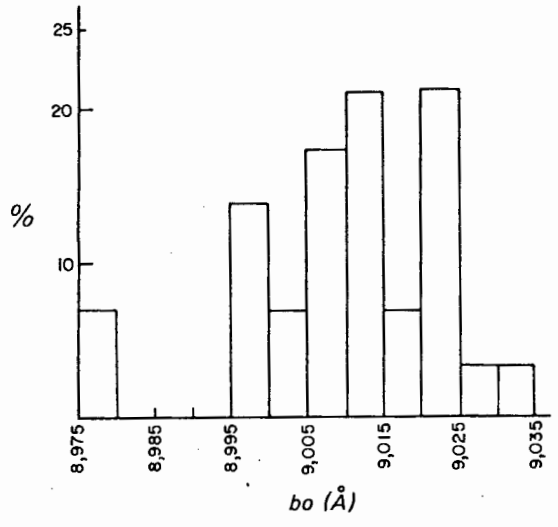

Fig. 6.18 Frequency distribution of b_o-values from the Devilscastle Schist Belt and related rocks. Note the wide spread of data and indications for at least three separate maxima

b_o-values of white micas (Fig. 6.5) in samples taken from the Devilscastle Schist Belt. They display characteristics different from other parts of the Richtersveld basement in that

a) the frequency distribution has three maxima (Fig. 6.18)
b) in many cases individual samples contain more than one maximum
c) the standard deviation is relatively high
d) the arithmetic mean of b_o= 9,0099Å is equivalent to facies series 3 of Sassi and Scolari (1974).

6.5.4. Interpretation of textural and mineralogical data

Mineralogical and textural data of the Devilscastle Event cannot be interpreted without taking into account its tectonic history and without reconciling conflicting observations as there are:

1) different degrees of recrystallisation
   a) on thin-section scale
   b) on outcrop scale
   c) on local scale
2) kyanite, indicating medium pressure type metamorphism
3) the mean of b_o-values, indicating low to intermediate pressure metamorphism (andalusite)
4) three-maxima frequency distribution of b_o-values

The interpretation of these contradictory observations, however, may be facilitated by considering the interrelationship of Devilscastle-type rocks and the intrusive sequence of the Richtersveld Igneous Complex which suggests not only a considerable period of time for the emplacement of the

intrusives but also for deformation and recrystallisation of Devilscastle rocks.

Taking this into account the tectonometamorphic history leading to mineralogy and textures described above could have been as shown in the following table. (See also Fig. 5.28.)

Table 6.17

time	*conditions and mechanisms of deformation*	*expected features*	*observed features*
	east west		
early ~ 900 my	shearing and recrystallisation, low-grade metamorphism: T ~500 P ~5 kb *	full recrystallisation following deformation; low-grade mineral assemblages, barrovian type b_o-characteristics	well-crystallised textures only partly anisotropic; kyanite, chloritoid garnet; b_o-characteristics representing facies series 4 (Fig. 6.5 Table 6.7)
	continuing uplift and deformation	renewed deformation and recrystallisation but finer grain size; low to intermediate pressure b_o characteristics	well recrystallised small grain-sized textures cutting through secondary or primary textures; central b_o peak in Fig. 6.18
~ 750 my (late)	continued deformation under near-surface conditions	renewed deformation and weak recrystallisation, formation of mylonites mainly in the east	mylonites and protomylonites, tectonic breccia; weak or no recrystallisation; possibly lowest b_o-peak in Fig. 6.18.

* Horizontal lines denote area of main tectonic activity

An alternative model of contemporaneous deformation and recrystallisation of all rocks of the Devilscastle Event would necessitate the presence of a rather small thermal dome in the southeastern Richtersveld. Although such a thermal dome could be imagined in connection with the emplacement of the Richtersveld Igneous Complex, particularly weak recrystallisation in the vicinity of these rocks rules out this possibility. As an additional alternative the effects of Gariep deformation and metamorphism should be taken into account. Although schists of the Devilscastle type are definitely cut by the unconformity, later reactivation and formation

Table 6.18 Metamorphism of the eastern Richtersveld, summary

domain	*metamorphism* *grade*	*evidence*	*age* *time (my)*	*evidence*
central Richtersveld	375±25°C 2 ± 0,5 kb	kao stable, biotite zone 2, mica facies series 2-3	older 1800 younger 1900	Orange River Group deformed; G_2 partly deformed; G_3 undeformed; inferred from radiometric data, Haib area (Reid, 1978)
HMC	675±15°C 5,5±1,5 kb	advanced stage melting of granodiorite, formation of sill (curve 1 in Fig. 6.14)	~1750	radiometric dating (Corner 1970, quoted in Köstlin, 1971)
PGU	660±10°C 4,5±1,5 kb	sill pseudomorphs and occasional fibrolite (curve 1 in Fig. 6.14)	peak (~1800) closing stage ~1000	main textural imprint predating G_2 inferred after radiometric ages of pegmatites
Noms River	*early:* (400°) (2 kb)	formation of biotite in metavolcanics, chlorite in metapelites bi and mu stable. low b_o origin of frequency distribution	(older than ~1800)	inferred
	late: (400°) >3 kb	late: same as above but mica facies series 4	~1000	radiometric dating (Welke *et al.*, 1978)
Blockwerf	*early:* (500 - 700°C) p unknown	migmatites, strong textural reconstitution	(older ~1800)	inferred
	late: unknown, probably low grade	occasional downgrading of biotite	~1000	radiometric dating (Welke *et al.*, 1978)
Devilscastle (SE Richtersveld)	*early:* +500°C ± 5 kb	ky, cltd, garnet, mica facies series 4	~1000 ~ 900	deformation of pegmatites, partial deformation of early RIC
	late: near surface	decreasing b_o, lack of recrystallisation	~700	inferred from radiometric data of RIC (Allsopp *et al.*, 1978)
(NE Richtersveld)	near surface	brittle fracture	~700-~900	inferred from SE Richtersveld

( ) : rough estimate

of new mica textures can nevertheless not be ruled out, but judging from the b_o-characteristics of Gariep rocks (Fig. 6.5) only the highest values could have been caused by Gariep metamorphism in the Devilscastle Schist Belt.

6.6. DISCUSSION

Metamorphic conditions in various parts of the Richtersveld have been summarised in Table 6.18. It appears from this summary that three trends of development can be recognised:

1. *Lateral variation of metamorphic grade*

Although exact boundaries of metamorphic zones can rarely be provided it is nevertheless evident that the lowest metamorphic grade occurs in the central northeastern Richtersveld while the highest grades are situated at the southern and northern margins. Particularly between the southeastern and the central Richtersveld the transition appears to be gradational and the same is the case, with the exception of the Blockwerf area, towards east and northeast, which is particularly striking if Blignault's (1977) data are also taken into account. And the gradual increase of grain size with metamorphic grade in supracrustal (mainly volcanic) rocks (Fig. 6.20) supports this view as well, although only in a qualitative manner.

2. *Change of the age of the last metamorphic imprint*

While in the central northeastern Richtersveld metamorphism predates the emplacement of G_3 of the Vioolsdrif Intrusive Suite and is largely contemporaneous with G_2 (~1900 my), radiometric data give ages around 1750 my in the Helskloof Migmatitic Complex and 1000 my for the latest metamorphic imprint in the Noms River area. For the Pink-gneiss Unit no radiometric ages are available, but if pegmatite ages of ~1000 my determined elsewhere are applicable here as well, and if the formation of the pegmatites is related to metamorphism (cf.8.1.4) they might indicate the approximate closing age of high-grade metamorphism.

It thus appears that the age of the last metamorphic imprint decreases when approaching the margins of the Richtersveld.

3. *Change of baric type of metamorphism with time*

While for the central northeastern Richtersveld a geothermal gradient of ~50°C/km can be inferred, a geothermal gradient of 35-40°C/km (but with a large uncertainty) can be calculated for the slightly younger

migmatites of the Helskloof and at least 25-30°C/km for the last metamorphic imprints at the Noms River and during the early Devilscastle Event. Since there is no evidence for a major metamorphic break between these two imprints, a slow decrease of the geothermal gradient between 1700 and 900 my must be assumed.

Table 6.19

	increasing age of last metam. imprint	increasing geothermal gradient	increasing grade of metamorphism	increasing distance from the NMC
BMC				
Noms River	↓	↓	↑	↓
Central Richtersveld	↑	↑	↓	↑
Helskloof				
PGU				

These trends of development, schematically shown in Table 6.19, are important insofar as they can easily be interpreted in terms of a change of metamorphic conditions with time and in terms of a continuous transition of metamorphic grade between the Richtersveld and the adjacent Namaqua Metamorphic Complex.

The metamorphic path deduced from data so far obtained is shown in Figure 6.19.

The earliest stage of metamorphism is represented by the central northeastern Richtersveld and characterised by a particularly high geothermal gradient. While in basinal sediments pressure can be expected to rise faster than temperature due to rapid subsidence and sediment accumulation resulting in a low geothermal gradient at the beginning of the metamorphic path, this possibility must be ruled out in an active volcanic terrain such as the Richtersveld at the time of the deposition of the Orange River Group. Instead it is possible that metamorphism started shortly after deposition and during subsidence of the supracrustal volcanics passing into the metamorphic stage without or with only a short period of diagenesis. This suggestion is important insofar as it tends to reconcile the conflicting observations as to the stability of kaolinite which already breaks down during diagenesis under natural conditions while it is stable up to much higher temperatures

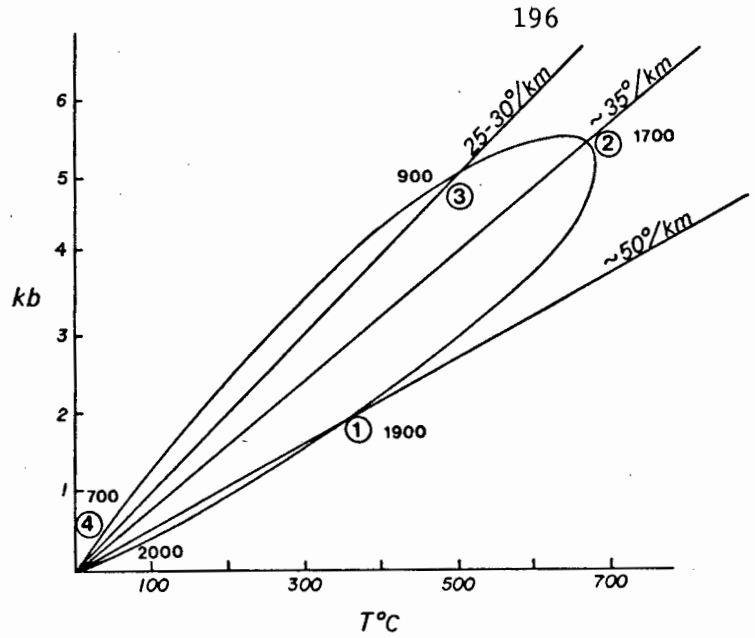

Fig. 6.19 Metamorphic path of the Richtersveld tectonothermal cycle as deduced from metamorphic data.

1) Central northeastern Richtersveld
2) Helskloof migmatisation
3) Early Devilscastle Event
4) Final stage of Devilscastle Event

2000, 1900, etc: approximate time of event (in my)

50°C/km etc: geothermal gradient

in experiments (Table 6.4), i.e. when metamorphic conditions are attained within a relatively short time. A rapid transition into the metamorphic stage, however, would approximate experimental conditions and thus provide an explanation for the presence of kaolinite in a metamorphic environment where it is commonly not observed.

A slightly later stage of metamorphism and a lower crustal level is represented by the Helskloof migmatites and characterised by a lower geothermal gradient. Since there are no indications for a major break in metamorphic conditions between 1) and 2) (Fig. 6.19) the Helskloof migmatites are unlikely to represent a Sederholm effect, which is defined by migmatisation of an intrusive rock after a period of uplift to near-surface conditions (Eskola, 1960).

No metamorphic assemblages are recorded that could with certainty be attributed to the time between Helskloof migmatisation and the Devilscastle Event and since also here indications for a break in metamorphic conditions are absent, a gradual and slow decrease of temperature between these two metamorphic imprints must be assumed, finally resulting in a geothermal gradient of 25-30°C/km during the early Devilscastle Event, subsequent to which uplift occurred in the southeastern Richtersveld and surface conditions were attained

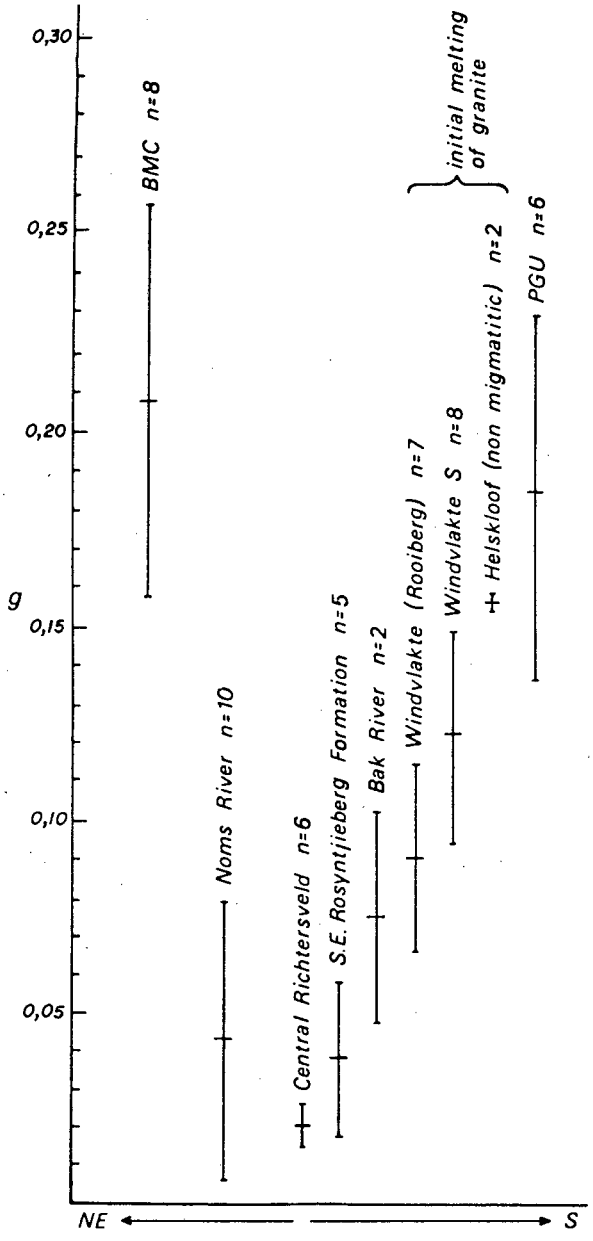

Fig. 6.20

Variation of grain size with metamorphic grade. The grain size is represented by the ratio

$$g = \frac{l\ (\text{mm})}{T}$$

T = number of transitions into minerals of the same or other species along the reference line l. Sericite- and epidote aggregates are treated as one mineral.

l = length of reference line in mm. The length chosen depends on homogeneity and (order of) the grain size of the sample. 50 to 200 transitions were regarded as sufficiently representative. Only samples of supracrustal origin were considered.

n = number of samples investigated per population.

Fig. 6.20 shows variation of parameter g with standard deviation s. Its mean displays a distinct and regular increase from the central Richtersveld to the S and the NE.

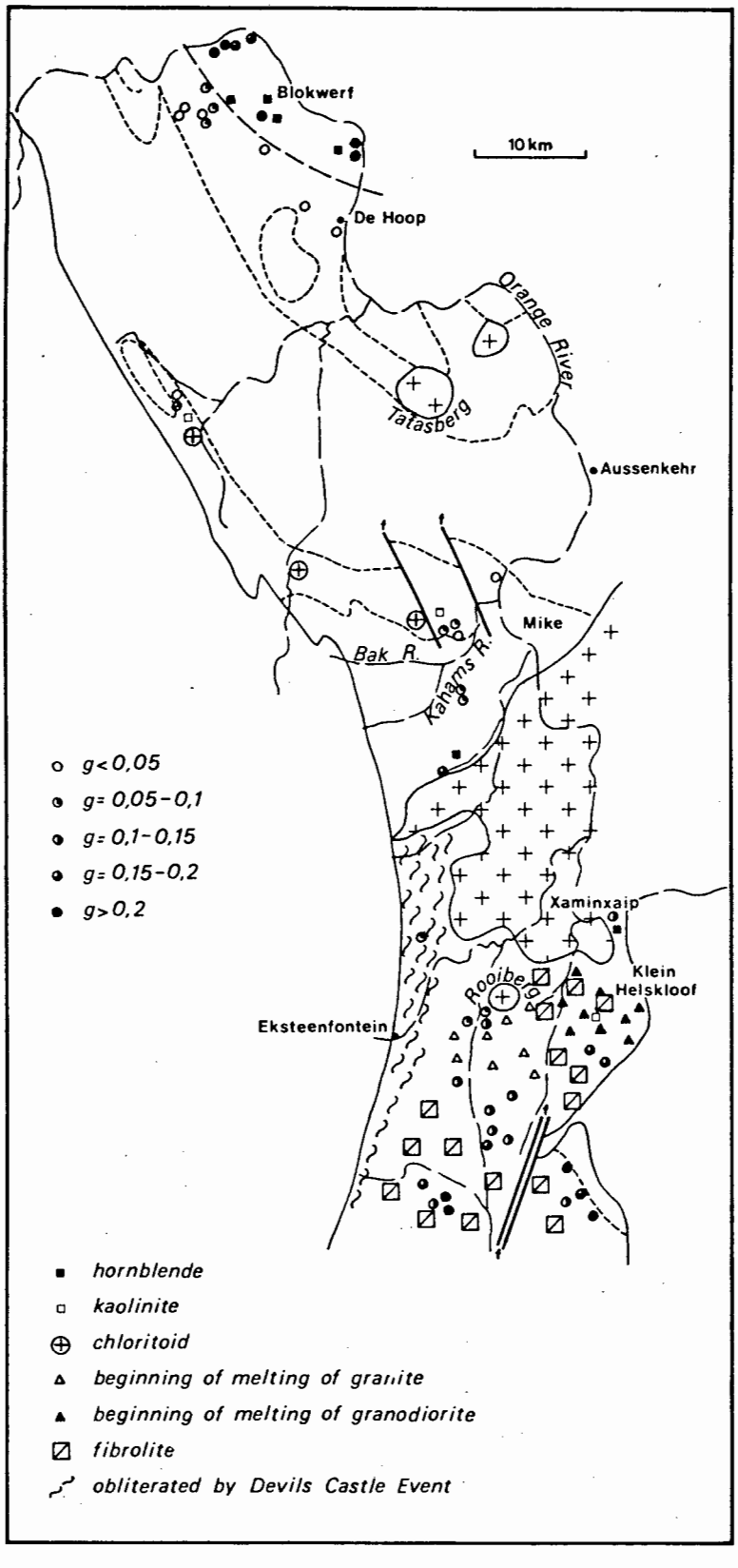

Fig. 6.21

Occurrence of index minerals and development of grain size in the eastern Richtersveld.

See Fig. 6.20 for explanation of g for grain size.

around 700 my ago.

The Richtersveld metamorphic cycle can thus be subdivided into a relatively short prograde part between 2000 and 1800 my ago followed by a retrograde part which consisted of a long period of slowly decreasing temperature and more or less stable pressure after which relatively rapid uplift took place. Uplift and cooling rates inferred from this development are listed in Table 6.20. Their comparison with data from the literature shows that they are at least one magnitude lower than those from Phanerozoic orogenies but agree rather well with data from Precambrian and anorogenic terrains.

Table 6.20 Comparison of uplift and cooling rates as inferred for the Richtersveld with data from the literature.

	time (in my)	*uplift (per 1000 years)*	*cooling in °C (per million years)*
Richtersveld:			
northeast-central	1700-1000	no uplift	
	700-900	no or weak uplift	
southeast	1700-1000	no uplift	0,25°
	700-900	9 cm	2,5°
Alps (Clark and Jäger, 1969)	30 my to present	40-100 cm	10°
Himalayas (Robinson, 1966)	present	100 cm	
Rocky Mountains (Robinson, 1966)	Upper Cretaceous	12-20 cm	
Damara (Haack, 1976)	550-480	7-8 cm	3-6°
Lewisian (partly calculated after Dickinson and Watson, 1976)	3000-2000	no or weak uplift	0,07-0,17°
	2000-1700	2-3 cm	1,3°
Margins of the Rhinegraben (Blackforest-Vosges) after Illies, 1970	since Middle Eocene (~45)	4,8 cm	
Colorado Basin (Robinson, 1966)	present	16,3 cm	

Chapter 7

STRATIGRAPHY, METAMORPHISM AND STRUCTURE OF ROCKS OVERLYING THE RICHTERSVELD BASEMENT

7.1 GENERAL

Investigations of rocks overlying the basement are not among the objectives of this study and have only been undertaken in order to assess the extent and degree to which later depositional and tectonothermal events may have influenced the basement.

7.2 STINKFONTEIN FORMATION

7.2.1. Stratigraphy

The stratigraphic relationships are only of interest with regard to the exact position of the unconformity since Kröner (1974) appears to regard the Stinkfontein conglomerates as the lowermost unit of the Stinkfontein Formation. Although this might frequently be the case the present investigations have shown that Stinkfontein conglomerate is at many places underlain by a succession of pink, arkosic rocks, which if sheared, are not easily distinguishable from the underlying rocks of the Devilscastle Schist Belt. Non-basement rocks underlying the Stinkfontein quartzites are particularly obvious in the village of Eksteenfontein where a 100 - 200 m thick succession of marble and biotite schists unconformably overlies melanocratic granodiorite (G_2) of the basement and thus belongs to the Gariep Group as opposed to the views of De Villiers and Söhnge (1959) and Kröner (1974).

The formation of a relatively thick succession of carbonates and pelitic rocks at this position and of possibly arkosic rocks elsewhere is particularly important with respect to the pre-Stinkfontein erosional (= uplift) history of the basement. Since granitoids also at present tend to weather more readily and form depressions, this area is likely to have

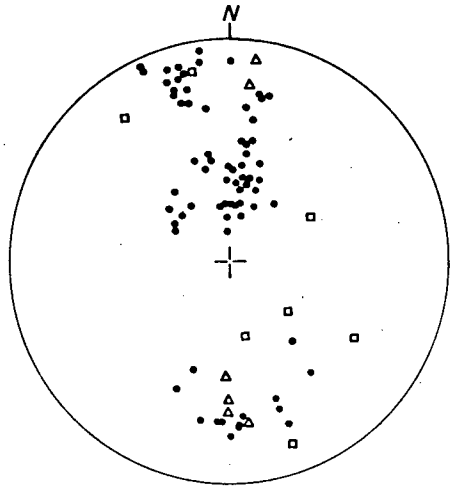

Fig. 7.1a

Linear elements at and near the unconformity, northeastern Richtersveld.

dots : lineation
triangles : slickenside,
squares: π

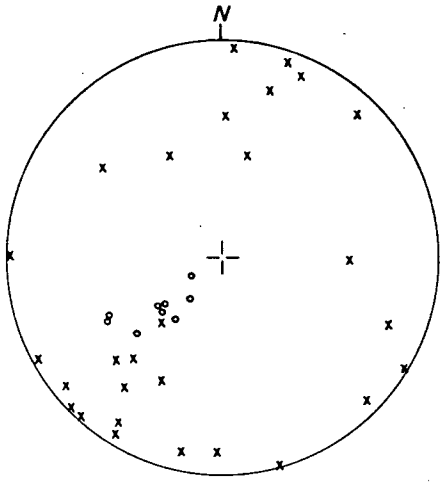

Fig. 7.1b

Planes of fracturing and kinking

crosses : basement

circles : Gariep Group at Helskloof

These planes display predominantly right-lateral displacement and agree therefore with photolineaments of similar direction and sense of displacement

been eroded to a relatively mature degree in pre-Stinkfontein times, when depressions were filled with evaporites and lakes of stagnant water prior to the deposition of the Stinkfontein quartzites.

7.2.2. Metamorphism

Samples of mainly pelitic rocks collected between Port Nolloth and Eksteenfontein have been investigated in a reconnaissance fashion. They contain quartz, muscovite, chlorite and biotite as major constituents and feldspar as an accessory. X-ray diffraction tests for stilpnomelane were negative. The Stinkfontein Formation in the Richtersveld has therefore attained the biotite zone of low grade metamorphism and not the chlorite zone as suggested by Kröner (1974).

The b_o-values obtained* must be regarded with caution since they have been measured on specimens from a large area with sampling localities as much as 100 km apart, and little accompanying petrographic work has been carried out. In addition, some specimens were so friable that only powder samples could be used which showed a rather high variation of b_o-values between different runs so that only means from several runs could be used for statistical evaluation.

Nevertheless, the values obtained reflect a celadonite content of the white micas considerably higher than in the basement. This, pending further investigation, must be regarded as being at least partly due to higher pressure during metamorphism and is in agreement with the occurrence of glaucophanitic amphiboles reported by Kröner (1974) from the Alexander Bay area and by Kaiser (1926) from parts of the Gariep trough farther in the north.

7.2.3. Structure

Linear structural elements collected in the northeastern Richtersveld in the vicinity of the unconformity are distributed along a north-south trending great circle (Fig. 7.1a) (in contrast to the northwest-southeast trending great circle of F_1-elements) which suggests overprinting of north-south striking axial elements of Pan-African deformation (Kröner, 1974, p.66) on northwest striking planar elements of the basement. In the basement, planes of deformation (kinkfolding of S_1) strike west to northwest, dip steeply (Fig. 7.1b) and display right-lateral displacement more frequently than left-lateral. They are therefore likely to represent the local equivalents of east-west trending photolineaments observed in Annexure 4, along which right-lateral displacement of the dykes of the Gannakouriep Suite occurs.

In the southeastern Richtersveld the basement appears to be even less affected and apart from shearing along the unconformity no fabric elements unambiguously due to Gariep deformation can be recognised. West-northwest striking faults which are at places associated with quartz impregnation and

* Fig. 6.5

mylonitisation display dextral displacement of the Gannakouriep dykes and the unconformity between Stinkfontein Formation and the basement but do not affect rocks of the Nama Group. Their possible vertical component becomes evident in the Helskloof area where the degree of migmatisation in some cases increases abruptly when crossing these faults in an easterly direction.

7.3 THE NAMA GROUP

7.3.1. Stratigraphy

Only basal parts of the Nama Group are exposed in the Richtersveld proper which have been studied by Middlemost (1963, his Kuibis Series) and consist mainly of sandstone, feldspathic sandstone and green, grey and red shale. During the present investigation light-grey limestone, partly containing angular limestone clasts of possible biogenic origin, has been found in its lowermost parts in the area east of Klipbok.

7.3.2. Metamorphism

In order to assess whether and to what extent the rocks of the Nama Group had undergone metamorphism measurements of the *illite crystallinity* had to be carried out. They were made by determining Hb_{rel} after Weber (1972a). Details and theoretical background are given in Appendix 2.

Ten samples of pelitic Nama sediments were collected at Vioolsdrif and Helskloof and an average Hb_{rel} = 154,5 (s=29,9) was determined on rock slabs cut parallel to the foliation. Two of the samples at M8 had the unrealistically low Hb_{rel} of 100 which is that of a fully developed muscovite. An average of 154, however, is well in agreement with determinations of illite crystallinity in Nama rocks to the north of the Richtersveld (Ahrendt *et al.*, 1978) according to which Hb_{rel} <200 can be expected in the Nama Group south and west of the Lower Fish River.

According to Weber (1972b), Hb_{rel} =150 corresponds to a *Kubler Index* (*KI*) of 5. As to the correlation of illite crystallinity and the current metamorphic classification, the data available are inconsistent. Kubler (1966) and Dunoyer de Segonzac *et al.*, (1968) drew the boundary between *diagenesis* and "*anchimetamorphism*" at *KI*=4 and that between "*anchimetamorphism*" and *low grade metamorphism* at *KI*= 2,5 while Teichmüller and Weber

(quoted in Ahrendt *et al*, 1978) assumed Hb_{rel}=350 to 500 for the *diagenetic-"anchimetamorphic"* boundary. Frey (1970) in a study of Jurassic rocks of the Alpine foreland correlated *KI*=4 to 7,5 with the *laumontite-prehnite-quartz*-facies and the *pumpellyite-prehnite-quartz*-facies and *KI*<4 with the *greenschist facies sensu* Winkler (1967). Weber (1972b), arrived at similar conclusions and drew the boundary between *low grade* and *very low grade* metamorphism at Hb_{rel}=100 (=*KI*~3) by comparing the mineral paragenesis of spilitic rocks with the illite crystallinity in adjacent pelitic rocks in the northeastern Rheinisches Schiefergebirge (West Germany). All that can be said is therefore that the metamorphism of the Nama rocks investigated has probably reached a stage at the transition between diagenesis and low grade metamorphism.

The increase of illite crystallinity towards the belt of Pan-African tectonic activity and K-Ar ages of syntectonic (Nama) muscovites of 530±10 my at and in the vicinity of the Naukluft Nappe (Ahrendt *et al.*, 1978) suggest that deformation as well as illite crystallinity of the Nama rocks of the Richtersveld are results of Pan-African tectonothermal influences.

7.3.3. Structure

The Richtersveld basement is bounded in the southeast by a zone of relatively strong deformation extending from near Doring River in the south along the Groenrivier to Geelfontein and from there in a northerly direction through Helskloof. Previously regarded as a shear zone (De Villiers and Söhnge, 1959) it was found during the present investigation to be characterised mainly by steeply dipping Nama upon which basement has repeatedly been thrust along steeply northwest-dipping thrust planes (cf. Ritter, 1978 Fig. 27). The compressional nature of post-Nama deformation is also evident from occasional folding around North-northeast trending axes with rather well developed axial-plane cleavage. A right-lateral sense of displacement is indicated by drag folds south of Helskloof although the position of the Pink-gneiss Unit west of Klipbok indicates left lateral movement. It is, however, likely that this structure owes its present form mainly to deformation during the Devilscastle Event and has only been *reactivated* after the deposition of the Nama Group.

7.4 OTHER OCCURRENCES

Rocks resembling diamictites occur at three localities at the eastern margin of the Richtersveld at Farm Aussenkehr; two of them are already known from the literature. Kröner and Germs (1971) investigated a sedimentary succession overlying the Richtersveld basement at Nabas north of Aussenkehr and found its basal part to be made up of Numees diamictite and overlain by Nama Group rocks ((1) in Fig. 7.2). Another occurrence of mixtitic sediments is mentioned by Martin (1965 p.103) and occurs

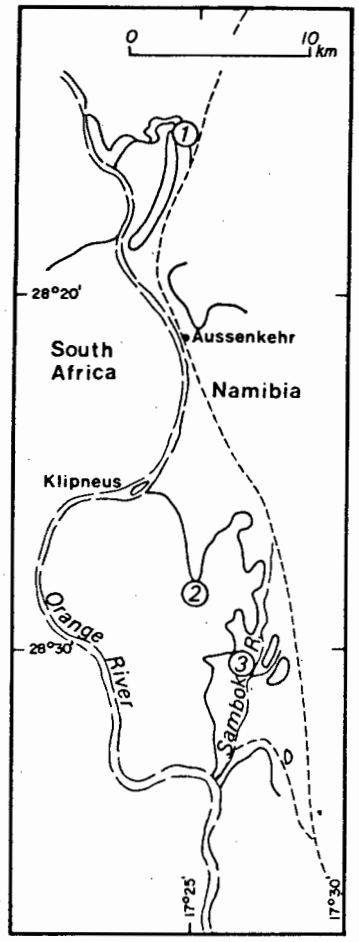

Fig. 7.2

Key map of mixtitic rocks at the eastern margin of the Richtersveld at Farm Aussenkehr.

1) Kröner and Germs (1971) (Numees mixtite)

2) mixtite, this report

3) mixtite, this report and Martin (1965)

approximately 20 km south of Aussenkehr (3). It is also overlain by Nama and Karoo and thought to be Numees tillite. A third occurrence has been found during the present investigation 10 km south of Aussenkehr (2) unconformably overlying volcanics of the Klipneus Formation and quartzites of the Rosyntjieberg Formation in a north-south-striking graben and resembling in outcrop the descriptions of the Nabas mixtite. A thin section of the fine-grained variety shows slightly rounded clasts of mineral fragments partly with mineral species not known from the Richtersveld (e.g. cordierite) and a largely un-recrystallised matrix. Macroscopic clasts contain quartzite, fragments of dykes of the Gannakouriep Suite, De Hoop metavolcanics and Vioolsdrif granodiorite.

The occurrence at (3) is much better recrystallised when viewed in thin section. Its fragments are more angular than at locality (2) and

appear to be mainly derived from the Richtersveld. In the light of the different degree of recrystallisation of the samples investigated it is unlikely that they are both of the same origin. While it is possible that the sample at (3) may be attributed to the Numees mixtite, the sample at (2) must be younger and may either be related to the Nama Group as suggested by Martin (1965) for the Nabas stage diamictite, or be an independent local facies variation at the base of the Nama at the margin of the Richtersveld.

7.5 DISCUSSION

Rocks of the Gariep Group have undergone at least low grade metamorphism and considerable deformation. On the other hand, texture and mineralogy of rocks of the basement can firmly be linked with tectonothermal events prior to the deposition of the Stinkfontein Formation. The question therefore arises why Pan-African metamorphism and deformation did not affect the basement more strongly. The following reasons may be suggested:

a) the grade of metamorphism is the same in basement and Gariep, although metamorphic facies series is different
b) lack of index minerals
c) lack of sufficient tectonic activity necessary to promote recrystallisation of older metamorphic textures

Particularly with respect to the b_o-values, previous investigators (e.g. Piccarreta and Zirpoli, 1974; Kräutner *et al.*, 1975) suggested that considerable tectonothermal influence is necessary to completely obliterate b_o-characteristics of previous metamorphic imprints. If therefore metamorphic recrystallisation is not aided by penetrative deformation, no recrystallisation of the pre-existing texture will take place despite the fact that appropriate metamorphic temperatures have been reached.

Nevertheless, the question remains why rocks in the immediate vicinity of Gariep tectonothermal activity could have remained unaffected. In the author's opinion the answer can at least partly be found in the fact that the basement-Gariep relationship as exposed today is that of a lateral juxtaposition rather than a vertical relationship, i.e. the presently exposed basement of the Richtersveld formed the *margin* of the Gariep trough and was not or only marginally affected by the tectonothermal processes taking place in it. *

---

* This relationship is partly implied by Kröner (1974 Fig. 41) but not explicitly stated.

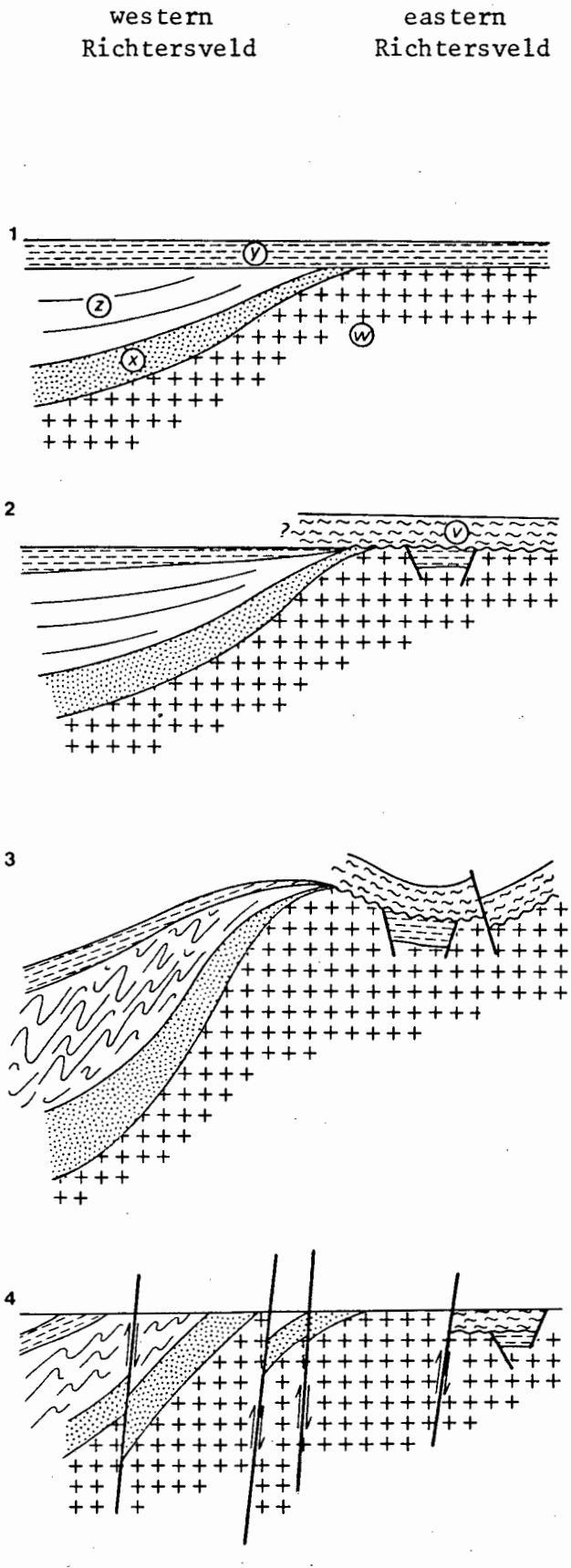

Fig. 7.3

Schematic presentation of the development of the basement-Gariep relationship

1) *Gariep sedimentary stage*
Subsidence of the Gariep trough in the W (a) but relative stability in the E (b). Only Numees mixtite as the uppermost formation of the Gariep Group transgresses on the basement towards the end of subsidence (b).

Evidence :

a) stratigraphic succession mainly after Kröner (1974)
b) Only Numees mixtite is found unconformably overlying the basement in the E of the unconformity; either primarily deposited in a graben structure or preserved there later

2) *Deposition of Nama*
After period of weak uplift deposition of Nama on the basement in the E.

Evidence :

Nama overlies Numees unconformably (Kröner & Germs, 1971) or is deposited on a well-peneplained erosion surface of the basement.

3) *Gariep deformation and metamorphism* by deep subsidence of Gariep rocks (a), weak deformation in marginal areas (b).

Evidence :

a) high pressure-low temperature metamorphism in Gariep rocks : b_o-characteristics of white micas (Fig. 6.5), occurrence of glaucophane (Kröner, 1974; Kaiser, 1926)
b) Nama affected by Pan-African deformation and metamorphism : Illite crystallinity, 530 my radiometric ages for Nama

In this regard attention should also be drawn to the fact that Nama Group rocks overlie a remarkably well-peneplaned basement (De Villiers and Söhnge, 1959) only 10 km to the east of the easternmost outcrops of Stinkfontein sediments, suggesting a long history of exposure under more or less static conditions. This implies either that Gariep rocks had never been deposited there or that they had been deposited but eroded already prior to Gariep tectonism, in both cases involving either considerable uplift or at least non-subsidence as opposed to strong subsidence farther in the west in the Gariep trough. However, since Numees mixtite, in turn unconformably overlain by the Nama Group, has been found overlying the Richtersveld basement, considerable uplift after its deposition is also unlikely and since illite crystallinity of Nama Group rocks indicates at most very low grade ("anchi") metamorphism, their subsidence must also have been rather limited. It is therefore likely that the area east of the unconformity was essentially stable during deposition and deformation of Gariep Group rocks. A possible model is proposed in Fig. 7.3.

Fig. 7.3 (continued from page opposite)

metamorphism (Ahrendt *et al.*,1978; this investigation)

4) *Rapid uplift of Gariep rocks in the west* subsequent to deformation.
This assumption explains best the present-day juxtaposition of deformed and metamorphosed Gariep rocks and unaffected basement and is supported by evidence of post-Nama faulting and upthrust of basement over Nama in the south-eastern Richtersveld.

Legend:

w) basement x) Stinkfontein Formation y) Numees mixtite z) other Gariep rocks v) Nama Group

Chapter 8

THE RICHTERSVELD PROVINCE IN ITS REGIONAL CONTEXT

8.1 THE RICHTERSVELD PROVINCE AND THE NAMAQUA METAMORPHIC COMPLEX

In this chapter stratigraphy, structure and metamorphism of the Richtersveld Province and the Namaqua Metamorphic Complex will be compared and discussed in the light of modern geotectonic concepts.

8.1.1. Stratigraphy

1. *Stratigraphic relationships within the Richtersveld Province*

Owing to the detailed mapping of the rocks of the Orange River Group it is now possible to establish a new scheme of stratigraphic correlations within the Richtersveld (Table 8.1). An attempt has also been made to correlate the volcanics of the Haib Subgroup with those of the De Hoop Subgroup based mainly on a tendency of the volcanics in both areas to become more mafic in the higher parts of the succession. However, in a subaerial volcanic terrain such as the Richtersveld Province a variety of eruptive centres can be expected which overlap in time and space and similarities of the stratigraphic succession in both areas are therefore not necessarily an indication for contemporaneous deposition.

2. *Stratigraphic relationships between Richtersveld Province and the Namaqua Metamorphic Complex*

Apparently contradictory observations have been made by different authors as to the stratigraphic relationships between Richtersveld and the Namaqua Metamorphic Complex. They are compiled in Table 8.2 and shown in Fig. 8.2 as an interpretative cross-section through the Richtersveld, demonstrating that these different observations can be brought onto a common denominator. Particularly Blignault's (1977) conclusion that some of the rocks in the Ais-ais area may overlie equivalents of Richtersveld volcanics

Table 8.1 Stratigraphic relationships within the Richtersveld Province and correlation with previous classifications

author	*northeastern Richtersveld*		*southeastern Richtersveld*	*Haib area*
De Villiers and Söhnge (1959)	Marydale Series	Kaaien Series	Wilgenhoutdrif Series	? Wilgenhoutdrif Series
Blignault (1974a) Kröner & Blignault (1977)	De Hoop Subgroup	Rosyntjie-berg Formation	Haib Subgroup	Haib Subgroup
this investigation and Blignault (1977) for Haib area	Kuamsrivier Formation Kookrivier Formation Abiekwa-rivier F.	Rosyntjie-berg F. Klipneus F. Paradysri-vier F.	Windvlakte Formation Pink-gneiss Unit (= NMC)	Nous Formation Tsams Formation

Table 8.2 Contrasting views on the stratigraphic relationship between the Richtersveld and the Namaqua Metamorphic Complex

Investigator	*Interpretation*	*Area*
Bertrand (1976)	Orange River volcanics grade laterally into volcano-sedimentary Bushmanland Sequence	Goodhouse
Moore (1977)	Bushmanland Sequence shallow basinal deposit overlying Archaean basement	Namiesberg
Blignault (1977)	Paragneiss unit overlying equivalent of Orange River volcanics (grey gneiss unit). Paragneiss unit = mudstone/wacke sequence	Aï-ais
This investigation	Orange River Group volcanics conformably overlying NMC (PGU =? Bushmanland Sequence)	SE Richtersveld

fits very well into the interpretation of the Richtersveld Province as a volcano-plutonic complex to be discussed later.

3. *Stratotectonic environment during the time of deposition*

In order to assess the stratotectonic environment (*sensu* Rutland, 1973) in which the rocks of the Lower Orange River area * have been formed, their lithology and stratigraphy as well as their chemistry are compared with known Cenozoic environments.

a) Lithology and stratigraphy

In Table 8.3 the rock assemblages of the Lower Orange River area have been compared with those found in Cenozoic active continental margins and geosynclines. Although some of the evidence is rather interpretative,

---

* The term Lower Orange River area is used here and in the following as sack term comprising the rock assemblages of the Richtersveld Province as well as the immediately underlying areas of the Namaqua Metamorphic Complex.

Table 8.3

Rock assemb	*tersveld and Lower Orange River area*
shallow mar	rpretative : parts of Bushmanland ence
coastal pla	sional in Bushmanland Sequence (Moore,
carbonates	1977)
Interbedded	-----
tholeiitic ultrabasics	-----
tholeiitic turbidites	-----
composition mature turb	
calc-alkali volcanics a	dant : Orange River volcanics, lsdrif Intrusive Suite
minor intru	ible in paragneiss unit, grey-gneiss
calc-alkali canic turbi	(Blignault, 1977)
continent-c coarse clas	rpretative:Paradysrivier F.,Klipneus F. lsdrif Intrusive Suite
intermedia acidic plut	inental : inferred from field ence and chemistry of volcanics
nature of ing crust	

a certain similarity of the Orange River area with Andean-type continental margins and Island-arc-type volcanic chains emerges while eugeosynclinal and trench environments can be ruled out. In Table 8.4, therefore, the rock assemblages of Andean-type mountain ranges have been compared in detail with those of the Richtersveld. It indicates clearly that their lithology and other geological features are well compatible.

Table 8.4 Sediments deposited on the continent in and near Andean-type mountain ranges (after Mitchell and Reading, 1969) and their comparison with Proterozoic rocks occurring in the Lower Orange River area

Andean-type mountain range	*Lower Orange River area*
Coarse, conglomeratic deposits (molasse type), deposited in fault-graben	Klipneus F., Paradysrivier F., Conglomerates and fanglomerates, cherts, quartzites, reworked volcanics, basin of Rosyntjieberg F., basin of Klipneus F.
parallel to the margin of the mountain range.	NW-SE trending coastline of Rosyntjieberg basin
Sediments are immature, consisting of calc-alkaline volcanic detritus or recycled igneous material with interbedded pyroclastics and lava flows	various degrees of reworking in Rosyntjieberg and Klipneus Formations; nature of volcanic intercalations in Rosyntjieberg Formation is closely related to adjacent volcanic activity particularly evident in Klipneus and Paradysrivier Formations.

b) Chemistry

In comparing chemical characteristics of volcanic arcs with their tectonic environments, Miyashiro (1974) found that

a) the proportion of calc-alkaline rocks tends to increase with advancing development of continental-type crust beneath the volcanic arc
b) the average SiO_2 and K_2O contents tend to increase with advancing development of continental-type crust
c) the proportion of alkaline and calc-alkaline volcanics tends to increase with decreasing rate of plate convergence and with increasing thickness of the underlying crust.

In the Richtersveld Province calc-alkaline volcanics predominate over tholeiitic and alkaline volcanics (Haib Subgroup : 10 percent tholeiitic,

Fig. 8.1 Comparison of Haib and Richtersveld volcanics with Cenozoic volcanic provinces. Average trend of Haib volcanics after Reid, 1977. Cenozoic volcanic provinces after Miyashiro, (1974).

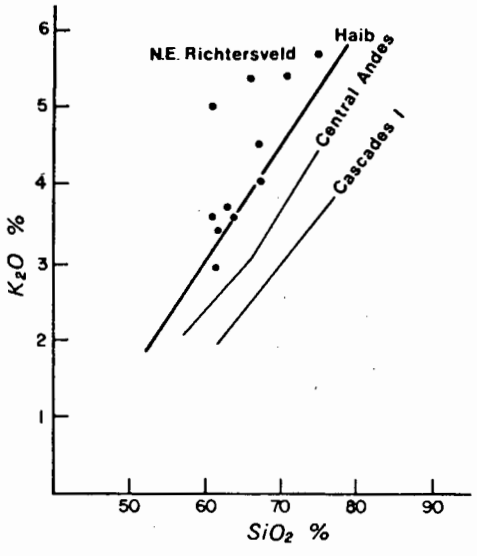

(a)
Variation of K_2O with SiO_2

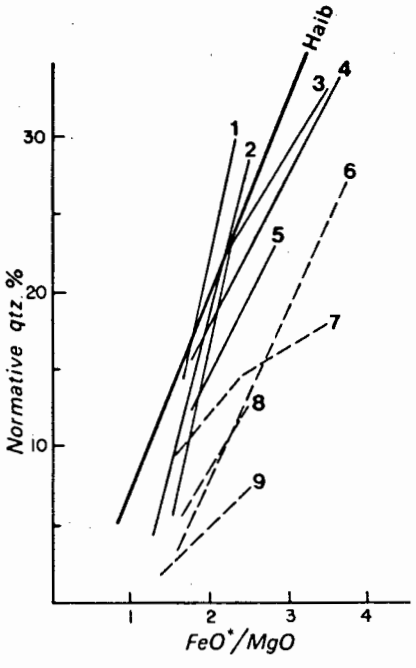

(b)
Variation of normative quartz with FeO^*/MgO ratio.
1) Cascades inner arc; 2) Cascades outer arc; 3) Central Andes; 4) NE Japan outer arc; 5) NE Japan inner arc.
Tholeiitic : 6) NE Japan outer arc;
7) Tongas; 8) NE Japan inner arc;
9) Kermadecs

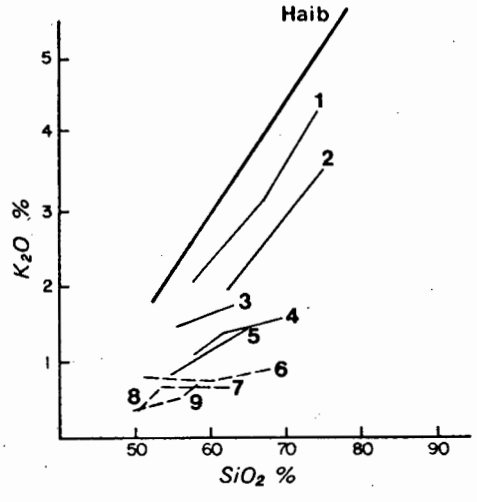

(c)
Variation of K_2O with SiO_2.
1) Central Andes
2) Cascades inner arc;
3) NE Japan inner arc;
4) Japan outer arc;
5) Cascades Outer arc;
Tholeiitic :
6) Central Kuriles outer arc;
7) NE Japan outer arc;
Kermadecs;8) NE Japan outer arc;
9) Tongas

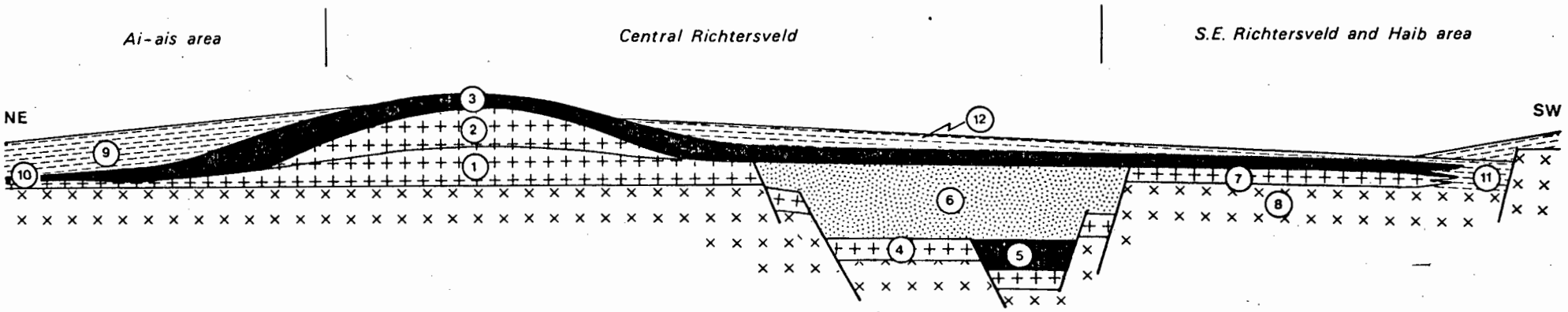

Fig. 8.2

Interpretative and schematic cross-section through the Richtersveld area prior to deformation and intrusion of the Vioolsdrif Suite, reconciling various views on the relationship between Namaqua Metamorphic Complex and Richtersveld Province.

Different possibilities for the relationship between Richtersveld Province and Namaqua Metamorphic Complex:

7/8) : Richtersveld overlying Namaqua Metamorphic Complex
9) : Namaqua Metamorphic Complex overlying Richtersveld
11) : lateral relationship either by lateral facies variation or faulting

Approximate position of formations and map units:
1) Abiekwarivier F.; 2) Kookrivier F.; 3) Kuamsrivier F; 4) Paradysrivier F.; 5) Klipneus F.; 6) Rosyntjieberg F.; 7) Windvlakte F.; 8) Pink-gneiss Unit (NMC); 9) Paragneiss Unit; 10) supracrustal component of Grey gneiss unit; 11) Bushmanland Sequence; 12) hypothetical greywacke sequence merging with Bushmanland Sequence

60 percent calc-alkaline, 20 percent alkaline; De Hoop Subgroup : 10 percent tholeiitic, 70 percent calc-alkaline, 20 percent alkaline*) It can therefore be grouped into group IIb of Miyashiro (1974 Table 5) which is characterised by well-developed continental crust and slow rate of plate convergence (e.g. Central Andes, Cascades Inner arc). The same conclusion is arrived at if FeO*/MgO and K_2O/SiO_2 ratios are compared (Fig. 8.1). Chemical evidence therefore suggests that the Orange River Group volcanics have been deposited on a continental crust of considerable thickness and maturity. This is in agreement with field evidence (e.g. Moore, 1977; Bertrand, 1976) and indicates that the basement on which the Richtersveld volcanics and the Bushmanland Sequence have been deposited consisted of consolidated crust, possibly of Archaean or early Proterozoic age. This conclusion is, however, contradicted by Köppel (1978) who arrived at isotopic ages for the Bushmanland Sequence between 1200 and 1500 my. It is therefore most important to note that these findings and the combined radiometric and geological evidence from the Lower Orange River area are mutually exclusive, i.e. : if the 1950 my old volcanics of the Orange River Group overlie and are intercalated in the Bushmanland Sequence, (the latter overlying a possible basement) they cannot be younger than 1950 my and Koeppel's results are not correct; alternatively, Reid's (1977) radiometric data of the Richtersveld Province are incorrect, implying that the Richtersveld Province is in fact younger than 1100 my. Since the latter is contradicted by field and reliable radiometric evidence, such a young age must be regarded as rather unlikely despite certain points in its favour resulting from some other isotopic data.

4. *Summary*

The supracrustal rocks of the Richtersveld have been subdivided into formations which display a complicated lateral relationship. In the SE Richtersveld they conformably overlie rocks of the Namaqua Metamorphic Complex while farther to the east, south of the Haib area, a lateral relationship between Richtersveld and Namaqualand Metamorphic Complex has been observed. North of the Richtersveld Province again rocks of the Richtersveld appear to be overlain by rocks of the Namaqua Metamorphic Complex. The relationships ensuing from this are tentatively shown in Fig. 8.2.

Lithology as well as geochemical criteria suggest, by analogy with Cenozoic stratotectonic environments, an origin for the Richtersveld Province as an Andean-type continental margin.

8.1.2. Structural relationships

Most investigators working in the high grade metamorphic terrain of the Namaqua Metamorphic Complex report several co-planar early events

---

* estimated from the number of available chemical analyses

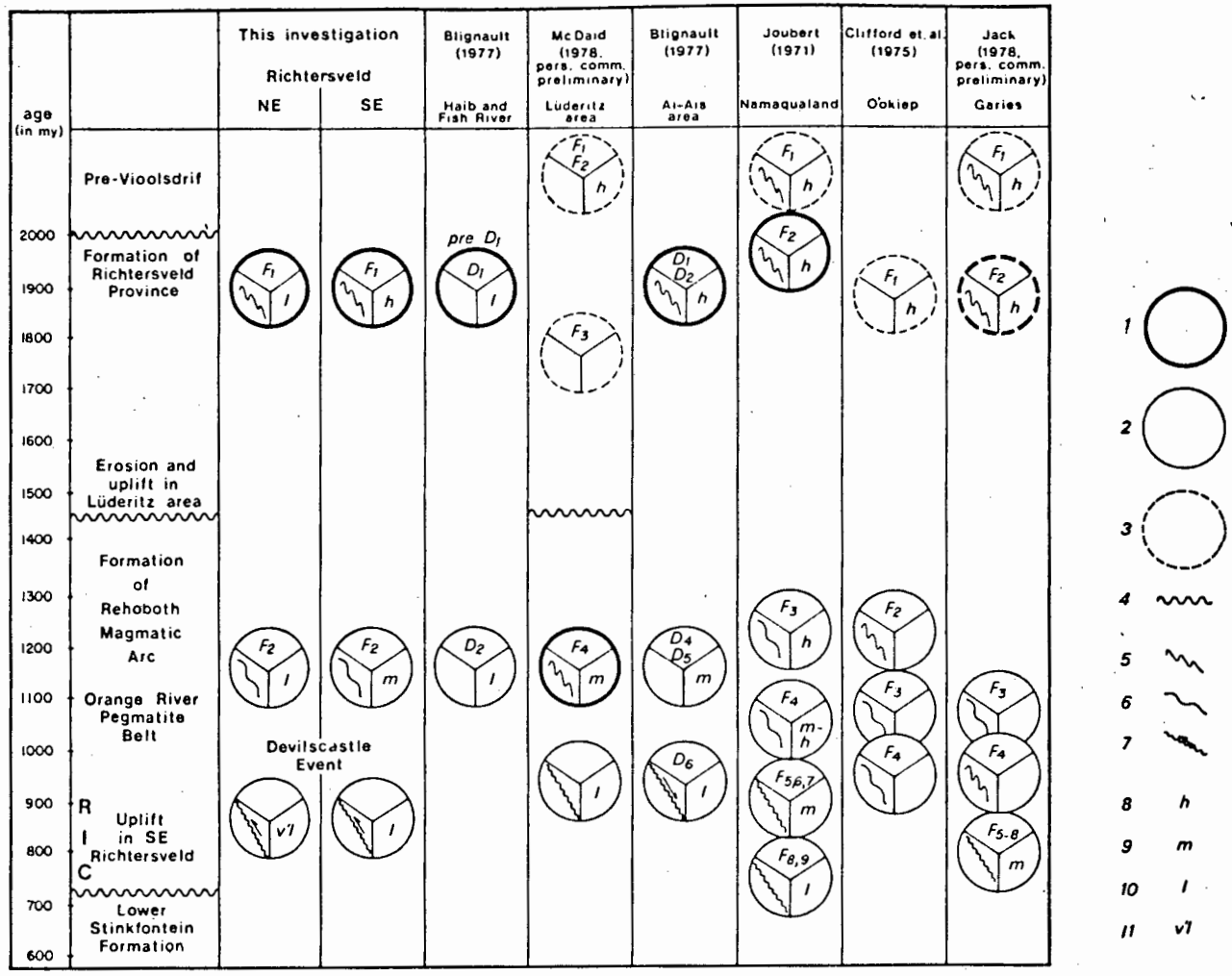

Table 8.5 Comparison of *deformational events* (*sensu* Joubert, 1971) *in Richtersveld Province and Namaqua Metamorphic Complex* as suggested by various authors. Three maxima of tectonic activities can be recognised. While the two earlier folding events are roughly contemporaneous with the formation of the Richtersveld Province and the Rehoboth Magmatic Arc respectively, shearing appears to postdate the formation of the Orange River Pegmatite Belt and to be roughly contemporaneous with the intrusion of the Richtersveld Igneous Complex.

Legend: 1) deformational event causing main structural imprint 2) approximate age as suggested by respective author 3) age unknown within limits indicated 4) unconformity

Character of deformation and accompanying metamorphism : 5) tight, isoclinal, recumbent, intrafolial folding 6) open folding 7) shearing, with sense of lateral displacement 8) high grade metamorphism 9) medium grade metamorphism 10) low grade metamorphism 11) very low grade metamorphism or near surface conditions.

with axial plane directions roughly east-west and a more or less cross-cutting later event resulting in open folds and shearing (e.g. Blignault *et al.*, 1974). This is particularly evident from Table 8.5 where results of those investigators able to provide some evidence for the ages of their deformational events have been compiled. It shows that three periods of intensified deformation can be distinguished between 2000 and 700 my in the Namaqua Metamorphic Complex as well as in the Richtersveld:

a) Early phases of folding, commonly clustering around 1800 and 2000 my in most cases bear the main structural imprint and tend to be defined by tight to isoclinal folds

b) A late phase of folding clustering mainly between 1200 and 1000 my and commonly forming large open but also recumbent and isoclinal folds

c) A final phase of deformation commonly postdating the intrusion of the pegmatites and defined mainly by N-S or NW trending shear zones

Additional features worth noting are:

a) The early folding coincides with the formation of the Richtersveld Province and the later folding with the formation of the Rehoboth Magmatic Arc (Watters, 1974) as well as with the first structural imprint in the Konipberg Sequence which unconformably overlies the Namaqua Metamorphic Complex in the Lüderitz area (McDaid, 1978, pers. comm.).

b) The final shearing event coincides with the intrusion of the alkaline Richtersveld Igneous Complex and the early Bremen Complex and with crustal uplift in the southeastern Richtersveld. Shearing appears to take place under increasingly higher metamorphic conditions from north to south.

Watters (1974) investigating volcanics of the Sinclair Group (southern Namibia), concluded tentatively that they might be part of a volcano-plutonic arc at the margin of the Kalahari Plate between 1400 and 950 my as the result of the subduction of an oceanic plate towards the southeast. This conclusion is supported by the recent discovery of the Konipberg Sequence in the Lüderitz area (McDaid, 1978, pers. comm.) which overlies unconformably rocks of the Namaqua Metamorphic Complex and has undergone medium grade metamorphism and deformation around 1200 my, i.e. coinciding with the formation of the Rehoboth Magmatic Arc and the later deformations in the Richtersveld and the Namaqua Metamorphic Complex. If these findings are correct, uplift at least in some parts of the area north of the Orange River must have occurred prior to approximately 1400 my, which implies at the one hand that the high grade metamorphism found there in the basement must be older than 1400 my and on the other hand that subsequent to uplift and erosion a new northeast-trending orogenic belt must have developed influencing the structural and metamorphic development also of the area farther in the south. Particularly a southeastward directed subduction as suggested by Watters (1974, 1977) would provide the compressional strain direction required to account for major shear zones in the Richtersveld and the Namaqua Metamorphic Complex

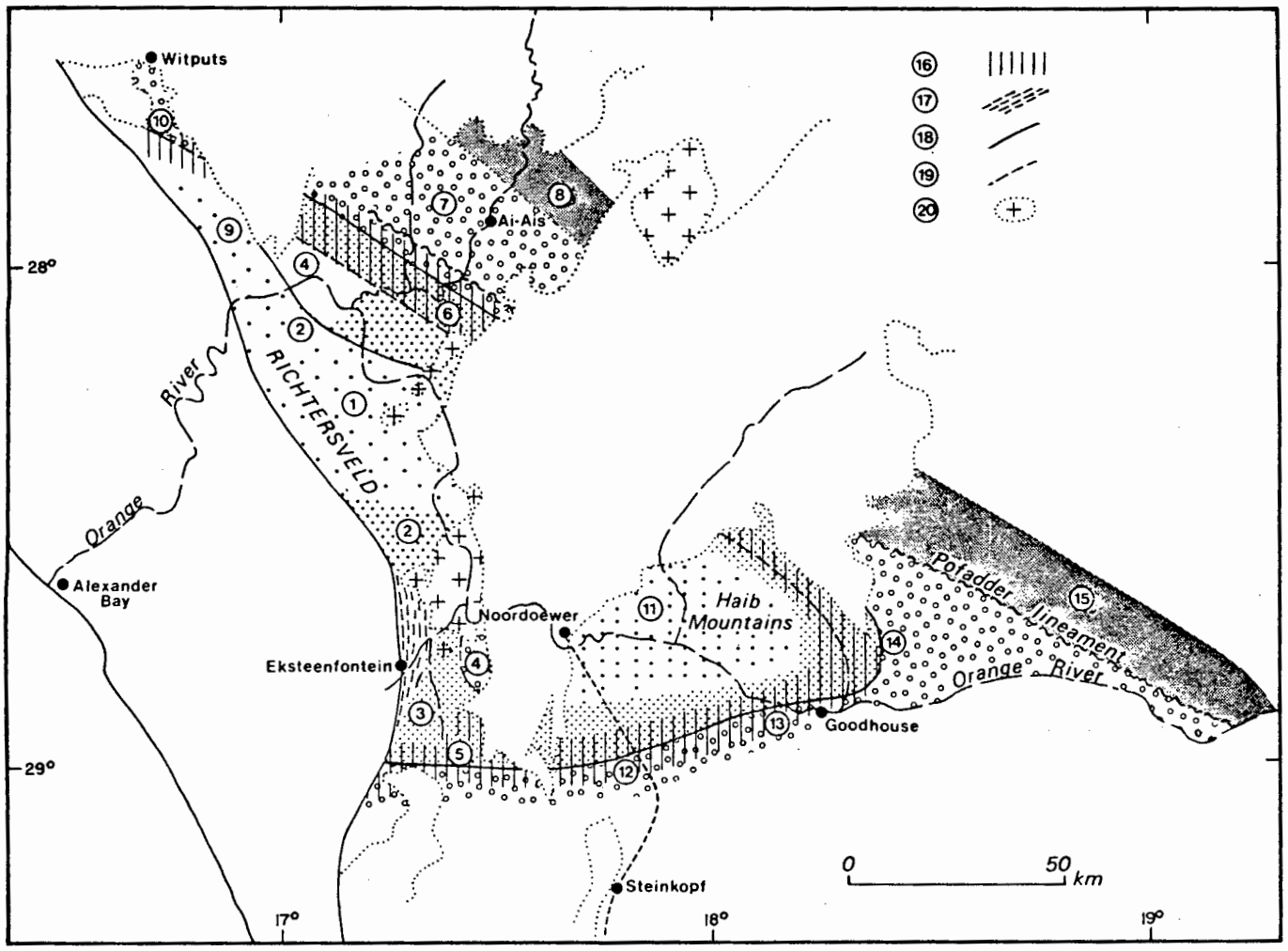

Fig. 8.3 Metamorphism of the Richtersveld in its regional context. Compiled after various investigators and the present investigation.

Comments:

1) Lower part of low grade metamorphism (<400°). Central NE Richtersveld (A)
2) Upper part of low grade metamorphism (~400°). Central Richtersveld (A); Lower Fish River area (a); muscovite plus chlorite zone.
3) Medium grade metamorphism (~500°) solidus granodiorite) (A)
4) High grade, melting of granodiorite; Helskloof-type rock assemblage in the NE Richtersveld (A,e)
5) High grade; Pink-gneiss Unit; mu pseudom. after sill (A), migmatisation of granodioritic rocks farther in the S (B)
6) Medium grade; muscovite plus chlorite out zone and lower part of sill zone, increased density of pegmatites (a)
7) High grade; minimum melt isograd, epidote out zone (a)
8) High grade ; Kf plus sill zone (a)

(cont.)

(Devilscastle shearing, Pofadder-type shearing) as well as for the later folding events. It would explain these features much better than a model proposed by Wynne-Edwards (1976 Fig. 8) who related the right-lateral and left-lateral shear zones of Namaqualand to transform faults of a spreading system farther in the northwest.

Summary

Three periods of deformation in the Namaqua Mobile Belt coincide with those observed in the Richtersveld Province not only in time but also with respect to the character of deformation. While the early deformational events which bear the main structural imprints are roughly coeval with the formation of the Richtersveld Province, the later folding coincides with the formation of the Rehoboth Magmatic Arc and the deformation and metamorphism of the Konipberg Sequence. Northwest-trending shear belts with right and left lateral displacement can possibly also be related to orogenic activities at and to the north of the Rehoboth Magmatic Arc.

Fig. 8.3 (caption continued)

9) Low grade undifferentiated, inferred (f)
10) High grade; migmatisation and posttectonic granites, pegmatites, similarity to Pink-gneiss Unit (f)
11) Low grade, undifferentiated (a,g)
12) High grade; cordierite-sill schist and gneiss; increased density of pegmatites (i); migmatisation of Vioolsdrif granodiorite (B)
13) High grade; migmatisation of Vioolsdrif granodiorite (d); increased density of pegmatites (k)
14) High grade; boundary of migmatisation (b); sill isograd (c); increased density of pegmatites (a)
15) High grade, sill-kf zone (h)
16) increased density of pegmatites
17) obliteration of metamorphic textures by later shearing
18) beginning of melting after various authors, in most cases melting of granodiorite implied
19) Namaqua front as conventionally seen
20) Late Precambrian and Paleozoic intrusives

References:

A) this investigation
B) this investigation, reconnaissance
a) Blignault 1977
b) Blignault *et al.*, 1974
c) Beukes, 1973
d) Bertrand, 1976
e) Mc Millan, 1965
f) Mc Millan, 1968
g) Reid, 1977
h) Toogood, 1976
i) Ward, 1977
k) Geol. map SA sheet No: 2817D Vioolsdrif

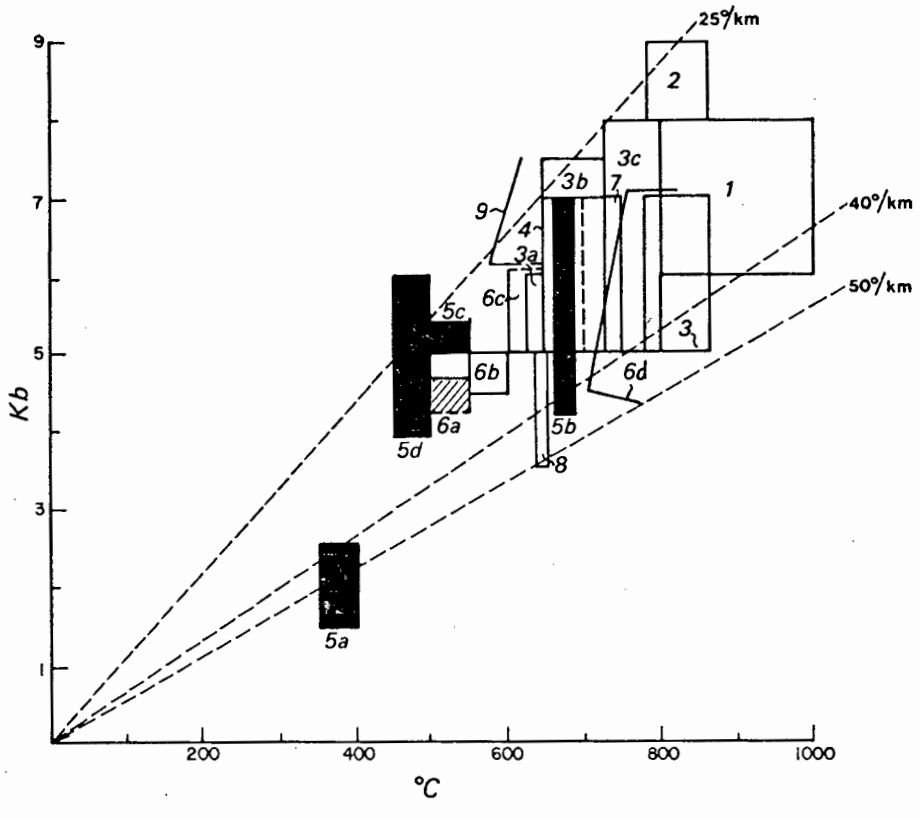

Fig. 8.4 Estimated metamorphic conditions from various parts of the Richtersveld Province and Namaqua Metamorphic Complex

References:

1) O'Okiep, Clifford *et al.*, (1975).
2) Onseepkans, Toogood, (1976), Kumian metamorphism.
3) Jackson (1976), Aus granulites.
3a) Zone I, medium stage, Aus, Jackson (1976.
3b) Zone II, high stage, Aus, Jackson (1976).
3c) Zone III, high grade, Aus, Jackson (1976).
4) Velloorian, Warmbad, Toogood (1976), North of Pofadder Lineament.
5a) Central northeast Richtersveld, this investigation.
5b) Helskloof, southeast. Richtersveld, this investigation.
5c) Southeast. Richtersveld, Devilscastle Event, this investigation.
5d) Northeastern Richtersveld, Noms River, late metamorphism, this investigation.
6a) Fish River area and Haib, Blignault (1977).
6b) Medium grade, Ais, Blignault (1977).
6c) Sillimanite zone, Ais, Blignault (1977).
6d) Kf-Sill zone, Ais, Blignault (1977).
7) Namiesberg, Bushmanland, Moore, (1977).
8) Velloorian, S of Pofadder Lineament, Toogood (1976).
9) N Namaqualand, sillimanite isograd, inferred after Joubert (1971).

Black : Richtersveld

Geothermal gradients are calculated at 0,275 kb/km.

8.1.3. Metamorphic relationships

In order to compare the P-T conditions of Richtersveld metamorphism with those of the Namaqua Metamorphic Complex, Figure 8.4 has been compiled. It is evident from this that although the metamorphic grade in the Richtersveld is generally lower, P-T ratios (i.e. geothermal gradient) are essentially similar inside and outside the Richtersveld and occupy with few exceptions the range between 30 and 40°C/km.

Deviations towards the higher gradient are found in the central northeastern Richtersveld and during Velloorian metamorphism south of the Pofadder Lineament (Toogood, 1976). Deviations towards lower gradients are found during Kumian metamorphism north of the Pofadder Lineament (Toogood, 1976) and in northern Namaqualand (Joubert, 1971). The latter, however, is estimated from the occurrence of the ky/sill isograd and is thus dependent on what experimental triplepoint for the alumina silicate modifications is used. It is furthermore evident from this compilation that the high pressure domain around O'Okiep postulated by Jackson (1976) does not seem to be real since the centre of the P-T field of this area falls well on the 35° geothermal gradient and is thus neither higher nor lower than the majority of the other estimates.

1. *The metamorphic transition between Richtersveld Province and Namaqua Metamorphic Complex : "Namaqua front" or continuous transition?*

One of the problems regarding the position of the Richtersveld Province within the Namaqua Metamorphic Complex is whether it constitutes a distinctly and sharply bounded domain as suggested by Blignault (1974b, 1977 p.187) or whether there is a continuous transition, favoured by the present investigation (see Fig. 8.3).

The continuity of a metamorphic zonation can be determined by comparing the observed metamorphic zones with the metamorphic zonation that can be expected in a particular facies series. This has been done for a geothermal gradient of 35°/km in Figure 8.5 (expected metamorphic zonation). In Figure 8.6 the width and sequence of the expected zonation are compared with the width and sequence of the observed zonation as inferred from mapping. This diagram is constructed by intersecting the width of each expected zone with that of the observed zone. Any break in the succession of the metamorphic zone (e.g. one zone missing, or less wide than expected or wider than expected due to tectonic repetition) would thus result in a change in steepness of the constructed slope or its interruption. This is not the case in two of the profiles, i.e. the metamorphic zonation between the central northeastern Richtersveld and the Ais-ais area and the southeastern Richtersveld respectively, appear to be undisturbed, although the latter should be regarded with caution since the boundaries of the observed zones

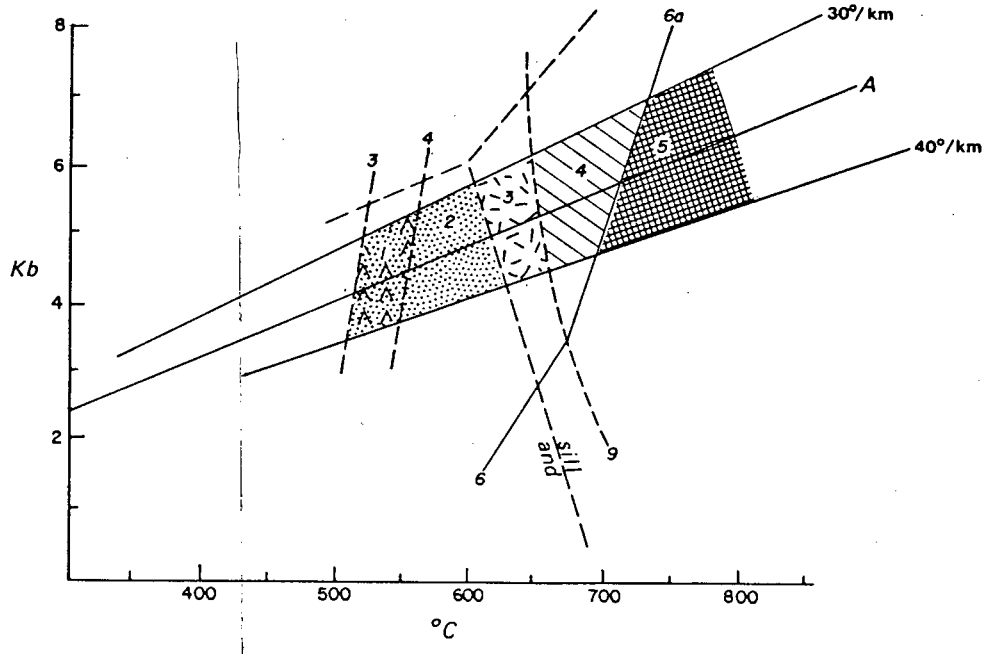

Fig. 8.5

Succession and width of metamorphic zones along geothermal gradients of 30 - 40°C/km and approximate erosion surface.

Phase boundaries:
3) An 17 + hbl in (Winkler, 1974)
4) 'Staurolite in' (Winkler, 1974)
6) mu + qtz = kf + sill + H_2O
6a) formation of sill (Storre and Karotke, 1972)
9) Beginning of melting of granodiorite (water saturated) (Piwinskii, 1968; Whitney, 1975a).

Zone 1 : upper low grade
Zone 2 : medium grade
Zone 3 : medium grade (lower "sill zone" of Blignault, 1977, Fig. 4.11)
Zone 4 : high grade (upper "sill zone" and "epidote-out" zone of Blignault, 1977 Fig. 4.11).
Zone 5 : high grade ("kf + sill zone" of Blignault, 1977, Fig. 4.11).

Only an erosion surface similar to that of A can account for width and succession of metamorphic zones as displayed in the field. Horizontal erosion surfaces do not account for the decrease of pressure with temperature which is evident from the present investigations.

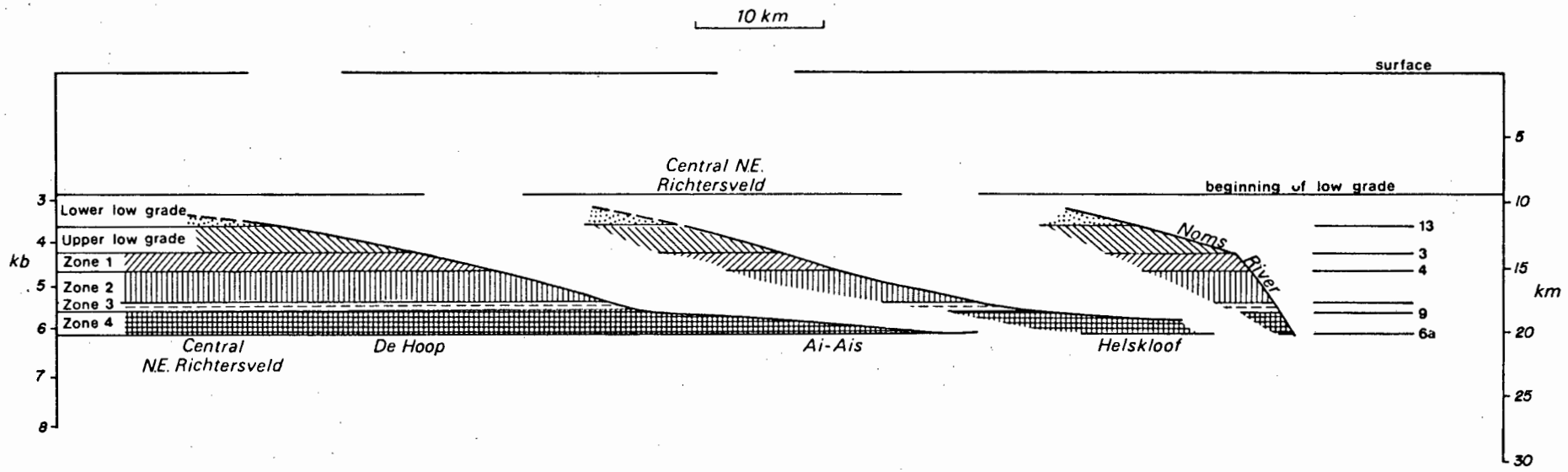

Fig. 8.6 Metamorphic profile through parts of the Richtersveld and the adjacent Namaqua Metamorphic Complex. Vertical metamorphic zonation is constructed with a geothermal gradient of $35^{o}C/km$ and using the phase boundaries of Figs. 8.5 and (13) : pyrophyllite = andalusite + quartz + H_2O (Kerrick, 1968).
Scale : vertical = horizontal.
The present-day erosion surface is constructed by intersecting the width of the observed mapped metamorphic zone with the respective expected metamorphic zone.
A regular slope indicates that no major discontinuity is present in the metamorphic profile.

are only approximately known. Only in the Noms River-Blockwerf area is a break in zonation evident from a rapid lateral transition from low to high grade rocks, but since this had already been detected without reconstruction it is merely included to illustrate the effects of such a disturbance. An undisturbed zonation is particularly evident from the profile between the central Richtersveld and Ais-ais where the more accurate data of Blignault have partly been used to construct Figure 8.6. From this regular zonation it is difficult to assume a sudden increase in temperature at a "Namaqua front zone" as indicated by Blignault (1977, Fig. 5.3). However, it is evident from his descriptions and diagrams that this misconception can only arise if the Richtersveld is regarded as a homogeneously low grade metamorphic terrain, i.e. lack of further metamorphic zonation within the Richtersveld Province, a view which appears to have been held more implicitly than explicitly by virtually all previous investigators mentioning the Richtersveld. This, however, underlines the importance of the present findings since only in the case of a metamorphic zonation in the Richtersveld is the transition between Richtersveld Province and the Namaqua Metamorphic Complex gradational and agrees with metamorphic models that see both as a unity and not as separate geological entities.

2. *A metamorphic model*

If the metamorphic zonation between the Richtersveld Province and the Namaqua Metamorphic Complex is continuous it is only logical to assume their formation by the same metamorphic event, an assumption which is rendered difficult by the difference in radiometric ages of nearly 1000 my between Richtersveld and Namaqua Metamorphic Complex.

The variation in age of metamorphic imprint, the regular variation of geothermal gradient and metamorphic grade, however, can be accounted for by the following model:

Early stage:

Main metamorphism reached its peak between 2000 and 1800 my, subsequent to which heat flow decreased over a long period of time, with crustal thickness remaining essentially the same. This may explain the cessation of metamorphism in the central Richtersveld at a relatively early stage by mere lowering of the geothermal gradient since it occupied relatively high crustal levels, and the preservation of 1900 my extrusive ages (Haib area) as well as the preservation of the earliest metamorphic imprints reflecting maximum or near maximum conditions (high geothermal gradient). For the same reasons textural imprints formed during later stages of metamorphism represent lower temperatures at unchanged pressures, i.e. a lower T/P ratio (see Fig. 6.19).

Late stage:

Possibly from around 1000 my ago epeirogenic differential uplift led to the exposure of relatively deep crustal levels in the area now underlain by the Namaqua Metamorphic Complex and the marginal Richtersveld while in the central Richtersveld no or less crustal uplift occurred and rocks of higher crustal level were preserved. This may explain the broad continuous metamorphic zonation and the ages of the high grade rocks of the Namaqua Metamorphic Complex and the marginal Richtersveld; i.e. since the highest grade rocks represent the lowest crustal levels they were the latest to be exposed to upper crustal conditions and thus the latest to close their isotopic systems.

The essential elements of this model are therefore : slow decrease of geothermal gradient over a long period at unchanged pressures followed by a relatively rapid period of differential uplift exposing the lowest crustal levels. Only in that way could the bimodal age distribution between the Richtersveld and the Namaqua Metamorphic Complex have been achieved while any other mechanism would have led to the continuous distribution of ages as well. For these reasons the assumption is justified that the present metamorphic pattern in northern Namaqualand is the result of differential crustal uplift of epeirogenic dimensions during and following Namaqua metamorphism and that the Richtersveld Province and the Namaqua Metamorphic Complex are part of the same crustal segment but represent different levels in it.

3. *Alternative models : Thermal dome*

Any metamorphic model trying to explain the metamorphic relationships between Richtersveld and Namaqua Metamorphic Complex has to take into account the normal temperature distribution within the Earth's crust. Unfortunately models based on the concepts of thermal domes, surges, plùmes, etc. (i.e. implying a lateral change of geothermal gradient) are still haunting the literature on the Namaqua Metamorphic Complex and the Richtersveld. They are even disregarding the laws of nature as can be seen particularly well in Pretorius (1974, Fig. 12) whose model implies a geothermal gradient going towards zero below the Kaapvaal Craton, a condition which is clearly impossible to realise in nature.

In a less extreme form lateral geothermal gradients are possible at the transitions between different structural domains in active continental margins (e.g. between arc and trench) and are generally assumed to be present at the transition between Precambrian cratons and mobile belts, although they have actually rarely been proved there (e.g. Saggerson and Turner, 1976, for the Rhodesian craton and Limpopo Belt).

Assuming nevertheless a thermal dome-origin for the Namaqua Metamorphic Complex - Richtersveld Province relationship, Table 8.6 and Figure 8.7 have been devised comparing some expected with some observed features in such a case. They show that the most crucial feature

Fig. 8.7 Distribution of metamorphic zones in the case of a thermal dome. Very high geothermal gradients in the centre and increasingly lower ones towards the margins are implied by this model. Level of erosion is indicated.

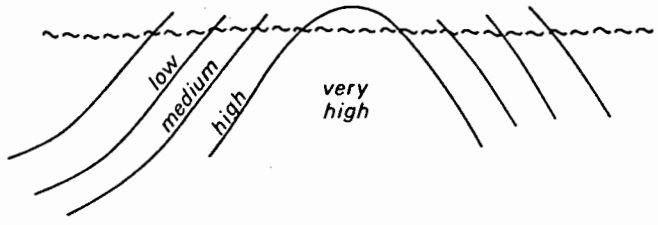

Table 8.6 Comparison of features expected in metamorphic zonation due to a thermal dome with features encountered in the Richtersveld Province and the Namaqua Metamorphic Complex. Particularly the similarity of metamorphic facies series in both domains rules out an origin as a thermal dome.

	met. grade	met. facies series	geotherm. gradient	radiometric ages
Richtersveld :				
expected	low	high p.	low	1900 my
observed	low	low p.	high ~50°/km (early) 25-30/km (late)	1900 my
Namaqua Metamorphic Complex:				
expected	high	very low	very high	1000 my
observed	high	low p.	high (~35°/km)	1000 my

of a thermal dome, the association of low grade metamorphism with a low geothermal gradient, is not found here. On the contrary, early metamorphism in the central Richtersveld appears to reflect a particularly high heat flow, a feature which is consistent with the volcanic nature of the area and would rather imply a thermal dome at the site of the Richtersveld and not the Namaqua Metamorphic Complex. Inferred gradients for later metamorphism again are not different enough to justify the assumption of a thermal dome underlying the Namaqua Metamorphic Complex during Kibaran times, particularly since it cannot be ruled out that some of the aberrant P-T determinations (Fig. 8.4) represent late stages of metamorphism; and the latest-stage Richtersveld metamorphism (Devilscastle) has no equivalent in the Namaqua Metamorphic Complex since it is younger than the mineral assemblages recorded there.

This leads to the conclusion that the two main requirements for the postulation of a thermal dome : lateral change of geothermal gradient and a particularly high geothermal gradient in the high grade metamorphic terrain are not met here and that thus the difference in metamorphic grade between Richtersveld Province and Namaqua Metamorphic Complex cannot be attributed to a mechanism involving a "thermal dome".

4. *Metamorphism and present-day areas of high heat flow*

It must also be emphasised that the geothermal gradients* inferred for Richtersveld and Namaqua metamorphism do not even constitute a particularly strong deviation from normal. It rather appears that the late Richtersveld metamorphism (Devilscastle) represents thermal conditions as they are presently found in crustal segments which have been consolidated in Late Precambrian and Paleozoic times (Fig. 8.8) while thermal gradients inferred for the main Richtersveld-Namaqua metamorphism are rather similar to those measured in Cenozoic back-arc areas. Takeuchi and Uyeda (1965) already suggested from terrestrial heat flow measurements that low-P type regional metamorphism may presently be underway beneath the high heat flow zone of the Japan Sea and Oxburgh and Turcotte (1971) presented a quantitative model for the thermal structure of crust and upper mantle in island-

---

* The comparison of geothermal gradients inferred from metamorphism with present-day heat flow values is of course only valid if it is assumed that the g-value was the same throughout the Earth's history and that heat flow and geothermal gradient are mainly caused by thermal conduction. Intrusion of magmatic rocks and volatiles ascending into higher crustal levels may lead to a lowering of the geothermal gradient with increasing depth (e.g. Oxburgh and Turcotte, 1971).
Geothermal gradients inferred from metamorphic data may therefore be slightly lower than the corresponding surface heat flow.

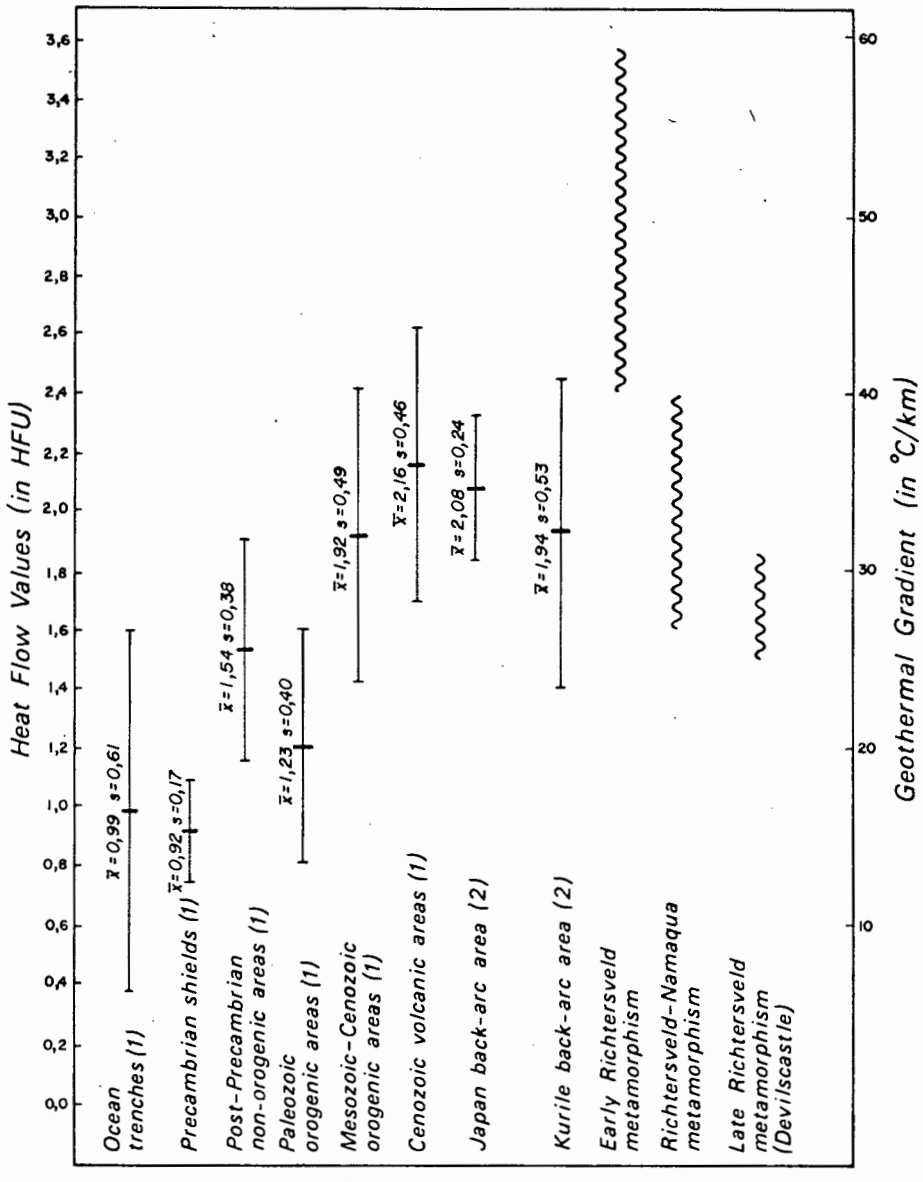

Fig. 8.8
Present-day surface heat flow values and approximate geothermal gradients for major geological features and their comparison with geothermal gradients inferred from Richtersveld and Namaqua metamorphism.
The values inferred from the main Richtersveld-Namaqua metamorphism are well in accordance with those measured in Mesozoic-Cenozoic orogenic areas. Values inferred from late Richtersveld metamorphism agree with those areas that have been consolidated in Late Precambrian and Paleozoic times. They support the view expressed in the text that the Richtersveld was in a state of consolidation at the time of the Devilscastle Event.

The geothermal gradient has been calculated using an average thermal conductivity of 6 (10^{-3}cal/cm sec ^{o}C).

1 HFU (= Heat Flow Unit) = 1 μcal/cm^{2}sec

References : 1) Lee and Uyeda (1965) 2) McKenzie and Sclater (1968).

arc areas and considered the implication of this structure for paired metamorphic belts and crustal extension behind the arcs. They also found that the vertical geothermal gradient in high heat flow areas behind the arc can give rise to P-T conditions of the andalusite-sillimanite and kyanite-sillimanite facies series.

The predominance of low-P type metamorphism in the Precambrian has long been a matter of discussion and is generally attributed to higher geothermal gradients in early stages of the Earth's history (De Roever, 1956; Roering, 1967; Martin, 1969; Ernst, 1972; Fyfe, 1976), but to the author's knowledge this fact has so far nowhere been proved conclusively. More recent discussions, however, stress that there is no evidence from mineral reactions and assemblages for a generally high heat flow in the Precambrian as compared with Phanerozoic and present-day terrains (e.g. Watson, 1978) and that heat flow in orogenic terrains might be more indirectly controlled by different thicknesses of plates and consequently different subduction angles and velocities, as suggested by Miyashiro (1972), according to whom plate motion in Precambrian time had been relatively slow resulting only in intermediate-P metamorphism in subduction zones.

That the velocity of plate descent has considerable influence on the thermal structure of an active continental margin has been verified by thermal models (e.g. Minear and Toksoz, 1970; Oxburgh and Turcotte, 1970, 1971). It has furthermore been emphasised by various investigators that the high-P mineralogy of a subduction zone can only be preserved if rapid uplift occurs soon after its formation (Miyashiro, 1972; Oxburgh and Turcotte, 1971; Ernst, 1972). Particularly Oxburgh and Turcotte (1971) drew attention to the importance of crustal accretion at the leading edge of the lithospheric plate and the consequent outward migration of the subduction zone. In this way the whole thermal structure of the plate margin migrates outward with respect to a fixed point on the plate and the trench metamorphics of high-P type will soon come under the influence of low-P type metamorphism unless they undergo rapid uplift or the movement along the subduction zone decelerates or stops entirely. For this reason the absence of a high-P metamorphic zone should not be regarded as a cogent argument against plate subduction. The absence of a subduction zone rather appears to be the necessary consequence of mechanisms closely related to subduction and the development of a continental margin.

The reason for increased heat flow in back arc regions is not yet well understood since a down-going slab of relatively cool oceanic crust should cause a low geothermal gradient in the area underlying the subduction zone. Dissipative heat generation at the surface of the down-going slab alone cannot be the answer either since the time for heat transfer solely by conduction would probably be greater than the lifetime of the trench and arc system (McKenzie and Sclater, 1968). It is therefore generally agreed that heat transfer by convection of large volumes of magma is essential to maintain the amount of heat flow that is common in back arc areas (e.g. McKenzie and Sclater, 1968; Oxburgh and Turcotte, 1971), an assumption which is justified in view of the large amounts of magma intruded and extruded in and

behind magmatic arcs. Oxburgh and Turcotte (1971) calculated that the amount of intrusives equivalent of a spreading rate of 5 cm/year corresponds to an intrusion rate sufficient to yield 4 μcal/cm^2 sec (= 4 HFU) surface heat flow affecting a 500 km wide belt behind the arc (i.e. intrusion of a dyke 5 cm wide across the width of the belt per year would be sufficient to maintain a heat flow of 4 HFU).

Since thus not only the baric type of metamorphism of Precambrian mobile belts is compatible with Cenozoic orogenic belts but also their length (several thousand kilometres, e.g. the Andes; Rutland, 1973) their width (several hundred kilometres) and duration of activity (several hundred my; Matsumoto, 1966; Miyashiro, 1973; Stewart *et al.*, 1973), it may not be too far fetched to assume processes similar to those presently taking place in the circum Pacific region to be responsible for metamorphism at least in some Precambrian mobile belts. In the present case this idea is particularly attractive in view of some geological and geochemical similarities of the Richtersveld Province with an Andean-type continental margin.

5) *Summary*

a) Metamorphic facies series in Richtersveld and Namaqua Metamorphic Complex are essentially similar although significant deviations do occur, and the metamorphic transition between these two domains is continuous.

b) Continuous zonation but variable ages can be explained by a model comprising as essential elements a slow decrease of geothermal gradient after the peak conditions of metamorphism had been reached (~1800 my) and epeirogenic differential uplift during later stages (~1000 my). Models involving "thermal domes" or similar mechanisms must be discarded since there are no indications for a significant difference of metamorphic facies series between Richtersveld and Namaqua Metamorphic Complex.

c) Geothermal gradients inferred for the main Richtersveld and Namaqua metamorphism agree well with gradients presently measured in Mesozoic-Cenozoic orogenic back-arc areas, and gradients inferred for the late Richtersveld metamorphism (Devilscastle) agree well with those presently measured in areas which have been consolidated in Late Precambrian and Paleozoic times.

8.1.4. The origin of the pegmatites

Pegmatites are commonly found at the margins of intrusive bodies but also occur in metamorphic terrains unrelated to major intrusions. Schneiderhöhn (1961) therefore distinguished pegmatites according to their

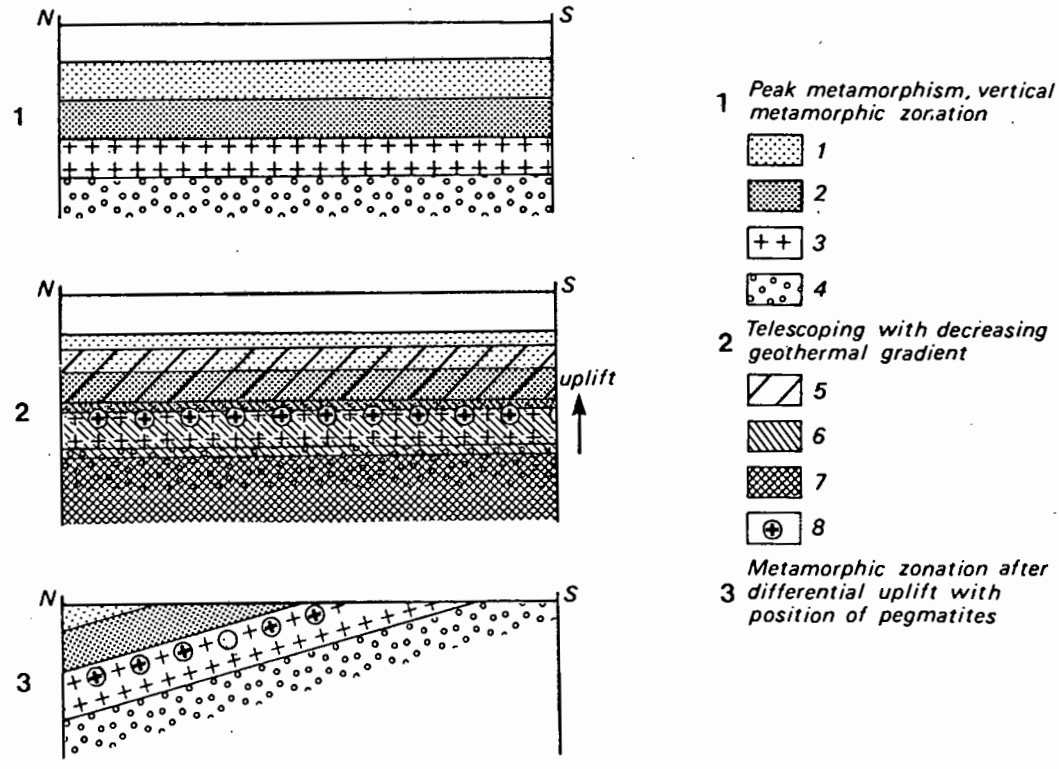

Fig. 8.9 Schematic sketch illustrating the formation of pegmatites and of metamorphic zonation.

Stage 1 : Vertical metamorphic zonation during the peak of metamorphism which formed the presently exposed metamorphic zoning.

Stage 2 : A decreasing geothermal gradient results in wider metamorphic zones, in the course of which the original high-grade (migmatitic) zone cools to medium grade, resulting in crystallisation of the magmatic phase. Pegmatites then form in a position determined by depth, geothermal gradient, and composition of the fluid phase above or in the upper part of the former high-grade zone.

Stage 3 : Epeirogenic differential uplift leads to the exposure of the metamorphic zonation, in which the pegmatites occupy a distinct position.

This model is a simplified one and applies best to the Richtersveld and surroundings. Complicating factors may occur such as retrogressive metamorphic reactions, deformation and vertical movements during Stage 2.

Legend:

1) low grade
2) medium grade
3) high grade (migmatisation)
4) granulite
5) low grade
6) medium grade
7) high grade
8) zone pegmatites

genetic relationships and termed the latter "pseudo pegmatites".

In the present case of a pegmatite belt of ~600 km in length (Hugo, 1969) a relationship to an intrusion or intrusive phase can be envisaged only with difficulty and would require the presence of a giant batholith underlying the full east-west length of the Namaqua Metamorphic Complex. Individual minor intrusions as a source of the pegmatites would fail to explain the rather consistent nature of this belt throughout its length. It would also fail to explain the fact that the pegmatites are concentrated in a rather narrow belt while other intrusive rocks are abundantly present elsewhere in the Namaqua Metamorphic Complex. Particular attention should also be drawn to the preferred occurrence of pegmatites not only at the southern but also at the northern margin of the Richtersveld Province (McMillan, 1965, 1968; Blignault, 1977), although not as abundant there as in the south.

Assuming an origin of the pegmatites as "pseudo pegmatites" *sensu* Schneiderhöhn (1961) the possible mechanism leading to their formation has been illustrated and explained in Figure 8.9. It is based on the uplift and cooling history of the Namaqua Metamorphic Complex.

Pegmatitic melts and fluids form at a late stage of crystallisation of a magmatic body when vapour pressure rises in the rest melt due to crystallisation of mainly anhydrous minerals in the magma. This gives rise to highly mobile solutions containing all those elements that could not be accommodated in the lattice of already crystallised minerals. Since the temperature at a given depth is determined by the geothermal gradient, pegmatites will form during Stage 2 in the upper parts of the high grade metamorphic zone, possibly partly overlapping with overlying rocks, at that very depth that is specific for their composition.

If this explanation is correct the Orange River Pegmatite Belt must be regarded as representing a distinct crustal level equivalent to the lower part of the high grade metamorphic zone. It would also indicate that the conditions leading to differential uplift acted throughout the western Orange River region.

8.1.5. Some remarks on possible geotectonic mechanisms

Much of the discussion so far has been conducted in terms of plate tectonics. It has been shown that the geology of the supracrustal rocks, the chemistry of the volcanics and some aspects of the structural development are in agreement with plate tectonic models and that in particular the occurrence of volcanics and intrusives of the Richtersveld Province must be seen in close relation to the early Namaqua-Richtersveld metamorphism. Nevertheless, important indicators for a plate tectonic regime such as eugeosynclinal or trench assemblages and high to intermediate pressure metamorphism are missing, and alternative models should therefore not entirely be neglected, although hardly any are available that account for both calc-alkaline volcanism and metamorphism. An aulacogen model as suggested by Martin

and Porada (1977) for the Damara orogen must be ruled out since there is no evidence for the accumulation of an excessively thick sedimentary sequence prior to the extrusion of the Orange River volcanics as required by such a model; and also all models involving upwelling of mantle material in one form or other can only account for metamorphism but not for intermediate volcanics and intrusives with the major and trace element characteristics encountered in the Richtersveld Province.

Models based on gravitational instability due to gabbro/eclogite transformation and resulting density inversion in the upper mantle have been proposed as parts of Martin and Porada's (1977) model for the Damara and by Ringwood and Green (1966). Particularly the latter model accounts for the formation of geosynclines, acid to intermediate volcanism, regional metamorphism and deformation. It is based on the fact that eclogite, formed from gabbroic rocks at the base of the oceanic crust at the prevailing geotherms, has a greater density than the underlying mantle pyrolite, is therefore gravitationally unstable and may, if decoupled from the overlying crust, sink into the mantle and undergo fractional melting, producing andesitic magmas which will raise the geotherms in the overlying crust and lead to acid and intermediate magmatism with geological, geochemical and thermal characteristics similar to those in conventional plate tectonic environments.

Although this model is not directly applicable to ensialic mobile belts of the Namaqua type, it nevertheless underlines the potential importance of gravitational instability within the upper mantle as an alternative to plate tectonics. If it could be established that basaltic layers could not only be formed beneath continental margins as suggested by Ringwood and Green (1966) but also within and beneath sialic plates (e.g. by fractional melting of mantle pyrolite), its subsequent transformation into eclogite (with decreasing geothermal gradient), decoupling and sinking into the mantle could provide a mechanism which could explain reworking of ancient crust in mobile belts cutting through older basement without any indications for overlying geosynclinal sediments, (e.g. Kröner, 1977) and the occurrence of continental margin-type magmatism within sialic plates.

8.2. THE RICHTERSVELD BASEMENT AND THE AGE OF THE STINKFONTEIN FORMATION

Since data of the basement geology important for the elucidation of the depositional history of the Stinkfontein Formation are scattered throughout this report, they have been compiled and condensed in Table 8.7. From these data it is evident that, if the unconformity cuts the Devilscastle Schist Belt and the Klipbokkop intrusion, it must be younger than the latter and that, if parts of the Klipbokkop intrusion display near-surface textural features, it must have been emplaced close to the surface and its age must represent the approximate time of the formation of the unconformity.

Table 8.7 Relationships of the Richtersveld Igneous Complex and deformational zones of the Devilscastle Event with the Stinkfontein unconformity.

rock unit/ event	*crustal level*	*evidence*	*age (in my)*	*evidence*	*relationship to other rock units*
Sjambok River Intrusion	low	coarse texture	910±10 864±12	Allsopp *et al.*, (1978): U-Pb zircon Rb-Sr whole rock isochron	deformed by Devilscastle Schist Belt
Black Face Mntn Xaminxaip Intrusion	low	coarse texture	850±20 896±90	Pb age (in Köstlin, 1971) Rb-Sr whole rock errorchron (Allsopp *et al.*, 1978)	deformed by Black Face Mountain Mylonite Belt
Rooiberg Intrusion	low and high	coarse and fine textures	809±102 751± 8 762(mu) 792 (fspr)	Rb-Sr errorchron (Allsopp *et al.*, *op. cit.*) Rb-Sr whole rock isochron Rb-Sr isochron mineral age (Köstlin, 1971)	intruded into Black Face Mntn Mylonite Belt
Klipbokkop Intrusion	high and near surface	fine and very fine-grained texture	696 ± 16	Rb-Sr whole rock isochron (Allsopp *op.cit.*)	intrudes Devilscastle Schist Belt and Black Face Mylonite Belt, cut by Stinkfontein unconformity
Devils castle Schist Belt	low (~18km ~500°C)	b_o-characteristics, mineral assemblage			deforms Sjambok River Intrusion
Black Face Mntn.Mylonite Belt	high	partly unrecrystallised			deforms Black Face Mountain Intrusion younger than Devilscastle Schist Belt
Stinkfontein unconformity					cuts Klipbokkop Intrusion and Devilscastle Schist Belt.

The crucial question in this case is therefore the reliability of the Rb-Sr whole rock ages determined in the Richtersveld Igneous Complex, i.e. whether they represent metamorphic resetting events as concluded by Allsopp *et al.*, (1978) or the true age of intrusion but reflecting a complicated intrusive history as supported by the following evidence:

a) there are no indications for metamorphic textural reconstitution of the wall rocks of the Richtersveld Igneous Complex after the Devilscastle Event

b) Rb-Sr whole rock ages are consistent with the relative sequence of intrusion as deduced from fieldwork

c) textural evidence in the youngest members of the Richtersveld Igneous Complex suggests refusion and may thus account for the discrepancy between whole rock and zircon ages,i.e. the zircons represent an earlier phase of crystallisation during repeated melting and "freezing" of the rock in the course of a complicated intrusive history (cf. 4.12/7).

For this reason it is here regarded as likely that the Rb-Sr whole rock ages reflect the true intrusive history of the Richtersveld Igneous Complex and that the 700 my age of the Klipbokkop intrusion represents the approximate age of the unconformity.

Thus arriving at a maximum age for the Stinkfontein Formation of ~700 my this investigation disagrees with suggestions by Kröner (1974) and Allsopp *et al.*, (1978) who argued in favour of a 900 my age. It is important to stress however, that the radiometric data (Allsopp *et al.*, 1978) have partly such a high uncertainty that they can also accommodate a 700 my Stinkfontein age: 662 ± 201 for the Stinkfontein lavas and 686 ± 32 for the Kapok and Hilda felsites can thus be taken as primary ages, since a low initial ratio need not indicate resetting. The Lekkersing granite (582 ± 70), occupying the southwesternmost extension of the Richtersveld Igneous Complex, would then constitute its last intrusive phase (which is in agreement with field evidence for increasingly younger ages of the Richtersveld Igneous Complex from northeast to southwest) while ages of 501±19 for Hilda and Kapok felsites as well as 481±20 for Numees shales would have to be interpreted as metamorphic ages (Numees shale is the only sedimentary rock on which ages have been obtained, which can therefore only be a metamorphic age, all other rocks dated are igneous), a conclusion which is not contradicted by the (post-metamorphic) Kuboos age of 525±60 my.

Without disregarding any of the data presented by Allsopp *et al.*, (1978) it is therefore possible to arrive at a totally different interpretation which renders Stinkfontein deposition and Garien metamorphism considerably younger than previously assumed. This interpretation is partly in agreement with new Rb-Sr radiometric ages from the Damara belt farther in the north which strongly argue in favour of two distinct Pan-African tectonothermal events at 665±34 and 474±16 my (Kröner *et al.*, 1978) and with K-Ar ages of syntectonic muscovite in rocks of the Nama Group in the Naukluft area of 530±10 my (Ahrendt *et al.*, 1978) which have been affected by Damaran tectonothermal processes.

Taking into account the regional distribution of illite crystallinity in Nama sediments between Naukluft (Ahrendt *et al.*, 1978, Fig. 2) and the Richtersveld, it can be concluded that the Gariep rocks were in any case affected by a metamorphic event close to 500 my ago. Earlier events such as in the Damara cannot be ruled out even if the depositional age of the Stinkfontein Formation is only 700 my (since a period of 20 to 50 my between deposition and metamorphism of a rock is not unduly short) and despite the fact that petrographic evidence from the Gariep Group rocks is not yet sufficient to prove this assumption.

8.3 SUMMARY AND CONCLUSION

The results relevant to the objectives of this study can be summarised as follows:

a) the Richtersveld overlies rocks of the Namaqua Metamorphic Complex in the south. Observations to the contrary to the north of the Richtersveld do not invalidate this finding but rather stress the complicated interrelationship of igneous and sedimentary processes prior and subsequent to the formation of the Richtersveld Province.

b) a continuous metamorphic transition exists between the central Richtersveld and the central parts of the Namaqua Metamorphic Complex. The metamorphic facies series develops in time from low pressure type at the earliest stage to intermediate pressure type during the last stage.

c) the Richtersveld and the Namaqua Metamorphic Complex have been affected by essentially the same tectonic events within the time postdating the deposition of the Orange River Group and predating Gariep tectogenesis.

d) Gariep deformation affected the Richtersveld only marginally and Gariep metamorphism was apparently not able to cause widespread reconstitution in the basement rocks of the Richtersveld.

e) evaluation of radiometric aga data in the light of textural and structural evidence from the basement strongly suggests a deposition of the Stinkfontein Formation not prior to 700 my.

The Richtersveld is therefore in stratigraphic, metamorphic and structural continuity with the surrounding Namaqua Metamorphic Complex and both have gone through essentially the same geological history. Differences in character of deformation as well as degree of metamorphism are secondary effects and can be accounted for by the different crustal levels of these two domains. The term *Richtersveld Tectonic Province* as defined by Kröner and Blignault (1977) is therefore no longer tenable and should be abandoned since it denotes a part of the Namaqua Province as defined by the same authors. The term *Richtersveld Province* should consequently only be used in the sense of an *"igneous province"* characterised by predominantly calc-alkaline extrusive and intrusive rocks of the Orange River Group and the Vioolsdrif Intrusive Suite (cf. also Bertrand, 1976).

The geological evolution of the eastern Richtersveld has been shown schematically in Table 8.8. It comprises 3 stages of development:

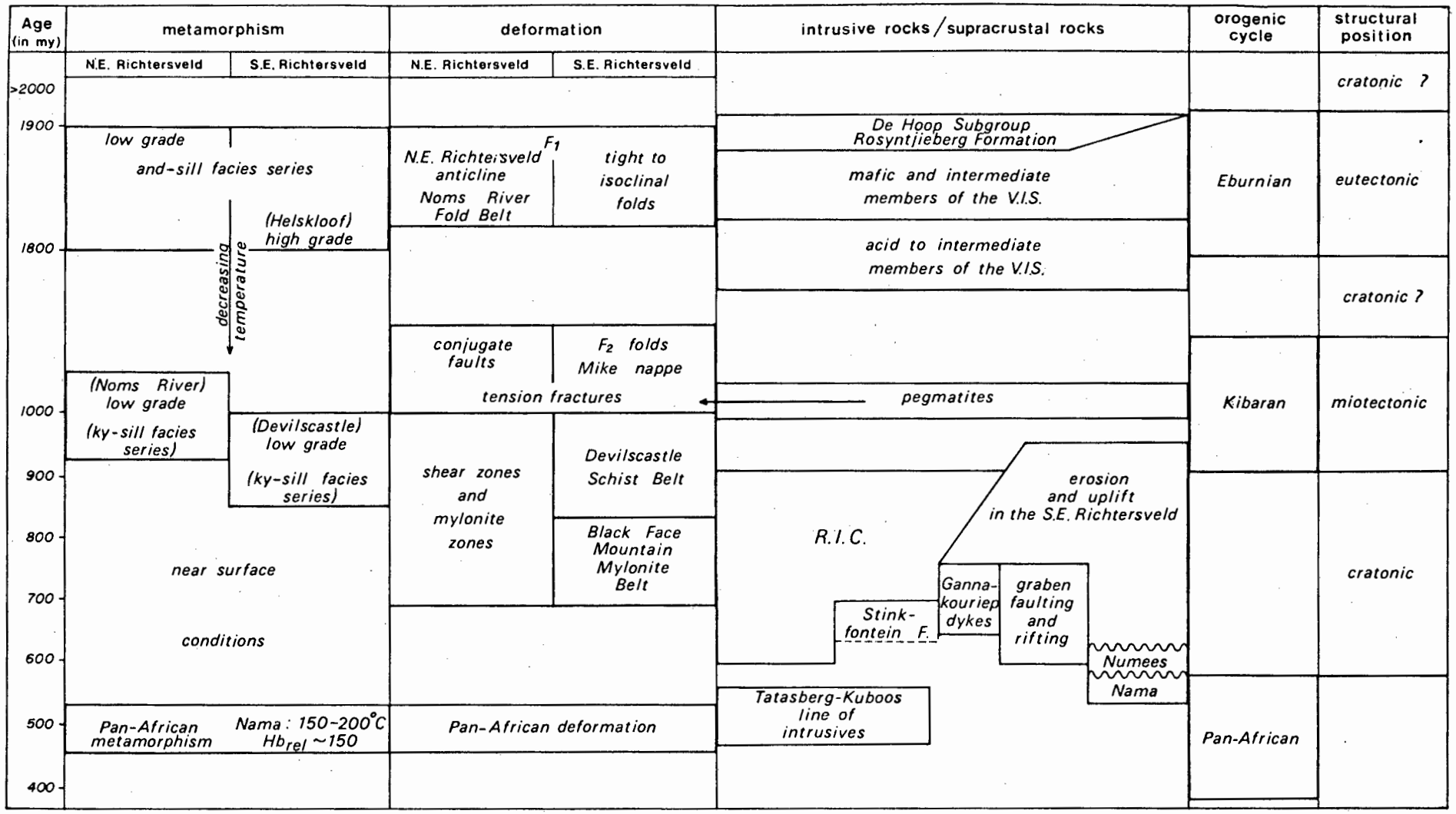

Table 8.8. Evolution of the eastern Richtersveld, summary. The column "structural position" refers to the respective orogenic cycle and is used after Rutland (1973).

Stage 1 includes the formation of the Richtersveld (igneous) Province. The main metamorphism and F_1 deformation also belong to this stage. Rock assemblages, stratigraphic relationships, general geology and certain chemical features of the volcanic rocks suggest, by analogy with Cenozoic orogenic areas, an origin as Andean-type continental margin.

Stage 2 is characterised by northeast-trending compressional features (F_2) and large-scale intraplate wrench-faulting or shearing which are interpreted as an expression of orogenic activities at and to the north of the Rehoboth Magmatic Arc. They may thus represent marginal (miotectonic) effects of a possible Kibaran eutectonic zone at and to the north of the Rehoboth Magmatic Arc. Epeirogenic crustal uplift in large parts of the Namaqua Metamorphic Complex may be due to the same orogenic activity and is regarded as being responsible for the cessation of metamorphism about 1000 my ago. For the time postdating 1000 my, emplacement of alkaline to peralkaline rocks (RIC) and indications for a relatively low geothermal gradient corresponding to present-day semi-consolidated areas suggest also increasing consolidation for the Richtersveld. Relatively strong crustal uplift between 700 and 900 my is restricted to the southeastern Richtersveld and may either be the cause or the result of the emplacement of the Richtersveld Igneous Complex.

Stage 3 (Pan-African) is initiated by rifting documented by the intrusion of mafic dykes of the Gannakouriep Suite along north-south trending lines of tensile stress and the deposition of the Lower Stinkfontein Formation in a developing graben system.

The geology of the Richtersveld therefore reflects the crustal development in the Lower Orange River area during various stages of the Proterozoic with respect to upper as well as lower crustal levels, which makes this area particularly suitable for the study of "stockwerk" phenomena and the discussion of the still controversial question of crustal growth and remobilisation during the Precambrian.

While previous views (e.g. Clifford, 1968, 1970) stress crustal growth around ancient nuclei, it is now generally agreed that most of the continental crust was already present at the end of the Archaean era (e.g. Watson, 1978; Heier, 1978; Kröner, 1977), that its thickness was comparable with that of present-day continental plates (Watson, 1978) and that major parts of the ancient continental plates have been rejuvenated and regenerated by later mobile belts (Kröner, 1977), possibly in a complicated "stockwerk pattern" with processes of regeneration particularly active in the middle crust while the lower crust (granulite) frequently retained older structural patterns and the uppermost parts of the crust were made up of new crustal material (Watson, 1973).

This concept is rather well confirmed in the present area where the rocks of the Richtersveld Province most probably represent juvenile crustal addition from the upper mantle (Reid, 1977) while geological and geochemical evidence suggest the presence of a much older continental basement underlying the Richtersveld Province. Both crustal levels subsequently underwent rejuvenation as is best exemplified by the migmatites of the Helskloof as well as Oenas and Kromnek-type posttectonic granites.

In the Lower Orange River area crustal thickness and continental outlines were therefore already established in Early/Middle Proterozoic times. Since also certain thermal, supracrustal and chemical features are similar to those found in present-day orogenic areas, it is difficult to assume processes markedly different from those acting today to be responsible for the formation of the Richtersveld Province. They may, if at all, have been different in degree rather than in kind.

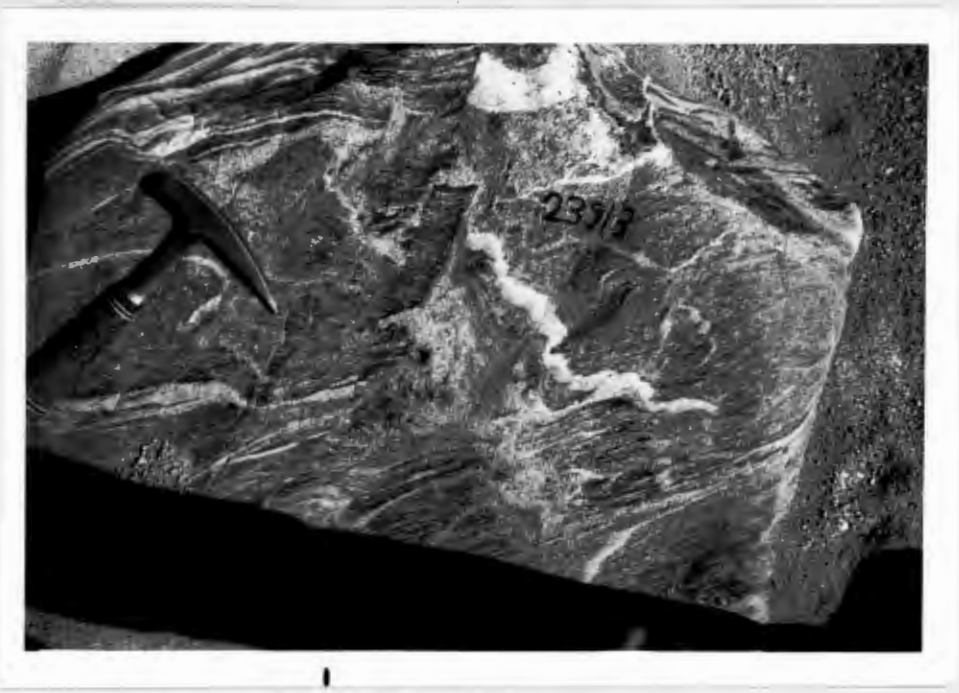

Plate 1. Migmatites of the Helskloof area : dictyonitic, phlebitic, and stromatic migmatites occur in close proximity.

Plate 2. Migmatised Vioolsdrif granodiorite. Reconstitution of the rock is continuously developed with unfoliated paleosome (1), foliated paleosome (2), foliated neosome (3), unfoliated, fine-grained neosome with schlierig to nebulitic structures (4).

Plate 3. Nebulitic migmatite

Plate 4. Folded (R6) quartzite in the valley of the Orange River, 2 km west of Mike; viewed across the Orange River towards north-west. See also Figure 5.3.

Plate 5. Parts of the Mike Nappe, viewed from northwest; R3 - stage quartzite is overlying volcanics and quartzites of the R4-stage. The underlying (authochthonous) rocks are cut off by banks of massive tectonic breccia at the base of a zone of intense deformation which is approximately 100 m thick.

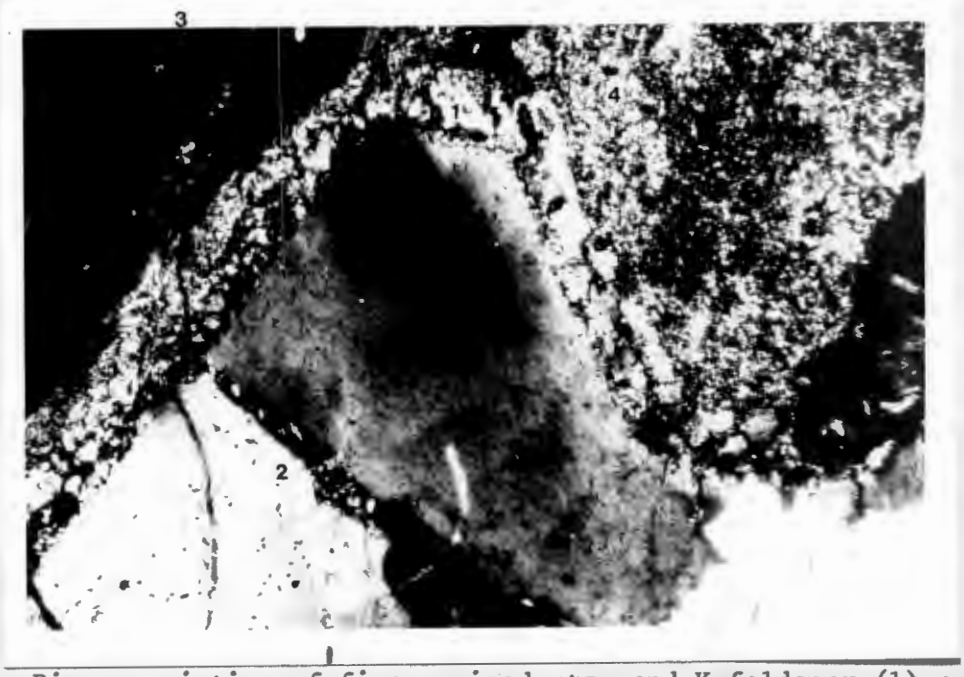

Plate 6. Rims consisting of fine-grained qtz and K-feldspar (1) caused by initial melting of Vioolsdrif granodiorite. Melting occurs at contact with qtz (2) and K-feldspar (3) and qtz and plg (4) only. Similar features have been described from melting experiments (Büsch *et al.*, 1974). Note, however, that melting of this kind occurs only at the contact with major dykes of the Gannakouriep suite and must not be seen in connection with migmatisation in the southeastern Richtersveld.

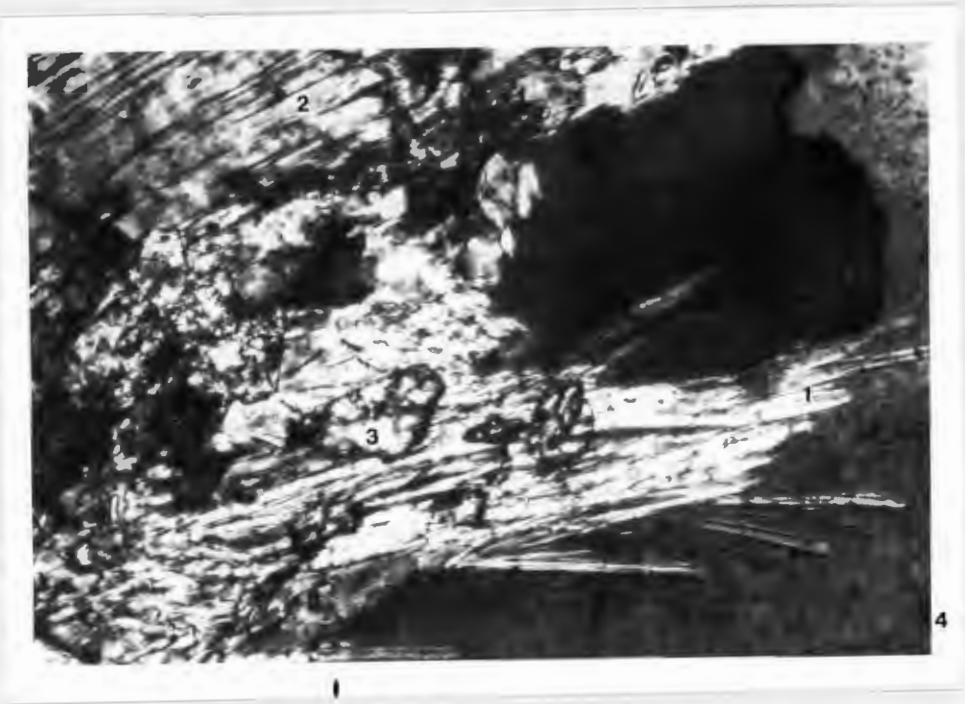

Plate 7. Formation of amphibole at contact of biotite and quartz during anatexis of granodiorites (biotite - hornblende - reaction as described in the text). Very fine needles of amphibole (1) at contact with quartz; biotite (2); epidote grains are retained from biotite (3); quartz (4).

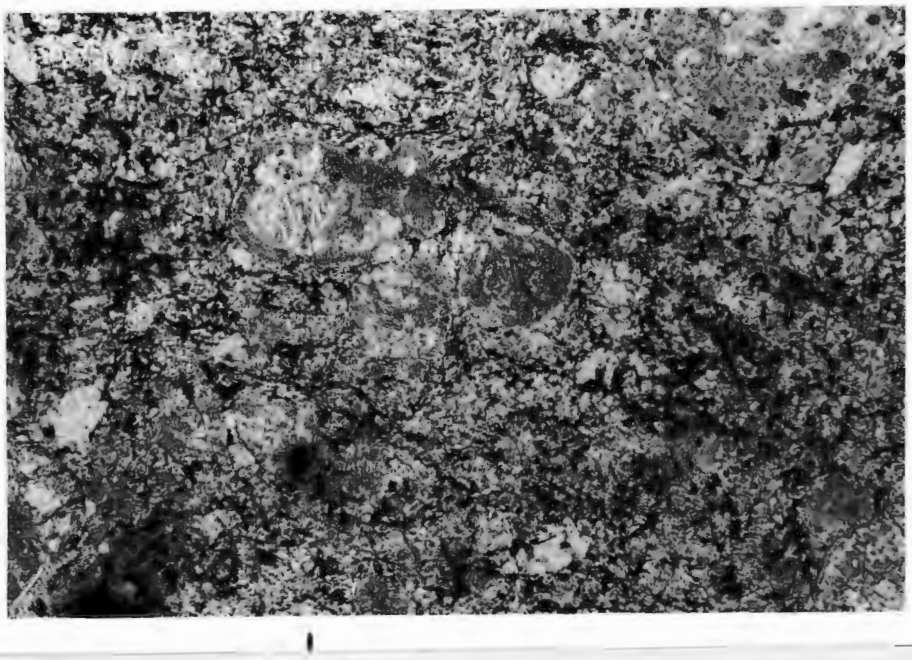

Plate 8. Irregularly zoned K-feldspar phenocrysts in a relatively fine-grained groundmass of a quartz-syenite of the Klipbokkop (RIC), suggesting at least partial refusion prior to the final emplacement, corroborating the view expressed in the text that resetting of radiometric ages in the RIC has been caused by remelting and not by regional metamorphism.

REFERENCES

*ACKERMAND, D. & KARL, F., 1972 - Experimental studies on the formation of inclusions in plagioclase from meta-tonalites, Hohe Tauern, Austria (Lower temperature stability limit of the paragenesis anorthite plus potash feldspar). *Contr. Miner. Petrol. 35,* 11-21.

AHRENDT, H., HUNZIKER, J.C., WEBER, K., 1978 - Age and degree of metamorphism and time of nappe emplacement along the southern margin of the Damara orogen, Namibia (South-West-Africa). *Geol. Rdsch. 67,* 719-742.

ALLSOPP, H.L., KÖSTLIN, E.O., WELKE, H., BURGER, A.J., KRÖNER, A. and BLIGNAULT, H.J., 1978 - Rb-Sr and U-Pb geochronology of late Precambrian and early Paleozoic igneous activity in the Richtersveld and southern South West Africa. *Trans. geol. Soc. S.Afr., (in press).*

*ALTHAUS, E., 1969 - Das System Al_2O_3- SiO_2- H_2O. *Neues Jb. Miner. Abh. 111,* 111-161.

_____, KAROTKE, E., NITSCH, K.H., WINKLER, H.G.F., 1970 - An experimental re-examination of the upper stability limit of muscovite and quartz. *Neues Jb. Miner. Mh.,* 325-336.

ASHWORTH, J.R., 1976 - Petrogenesis of migmatites in the Huntly-Portsoy area, northeast Scotland. *Miner. Mag. 40,* 661-682.

BENEDICT, P.C., WILD, D.de N., CORNELISSEN, A.K. & staff, 1964 - Progress report on the geology of the O'okiep Copper district. *In:* Haughton, H.S. (Ed.). The geology of some ore deposits in South Africa. *Geol. Soc. S.Afr. 2,* 238-318.

BERTRAND, J.M., 1976 - Granitoids and deformation sequence in the Goodhouse-Henkries area. A new interpretation of the relationship between the rocks in the Vioolsdrif-Goodhouse area and the Namaqualand and Bushmanland gneisses. *Ann. Rep. Precambr. Res. Unit, Univ. Cape Town, 13,* 61-70.

*BLACKWELL, D.D., 1969 - Heat-flow determinations in the northwestern United States. *J. Geophys. Res., 74,* 992-

*_____, 1971 *In*: Peacock (Ed.). *The structure and physical properties of the earth's crust.* Washington, 1971.

BAILEY, D.K., 1964 - Crustal warping and a possible tectonic control of alkaline magmatism. *J. Geophys. Res., 69,* 1103-1111.

_____ 1974 - Continental rifting and alkaline magmatism. Melting in the deep crust. *In:* Sørensen (Ed.). *The alkaline rocks. p.148-159; 436-442.* Wiley, London, New York.

BEUKES, G.J., 1973 - *'n Geologiese ondersoek van die gebied suid van Warmbad, Suidwes-Afrika, met spesiale verwysing na die metamorf-magmatiese assosiasies van die Voorkambriese gesteentes.* Unpubl. D.Sc. thesis, Univ. Orange Free State.

BLIGNAULT, H.J., 1974a - The tectonic zonation of part of the Namaqua Province in the lower Fish River/Narubis cross-section. *Ann. Reps. Precambr. Res. Unit, Univ. Cape Town 10 & 11,* 43-45.

BLIGNAULT, H.J., 1974b - Aspects of the Richtersveld Province, *In:* Kröner, A. (Ed.). Contributions to the Precambrian geology of southern Africa. 49-56. *Bull. Precambr. Res. Unit, Univ. Cape Town,* 15, 213p.

_____ 1977 - Structural-metamorphic imprint on part of the Namaqua Mobile Belt in South West Africa. *Bull. Precambr. Res. Unit, Univ. Cape Town,* 23, 197p.

_____ JACKSON, M.P.A., BEUKES, G.J. and TOOGOOD, D.J., 1974 - The Namaqua tectonic province in South West Africa. *In:* Kröner, A. (Ed.). Contributions to the Precambrian geology of southern Africa. *Bull. Precambr. Res. Unit, Univ. Cape Town,* 15.

* BURCHFIELD, B.C. and DAVIS, G.A., 1972 - Structural framework and evolution of the southern part of the Cordilleran orogen, western United States. *Amer. J. Sci.,* 272, 97-118.

BURGER, A.J., HUGO, P.J. & STRELOW, F.W.E., 1965 - The radiometric dating of certain pegmatites occurring in the Kenhardt and Gordonia districts, Cape Province, South Africa. *Ann. geol. Surv. S.Afr.,* 4, 87-98.

BÜSCH, W., SCHNEIDER, G. and MEHNERT, K.R., 1974 - Initial melting at grain boundaries Part II : Melting in rocks of granodioritic, quartzdioritic and tonalitic composition. *Neues Jb. Miner. Mh.* 345-370.

BUTAKOVA, E.L., 1974 - Regional distribution and tectonic relations to the alkaline rocks of Siberia, p.172-189. *In:* Sørensen (Ed.) *The alkaline rocks.* Wiley, London, New York, 622p.

CANN, J.R., 1970 - Upward movement of granitic magma. *Geol. Mag.* 107, 335-340.

CANTANZARO, E.J., 1968 - The interpretation of zircon ages. *In:* Hamilton, E.I., Farquhar, R.M. (Eds.) *Radiometric dating for geologists.* Interscience Publ., London.

* CIPRIANI, C., SASSI, F.P. & SCOLARI, A., 1971 - Metamorphic white micas: Definition and paragenetic fields. *Schweiz. Mineralog. petrogr. Mitt.* 51, 259-295.

CLARK, S.P. & JÄGER, E., 1969 - Denudation rate in the Alps from geochronologic and heat flow data. *Am. J. Sci.* 267, 1143-1160.

CLIFFORD, T.N., 1968 - Radiometric dating and the pre-Silurian geology of Africa. *In:* E.I. Hamilton and R.M. Farquhar (Eds.) *Radiometric dating for geologists.* Interscience Publ. London, 299-416.

_____ 1970 - The structural framework of Africa. *In:* Clifford, T.N. and Gass, I.G. (Eds.) *African magmatism and tectonics.* Oliver and Boyd, Edinburgh, 1-26.

*CLIFFORD, T.N., 1974 - Review of African granulites and related rocks. *Spec. Pap. geol. Soc. Am., 156.*

_____ GRONOW, J., REX, D.C. & BURGER, A.J., 1975 - Geochronological and petrogenetic studies of high-grade metamorphic rocks and intrusives in Namaqualand, South Africa. *J. Petrology 16 (1),* 154-188.

COBBOLD, R., COSGROVE, J.W., SUMMERS, J.M., 1971 - Development of internal structures in deformed anisotropic rocks. *Tectonophysics 12,* 23-53.

COETZEE, C.B., 1941 - The petrology of the Goodhouse-Pella area, Namaqualand, South Africa. *Trans. geol. Soc. S.Afr. 28,* 199-205.

CORNELL, D.H., 1977 - A post-Transvaal age for the Marydale formation, Kheis Group, southern Africa. *Earth Planet. Sc. Lett. 37,* 117-123.

CURRIE, J.B., PATNODE, H.W. & TRUMP, R.P., 1962 - Development of folds in sedimentary strata. *Bull. geol. Soc. Am. 73,* 655-74.

*DICKINSON, W.R., 1972 - Evidence for plate tectonic regimes in the rock record. *Am. J. Sci., 272,* 551-576.

DICKINSON, B. & WATSON, J., 1976 - Variations in crustal level and geothermal gradient during the evolution of the Lewisian complex of northwest Scotland. *Precambrian Research 3,* 363-374.

DE ROEVER, W.P., 1956 - Some differences between post-Paleozoic and older regional metamorphism. *Geologie Mijnb (NS) 18e,* 123-127.

DE VILLIERS, J. & SÖHNGE, P.G., 1959 - The geology of the Richtersveld. *Mem. geol. Soc. S.Afr. 48.*

DI PIERRO, M., LORENZONI, S., ZANETTIN LORENZONI, E., 1973 - Phengites and muscovites in Alpine and pre-Alpine phyllites of Calabria (southern Italy). *Neues Jb. Miner. Abh. 119,* 57-64.

DUNOYER DE SEGONZAC, G., FERRERO, J. & KUBLER, B., 1968 - Sur la Cristallinité de l'Illite dans la diagenese et l'Achimetamorphisme. *Sedimentology 10,* 137-143.

*_____ 1970 - The transformation of clay minerals during diagenesis and low-grade metamorphism : A review. *Sedimentology 15,* 281-346.

ERNST, W.G., 1963 - Significance of phengitic micas from low-grade schists. *Am. Miner. 48,* 1357.

_____ 1972 - Occurrence and mineralogic evolution of blueschist belts with time. *Am. J. Sci., 272,* 657-668.

*_____ 1974 - Metamorphism and continental margins. *In:* Burk, C.A., Drake, C.L. (Eds.) : *The geology of continental margins.* Springer, 1974.

ESKOLA, P., 1960 - Granitentstehung bei orogenese und epirogenese. *Geol. Rdsch., 50,* 105-123.

EVANS, B.W., 1965 - Application of a reaction-rate method to the breakdown of equilibria of muscovite and muscovite plus quartz. *Am. J. Sci. 263,* 647-667.

_____ GUIDOTTI, Ch.V., 1966 - The sillimanite-potash feldspar isograd in western Maine, USA. *Contr. Miner. Petrol., 12,* 25-62.

FETTES, D.J., GRAHAM, C.M., SASSI, F.P. & SCOLARI, A., 1976 - The basal spacing of potassic white micas and facies series variation across the Caledonides. *Scott. J. Geol., 12, (3),* 227-236.

FLINN, D., 1969 - Grain contacts in crystalline rocks. *Lithos., 3,* 361-370.

FREY, M., 1970 - The step from diagenesis to metamorphism in pelitic rocks during Alpine orogenesis. *Sedimentology, 15,* 261-79.

FYFE, W.S., 1976 - Heat flow and magmatic activity in the Proterozoic. *Phil. Trans. R. Soc. Lond. A280,* 655-660.

GASS, I.G., CHAPMAN, D.S., POLLACK, H.N. & THORPE, R.S., 1978 - Geological and geophysical parameters of mid-plate volcanism. *Phil. Trans. R. Soc. Lond. A288,* 581-595.

GEVERS, T.W., PARTRIDGE, F.C. & JOUBERT, G.K., 1937 - The pegmatite area south of the Orange River in Namaqualand. *Mem. geol. Surv. S.Afr., 31,* 180p.

GIBBON, D.L. & WYLLIE, P.J., 1969 - Experimental studies of igneous rock series : Farrington Complex, North Carolina, and the Star Mountain rhyolite, Texas. *J. Geol., 77,* 221-239.

GINGERICH, P.D., 1969 - Markov analysis of cyclic alluvial sediments. *J. sedim. Petrol., 39,* 330-332.

GUIDOTTI, C.V., 1973 - Compositional variation of muscovite as a function of metamorphic grade and assemblage in metapelites from northwest Maine. *Contr. Miner. Petrol., 42,* 33-42.

_____ & SASSI, F.P., 1976 - Muscovite as a petrogenetic indicator mineral in pelitic schists. *Neues Jb. Miner. Abh., 127,* 97-142.

HAACK, U., 1976 - Rekonstruction der Abkühlungsgeschichte des Damara Orogens in Südwest-Afrika mit Hilfe von Spaltspuren Altern. *Geol. Rdsch., 65,* 967-1002.

HALFERDAHL, L.B., 1961 - Chloritoid : Its composition, X-ray and optical properties, stability and occurrence. *J. Petrology, 2 (1),* 49-135.

HEIER, S., 1978 - The distribution and redistribution of heat-producing elements in the continents. *Phil. Trans. R. Soc. Lond. A228,* 393-400.

HIGGINS, M.W., 1971 - Cataclastic rocks. *Prof. Pap. U.S. geol. Surv., 687.*

HOBBS, B.E., MEANS, W.D. & WILLIAMS, P.F., 1976 - *An outline of structural geology.* Wiley, London, 571p.

HÖCK, V., 1974 - Coexisting phengite, paragonite and margarite in metasediments of the Mittlere Hohe Tauern, Austria. *Contr. Miner. Petrol.* 43, 261-273.

* HOFFMAN, P., 1973 - Evolution of an early Proterozoic continental margin : the Coronation geosyncline and associated aulacogens of the northwest Canadian Shield. *Phil. Trans. R. Soc. Lond., A273,* 547-81.

HOLLAND, H.B., 1972 - Granites, solutions and base metal deposits. *Econ. Geol., 67, (3),* 281.

* HSU, L.C., 1968 - Selected phase relationships in the system Al-Mn-Fe-Si-O-H: Model for garnet equilibria. *J. Petrology, 9,* 40-83.

HUGO, P. J., 1969 - The pegmatites of the Kenhardt and Gordonia districts, Cape Province. *Mem. geol. Surv. S.Afr., 58.*

HUTCHINSON, R.W., 1978 - Geological and geochemical evolution of massive sulphide deposits. *Econ. geol. Res. Unit., Univ. Witwatersrand.* Programme of post-graduate course in Economic Geology, 10, 1978.

ILLIES, H.J., 1970 - Graben tectonics as related to crust and mantle interaction, p.4-27. *In:* Graben problems, Illies, J.H., Mueller, St. (Eds.) *Internat. Upper Mantle Proj. Sci. Report 27.* Schweitzerbart, Stuttgart.

JACKSON, M.P.A., 1976 - High-grade metamorphism and migmitisation of the Namaqua Metamorphic Complex around Aus in the southern Namib desert, South West Africa. *Bull. Precambr. Res. Unit, Univ. Cape Town, 18*

JAEGER, J.C., 1957 - The temperature in the neighbourhood of a cooling intrusive sheet. *Am. J. Sci., 255,* 306-318.

_____1961 - The cooling of irregularly shaped igneous bodies. *Am. J. Sci., 259,* 721-734.

JAHNS, R.H. & BURNHAM, C.W., 1969 - Experimental studies of pegmatite genesis : I.A. Model for the derivation and crystallisation of granitic pegmatites. *Econ. Geol., 64, (8),* 843-863.

JAMES, H.L., 1954 - Sedimentary facies of iron formation. *Econ. Geol., 49,* 235-93.

JOUBERT, P., 1971 - The regional tectonism of the gneisses of part of Namaqualand. *Bull. Precambr. Res. Unit, Univ. Cape Town 10.*

* _____ & KRÖNER, A., 1971 - The Stinkfontein formation south of the Richtersveld. *Trans. geol. Soc. S.Afr. 75,* 47-54.

JUNG, J. & BROUSSE, R., 1959 - *Classification modale des roches éruptives.* Masson, Paris, 122p.

KAISER, E., 1926 - Die Eruptivgesteine der Chloritschieferstufe, der Konkip- und der Namaformation und die Amphibolitisierung in diesen Stufen. *In:* Kaiser, E. (Ed.) *Die Diamantenwüsten Südwestafrikas.* D. Reimer, Verlag, Berlin, 190-208.

KERRICK, D.M., 1968 - Experiments on the upper stability limit of pyrophyllite at 1,8 and 3,9 kilobars water pressure. *Am. J. Sci., 266,* 204-214.

KLEINSCHMIDT, G., SASSI, F.P. & ZANFERRARI, A., 1976 - A new interpretation of the metamorphic history in the Saualpe basement (eastern Alps). *Neues Jb. Geol. Paläont. Mh. 11,* 653-670.

_____, NEUGEBAUER, J; SCHÖNENBERG, R., 1975 - Gesteinsinhalt und Stratigraphie der Phyllitgruppe in der Saualpe. *Clausth. Geol. Ahb., 1,* 11-44.

_____ & RITTER, U., 1976 - Geologisch-petrographischer Aufbau des Koralpenkristallins südlich von Soboth/Steiermark-Kärnten (Raum Hühnerkogel-Laaken). *Carinthia II, 166/86,* 57-91.

KNABE, W., 1970 - Reaktionen des Biotits bei der Anatexis. *Jb. Geol. 88,* * * 355-372.

KÖSTLIN, E.O., 1971 - *The Rb-Sr radiometric ages of the Richtersveld Complex and neighbouring Bostonite dykes.* Unpubl. M.Sc. thesis, Univ. Witwatersrand.

KRÄUTNER, H.G., SASSI, F.P., ZIRPOLI, G. & ZULIAN, T., 1975 - The pressure characters of the pre-Alpine metamorphisms in the east Carpathians (Romania). *Neues Jb. Miner. Abh. 125,* 278-296.

*KRETZ, R., 1963 - Note on some equilibria in which epidote and plagioclase participate. *Am. J. Sci., 261,* 973-988.

_____ 1969 - On the spatial distribution of crystals in rocks. *Lithos., 2,* 39-66.

*KROGH, E.J., 1977 - Evidence of Precambrian continent-continent collision in western Norway. *Nature, 267,* 17-19.

KRÖNER, A., 1974 - The Gariep Group, Part I, Late Precambrian Formations in the western Richtersveld, Northern Cape Province. *Bull. Precambr. Res. Unit, Univ. Cape Town, 13.*

_____ 1977 - The Precambrian geotectonic evolution of Africa : Plate accretion versus plate destruction. *Precambrian Research, 4,* 163-213.

_____, GERMS, G.J.B., 1971 - A re-interpretation of the Numees-Nama contact at Aussenkjehr, South West Africa. *Trans. geol. Soc. S.Afr., 74,* 69-74.

_____, BLIGNAULT, H.J., 1977 - Towards a definition of some tectonic and igneous provinces in western South Africa and southern South West Africa. *Trans. geol. Soc. S.Afr., 79,* 232-238.

_____, RICHARDSON, M.H., JACOB, R.E., 1978 - Rb-Sr geochronology in favour of polymetamorphism in the Pan-African Damara belt of Namibia (South West Africa). *Geol. Rdsch., 67,* 688-705.

KUBLER, B., 1966 - La cristallinité de l'illite et les zone tout à fait supérieur du métamorphism. *In: Colloque sur les etages tectoniques,* A. lá Baconnière, Neuchatel, 105-122.

KUNO, H., 1968 - Differentiation of basalt magmas. *In:* Hess, H.H., (Ed.) *Basalts. The Poldervaart treatise on rocks of basaltic composition.* 2, Interscience, 623.

LAMBERT, I.B., ROBERTSON, J.K., WYLLIE, P.J., 1969 - Melting reactions in the system $KAlSi_3O_8$ - SiO_2 - H_2O to 18,5 kilobars. *Am. J. Sci., 267,* 609-626.

LAMBERT, T.W. & WYLLIE, P.J., 1974 - Melting of tonalite and crystallisation of andesite liquid with excess water to 30 kb. *J. Geol., 82,* 88-97.

LEE, W.H.K. & UYEDA, S., 1965 - Review of heat flow data. *In:* Lee, W.H.K. (Ed.) *Terrestrial heat flow.* Geophys. Monograph. series Nr. 8, Amer. Geophys. Union Publication Nr. 1288.

MAALØE, S. & WYLLIE, P.J., 1975 - Water content of a granite magma deduced from the sequence of crystallisation determined experimentally with water-undersaturated conditions. *Contr. Miner. Petrol., 52,* 175-191.

MARTIN, H., 1965 - The Precambrian geology of South West Africa and Namaqualand. *Precambr. Res. Unit, Univ. Cape Town,* Rustica Press, Wynberg, 159p.

_____ 1969 - Problems of age relations and structure in some metamorphic belts of Southern Africa, *In:* Wynne-Edwards, H.R. (Ed.) *Age relations in high grade metamorphic terrains.* Geol. Ass. Canada Spec. Paper 5, 17-36p.

_____ & PORADA, H., 1977 - The intracratonic branch of the Damara Orogen in South West Africa. I. Discussion of geodynamic models. *Precambrian Research 5,* 311-338.

MARTIN, R.F. & BONIN, B., 1976 - Water and magma genesis : The association hypersolvus granite - subsolvus granite. *Can. Miner., 14, (3),* 228-237.

MATHER, J.D., 1970 - The biotite isograd and the lower greenschist facies in the Dalradian rocks of Scotland. *J. Petrology, 11,* 253-275.

MATHIAS, M., 1940 - A comparative study of the Namaqualand granites. *Trans. geol. Soc. S.Afr., 42,* 175-203.

MATSUMOTO, T., 1966 - Fundamental problems in the circum-Pacific orogenesis, *Tectonophysics, 4,* 595-613.

MAY, P.R., 1971 - Pattern of Triassic-Jurassic diabase dykes around the north Atlantic in the context of predrift position of the continents. *Bull. geol. Soc. Am., 82,* 1285-92.

MCDOWELL, S.D. & WYLLIE, P.J., 1971 - Experimental studies of igneous rock series : The Kungnat syenite complex of southwest Greenland. *J. Geol.,* 173-194.

MCKENZIE, D.P. & SCLATER, J.G., 1968 - Heat flow inside the island arcs of the northwestern Pacific. *J. Geophys. Res., 73,* 3173-3179.

MCMILLAN, M.D., 1965 - Preliminary report on the geology of the lower Fish River area, South West Africa. *Ann. Rep. Precambr. Res. Unit, Univ. Cape Town, 3,* 6-16.

MCMILLAN, M.D., 1968 - The geology of the Witputs Sendelingsdrif area. *Bull. Precambr. Res. Unit, Univ. Cape Town, 14.*

MEANS, W.D., WILLIAMS, P.F., 1972 - Crenulation cleavage and faulting in an artificial salt-mica schist. *J. Geol., 80,* 569-91.

MEHNERT, K.R., 1968 - *Migmatites and the origin of granitic rocks.* Elsevier, Amsterdam, 1968.

_____, BÜSCH, W., & SCHNEIDER, G., 1973 - Initial melting at grain boundaries of quartz and feldspar in gneisses and granulites. *Neues Jb. Miner. Mh.* 165-183.

MINEAR, J.W., TOKSÖZ, M.N., (1970) - Thermal regime of a downgoing slab. *Tectonophysics, 10,* 367-390.

MIDDLEMOST, A.E.K., 1963 - *Geology of the southeastern Richtersveld.* Unpubl. Ph.D. thesis, Univ. Cape Town.

* _____, 1964-Petrology of the plutonic and the dyke rocks of the southeastern Richtersveld. *Trans. Soc. S.Afr., 67,* 227-261.

* MILLER, R.MC.G., 1973 - The implication of albite rims in granite studies. *In:* Lister, L.A. (Ed.) Symposium on granites, gneisses and related rocks. *Spec. Pap. geol. Soc. S.Afr., 3.*

MITCHELL, A.H. & READING, H.G.(1969) - Continental margins, geosynclines and ocean floor spreading. *J. Geol. 77,* 629-

* _____1971 - Evolution of island arcs. *J. Geol., 79,* 253- .

MIYASHIRO, A., 1972 - Metamorphism and related magmatism in plate tectonics. *Am. J. Sci., 272,* 629-656.

_____ 1973 - *Metamorphism and metamorphic belts.* Allen, London.

_____ 1974 - Volcanic rock series in island arcs and active continental margins. *Am. J. Sci., 271,* 321-355.

MOODY, J.D. & HILL, M.J., 1956 - Wrenchfault tectonics. *Bull. geol. Soc. Am., 67,* 1207-1246.

* MOORBATH, S., 1978 - Age and isotope evidence for the evolution of the continental crust. *Phil. Trans. R. Soc. Lond., A288,* 401-413.

MOORE, A.C., 1970 - Descriptive terminology for the textures of rocks in granulite facies terrains. *Lithos 3,* 123-127.

_____, 1975 - The petrography and the regional setting of the Tantalite Valley Complex, South West Africa. *Trans. geol. Soc. S.Afr. 78,* 235-49.

MOORE, J.M., 1977 - The geology of Namiesberg, northern Cape. *Bull. Precambr. Res. Unit, Univ. Cape Town, 20,*

OXBURGH, E.R. & TURCOTTE, D.L., 1970 - The thermal structure of island arcs. *Bull. geol. Soc. Am., 81,* 1665.

OXBURGH, E.R. & TURCOTTE, D.L., 1971 - Origin of paired metamorphic belts and crustal dilatation in island arc regions. *J. Geophys. Res.*, *76*, 1315-1327.

PARSONS, I. & BOYD, R., 1971 - Distribution of potassic feldspar polymorphs in intrusive sequences. *Min. Mag.*, *38*, 295-311.

PATERSON, M.S. & WEISS, L.E., 1966 - Experimental deformation and folding in phyllite. *Bull. geol. Soc. Am.*, *77*, 343-74.

PICCARRETA, G. & ZIRPOLI, G., 1974 - The barometric significance of the potassic white micas of the metapelites outcropping south of the low Savuto valley (Calabria, southern Italy). *Neues Jb. Miner. Mh. H.10*, 454-461.

PILGER, A., 1952 - Zur Gliederung und Kartierung der Siegener Schichten, I, II. *Geol. Jb.*, *66*, 703-722.

_____, SCHÖNENBERG, R. & WEISSENBACH, N. (Herausgeber)1975 - Geologie der Saualpe. *Clausthaler Geol. Abh., Sonderband.*

PIWINSKII, A.J. 1968 - Experimental studies of igneous rock series : Central Sierra Nevada batholith, California. *J. Geol.*, *76*, 548-

_____ & WYLLIE, P.J. (1970) - Experimental studies of igneous rock series : felsic body suite from the Needle Point pluton, Wallowa batholith. *J. Geol.*, *78*, 52-76.

PRETORIUS, D.A., 1974 - The structural boundary between the Kaapvaal and the Sonama crustal provinces. *Inform. Circ. econ. Geol. Res. Unit, Univ. Witwatersrand*, *88*,

RAMBALDI, E.R., 1973 - Variation in the composition of plagioclase and epidote in some metamorphic rocks near Bankroft/Ontario. *Can. J. Earth Sci.*, *10*, 852-868.

RAMBERG,H., 1963 - Fluid dynamics of viscous buckling applicable to folding of layered rocks. *Bull. Am. Ass. Petrol. Geol.* *47*, *(3)*, 484-505.

_____1964 - Selective buckling of composite layers with contrasted rheological properties, a theory for simultaneous formation of several order folds. *Tectonophysics*, *1*, 307-41.

RAMSAY, J.G., 1967 - *Folding and fracturing of rocks.* McGraw-Hill, 1967.

REID, D.L., 1974 - Preliminary report on petrologic studies of volcanic and intrusive rocks in the Vioolsdrif region, lower Orange River, *In:* Kröner, A. (Ed.) : Contributions to the Precambrian geology of southern Africa, 57-67. *Bull. Precambr. Res. Unit, Univ. Cape Town*, *15*, 213p.

*REID, D.L., 1976 - Geochronology of the Haib - Vioolsdrif igneous province. *Ann. Rep. Precambr. Res. Unit, Univ. Cape Town, 13,* 49-60.

_____ 1977 - Geochemistry of Precambrian igneous rocks in the lower Orange River region. *Bull. Precambr. Res. Unit, Univ. Cape Town, 22,*

_____ 1978a - Total rock Rb-Sr and U-Th-Pb isotopic study of Precambrian metavolcanic rocks in the lower Orange River region, South Africa. *Earth Planet. Sc. Lett., in press.*

_____ 1978b - Age relations within the Proterozoic Vioolsdrif batholith, lower Orange River region, South Africa. *Precambrian Research, in press.*

RHODES, R., 1971 - Structural geometry of subvolcanic ring complexes as related to pre-Cenozoic motions of continental plates. *Tectonophysics, 12,* 111-117.

RICHARDSON, S.W., GILBERT, M.C. & BELL, P.M., 1969 - Experimental determination of kyanite - andalusite and andalusite - sillimanite equilibria. *Am. J. Sci., 267,* 259-72.

RINGWOOD, A.E. & GREEN, D.H., 1966 - An experimental investigation of the gabbro-eclogite transformation and some geophysical implications. *Tectonophysics, 3,* 383-427.

*RITTER, U., 1976 - Preliminary report on the geology of the northeastern Richtersveld. *Ann. Rep., Precambr. Res. Unit, Univ, Cape Town, 13,* 42-48.

_____1978 - The southeastern Richtersveld between Eksteenfontein and Klein Helskloof, its relationship to Gariep metamorphism and tectonism and to the Namaqua Metamorphic Complex. *Ann. Rep. Precambr. Res. Unit, Univ. Cape Town, 14 & 15.*

ROBERTS, B. & SIDDANS R.W.B., 1971 - Fabric studies in the Lewyd Mawr Ignimbrite, Coernarvonshire, North Wales. *Tectonophysics, 12,* 283-306.

ROBERTSON, J.K. & WYLLIE, P.J., 1971 - Rock-water-systems, with special reference to the water deficient region. *Am. J. Sci., 271,* 252-277.

ROBINSON, P.,1966 - Alumino silicate polymorphs and paleozoic erosion rates in central Massachusetts. *Abstr. Trans. Am. geophys. Un., 47,* 424.

ROERING, C., 1967 - Non-orogenic granites in the Archaean geosyncline of the Barberton mountain-land. *Inform. Circ. econ. Geol. Res. Unit, 35,* 1-13.

*ROGERS, A.W., 1907 - Geological survey of parts of Vryburg, Kuruman, Hay and Gordonia. *Ann. Rep. geol. Comm., C.G.A. for 1907,* 11-122.

_____ 1915 - The geology of part of Namaqualand. *Trans. geol. Soc. S.Afr., 18,* 72-100.

RODDICK, J.C., COMPSTON, W. & DURNEY, D.W., 1976 - The radiometric age of the Mount Keith granodiorite, a maximum age estimate for an Archean greenstone sequence in the Yilgarn Block, Western Australia. *Precambrian Research, 3,* 55-78.

*RUTLAND, R.W.R., 1962 - Feldspar structure and the equilibrium between plagioclase and epidote : a reply. *Am. J. Sci., 260,* 153-157.

_____ 1973 - On the interpretation of Cordilleran orogenic belts. *Am. J. Sci., 273,* 811-849.

SAGGERSON, E.P. & TURNER, L.M., 1976 - A review of the distribution of metamorphism in the ancient Rhodesian craton. *Precambrian Research, 3,* 1-53.

SANDER, B., 1950 - *An introduction to the study of fabrics of geological bodies.* Pergamon Press, Lond.

SASSI, F.P. & SCOLARI, A., 1974 - The b_o value of the potassic white micas as a barometric indicator in low-grade metamorphism of pelitic schists. *Contr. Miner. Petrol., 45,* 143-152.

SCHERMERHORN, L. J. G., PRIEM, H.N.A., BOERIJK, N.A.I.M., HEBEDA, E.A., VERDURMEN, E.A.Th. & VERSCHURE, R.H., 1978 - Age and origin of the Messejana fault-dike system (Portugal and Spain) in the light of the opening of the north Atlantic ocean. *J. Geol., 86,* 299-309.

SCHNEIDERHÖHN, H., 1961 - *Die Erzlagerstätten der Erde, Bd. II : Die Pegmatite.* Fischer, Stuttgart, 1961.

SCRUTTON, R.A., 1973 - The age relationship of igneous activity and continental break-up. *Geol. Mag., 110,* 227-34.

SHAW, H.R., 1974 - Diffusion of H_2O in granitic liquids : Part I : Experimental data; Part II : Mass transfer in magma chambers. *In:* Geochemical transport and kinetics (A.W. Hofmann, B.J. Giletti, H.S. Yoder and R.A. Yund, Eds.), *Carnegie Inst. Wash. Publ. 634,* 139-170.

SILLITOE, R.H., 1973 - The tops and bottoms of porphyry copper deposits. *Econ. Geol., 68,* 799-815.

SØRENSEN, H. (Ed.), 1974 - *The Alkaline rocks, I-II.* Wiley, London, New York, 622p.

SPRY, A., 1969 - *Metamorphic textures.* Pergamon Press, Lond., 350p.

STEWART, J.W., EVERNDEN, J.F. & SNELLING, N.J., 1974 - Age determinations from Andean Peru : A Reconnaissance survey. *Bull. geol. Soc. Am., 85,* 1107-1116.

STORRE, B. & KAROTKE, E., 1972 - Experimental data on melting reactions of muscovite-quartz in the system K_2O-Al_2O_3-SiO_2-H_2O to 20 kb water pressure. *Contr. Miner. Petrol. 36,* 343-345.

STRECKEISEN, A., 1973 - Classification and nomenclature of plutonic rocks, recommendations. *Neues. Jb. Miner. Mn., H4,* 149-164.

TAKEUCHI, H. & UYEDA, S., 1965 - A possibility of present-day regional metamorphism. *Tectonophysics, 2,* 59-68.

*TCHALENKO, J.S., 1970 - Similarities between shear zones of different magnitudes. *Bull. geol. Soc. Am., 81,* 1625-1640.

THOMPSON, A.B., 1970 - A note on the kaolinite-pyrophyllite equilibrium. *Am. J. Sci., 268,* 454-458.

TOOGOOD, D.J., 1974 - Preliminary report on the geology of the Onseepkans area, southeastern South West Africa. *Ann. Rep. Precambr. Res. Unit, Univ. of Cape Town, 10-11,* 31-37.

_____, 1976 - Structural and metamorphic evolution of a gneiss terrain in the Namaqua belt near Onseepkans, South West Africa. *Bull. Precambr. Res. Unit, Univ. Cape Town, 19,*

*TORSKE, T., 1977 - The south Norway Precambrian region - a Proterozoic cordilleran-type orogenic segment. *Norsk. geol. Tidsskr., 57,* 97-120.

TRÖGER, E.W., 1971 - *Optische Bestimmung der Gesteinsbildenden Minerale Bd.I,* Stuttgart, 1971.

*UYEDA, S. & HORAI, K., 1964 - Terrestrial heat flow in Japan. *J. Geophys. Res., 69,* 2121-

VELDE, B., 1965 - Phengite micas : synthesis, stability and natural occurrence. *Am. J. Sci., 263,* 886-913.

_____1967 - Si^{4+} content of natural phengites. *Contr. Miner. Petrol., 14,* 250-258.

VISTELIUS, A.B., 1966 - Genesis of the Mt. Belaya granodiorite, Kamchatka (an experiment in stochastic modelling). *Dokl. (Proc.) Acad. Sci., U.S.S.R., 167,* 48-50 *(Dokl. Akad. Nauk. U.S.S.R., 167,* 1115-8).

_____ 1972a - Ideal granite and its properties. I. The stochastic model. *J. Int. Ass. Math. geol., 4,* 89-102.

_____1972b - Ideal granites and their metasomatic transformation : stochastic model, statistical description and natural rocks. *Int. geol. Congr. Canada, XXIV, Abstr.,* 518-19.

WADSWORTH, W.B., 1975 - The petrogenetic significance of grain transition probabilities, Cornelius pluton, Ajo, Arizona. *Mem. geol. Soc. Am., 142,*

WARD, J.H.W., 1977 - The geology of the area south of Vioolsdrif. *Rep. Atomic Energy Board, PEL-257,* 48p.

WATSON, J.V., 1973-Effects of reworking on high grade gneiss complexes. *Phil. Trans. R. Soc. Lond. A273,* 443-455.

_____1978 - Precambrian thermal regimes. *Phil. Trans. R.Soc. Lond, A288,* 431-440.

WATTERS, B.R., 1974 - Stratigraphy, igneous petrology and evolution of the Sinclair Group in southern South West Africa. *Bull. Precambr. Res. Unit, Univ. Cape Town, 16,*

_____1977 - The Sinclair Group : Definition and regional correlation. *Trans. geol. Soc. S.Afr., 80,* 9-16.

WEAVER, C.E., 1960 - Possible use of clay minerals in search for oil. *Bull. Am. Ass. Petrol. Geol., 44,* 1505, 1518.

WEBER, K., 1972a - Notes on determination of illite crystallinity. *Neues Jb. Miner. Mh.,* 267-276.

_____1972b - Kristallinität des Illits in Tonschiefern und andere Kriterien schwacher Metamorphose im nordöstlichen Rheinischen Schiefergebirge. *Neues Jb. Miner. Abh. 141,* 333-363.

WELKE, H.J., BURGER, A.J., CORNER, B., KRÖNER, A., & BLIGNAULT, H. J., 1978 - U-Pb and Rb-Sr age determinations on middle Proterozoic rocks from the lower Orange River area, southwestern Africa. *Trans. geol. Soc. S.Afr. (in press).*

WHITNEY, J.A., 1975a - The effects of pressure, temperature and X_{H_2O} on phase assemblage in four synthetic rock compositions. *J.geol., 83,* 1-31

_____ 1975b - Vapour generation in a quartzmonzonite magma : A synthetic model with application to porphyry copper deposits. *Econ. Geol. 70,* 346-358.

WHITTEN, E.H.T. & DACEY, M.F., 1975 - On the significance of certain Markovian features of granitic textures. *J. Petrology, 16, (2),* 429-453.

WILCOX, R.E., HARDING, T.P. & SEELY, D.R., 1973 - Basic wrench tectonics. *Bull. Am. Ass. Petrol. Geol., 57,* 74-96.

* WILLIAMSON, D.H., 1953 - Petrology of chloritoid and staurolite rocks north of Stonehaven, Kincardineshire. *Geol. Mag., 90,* 351-61.

WINKLER, H.G.F., 1974 - *Petrogenesis of metamorphic rocks.* Springer, Berlin.

WRIGHT, J.B., 1969 - A simple alkalinity ratio and its application to questions of non-orogenic granite genesis. *Geol. Mag. 106,* 370-384.

* WRIGHT, T.L., 1968 - X-ray and optical study of alkali feldspar : II. An X-ray method for determining the composition and structural state from measurement of 2 theta values for three reflections. *Am. Miner., 53,* 88-102.

WYNNE-EDWARDS, H. R., 1976 - Proterozoic ensialic orogenesis : The Millipede model of ductile plate tectonics. *Am. J. Sci., 276,* 927-953.

YODER, H.S., 1952 - Change of melting point of diopside with pressure. *J. Geol.*, *60*, 364-374.

ZEN, E-an, 1960 - Metamorphism of lower Paleozoic rocks in the vicinity of the Taconic range in west-central Vermont. *Am. Miner.*, *45*, 129-

_____ 1961 - Mineralogy and petrology of the system Al_2O_3-SiO_2-H_2O in some pyrophyllite deposits of north Carolina. *Am. Miner.*, *46*, 52-66.

ZWART, H.J., 1962 - On the determination of polymetamorphic mineral associations and its application to the Bosost area (Central Pyrenees). *Geol. Rdsch.*, *52*, 38-65.

* _____ 1969 - Metamorphic facies series in the European orogenic belts and their bearing on the causes of orogeny. *In:* Wynne-Edwards, H.R. : Age relations in high-grade metamorphic terrains. *Spec. Pap. Geol. Soc. Can.*, *5*, 7-16.

* Consulted but not quoted in the text

* * Inserted after completion of thesis:

KÖPPEL, V., 1978 - Lead isotope studies of stratiform ore deposits of Namaqualand, Northwest Cape Province, South Africa and their implications on the age of the Bushmanland Supergroup, In: Zartman, R.E. (Ed) : Short papers of the fourth international conference, Geochronology, Cosmochronology, Isotope Geology. *Geol. Survey Open-File Report 78-701*, 223-226.

Appendix 1

THE CONCEPT OF GRAIN TRANSITION PROBABILITIES

a) *Historical background*

Quantitative textural studies of intrusive and metamorphic rocks have only developed slowly, mainly because of the complexity of their fabrics and the difficulties in defining and measuring textural properties. The earliest known approach has been ventured by Sander (1950) who suggested a numerical evaluation of the "openness" of a texture with respect to a particular mineral species by relating the total number of grains of a given species and the number of grains of the same species touching each other. His *Proximity Index N* goes into the same direction and determines the number of grains with which a mineral grain is in immediate contact.

A more promising approach has been introduced during recent years mainly by Russian workers and consists of the analysis of grain contact frequencies. These data can be objectively obtained and tested according to statistical methods. In its basic form, *the sequence of transitions from one crystal or one mineral species to another along a line on a section through the rock is recorded.* The number of transitions of each type may then be displayed in the form of a *transition frequency* matrix and compared with random frequencies. In its more sophisticated form data thus obtained may be tested for their Markov properties, i.e. whether and to what extent the position of grains of a mineral-species are dependent on the position of mineral grains of the same or other species. It is therefore possible to introduce a stochastic model of crystallisation in granites as Vistelius (1966 , 1972) did and test real plutons against this model.

On empirical grounds, Vistelius and coworkers found that non-metasomatic "ideal" granites correspond to first order Markov chains while metasomatically altered granites correspond to second order Markov chains and that chi^2-values increase with increasing metasomatism (their Markovity index). In view of the frequent correlation of metasomatism and ore deposits the reality of this index is of considerable importance.

In western countries a small but growing number of workers has been dealing with grain transition frequencies in connection with textural problems in granites and metamorphic rocks. Whitten and Dacey (1975) gave a comprehensive account on the results and theories of the Russian working group around Vistelius and concluded that the Markov property of certain granitic textures was likely to reflect petrologically important but still unidentified factors but nevertheless rejected Vistelius' and coworkers' petrogenetic justification for it on the grounds of theoretical considerations.

Kretz (1969) investigated the distribution of crystals in a pyroxene-

scapolite-sphene granulite from Quebec and found random distribution of its main constituents within homogeneous portions of his slides. For these reasons he concluded that mineral nucleation sites apparently were located at random with complete disregard for other crystals in the vicinity. Flinn (1969), on the other hand, obtained similar data from gneisses from Shetland and Siberia and found by different methods of statistical evaluation that the distribution of mineral grains was non-random and that grains of the same mineral species showed the tendency to occur in contact with each other.

A slightly different approach was undertaken by Ashworth (1976) and Wadsworth (1975) who dealt more realistically with the degree of randomness of a texture rather than with the fruitless theoretical question when exactly randomness in the statistical sense begins. Ashworth (1976), investigating migmatites from northeast Scotland, concentrated on the different possibilities of the departure of a texture from randomness and regarded as a measure of the latter the value of chi^2 calculated against the matrix of expected frequencies. He was thus able to show textural differences between paleosomes and leucosomes. Wadsworth (1975) was the first to attempt to structure grain transition data according to a model of embedded Markov chains, i.e. transitions from a given state into itself were not recorded, as already previous authors had mentioned the difficulty to determine the exact boundary within grains of the same types (problem of subgrains, twins, etc.) Errors in measurement were therefore reduced to misidentification of mineral species. By calculating and comparing a *transition probability matrix* with an *independent trials probability matrix* he established grain sequence types and was thus able to map different types of textures within the Cornelia pluton, Arizona. His approach is regarded as the most realistic and many of his procedures have therefore been adopted in the investigation of the Vioolsdrif Intrusive Suite.

Although the reasons for granitic textures frequently having Markov properties may not be known, the relative and absolute values of the departure of their textures from randomness might still be a useful parameter. Grain transition frequencies in their basic form are useful in any case since they contribute one more dimension to the description of textural features and are in addition of a relatively objective and quantifiable nature.

b) *The application of grain transition probabilities in rocks of the eastern Richtersveld*

The procedure adopted is described below as far as necessary for the understanding of the basic principles. For mathematical and theoretical details the reader is referred to Whitten and Dacey (1975) and Wadsworth (1975) whose method has been adopted here to some extent. One thin section per specimen was investigated by the *line transect method* (Kretz, 1969), recording identity changes between mineral species along a line as shown in Figure A1.1.

All transitions between different mineral species were recorded and no restrictions were taken into account, e.g. that each grain along the line be encountered only once, as intergrowth of mineral grains is part

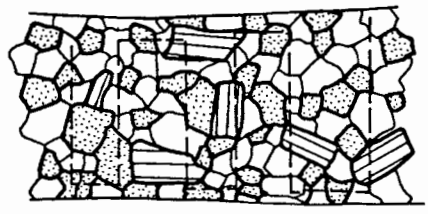

Fig. A1.1.

of the texture to be investigated and since it is generally impossible to determine whether an inclusion is real or connected with an adjacent grain outside the plane of the thin section (Wadsworth, 1976, p.262). 400 to 600 transitions were recorded in each thin section and entered into a *transition-frequency-matrix* (TFM):

TFM		state entered				
		qtz	*plg*	*kf*	*M*	row sum
state excited	*qtz*	-	89	34	102	225
	plg	94	-	23	27	144
	kf	36	24	-	24	84
	M	101	23	29	-	153
Column sum		231	136	86	153	606 matrix sum

It shows the frequency of identity changes between *different* mineral species. As transitions have been taken in both directions, the matrix must be symmetrical. From the TFM the *transition-probability-matrix* (TPM) is calculated by dividing each entry in the TFM by its corresponding row sum, e.g. in the present case the transition *qtz-plg* = 89/225 = 0,396, which means as each row sum equals one that the probability of entering from *qtz* into *plg* is 39,6%.

TPM				
	qtz	*plg*	*kf*	*M*
qtz	-	0,396	0,151	0,453
plg	0,652	-	0,160	0,188
kf	0,429	0,286	-	0,286
M	0,660	0,150	0,190	-

In contrast, the *independent-trials-probability-matrix* (ITPM) shows what the transition probabilities would be if the distribution of mineral species were at random. Calculating the transition *qtz-plg:*

$$\frac{\text{row sum } plg}{\text{matrix sum} - \text{row sum } qtz} = \frac{144}{606 - 225} = 0{,}378$$

Which means : taking into account the relative amounts of *plg* and *qtz* the probability of entering from *qtz* into *plg* is 37,8% in case of random distribution of mineral species.

ITPM

	qtz	*plg*	*kf*	*M*
qtz	-	0,378	0,220	0,402
plg	0,487	-	0,182	0,331
kf	0,431	0,276	-	0,293
M	0,497	0,318	0,185	-

For the recognition of grain sequence types the *difference-matrix* (DM) is obtained by subtracting the ITPM from the TPM. The DM has first been introduced by Gingerich (1969) in investigations of cyclic alluvial sediments and simplifies the recognition of probabilities which have either a positive or a negative deviation from randomness. The DM can be calculated in one step from the TFM with a programmable calculator and the whole procedure thus takes no more time than an ordinary modal analysis.

DM

	qtz	*plg*	*kf*	*M*
qtz	-	0,018	-0,069	0,051
plg	0,165	-	-0,022	-0,143
kf	-0,002	0,010	-	-0,007
M	0,163	-0,168	0,005	-

The values of the DM can be diagrammatically arranged as shown in Fig. A1.2. In this diagram values of the DM deviating positively from randomness are shown by an arrow. Although diagrams of this kind depict strictly speaking grain *sequences*, the grain sequence pattern as such can be interpreted as describing grain *associations*. For this reason the more inaccurate term "grain association diagram" is the better one and has been used in this investigation.

During the early stages of the investigation the grain sequence was recorded by assigning a number to each mineral species involved and by noting

the mineral species in their succession of occurrence. From this primary list the number of transitions had to be extracted and recorded in the transition-frequency-matrix. However, since the transitions are taken in

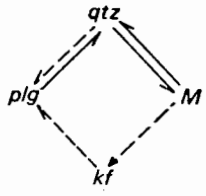

Fig. A1.2.
Grain association diagram. Arrows describe positive deviation from randomness. Different types of arrows can be used for different degrees of deviation.

both directions the TFM must be symmetrical, i.e. the transition *qtz* → *plg* must have the same number of entries as the transition *plg* → *qtz*. Since during practical determination the values within a pair of transitions hardly ever varied by more than 5%, the procedure could be simplified considerably by recording only each *pair* of transitions. That way a laboratory counter could be used in which one key was assigned to each pair of transitions, i.e. the transitions and not the individual mineral species were recorded and could be entered into the TFM directly. This procedure was adopted for most of the investigations presented here.

Appendix 2

ILLITE CRYSTALLINITY

In order to assess whether rocks of the Nama group had undergone metamorphism and to what extent, measurements of the Illite crystallinity had to be carried out.

a) *Theoretical background*

The formation of white micas out of clay minerals (illite) takes place gradually during diagenesis and very low grade metamorphism. The degree of transformation into white mica (illite crystallinity) can therefore be used to define the relative degree of diagenesis and very low grade metamorphism. It was determined for the first time by means of X-ray diffraction reflections by Weaver (1960) who used the ratio of the (001) illite reflection at 10Å to the height of the same reflection at 10,5Å (sharpness ratio of Weaver = *Weaver index*). Kubler (1966) for the same purpose used the *width* of the (001) illite peak at half height. More recently Weber (1972a) determined illite crystallinity by relating the width of the (001) illite reflection to the width of the (100) quartz reflection:

$$Hb_{rel} = \frac{Hb\ (001)\ illite\ (mm)}{Hb\ (100)\ qtz\ \ (mm)} \times 100$$

Hb = width of reflection at half height (Halbwertsbreite)

Hb_{rel} = rel. width of reflection at half height (relative Halbwertsbreite)

That way the measurement is independent of the instrumental setting and a possible instrumental error can be minimised.

b) *Measuring method*

Webers method was applied using slightly polished rockslabs and powder samples collected at two localities : M27 at Vioolsdrif, M8 at Helskloof. Measurements were carried out with a Philips Diffractometer with the following setting : Cu Kα, 40kV, 20mA, $\frac{1}{2}^{o}$ slit, Tc 4, $\frac{1}{4}^{o}$/min scanning speed, 0,5 cm/min chart speed. Quartz standards were determined 4 times before and after the samples were run. The following results were obtained:

M8; n=6, $\bar{x}$ = 146,6 s = 37,2
M27 ; n=4, $\bar{x}$ = 166,3 s = 8,3

Total: n=10, $\bar{x}$ = 154,5 s = 29,9

$\bar{x}$ = Hb_{rel} (mean)
s = standard deviation
n = number of samples investigated.

Appendix 3

THE ESTIMATE OF PRESSURE CONDITIONS IN LOW GRADE METAMORPHIC ROCKS

Despite rapid progress in the field of metamorphic petrology during recent years, rather insufficient means are still available to determine pressure conditions particularly in low grade metamorphic terrains. For these reasons a newly developed method has been applied here which is based on the measurement of b_o of white micas by X-ray diffractometry and provides a relative pressure scale for low grade metamorphism.

a) *Theoretical background*

Ernst (1963) was among the first to find that many white micas from glaucophane schists and low grade greenschist metamorphism are high in silica and contained relatively high amounts of MgO, FeO and Fe_2O_3 and therefore represented a solid solution between muscovite and celadonite to which he referred to as phengite. He suggested that the phengite content of white mica may be controlled by the reaction 8 phengite + chlorite = 5 muscovite + 3 biotite + 7 quartz + H_2O and pointed out that the phengite-chlorite assemblage is favoured by high ratios of fluid pressure to total pressure and by low temperatures. Velde (1965) determined the upper stability limit of phengite experimentally and, comparing his results with micas formed under natural conditions, concluded that the presence of phengite is in most cases indicative of metamorphism under high pressure with PH_2O approaching P_{tot} but that higher temperatures lead to micas containing smaller amounts of celadonite. Confirming this conclusion by the analysis of white micas from rocks of the glaucophane and greenschist facies (Velde, 1967), he noted the constancy of the Si-content in micas from rocks of different bulk composition formed under similar physical conditions and concluded, also based on his previous experiments, that the silica content of potassic white micas can be used to estimate the pressure and temperature conditions during their formation.

Guidotti (1973) presented chemical data of muscovites from medium and high grade metamorphic terrains. He also found increasing phengite content with increasing pressure but pointed out that bulk composition, too, has a great influence on phengite content. He therefore recommended that only limiting assemblages be used to determine the metamorphic grade. (Limiting assemblage : the number of phases present equals the number of components required to describe the phases).

Guidotti and Sassi (1976) reviewed all previous research and gave a comprehensive account of muscovite as a petrogenetic indicator mineral. They discussed its control in terms of T, P, aH_2O and rock bulk composition and showed that the b_o-values of white micas calculated from the position of the d(060) reflection by X-ray diffraction can be used to determine the

approximate celadonite content and that an increase of b_o reflects an increase in pressure if temperatures and rock bulk compositions are roughly constant. As for the application of this method, they recommended the following precautions:

1) Only samples with similar bulk composition or mineral assemblage should be compared. Paragonite, margarite, pyrophyllite, K-feldspar, carbonate, hematite and magnetite should be absent.
2) The number of the samples employed should be as large as possible in order to facilitate a statistical approach.
3) The samples should be from low grade rocks.
4) Mylonite zones and contact aureoles should be avoided.

On the basis of this approach Sassi and Scolari (1974) had already established an empirical pressure scale by determining b_o from 410 samples collected in low grade pelitic schists in metamorphic terrains ranging from very low pressure (Central Pyrenees) to glaucophanitic greenschist facies (Sanbagawa) (Table 6.7). Since then various further investigations have been carried out (Di Pierro *et al.*, 1973; Piccarreta and Zirpoli, 1974; Kräutner *et al.*, 1975; Fettes *et al.*, 1976; Kleinschmidt *et al.*, 1976) which all confirmed that pressure within low grade metamorphic terrains appears to be much more variable than previously suspected.

b) *Present investigation*

Investigations were carried out with a Philips Diffractometer on slices and thin sections cut perpendicularly to the foliation, using the following instrumental setting : c/s 2×10^2 or 4×10^2, tc4, scanning speed $\frac{1}{4}^o$/min, chart speed 1600 mm/h, slit 1^o, CuKα radiation. Each sample was scanned between 59,5 and 62^o 2θ and the position of the d(060) reflection determined using the quartz d(211) reflection as an internal standard.

The samples taken from the Richtersveld basement consisted of quartz and white mica with only minor amounts of chlorite. Chloritoid and magnetite were sometimes present in small amounts and did not affect the measurement significantly. Only very quartz-rich samples (muscovite bearing quartzite) showed an increase of 0,007 Å from the mean of the pelitic samples and were disregarded. The samples from the Devilscastle Schist Belt were quartz-mica schists as described in Chapter 5 and 6 (i.e. most probably recrystallised mylonite), although Guidotti and Sassi (1976) warned against using mylonitised rocks. However, for the purpose of this study the samples investigated can safely be regarded as metamorphic rocks since it is evident from the frequently random nature of the textures encountered that recrystallisation is essentially posttectonic. Only samples with high magnetite contents showed strongly aberrant b_o-values and were omitted from statistical evaluation.

Due to variable contents of white mica in the samples investigated and variable contents of celadonite in the white micas, d(060) peaks occur in various shapes, the three basic types of which are shown in Fig.A3.1; they may occur in various combinations. Particularly type b) and c) tend to be combined

and thus allow for a considerable subjective component in the determination of the exact position and the number of peaks. Regardless of shape the position of all peaks was measured at the top. To eliminate instrument error, d(060) had to be related to d(211) of quartz using the relationship (Fig. A3.1.a)

$$x = z + y$$

with $y = d(211) = 59{,}98^{\circ}2\theta$, $x = d(060)$, corrected position, and z = distance between y and x measured in $^{\circ}2\theta$.
From these values b_o as listed in the following tables was calculated.

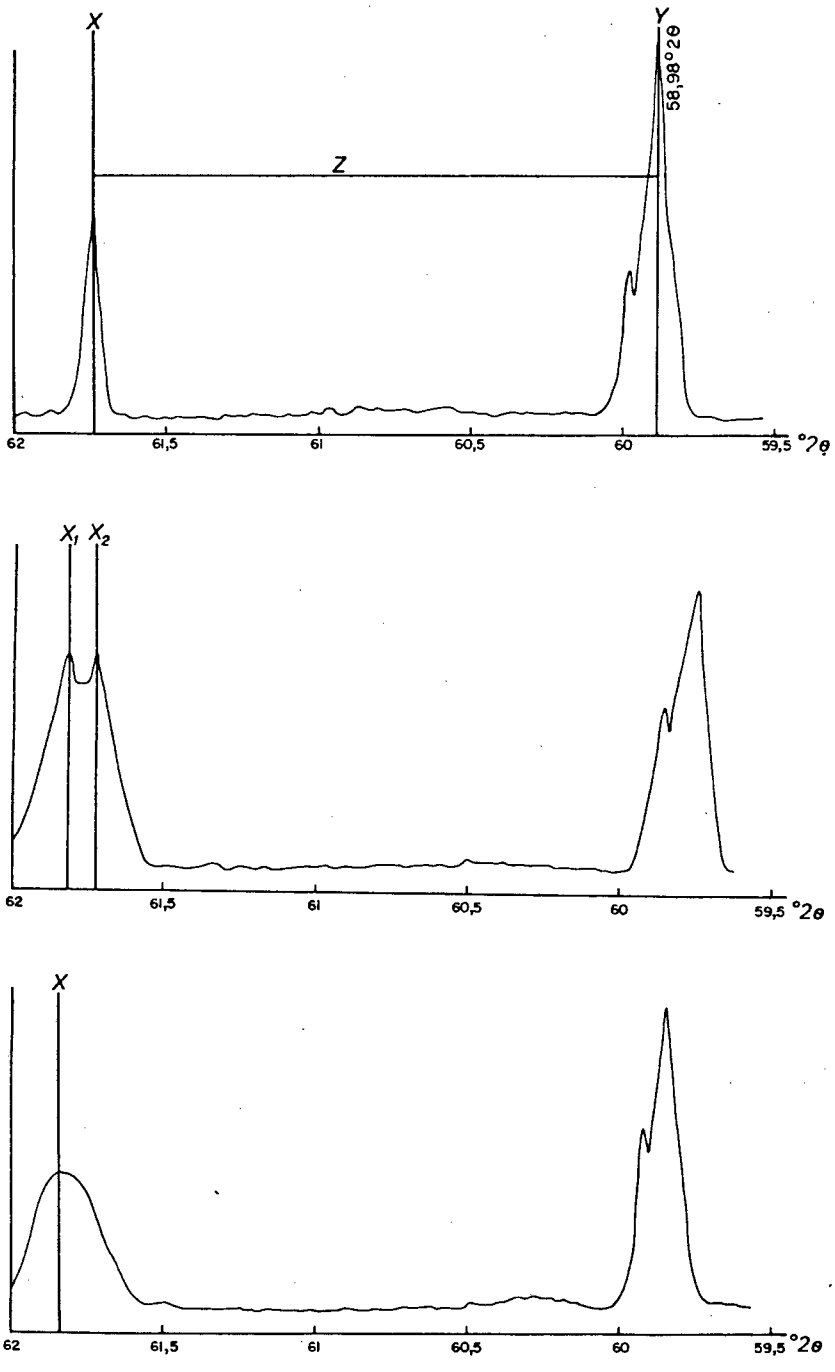

Fig. A3.1.
Three basic types of d(060) reflections

a) Sharp peaks and relationship of d(060) and d(211) (quartz)

b) Bifurcated peak suggesting two different maxima of b_o. Up to three subpeaks were encountered and usually measured separately

c) Wide peak with indistinct maximum. It is possible that peaks of this type are "disguised" furcated peaks in which the variation of celadonite content takes place gradually and does not form sharp maxima.

Table A1.1.

Grain transition frequencies:

System: *qtz - plg - kf - M*

Sample Nr	*qtz/plg	qtz/kf	qtz/M	plg/kf	plg/M	kf/M
11/2	27	39	0	32	0	0
43/	183	70	203	47	50	53
90/	227	600	49	111	7	12
131/	51	7	35	14	13	13
133/1	42	42	61	8	4	10
146/	142	145	14	120	14	26
198/32	81	81	70	45	25	47
213/2	105	33	12	83	28	14
213/10	287	76	162	88	132	49
214/2	119	38	51	116	72	36
248/2	206	220	40	148	15	13
303/2	148	93	45	131	89	37
312/1	43	42	0	71	10	0
408/	54	217	101	26	16	32
420/	43	54	111	82	50	30
421	63	46	23	33	19	8
422/	48	65	35	65	14	29
423/	95	61	135	75	60	54
424/	74	67	86	60	15	39
425/	101	82	117	67	54	41
427/	226	344	127	43	16	25
428/	42	76	130	46	27	49
429/	59	45	79	121	52	22
430/	58	229	50	70	8	58
431/	27	129	12	62	6	8
433/	109	145	56	52	14	22

* represents pair of transitions, i.e. *qtz/plg* and *plg/qtz*, etc.

Table A1.2.

Grain transition frequencies:

System: *qtz - plg - kf - b_f - b_a (hbl)* :
If * at sample number, read *hbl* instead of b_a

Sample Number	qtz/ plg	qtz/ kf	qtz/ ba	qtz/ bf	plg/ kf	plg/ ba	plg/ bf	kf/ ba	kf/ bf	ba/ bf
301/1*	92	28	37	35	23	13	26	3	15	28
328/2a*	163	56	58	59	43	13	49	5	17	31
328/2b*	95	27	33	34	21	2	44	1	16	30
420/	167	95	33	24	134	105	18	44	9	9
425/	156	76	43	28	75	116	35	40	7	10

Table A1.3.

System: *qtz - plg - bi - hbl* :

Sample Nr	qtz/plg	qtz/hbl	qtz/bi	plg/hbl	plg/bi	hbl/bi
208/2	189	166	79	82	99	44

Table A1.4

System: *qtz - plg - kf - ser - mu:*

Sample Number	qtz/ plg	qtz/ kf	qtz/ ser	qtz/ mu	plg/ kf	plg/ ser	plg/ mu	kf/ ser	kf/ mu	ser/ mu
389/4	152	124	48	65	71	60	12	36	7	36

Table A3.1

b_o - values of white micas

Central Richtersveld:

Sample number	b_o (Å)	location	remarks
M33,1	8,9994	Rosyntjiewater	
M33,2	9,0006	"	
M33,3	8,9964	"	
M33,4	8,9994	"	
M34,5	9,0096	"	
M43,6	9,0138	"	
M47,1	9,003	Upper Gannakouriep River	
M47,3	9,0204	"	
18/4	9,0108	"	
149	8,9934	Peilkop	
M35,1	8,9952	"	
M35,2	8,9928	"	
M35,3	9,003	"	

Table A3.2

Southeastern Rosyntjieberg Formation:

Sample number	b_o (Å)	location	remarks
M20	9,0006	Aussenkehr	
M21	9,003	"	
M25	9,0042	Mike/Orange River	
M25/3	9,024	"	
M25,4	8,9994	"	
151/1	9,0042	Klipneus	
151/2	9,0096	"	

Table A3.3

Noms River Fold Belt:

Sample number	b_o (Å)	location	remarks
M37,2	9,0192	Upper Noms River	
M37,3	9,0216	"	
M37,5	9,024	"	
M37/6	9,0138	"	
M40	9,024	Kuams River	
M41	9,0372	"	
M42	9,036	Lower Noms River	
M43	9,0372	"	
M44,4	8,9964	"	
M44,5	9,0006	"	
M46,1	9,0282	Kook River, 2 km W De Hoop	
M46,2	9,0336	"	
138/17	9,0303	Kuams River	

Table A3.4

Samples not included in final calculations:

Sample number	b_o (Å)	location	remarks
84/2	9,0126	Paradys River	too quartz-rich
84/3	9,015	"	"
84/4	9,0096	"	"
142/2	9,0144	Upper Oudannissiep River	"
339/	9,0021	Rosyntjieberg F.	too chlorite-rich
M47/2	9,027	upper Gannakouriep River	aberrant value

Table A3.5.

Devilscastle Schist Belt

Sample number	b_o (Å)	location	remarks
M7,2	8,9982	Eksteenfontein	
M12	8,9784	"	
M10	9,0006	"	
204/33	9,0180	Skimmelberg	weak peak
204/43	9,0108	"	
205/2	9,0120	Eksteenfontein	
205/33	9,036	"	
	9,0426		magnetite bearing, weak bifurcated peak, not included in analysis
212/11	8,9964	Skimmelberg	
	9,0042 *		
212/12	9,0126	"	Wide peak
243/1	9,0096	"	
	9,006		
243/2	9,0306	"	Van Zylsrus, at unconformity
	9,0246		
273/1	9,015	"	
275/1	9,0006	"	mean from two runs, distinctly bifurcated
	8,9955		
275/4	8,96	"	very weak peak, disregarded
275/5	8,9952	"	
280	9,0234	Eksteenfontein	at unconformity
307/21	9,0096	"	
	9,0018		
307/24	9,0117	"	wide peak, trifurcated mean from two runs
	9,0168		
	9,0237		
387/5	9,024	Kouefontein	
395/1	9,0324	cast of Die Plate	unconformity, sheared
395/2	9,0338	"	sheared granite

* Numbers underlined indicate main reflection

Table A3.6.

b_o - values of rocks of the Gariep Group

Sample number	b_o (Å) (individual run)	b_o (Å) (mean)	location	remarks
M3,1	9,0576	9,0495	W Eksteenfontein	powder
	9,0414			"
M3,2	9,0768	9,0597	"	"
	9,0426			
M33,1	9,0534			
	9,0402	9,0446	"	"
	9,0402			
M33,1	9,0438	9,048	"	"
	9,0522			
M33,2	9,0528		"	"
M3,4'	9,0336	9,0429	"	"
	9,0522			
M3,4	9,0336			
	9,0468	9,0366	"	slide
	9,0294			
M14	9,024		Hilda F.(Near Hogsback)	slide
M15	9,0468		"	powder
M16,1	9,0696		Port Nolloth	"
M16,2	9,0534	9,060	"	"
	9,0660			
M16,3	9,0402			
	9,060	9,0512	"	"
	9,0534			
M16,4	9,0576		"	"
M48,1	9,0402		phyllite, 15 km S Alexander Bay at road to Port Nolloth	slide
M48,2	9,0336			"
M48,3	9,0216			"
M49	9,0438		Mica schist, bed of Holgat River, road Alexander Bay Pt Nolloth.	"
395/32	9,0522		Die Plate	slide

Table A4.1 Modal analyses - Intrusive rocks of the VIS

Sample number	*qtz*	*plg*	*kf*	*M*	*Acc.*
3/2	27,3	45,8	9,8	16,9•	0,2
7/3	38,8	29,3	23,6	6,1	2,2
11/2	33,5	18,5	47,9	0	0
25/	27,7	37,3	7,8	27,2	-
35/1	27,3	43,3	9,9	18,5	1,0
35/2	28,6	42,7	10,4	18,2•	-
43/1	33,0	39,3	9,8	14,8	-
62/	36,5	33,9	20,0	9,6	-
64/	25,6	49,5	13,5	10,8•	0,9
68/3	29,9	54,8	6,7	9,6	-
90/	46,7	15,8	36,1	-	1,4
117/3	43,3	35,4	16,4	4,8	0,1
131/	31,6	41,3	13,6	14,2	0,3
132/	25,2	42,7	20,4	11,1	0,6
133/1	34,0	41,9	6,7	17,4	-
135/	31,4	41,8	3,2	20,2	3,4
137/	25,4	40,8	8,8	23,2	1,8
140/	31,8	43,9	7,1	17,2	-
148/	23,4	49,0	0,5	26,9	-
146/	34,6	27,8	36,2	1,3	-
199/2	27,2	46,3	0	26,5	-
199/3	45,1	25,5	23,2	3,3	2,9
199/4	35,1	41,2	17,4	6,2	-
199/42	25,7	36,7	26,3	10,3	1,0
199/5	24,2	45,2	2,4	25,7	2,5
199/6	24,8	34,8	33,0	3,6	3,7
199/7	28,2	42,8	19,5	9,0	0,7
208/2	15,5	47,2	0	34,0•	3,3
241/	29,3	47,8	7,2	14,7	1,1
244/11	28,3	53,1	3,4	15,3	-
244/12	27,2	50,4	7,2	11,4	3,8
244/42	35,2	40,1	22,5	1,9	0,3
248/2	40,8	28,8	29,2	1,3	-
248/3	28,6	44,7	16,1	10,5	-
248/4	47,4	37,3	5,3	7,3	2,2
249/	30,7	41,3	10,0	16,1	1,7
252/	25,3	36,1	9	32,5	-
276/	19,5	51,5	14,7	13,9	0,5
279/	26,7	35,5	16,9	18,0	3,0
284/3	29,3	28,3	14,3	22,0	6,0
287/1	37,7	43,1	3,2	9,9	6,7
295/	23,8	46,9	12,9	11,9	4,4
300/1	26,3	52,5	5,3	13,8	2,1
312/2	36,7	40,5	10,1	11,8	1,00

Table A4.1 (continued)

Sample number	*qtz*	*plg*	*kf*	*M*	*Acc.*
420/	30,3	31,4	21,6	12,5	4,3
422/	25,2	34,4	30,9	8,8	0,7
423/	29,0	40,2	16,3	9,2	5,4
424/	31,0	25,9	33,0	7,9	2,2
425/	28,3	34,9	19,5	15,4	1,9
427/	25,7	32,2	31,6	7,1	3,4
428/	27,1	37,3	20,6	11,6	3,5
429/	35,0	31,2	27,2	5,1	1,6
433/	35,5	28,2	30,7	4,5	1,1

• hornblende bearing

M mafic minerals : chlorite, biotite, epidote not occurring as alteration products of plagioclase

Table A4.2 - Migmatites of the Helskloof

Sample number		*qtz*	*plg*	*kf*	*M*	*Acc.*
198/21	P	36,9	40,0	10,5	12,1	0,5
198/22	M	32,5	37,0	-	27,8	7,6
198/31a	L	27,3	52,8	0	20,0	-
	M	19,1	22,9	0	58,0	-
198/31b	L	39,2	46,9	0	13,9	-
	M	4,5	24,8	0	70,7	-
198/31c	L	29,8	48,5	0	21,8	-
	L	47,1	44,7	0	8,2	-
	M	21,9	31,4	0	46,7	-
	L	39,1	45,2	5,3	10,3	-
198/32	L	46,0	23,0	24,4	5,0	1,6
208/12	P	38,7	45,9	4,2	11,0	0,3
213/1	D	45,0	31,4	12,5	10,0	1,1
213/2	D	31,9	39,7	21,0	7,3	-
213/3	D	30,0	42,0	16,1	11,9	-
213/9	D	31,6	34,4	25,8	8,2	-
213/10	D	30,0	32,9	17,7	19,1	0,2
234/23	P	32,2	34,6	2,9	30,3	-
237/	D	32,0	46,4	10,8	10,7	-
238/5	D	32,2	35,5	18,9	11,6	0,7
239/31	M	7,8	27,2	1,9	60,2	2,9
	L	30,7	41,5	13,3	14,5	-
	L	30,6	34,9	25,5	13,5	-
239/32a	M	20,0	27,6	6,0	45,6	0,8
	L	31,3	25,5	34,4	8,6	0,5
239/32b	M	18,9	4,6	45,9	30,6	-
	L	26,4	3,0	57,9	12,6	-
239/32c	M	6,3	64,3	3,1	24,9	1,4
	L	35,3	50,8	2,4	10,9	0,3
239/41	L	37,2	50,6	0	12,1	-
239/6	D	30,8	34,0	18,6	6,6	-
301/1	P	27,5	33,5	12,1	23,3	3,0
303/2	D	30,3	34,3	27,3	7,0	1,1
306/3	P(KrM)	21,1	41,4	0,4	33,3	3,9
308/1	P	35,7	42,2	2,4	16,8	2,8
308/2	D	41,5	33,4	19,9	5,1	-
309/	L	37,0	30,5	23,2	9,3	-
	L	45,6	49,8	0	3,7	-

P - Paleosome
M - Melanosome
L - Leucosome
Krm - in situ melting referred to in the text as kryptomigmatite

Alphabetical list of place names used in the text

	latitude	longitude
Abikwarivier	28 15'	17 11'
	28 19'	17 05'
Aussenkehr	28 22'	17 25'
Bakrivier	28 31'	17 16'
Black Face Mountain	28 43'	17 19'
Blockwerf	28 04'	17 07'
Bluff	28 55'	17 28'
Claim Peak	28 21'	17 09'
De Hoop	28 11'	17 10'
Devilscastle	28 47'	17 18'
Devils Tooth	28 28'	17 16'
Die Koei	28 17'	17 00'
Die Plate	28 54'	17 13'
Doringrivier	29 00'	17 22'
Eksteenfontein	28 49'	17 13'
Gannakouriep	28 17'	17 09'
Gorgons Head	28 20'	17 19'
Grasdrif	28 20'	17 22'
Groenrivier	28 49'	17 28'
Helskloof	28 45'	17 28'
Kahams	28 36'	17 15'
Kahamsrivier	28 33'	17 17'
Klipbok	28 53'	17 22'
Klipbokkop	28 38'	17 15'
Kliphoogte	28 57'	17 21'
Klipneus	28 25'	17 23'
Kouefontein	28 59'	17 24'
Kodaspiek	28 14'	16 59'
Koeroegab	28 15'	17 04'
Kookrivier	28 14'	17 04'
Krommek	28 57'	17 17'

	latitude	longitude
Kuamsrivier	28 06'	17 01'
Kwaggarug	28 24'	17 17'
Maerpoort	28 13'	17 08'
Mount Terror	28 27'	17 16'
Mike	28 30'	17 23'
Nabasberg	28 19'	17 20'
Nomsrivier	28 08'	17 06'
Oenas	28 04'	17 01'
Omsberg	28 27'	17 10'
Oudannisieprivier	28 2?'	17 21'
Paradyskloof	28 20'	17 00'
Peilkop	28 11'	17 01'
Pokkiespramberge	28 05'	16 58'
Rooiberg (NE Ri)	28 12'	17 09'
Rooiberg (SE Ri)	28 47'	17 21'
Rosyntjieberg	28 27'	17 12'
Sambokrivier	28 32'	17 27'
Sendelingsdrif	28 07'	16 54'
Skimmelberg	28 40'	17 17'
Soetgat	28 45'	17 16'
Springbokkloof	28 21'	17 18'
Stinkfontein se Rivier	28 43'	17 22'
Struishoek	28 51'	17 17'
Tatasberg	28 20'	17 15'
Tswales	28 24'	17 05'
Vandersterrberg	28 24'	17 03
Vanzylsrivier	28 32' 28 39'	17 21' 17 18'
Windvlakte	28 50'	17 19'
Xaminxaip	28 43'	17 25'

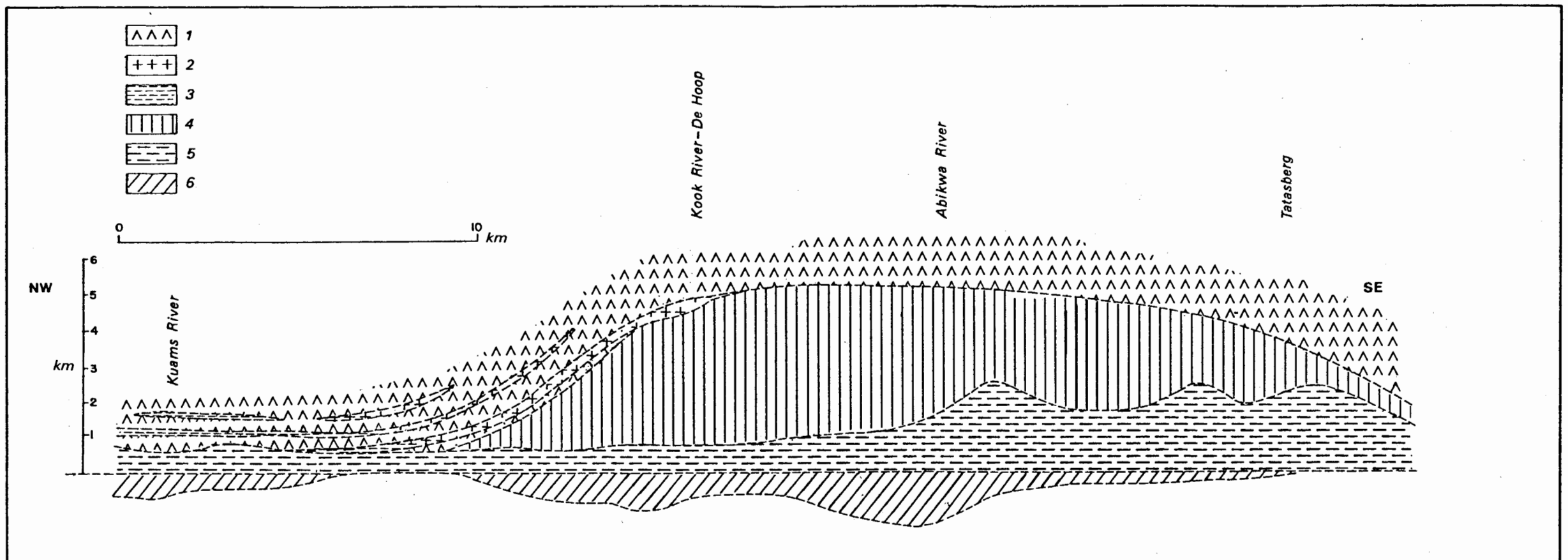

Palinspastic reconstruction of the supracrustal rocks between Oenas and Tatasberg in the northeastern Richtersveld. The reconstruction is based on the present day outcrop pattern and depicts the geological profile prior to the emplacement of the Vioolsdrif intrusives. The boundary Lower/upper Abikwarivier Formation has arbitrarily been used as reference line.
1) melanocratic volcanics 2) leucocratic volcanics 3) laminated gneiss (Kuamsrivier Formation) 4) quartz-feldspar porphyry (Kookrivier Formation) 5) Upper Abikwarivier Formation 6) Lower Abikwarivier Formation.
The upper limits are unknown but are unlikely to exceed those indicated in the profile.

Annexure 3b

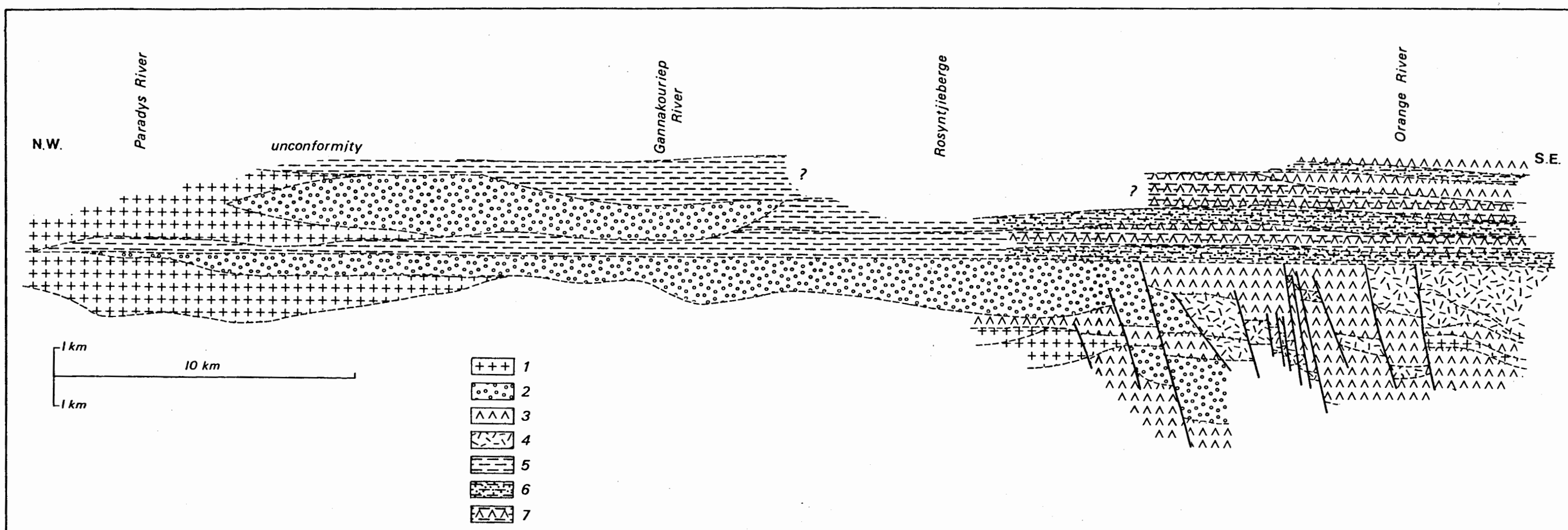

Palinspastic reconstruction of the supracrustal rocks between Aussenkehr and Paradys River in the northeastern Richtersveld. The reconstruction is based on the present day outcrop pattern and depicts the geological profile prior to the emplacement of the Vioolsdrif intrusives. The base of the Rosyntjieberg Formation has arbitrarily been used as reference line. Block faulting underlying the Rosyntjieberg Formation is interpretative in detail, but provides the best explanation for the attitude of layering and the type of unconformity with the Rosyntjieberg Formation. It indicates increased tectonic activity in the southeast prior to the deposition of the Rosyntjieberg Formation.

1) leucocratic volcanics - 2) mesocratic volcanics - 3) melanocratic volcanics - 4) metasediments and redeposited volcanics - 5) Rosyntjieberg Formation undifferentiated - 6) Rosyntjieberg quartzite - 7) reworked melanocratic volcanics with intercalated quartzites

Annexure 3a

Profiles across the Abikwarivier Formation : a) west of the Tatasberg, b) Abikwa River c) road from Abikwa River to Maerpoort.
1) leucocratic lavas, tuffs and ash-flow tuffs. 2) mesocratic volcanics, mostly tuffaceous. 3) mesocratic to melanocratic volcanics. 4) volcanoclastics, fine, coarse. 5) vesicular, amygdaloidal. 6) flowbanding. 7) quartz, feldspar phenocrysts in hand specimen.

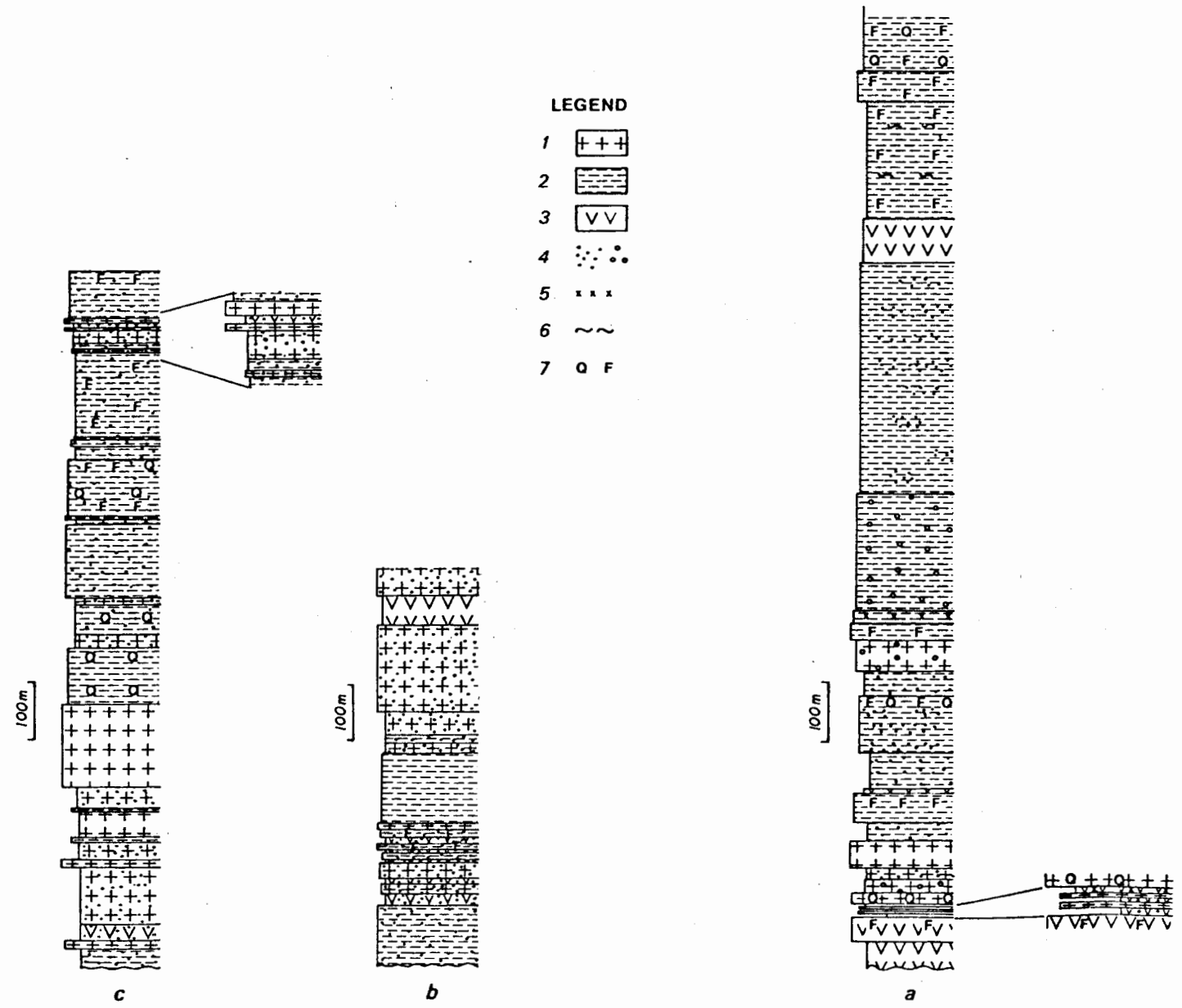

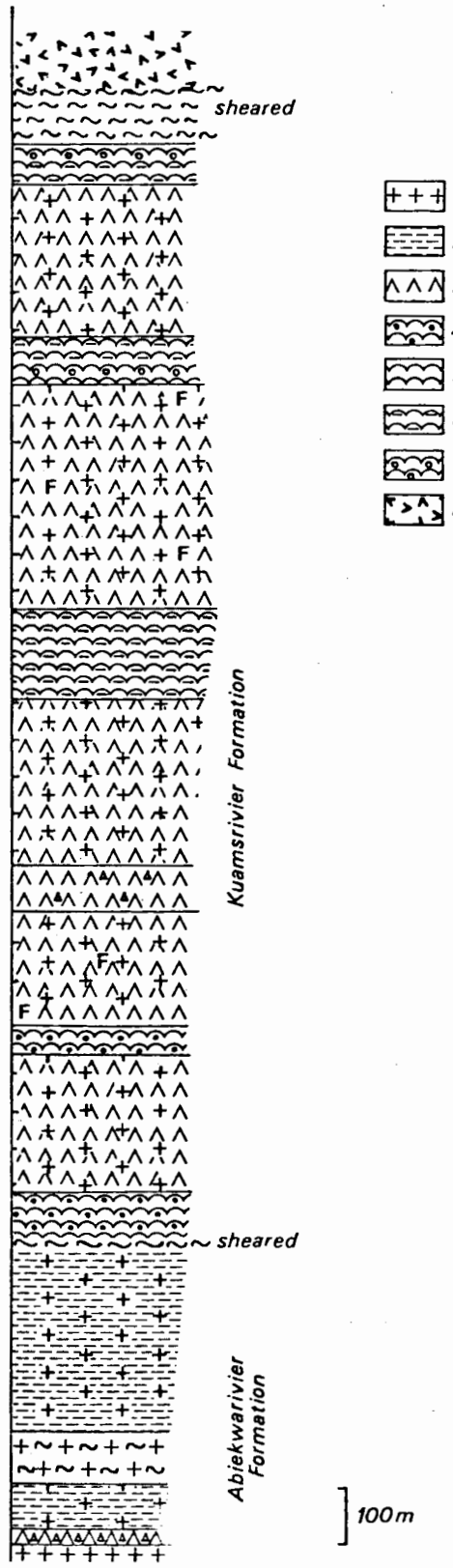

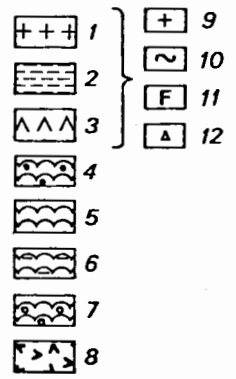

Profile along the Kuams River with Abikwarivier Formation and Kuamsrivier Formation. Repetition by folding of the Kuamsrivier Formation is not shown.
Legend: 1)leucocraticvolcanics 2)mesocratic volcanics 3)melanocratic volcanics 4)reworked volcanics and sediments 5) chlorite-sericite schist 6) finely laminated gneiss with biotite porphyroblasts 7)conglomerate 8)biotite gneiss and schist, amphibole 9)massive 10)flowbanding 11)feldspar phenocrysts 12)volcanic breccia

Annexure 2

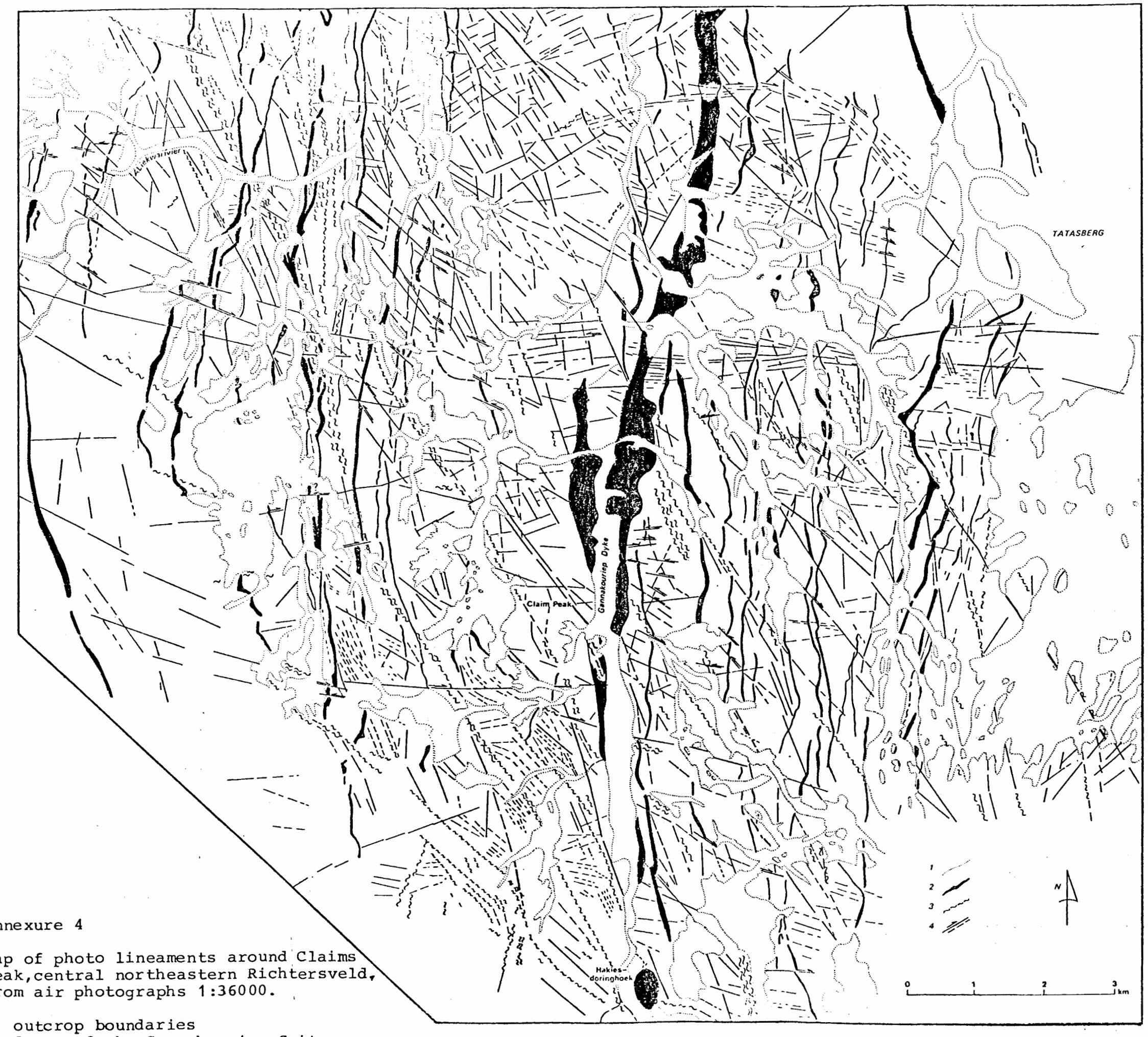

Annexure 4

Map of photo lineaments around Claims Peak, central northeastern Richtersveld, from air photographs 1:36000.

1) outcrop boundaries
2) dykes of the Gannakouriep Suite
3) zones of mylonitization and quartz impregnation (deformation of the Devilscastle Event)
4) photolineaments with/without sense of displacement